UNIVERSITY OF EAST ANGLIA

Modelling the Economic Impacts of Compound Hazards through the Production Supply Chain in the Post-pandemic World

YIXIN HU

Submitted in accordance with the requirements for the degree

of Doctor of Philosophy

University of East Anglia

School of Environmental Sciences

30 September 2022

Abstract

Climate change and fast urbanization are increasing the likelihood of compound hazards - events where multiple drivers and/or hazards interact with multiplicatively destructive environmental and socio-economic consequences. This includes increases in the frequency of not only concurrent natural extremes (heatwaves and droughts, storm surges and extreme rainfalls, etc.), but also collisions between natural and manmade disasters (air pollution, infectious disease transmission, trade wars, etc.) particularly in the post-pandemic world. Entanglement of different hazardous factors increases the complexity of impact accounting and risk management and requires an integrated solution to tackle the vulnerabilities of human societies towards compound risks. However, most of the research in disaster analysis investigates one hazard at a time. Only a few emerging perspectives have noticed or warned the potential of compound hazards, but they are still far from capacity building for the compound resilience to future crises.

This PhD thesis presents a full set of methodology to systematically assess the economic impacts from single to compound hazards. The concept of 'disaster footprint' is used here to capture the direct and indirect impacts rippling through the economic supply chain during a single or compound disaster event. A four-stage research framework is proposed. It starts from the direct disaster footprint assessment, which links physical characteristics of hazards with property damage or health impairment by simulating hazard-specific exposure-damage functions. The direct footprint is then fed into an input-output-based (IO-based) hybrid economic model to calculate the indirect disaster footprint that propagates through intersectoral and interregional connections to wider economic systems. The improved IO-based disaster footprint model is built here for single hazard analysis, with innovations regarding inventory adjustment and cross-regional substitutability. Third, within the same disaster footprint

framework, the economic interplays between diverse types of hazards are synthesized into the impact assessment, and thereby a Compound Hazard Economic Footprint Assessment (CHEFA) model is developed for compound events. Finally, favourable response and recovery plans, which are aimed to mitigate the total disaster footprint, are suggested by comparing the modelling results under wide ranging scenarios and identifying crucial influencing factors through sensitivity analysis. A major contribution of this thesis is that it takes the first step in the field of disaster analysis to integrate multiple hazardous factors within a macro-economic impact assessment framework that accounts for both direct and indirect disaster footprint into sectoral and regional details.

The proposed modelling framework is first applied to three types of hazards (i.e., heat stress, air pollution and climate extremes) on the provincial and national scales in China to demonstrate its flexibility for a wide range of disaster risks. The total economic costs of heat stress, air pollution and climate extreme events in China have increased from US$207.9 billion (1.79% of GDP) in 2015 to US$317.1 billion (2.16% of GDP) in 2020. Despite the decreasing economic costs of air pollution and climate extreme events, the economic costs from heat-related health impacts have continued the concerning growing trend. Among the three types of hazards, the economic costs of heat stress were the biggest and accounted for over 70% of the total costs. Heat stress affects the economy mainly by reducing labour productivity. For each unit of direct costs, heat stress was also inclined to cause more indirect supply chain costs than air pollution and climate extremes. Most of the heat-induced direct costs occurred outdoors in the agriculture and construction sectors, while most of the heat-induced indirect costs happened indoors in the manufacture and service sectors. At the regional level, hotspot provinces with prominent economic risks from these hazards have been identified for China. Southern provinces were more economically vulnerable to heat stress than northern provinces, while northern provinces tended to suffer larger

economic costs from air pollution than southern provinces. By contrast, the economic impacts of climate extreme events were more spatially distributed in China than the other two types of hazards. Location-specific economic impacts of climate change require location-specific responses, including enhancing inter-departmental cooperation, strengthening climate emergency preparedness, supporting scientific research, raising public awareness, and promoting climate change mitigation and adaptation.

Economic implications of climate change are also evaluated with a focus on future flood risks in six developing countries (i.e., Brazil, China, India, Egypt, Ethiopia and Ghana) around the end of 21st century (2086-2115). A physical model cascade of climate-hydrological-flood models is linked with the disaster footprint economic model through a set of country and sector specific depth-damage functions. The total (direct and indirect) economic losses of fluvial flooding are projected for each country, with or without socio-economic development, under a range of warming levels from <1.5°C to 4°C. As a share of national GDP, Egypt suffers the largest flood-induced losses under both climate change (CC) and climate change plus socio-economic development (CC+SE) experiments, reaching 2.3% and 3.0% of GDP under 4°C warming. Climate change acts as a driving factor that increases the flood losses in all countries, but the effect of socio-economic development differs among the countries and warming levels. For Ethiopia and China, future flood losses as a proportion of GDP under different warmings decline from the baseline levels when socio-economic development is modelled, suggesting a more resilient economic growth that helps reduce future flood risks. However, for Brazil, Ghana, and India, while losses as a proportion of GDP initially decline at lower warming levels, increases are seen from 2.5°C or 3°C warming onwards, suggesting a tipping point where increasing flood risk outweighs any relative benefits of socio-economic development. These results highlight the importance of including socio-economic development when estimating

future flood losses, essential to provide a more comprehensive picture of potential losses that will be important for decision makers.

With the development of the CHEFA model, the economic interaction between concurrent hazardous factors comes into analysis. A hypothetical perfect storm consisting of floods, pandemic control, and trade restrictions (as a proxy for deglobalization) is assumed to test the applicability and robustness of the model. The model also considers simultaneously cross-regional substitution and production specialization, which can influence the resilience of the economy to multiple shocks. Scenarios are first designed to investigate economic impacts when a flood and a pandemic lockdown collide and how these are affected by the timing, duration, intensity/strictness of each event. The results reveal that a global pandemic control aggravates the flood impacts by hampering the post-flood capital reconstruction, but a flood exacerbates the pandemic impacts only when the flood damage is large enough to exceed the stimulus effect of the flood-related reconstruction. Generally, an immediate, stricter but shorter pandemic control policy would help to reduce the economic costs inflicted by a perfect storm. The study then examines how export restrictions and retaliatory countermeasures during the pandemic and floods influence the economic consequences and recovery, especially when there is specialization of production of key sectors. It finds that the trade restriction of a region to ‘protect’ its product that can be substituted by the same product made elsewhere, while hampering the global recovery, may alleviate the region’s own loss during the compound disasters if the increasing domestic demand exceeds the negative impacts of falling exports. By comparison, the trade restriction on a non-substitutable product has greater negative impacts on the global recovery, which ultimately propagates backward to the region through the supply chain and exacerbates its own loss. The results also indicate that the potential retaliation from another region and sector would further deteriorate the global recovery and make everyone lose, with the region which initiates the trade war

losing even more when the retaliatory restriction is also imposed on a non-substitutable product. Therefore, regional or global cooperation is needed to address the spillover effects of such compound events, especially in the context of the risks from deglobalization.

The CHEFA model has been then successfully applied to a real compound event of the 2021 extreme floods and a COVID-19 wave in Zhengzhou, the capital city of Henan province in China. The event was rare in history and has caused enormous economic consequences (direct damage worthy of 66,603 million yuan and indirect losses worthy of 44,340 million yuan) to the city, reaching a total of 10.28% of its GDP during the previous year. The negative impacts also spilled over to the whole nation through the production supply chain, making the total economic losses amount to 131,714 million yuan (0.13% of China's GDP in the previous year). The local lockdown to control the spread of COVID-19 has increased the indirect losses by 77% and the indirect/direct loss ratio from 0.55 to 0.98. While a majority (29%) of direct losses happened in Zhengzhou's real estate industry, the indirect losses were more distributed in Zhengzhou's non-metallic mineral products (13%), food and tobacco (10%), and transportation services (10%). Zhengzhou's non-metallic mineral sector is also a critical sector with strong propagation effects. The reduction in its production has triggered a supply chain loss of 10,537 million yuan in terms of trades with other sectors and regions, which nearly doubled its value-added loss. In regions outside Zhengzhou, the agriculture, mining, petroleum and coking, chemical products, accommodation and restaurants, and financial services were the sectors significantly affected by this compound event. Among them, the agriculture in Henan (outside Zhengzhou) suffered the greatest indirect (or value-added) loss at 2,760 million yuan. The study also finds that the post-disaster economic resilience is most sensitive to factors such as road recovery rate, reconstruction efficiency and consumption subsidies, and the COVID-19 control tends to reduce the marginal economic benefits

of flood emergency efforts. As low-likelihood compound extreme events become more frequent with global warming, concerted actions are in urgent need to address the intricate dilemma between disaster relief, disease control and economic growth at both individual and institutional levels.

Overall, this PhD study develops an integrated assessment framework for the direct and indirect economic impacts from single to compound hazardous events. Within this framework, consistent and comparable loss metrics are elicited for different types of hazards, either single or compound ones, advancing the understanding of their economic risk transmission channels through the production supply chain. Knowing the economic complexity intrinsic to the disaster mixes will foster a sustainable risk management strategy that balances different emergency needs at the minimal economic costs, and guide investment to risk preparedness against the growing threats under climate change. In addition, collaborative efforts are required from the local to global levels to enhance the economic resilience towards future crises in complex situations. This is crucial to achieve the mitigation and adaptation targets in the Paris Agreement and Sendai Framework for Disaster Risk Reduction.

List of Contents

List of Tables

List of Figures

List of Appendix Tables

List of Appendix Figures

Abbreviations

Abbreviations	Descriptions
ARIO	Adaptive Regional Input-Output
BDI	Basic Dynamic Inequalities
CaMa-Flood	Catchment-based Macro-scale Floodplain
CGE	Computable General Equilibrium
CHEFA	Compound-Hazard Economic Footprint Assessment
CMIP	Climate Model Intercomparison Project
DALY	Disability-Adjusted Life Year
DF	Disaster Footprint
DIVA	Dynamic Interactive Vulnerability Assessment
EAR	Economic Amplification Ratio
ECMWF	European Centre for Medium-Range Weather Forecasts
EMEP	European Monitoring and Evaluation Programme
ERF	Exposure-Response Function
ESA CCI	European Space Agency Climate Change Initiative
GAINS	Greenhouse Gas - Air Pollution Interactions and Synergies
GBD	Global Burden of Disease
GCM	Global Climate Model
GDP	Gross Domestic Product
GEM	Global Earthquake Model
GTAP	Global Trade Analysis Project
GVA	Gross Value Added
HBV	Hydrologiska Byrans Vattenbalansavdelning
IEA	International Energy Agency

IFRC	International Federation of Red Cross and Red Crescent Societies
IIM	Inoperability Input-output Model
IO	Input-Output
IPCC	Intergovernmental Panel on Climate Change
JIT	Just-In-Time
MR-BRT curve	Meta-Regressed Bayesian Regularized Trimmed curve
MRIA	Multi-Regional Impact Assessment
MRIO	Multi-Regional Input-Output
NDC	Nationally Determined Contribution
NPI	Non-Pharmaceutical Intervention
$PM_{2.5}$	Fine Particulate Matter
PPE	Personal Protective Equipment
PWHL	Potential Work Hours Lost
RCP	Representative Concentration Pathway
RO	Research Objective
RQ	Research Question
RR	Relative Risk
SEIR	Susceptible-Exposed-Infected-Recovered
SRES	Special Report on Emissions Scenarios
SSP	Shared Socioeconomic Pathway
TFP	Total Factor Productivity
TMREL	Theoretical Minimum-Risk Exposure Level
UNISDR	United Nations Offices for Disaster Risk Reduction
VSL	Value of Statistical Life
WBGT	Wet Bulb Globe Temperature
WDI	World Development Indicators
WHL	Work Hours Lost

WLF	Work Loss Factor
YLL	Years of Life Lost

Acknowledgements

I would like to acknowledge both University of East Anglia (UEA) and Southern University of Science and Technology (SUSTech) for offering me the opportunity to do this site-split PhD programme. UEA confers my doctorate and SUSTech provides me the scholarship. Both universities offer inclusive and diverse environment for me to carry out my PhD study, and staff at both universities are always glad to provide timely help. I will always cherish my time in Norwich, UK and Shenzhen, China, two lovely but very different cities, which have enriched my life experience and widened my horizons.

I am also sincerely grateful to my supervisors at UEA and SUSTech: Dabo Guan, Lili Yang, and Helen He. Their continuous support and guidance throughout the programme have been invaluable. I am especially indebted to Dabo Guan for introducing me into the field of climate change economics and for the patience and trust in me when I make slow progress. He is a man of foresight and gives creative insights that enlighten my research. I also thank Lili Yang and Helen He for their precious advice on not only academic but also life and career.

Beside my supervisors, I would like to extend my thanks to my thesis examiners: Rosalind Bark and Lirong Liu. I really appreciate their time and efforts in examining this work and their insightful comments, which encourages me to widen my research from various perspectives.

It has been an amazing experience working between two research groups from UEA and SUSTech, particularly with teammates from diverse backgrounds. An immense thank to everyone I have worked with and from whom I have learned so much. I have really enjoyed the companionship of Huiqing Wang, Jiamin Ou, Yuli Shan, and Heran

Zheng during my time at UEA, as well as Xian Li, Feiyu E, Zongjia Zhang, and Wenwu Gong when I was at SUSTech. The time we spent together, the places we went together, and the good or bad emotions we shared have lighted up my PhD life and will be memorized forever. Thanks of course to the Disaster Footprint team I have worked so closely with: Zhiqiang Yin, Daoping Wang, Zhao Zeng, and Yida Sun. I am so pleased to have them working on disaster impact modelling with me and being able to discuss ideas with them really has been invaluable.

In addition, I would like to express my deep gratitude to everyone I have collaborated with externally: Rachel Warren, Katie Jenkins, and other team members on the BEIS project at the Tyndall Centre for Climate Change Research, plus Wenjia Cai, Chi Zhang, and other team members on the China Report of Lancet Countdown. Heartfelt thanks to all of them for their support and input.

My gratitude also goes to my family and friends for always standing by my side over the past years. I have the best parents, Anhong Li and Zhiwei Hu, in the world as they support every decision I make with unconditional love. A special thank is delivered to my boyfriend Nian Yu for his unlimited company and support for me to explore the academic world. All these people brighten up my mood every single day of my PhD study. I treasure them more than I can say.

I also want to thank myself for taking up the PhD challenges four years ago, not giving up halfway, and eventually getting to this stage. The experience and skills I have gained will become treasurable assets on my future journey to the next stage of my academic career.

Finally, and foremost, thank you God for guiding me through all the ups and downs throughout my PhD journey. I am truly grateful for all the blessings you have given

me in my life.

Yixin Hu

25 November 2022 in Norwich

PhD Achievements

Published Papers: ([#] first co-author; * corresponding author)

Hu, Y., Yang, L., & Guan, D*. (2022). Assessing the economic impact of "natural disaster-public health" major compound extreme events: a case study of the compound event of floods and COVID epidemic in Zhengzhou China (in Chinese). *China Journal of Econometrics, 2*(2), 257-290. https://doi.org/10.12012/CJoE2021-0090 (Chapter 7)

Yin, Z.[#], **Hu, Y.[#]**, Jenkins, K., …, Guan, D*. (2021). Assessing the economic impacts of future fluvial flooding in six countries under climate change and socio-economic development. *Climatic Change, 166*(3), 38. https://doi.org/10.1007/s10584-021-03059-3 (Chapter 5)

Mendoza-Tinoco, D.[#], **Hu, Y.[#],** Zeng, Z., …, Guan, D*. (2020). Flood footprint assessment: a multiregional case of 2009 Central European floods. *Risk Analysis, 40*(8), 1612-1631. https://doi.org/10.1111/risa.13497

Wang, H., **Hu, Y.,** Zheng, H., …, Guan, D*. (2020). Low-carbon development via greening global value chains: a case study of Belarus. *Proceedings of the Royal Society A: Mathematical, Physical and Engineering Sciences, 476*(2239), 20200024. https://doi.org/10.1098/rspa.2020.0024

Cai, W.[#], Zhang, C.[#], Zhang, S.[#], …, **Hu, Y.,** …, Gong, P*. (2022). The 2022 China report of the Lancet Countdown on health and climate change: leveraging climate actions for healthy ageing. *The Lancet Public Health*. https://doi.org/10.1016/s2468-2667(22)00224-9 (Chapter 4)

Cai, W.[#], Zhang, C.[#], Zhang, S.[#], …, **Hu, Y.,** …, Gong, P*. (2021). The 2021 China report of the Lancet Countdown on health and climate change: seizing the window of opportunity. *The Lancet Public Health, 6*(12), e932-e947. https://doi.org/10.1016/S2468-2667(21)00209-7 (Chapter 4)

Cai, W.[#], Zhang, C.[#], Suen, H. P.[#], …, **Hu, Y.,** …, Gong, P*. (2021). The 2020 China

report of the Lancet Countdown on health and climate change. *The Lancet Public Health, 6*(1), e64-e81. https://doi.org/10.1016/S2468-2667(20)30256-5 (Chapter 4)

Cai, W.[#], Zhang, C.[#], Suen, H. P.[#], …, **Hu, Y.**, …, Gong, P*. (2021). Location-specific health impacts of climate change require location-specific responses (in Chinese). *Chinese Science Bulletin, 66*(31), 3925-3931. https://doi.org/10.1360/TB-2021-0140 (Chapter 4)

Working papers:

Hu, Y., Wang, D., Huo, J., …, Chemutai, V. (2021). *Assessing the economic impacts of a 'perfect storm' of extreme weather, pandemic control and deglobalization: a methodological construct* [Working Paper No. 160571]. World Bank. https://documents.worldbank.org/en/publication/744851623848784106 (Chapter 6)

Book Sections:

Sonja S. Teelucksingh, Nesha C. Beharry-Borg, **Hu, Y.,** Zeng, Z., & Guan, D. (2020). Chapter Ten: Water Economics. In J. Holden (Ed.), *Water Resources: An Integrated Approach* (2nd ed.). London and New York: Routledge. https://doi.org/10.4324/9780429448270

Papers Forthcoming:

Hu, Y., Wang, D., Huo, J., …, Guan, D*. (2022). Assessing the economic impacts of a perfect storm of extreme weather, pandemic control and deglobalization: a methodological construct. *Risk Analysis,* under review. (Chapter 6)

Cai, W.[#], Zhang, C.[#], Zhang, S.[#], …, **Hu, Y.,** …, Gong, P*. (2022). Seizing the window of opportunity to mitigate the impact of climate change on the health of people in China (in Chinese). *Chinese Science Bulletin,* under review. (Chapter 4)

Chapter 1 Introduction

1.1. Compound Hazards in the Post-pandemic World

As the world enters the third year of the COVID-19 pandemic, human development faces unprecedented challenges from multiple environmental, social, economic, and political hazards. These hazards may interrelate and develop in confluence to generate disastrous compounding impacts. Yet current understanding of these hazards is often isolated and fragmented, leading to biased impact evaluation and inadequate emergency response. Therefore, a holistic approach that integrates multiple, or compound hazards is in urgent need to address the complex disaster impacts in the post-pandemic interconnected world.

At the time of writing, the COVID-19 pandemic has affected 500 million people with 6.2 million deaths in 226 countries and territories[1]. Waves of lockdowns, which usually last for several months, have been implemented to contain the spread of the virus around the world. As the COVID-19 pandemic and its response measures continue to affect public health and economic activities, the collisions with a number of other environmental and socioeconomic shocks and disruptions are inevitable, leading to increased risks of compound events (Phillips et al., 2020). For instance, from March 2020 to August 2021, 433 extreme weather events coincided with the COVID-19 pandemic, affecting an estimated 139.2 million people; additionally, 658.1 million people were exposed to extreme heat, and 0.8 million people were affected by wildfires (Walton et al., 2021).

On a broader scale, the recent climate and COVID-19 pandemic crises were also

[1] Data source: https://covid19.who.int/ (accessed on 19 April 2022).

overlapping with the deglobalization trend that had been rising prior to the COVID-19 pandemic. The 2020 World Development Report reports that growth in global value chains has flattened (World Bank, 2019). The contraction in global trade that began in mid-2018 deepened in March 2020, with the global exports and imports declining by around 12% year-on-year respectively (Ferrantino et al., 2020). Additionally, country and regional reform agendas have either experienced a reversal or have stalled. China's recent move towards promoting local industries and the falling share of exports as a share of GDP (from 32.6% in 2008 to just 18.5% in 2020) further brightens this signal (World Bank, 2021). Recent years also saw increasing trade tensions, especially in relations between the US and China, as well as the UK withdrawing from the EU, but also in some of the responses by governments to the COVID-19 pandemic (Eaton, 2021; Espitia et al., 2020; Hatzigeorgiou and Lodefalk, 2021; Zhang, Lei, et al., 2019). Countries turning inward closes the window of opportunities to enhance regional or global cooperation, increasing the uncertainty of global recovery in the post-pandemic era (Shahid, 2020).

Apart from the intersections between the pandemic (including COVID-19) and other hazards, compound events could also arise from the co-occurrence of non-pandemic hazards, such as multiple climatic hazards. In fact, the concept of 'compound events' is originated from climate research and developed by Zscheischler et al. (2018, p. 470) to describe 'the combination of multiple drivers and/or hazards that contributes to societal or environmental risk'. The combination of two or more weather or climate events, whether of similar types or of different types, can occur 1) at the same time, 2) in close succession, or 3) concurrently in different regions (Zscheischler et al., 2020). Many major weather- and climate- related catastrophes are inherently of a compound nature. For example, the widespread wildfires can be related to the co-occurrence of the extremely dry and hot conditions (Witte et al., 2011). The compounding of storm surge and precipitation extremes can cause coastal floods (Wahl et al., 2015).

Precipitation and heat extremes can occur in close succession due to abnormal climate conditions (Liao et al., 2021). Recent years have seen a more frequent occurrence of such compound events and their frequency and magnitude are projected to increase in the future due to both global warming and human activities (Seneviratne et al., 2021).

1.2. Interplay between Different Hazards and its Economic Implications

The compound events attributable to multiple hazards can cause devastating impacts at a scale well beyond that resulting from any one of these hazards in isolation (Hao and Singh, 2020). This is because the overlapping hazards can exceed the coping capacity of a system more quickly (Zscheischler et al., 2020). More interdisciplinary, cross-sectoral risk assessments are needed to capture the interactions between individual and interrelated hazards and address the trade-offs between sectors at different scales under a range of scenarios (Phillips et al., 2020).

An emerging body of research discovers that the collision between pandemic and natural hazards often puts governments into a dilemma where the goals for disaster relief and pandemic containment conflict with each other. On the one hand, standard mitigation strategies, such as mass sheltering and population evacuation, increase the risk of viral transmission by moving large groups of people and gathering them close together (Salas et al., 2020). On the other hand, strict measures to prevent viral transmission can result in inadequate response towards natural disasters (Ishiwatari et al., 2020) and constrain the economic flows required by post-disaster recovery, aggravating the disaster impacts. Swaisgood (2020) suggested that the economic consequences of such compound events are underestimated if the interplay between individual hazards is not considered. Similar perspectives are proven by Dunz et al. (2021), who found that non-linear dynamics that amplify the economic losses emerge

when COVID-19 and extreme weather events compound within an economy.

The pandemic and natural hazards can also intertwine with other social or economic risk factors, leading to complex situations. Some have argued that the COVID-19 pandemic and climate change have further fuelled the process of deglobalization by reinforcing concerns about unstable global supply chains (Abdal and Ferreira, 2021; Irwin, 2020; Shahid, 2020; Sneader and Lund, 2020). A number of countries have responded by introducing export restrictions on critical medical equipment and food and even on vaccines during the COVID-19 pandemic (Eaton, 2021; Espitia et al., 2020). Extreme weather shocks also have profound impacts on production and trade, especially in agriculture and developing countries, by either damaging trade-related transport and logistics infrastructure or generating shortage of supply in critical goods and services, i.e., food, medicines, and emergency workers (Brenton and Chemutai, 2021). These effects are compounded with amplifying adverse economic impacts if the restrictive trade policy measures undermine the efforts of countries simultaneously battling natural and pandemic crises (Hu et al., 2021; Mahul and Signer, 2020).

Even for simple scenarios compounded by merely multiple natural or climatic hazards, the interrelation between the occurring extreme events may still overwhelm the systems and aggravate the negative impacts (Ridder et al., 2020). Taking the sequential flood-heat extremes in Japan in the summer of 2018 as an example, heavy rains left many people without electrical power during a record-breaking heatwave, which killed more than 1000 people (Imada et al., 2019). Zeng and Guan (2020) also investigated the economic impacts of a hypothetical two-flood event. They found that the subsequent flood may disrupt the recovery of capital damaged by the first flood if the two events hit the economy in close succession. The total economic impacts of such a compound flood exceed the sum of the economic impacts of each individual flood due to the interplay between each flood during the economic recovery.

Growing evidence indicates that compound events usually affect and interweave numerous dimensions of social life and can be perceived as mixtures of exogenous shocks to the economic dynamics. They require a different way of accounting for the cumulative hazard impacts to the affected systems. There is increasing literature calling for an integrated approach to analyse the interaction between individual and interrelated hazards, so as to ascertain the potential impacts cascading across sectors and regions, as well as to inform advanced preparedness for future risks in complex situations (Kruczkiewicz et al., 2021; Mahul and Signer, 2020; Phillips et al., 2020).

1.3. Economic Impact Assessment for Disaster Events

Mitigating disaster economic impacts has long been one of the major targets of global disaster risk prevention and reduction. The Sendai Framework for Disaster Risk Reduction 2015-2030, which was adopted at the Third UN World Conference, underscored the importance of systematically evaluating the disaster economic impacts in understanding disaster risks and guiding disaster-resilient investments (UNISDR, 2015).

Consistent with the goal of the Sendai Framework, countries and international institutions have developed disaster loss assessment systems, such as the HAZUS model developed by the Federal Emergency Management Agency in the United States (FEMA, 2009), the EMA-DLA system developed by the Emergency Management Australia (EMA, 2002), the DaLA system developed by the World Bank (Jovel and Mudahar, 2010), etc., to facilitate disaster risk management. In addition, global disaster databases, such as EM-DAT, NatCatSERVICE, and SIGMA, developed by insurance companies or research institutes, have also become valuable tools for tracking disaster impacts (Mazhin et al., 2021).

Current assessment systems and tools usually measure or report two categories of economic impacts, that is, direct and indirect ones, resulting from disasters. The direct economic impacts refer to damages to humans, physical assets (e.g., buildings and infrastructure), and any other elements due to direct contact with disasters, relating directly in space and time to the disaster events (de Moel et al., 2015; Merz et al., 2010); while the indirect economic impacts are the subsequent changes in economic activities induced by direct ones, including the business interruption of affected economic sectors and regions, the spread of these impacts towards other initially non-affected sectors and regions, and the costs of recovery processes. They often occur, in space or time, after or outside the disaster events. Positive spillover effects may occur due to the substitution of production and the demand for reconstruction (Koks and Thissen, 2016). The indirect impacts of a disruptive event are more likely to be ignored in many cases. Most global disaster databases, for instance, only present the direct damage to human lives and physical properties induced by disasters. The disaster loss accounting system in China has not considered the indirect impacts of disasters to the economic system yet (Wang and Zhou, 2018). This may be related to the fact that the indirect impacts are intangible and hard to be traced. Nonetheless, the indirect impacts could account for a large proportion of the total impacts of a disaster event due to the close inter-sectoral linkages within the economic network (Oosterhaven and Többen, 2017). In particular, more industrialized countries tend to suffer severer indirect impacts than less industrialized ones, in spite of being less vulnerable to direct shocks (Mendoza-Tinoco et al., 2020). The uneven distribution of disaster impacts among nations or economies makes it important to enhance the understanding of the full economic consequences of disaster events, which requires a reliable and systematic assessment tool to capture both the direct and indirect impacts.

To reduce the uncertainty and increase the quality of disaster economic impact metrics,

it is necessary to develop common protocols or methods for impact assessment applicable to various scenarios across countries (Wirtz et al., 2014). Fortunately, the assessment of direct impacts has been developed to a comparatively mature degree, which combines primary data collection with computational models. It usually follows a standard procedure of field investigation to collect primary loss data on people affected, property loss, infrastructure damage, economic sector damage, etc. Catastrophe models, which interprets hazard characteristics into damage to exposed people and property according to a set of hazard-specific vulnerability curves or functions, are also adopted to supplement direct loss information (Botzen et al., 2019). By contrast, however, the assessment of indirect impacts is more challenging due to the complexity inherent in the macro-economic system and a unified methodological framework has not been well established yet. The most commonly used methods for indirect impact quantification include the Input-Output (IO) models (Jonkman et al., 2008; van der Veen and Logtmeijer, 2005), the Computable General Equilibrium (CGE) models (Carrera et al., 2015; Rose and Liao, 2005), and their hybrids, such as the ARIO model (Hallegatte, 2008, 2014) and the MRIA model (Koks and Thissen, 2016; Koks et al., 2019). These models use direct disaster impacts as input variables and simulate the cascading impacts of the initial disaster shock through interdependencies between sectors and regions within an economy. Yet, they vary in the assumptions about market flexibility and product substitutability, and thus fit for different temporal scales and yield different estimates on the indirect economic impacts of a disaster (Koks et al., 2016).

Many studies have focused on assessing the economic impacts of climate extremes (Hallegatte, 2008, 2014; Koks et al., 2015; Koks and Thissen, 2016; Lenzen et al., 2019; Mendoza-Tinoco et al., 2020; Oosterhaven and Többen, 2017; Willner et al., 2018; Xia, Li, et al., 2018; Zeng et al., 2019), and unsurprisingly research on biological hazards such as the COVID-19 pandemic is still new (Guan et al., 2020; McKibbin

and Fernando, 2020; Porsse et al., 2020), and even fewer studies have looked into the economic consequences of compound events (Dunz et al., 2021; Zeng and Guan, 2020). A consistent metric that bridges the economic impact assessment from single-hazard to compound-hazard events is still lacking. Mendoza-Tinoco et al. (2017) developed the concept of 'flood footprint' to summarize the total economic impacts that is directly and indirectly caused by a flood event in the region and the wider economic system. Later Zeng and Guan (2020) applied this concept for the assessment of a hypothetical two-flood event. This thesis extends the concept of 'flood footprint' to 'disaster footprint' to describe the compound economic impacts of a multi-disaster mix comprising of different hazard types. This concept emphasizes the economic footprint of an exogenous shock that propagates through the supply chain from one sector to another and one region to another within the economic network, as well as the recovery dynamics of the affected economic system in the disaster aftermath. The adoption of this concept could provide a consistent and comparable impact indicator between single-hazard and compound-hazard events and lay the foundation for further economic impact assessment in complex situations.

1.4. Research Questions and Objectives

1.4.1. Research Gaps and Questions

As compound hazards become more frequent and intense due to climate change and human influences, integrated solutions are in urgent need to mitigate their potential economic impacts. However, current impact assessment is usually performed for a single hazard at a time and not able to reflect on the interaction between hazards of different types. An emerging body of literature has started to rethink about risk governance or resilience building in the context of compound hazards. However, much of this literature is limited to qualitative analysis (Kruczkiewicz et al., 2021; Mahul and Signer, 2020; Phillips et al., 2020). Increasing the resilience of an economy also

means reducing the economic impacts of various types of hazards (Hammond et al., 2015; Oosterhaven and Többen, 2017). However, a systematic quantitative assessment of the economic impacts for compound hazards is still lacking.

Given the current research gaps, this PhD thesis analyses the methodological evolution from single-hazard to compound-hazard economic impact assessment with an attempt to address the following primary research aim:

"How to measure the economic impacts of a compound hazard cascading through the production supply chains?"

In relation to this primary research aim are four research questions (RQs):

RQ1) What are the unique characteristics of a compound hazard in terms of disrupting the production supply chains?

RQ2) What is the most suitable framework applied to assess the economic impacts of a traditionally single hazard considering supply chain effects?

RQ3) How to incorporate the characteristics of a compound hazard into this framework, which is previously intended for a single hazard, in order to properly assess the compound impacts?

RQ4) How to evaluate the relevant factors that may influence the economic resilience towards such a compound hazard?

1.4.2. Research Objectives and Contributions

To address these research questions, this thesis aims to develop a robust model for the economic impact assessment of compound hazards, which are combinations of multiple individual hazards categorised into biological, environmental, geological, hydrometeorological, technological and other types (UNISDR, 2017). The model will adopt the concept of 'disaster footprint' to provide a consistent metric with traditional single-hazard assessment, allowing for further comparative analysis. It will also be

modularized with flexibility to adapt to the needs of various compound hazard scenarios. The specific research objectives (ROs) are:

RO1) To unlock the interplay between concurrent hazards, either of similar or different types, in terms of their economic impacts and risk transmission channels within the economic system. *This contributes to RQ1 and is discussed in Chapter 1.*

RO2) To present a systematic review of the existing literature on the assessment of both direct and indirect economic impacts resulting from natural and manmade disasters, as well as the potential risks arising from compound hazards. *This contributes to RQ2 and is discussed in Chapter 2.*

RO3) To improve the traditional methods of accounting for the hazard-induced indirect economic impacts from the perspectives of supply chain cascading effects. *This contributes to RQ2 and is discussed in Chapter 3.*

RO4) To construct a methodological framework to assess the economic footprint of compound hazards, which is evolved from an improved single-hazard assessment framework. *This contributes to RQ3 and is discussed in Chapter 3.*

RO5) To apply the models developed in this thesis to both individual and compound hazards of various types and test their robustness under a range of past or projected and hypothetical or real hazard scenarios. *This contributes to RQs2, 3 and is discussed in Chapter 4 to Chapter 7.*

RO6) To explore factors that may influence the compound resilience of the economic system and offer suggestions on the response and recovery strategies for policy makers to mitigate the disaster impacts. *This contributes to RQ4 and is discussed in Chapter 6 to Chapter 8.*

By fulfilling the above objectives, this thesis could be a meaningful first step to embed multiple hazards within an economic risk assessment framework that accounts for both direct and indirect disaster footprint with sectoral and regional details. The modelling process can be generalized to the impact assessment of a wide variety of individual or

compound hazards, pushing the boundaries of applications and knowledge in relevant fields. The results will convey useful information on the total economic costs that can be saved from active risk reduction and adaptation strategies, as well as where bottlenecks can occur in the economy after a compound event and where to prioritize recovery funds. All these information will inform policies and investment in compound risk mitigation and compound resilience enhancement and eventually contribute to the formation of an integrated risk governance in advanced preparedness for future risks. This is important to achieving the targets of the Sendai Framework for Disaster Risk Reduction, which explicitly calls for a multi-hazard and multi-sectoral approach to increase the efficiency and effectiveness of disaster risk reduction practices (UNISDR, 2015).

1.5. Research Framework and Outline

A disaster event, emanating from either a single hazardous factor or compound hazardous factors, can cause direct and indirect impacts to the economic system. To assess its full economic footprint, a four-stage research framework is proposed in this thesis, as shown in Figure 1-1.

- **Step 1. Direct economic footprint assessment for individual hazards**

The first step aims to assess the direct economic footprint of individual hazards, with a special focus on that of flooding, heat stress, and air pollution. Hazard-specific catastrophe models are used, together with high-resolution land cover maps and demographic information, to interpret physical characteristics of these hazards into property damage or health impairment. Detailed methods can be referred to Section 3.1.1. This step eventually calculates the hazard-induced changes in the supply of two important primary production factors, i.e., labours and capital, by economic sectors.

- **Step 2. Indirect economic footprint assessment for individual hazards**

The second step explores how the direct shocks of individual hazards disrupt economic relations and propagate across sectors through the supply chain, hence the indirect economic footprint. Changes in labour and capital supplies, which are directly caused by the hazards, are fed into an IO-based hybrid economic model (i.e., the disaster footprint model) to simulate the risk transmission and economic recovery dynamics during and after the disruptive event. The disaster footprint model is extended from previous models by incorporating inventory adjustment and cross-regional substitutability. A detailed description of the methods can be found in Section 3.1.2. Changes in the production of economic sectors, relative to the pre-disaster levels, are accumulated over time in the disaster aftermath, indicating the ultimate size of indirect economic footprint resulting from the occurring hazards.

- **Step 3. Compound hazard economic footprint assessment**

The third step combines the methods of the previous two steps and extends the economic footprint assessment to compound hazards in the triple context of climate change, pandemic, and deglobalisation. The interaction between natural hazards, disease control, and trade frictions regarding their economic impacts and risk transmission channels within the economic system are carefully investigated and integrated into the Compound-Hazard Economic Footprint Assessment (CHEFA) model. The model is developed in Section 3.2 to assess the full economic footprint of compound events.

- **Step 4. Response and recovery planning formulation**

The final step intends to offer suggestions on favourable response and recovery plans to reduce the disaster-induced economic impacts, i.e., increase the economic resilience. Scenarios are built for disaster footprint analysis when hazardous events with different durations and magnitudes collide on different spatial and temporal scales. Sensitivity

analyses on modelling parameters, such as the duration and strictness of lockdowns, the labour and transportation recovery rates, the degrees of export restrictions, the inventory sizes, overproduction characteristics, external funds and subsidies, etc., are also conducted to recognize the crucial factors that influencing the disaster footprint or economic resilience. By unveiling how disaster footprint, at sectoral and regional levels, are related to some of the response and recovery characteristics under wide ranging scenarios, stakeholders or policy makers can draw useful information to act better in future risk mitigation and adaptation.

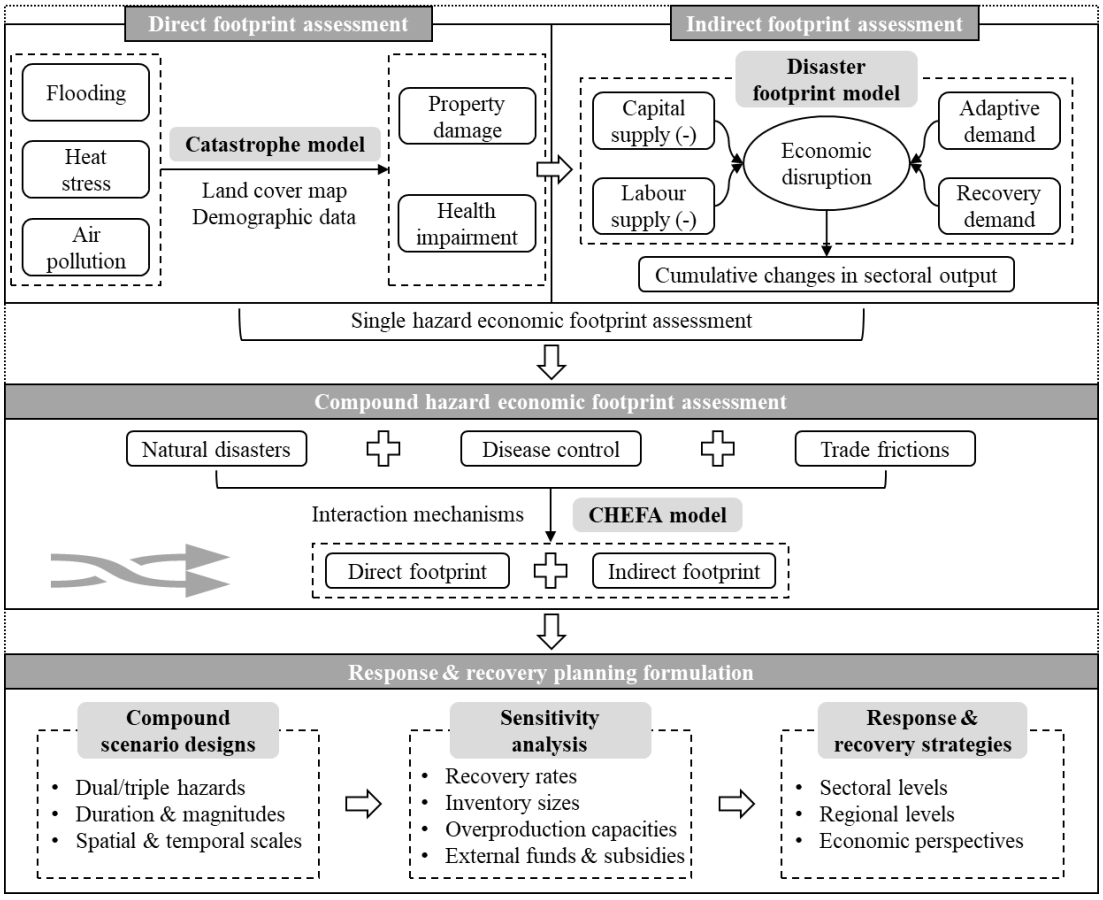

Figure 1-1: Research framework of economic footprint assessment for both individual and compound hazards.

The outline of this thesis is organized in accordance with the proposed framework and divided into 8 chapters.

Chapter 1 gives a brief introduction of this thesis' research background with a special focus on the potential interplay between multiple hazards and their compound economic implications *(RQ1 and RO1)*. This chapter highlights the necessity to study the economic impacts of compound hazards, identifies the research gaps, questions, and objectives, and sets out the research framework and outline.

Chapter 2 presents an overview of current literature on modelling economic impacts of natural or manmade disasters, as well as an emerging concern for the increasing likelihood of compound hazards *(RQ2 and RO2)*. The basic concepts of compound hazards and disaster footprint are clarified in this chapter to underpin the research scope of this thesis. This is followed by an appraisal of the mainstream economic models commonly used for traditional hazard analysis, alongside their applications and validations. In the end, this chapter specifically summarizes the progress in compound hazard analysis and thereafter identifies the research gaps to be filled.

Chapter 3 describes the methodology developed in this thesis to assess the comprehensive economic impacts resulting from individual or compound hazards *(RQs2, 3 and ROs3, 4)*. It starts with a methodological review for both direct and indirect economic impact assessment. The former is notably focused on three types of natural or manmade hazards, that is, flooding, heat stress and air pollution, and the latter introduces the fundamentals of the IO analysis and its development in disaster impact assessment. Built on the contributions of previous models, the Disaster Footprint model and the CHEFA model are constructed respectively for single- and compound-hazard impact analysis. The interactions between diverse hazards are integrated into the analysis from an economic perspective, linking the theoretical basis between the two models.

Chapter 4 and Chapter 5 demonstrate the proposed Disaster Footprint model in single-

hazard analysis for past and projected cases *(RQ2 and RO5)*. In particular, Chapter 4 focuses on the economic footprint of heat stress, air pollution, and extreme weather events in China over the past decades. The analysis is performed both on the national and provincial scales. Chapter 5 projected the economic consequences of future fluvial flood hazards in six vulnerable countries (i.e., Brazil, China, India, Egypt, Ethiopia, and Ghana) around the end of the 21st century. Scenarios are designed by combining climate change and socio-economic development to capture the long-term trend of river flood risks in the six countries.

Chapter 6 and Chapter 7 illustrate the proposed CHEFA model in compound-hazard analysis for hypothetical and real cases *(RQs3, 4 and ROs5, 6)*. Chapter 6 simulates the economic footprint of a hypothetical perfect storm comprising of flooding, pandemic control, and trade restrictions in a hypothetical global economy. Scenarios involve hazardous events with various duration and magnitudes co-occurring at different timings and places, demonstrating the modelling process of the CHEFA model. In addition, extensive sensitivity analyses for key model parameters are conducted to test the robustness and flexibility of the model. Then in Chapter 7, the CHEFA model is applied to a real compound event of extreme floods and COVID-19 control striking the Zhengzhou city in central China in 2021. The study is performed at multiregional levels to track down the economic footprint rippling across the nation. Economic and policy factors that significantly influence the post-event recovery and resilience are identified through the sensitivity analysis approach.

Chapter 8 summarises the main findings of this thesis and draws policy implications *(RO6)*. Contributions and limitations of this work are also discussed, and ideas concerning future work are then put forward accordingly.

The disaster footprint model in Chapter 3 and its applications in Chapter 4 were

integrated to parts of the 2020-2022 China reports of the Lancet Countdown on health and climate change. The reports have been published online by the journal of *The Lancet Public Health* at https://doi.org/10.1016/s2468-2667(22)00224-9, https://doi.org/10.1016/S2468-2667(20)30256-5, and https://doi.org/10.1016/S2468-2667(21)00209-7. The author of this PhD thesis contributed 3 (out of 27) indicators on the economic impacts of heat stress, air pollution, and climate-related extreme events to each report. Another application of the disaster footprint model in Chapter 5 has been published by the journal of *Climatic Change* and available at https://doi.org/10.1007/s10584-021-03059-3. The thesis author is one of the two co-first authors of this journal paper by contributing to the indirect impact modelling, result interpretation and drafting.

The CHEFA model developed in Chapter 3 and its illustration for a hypothetical compound event in Chapter 6 were parts of the work program of the World Bank on trade and climate change, which were later integrated into a journal paper submitted to *Risk Analysis* and under the 2nd round of review. Its application to a real case in China in Chapter 7 has been published in the *China Journal of Econometrics* and available at https://www.cjoe.ac.cn/CN/10.12012/CJoE2021-0090. This thesis author claims the lead authorship for both papers with over 90% of the contribution by study design, data collection, impact modelling, result interpretation and drafting.

The thesis author acknowledges all the contribution made by the co-authors and supervisors of the publications covered in this PhD thesis.

Chapter 2 Literature Review

Chapter 2 offers a critical review of the existing literature related to the research topic of this PhD thesis. It is divided into four sections. Section 2.1 introduces the basic concepts of compound hazards and disaster footprint, clarifying the research scope of this thesis. This is followed by an appraisal of the mainstream economic models commonly used for traditional hazard analysis, alongside their applications and validations, in Section 2.2. Advances and limitations are evaluated for each of the modelling techniques and then the appropriate methodological framework for this thesis' research objectives is determined. Section 2.3 discusses the emerging concerns for compound hazards and their mixed impacts to human society, especially to the economic system. After summarizing the research progress in relevant fields, this chapter ends with an analysis of the research gaps to be filled by the following parts of this thesis in Section 2.4.

2.1. Key Definitions

2.1.1. Compound Hazards

2.1.1.1. What is a hazard?

The United Nations Offices for Disaster Risk Reduction (UNISDR) defines a hazard as "a process, phenomenon or human activity that may cause loss of life, injury or other health impacts, property damage, social and economic disruption or environmental degradation" (UNISDR, 2017, https://www.undrr.org/terminology/hazard). It may arise from a natural or anthropogenic factor or be associated with a combination of natural and anthropogenic origins (ibid.). According to the type of factor that triggers a hazard, UNISDR classifies hazards into five categories. That is, biological, environmental, geological, hydrometeorological, and technological hazards. Table 2-1 presents some

examples of these hazard types.

Table 2-1: Examples of hazards according to their categories.

Hazard types	Examples
Biological	Bacteria, viruses, parasites, venomous wildlife and insects, poisonous plants, mosquitoes carrying disease-causing agents, etc.
Environmental	Soil degradation, deforestation, loss of biodiversity, salinization, sea-level rise, air pollution, etc.
Geological	Earthquakes, volcanic activity and emissions, mass movements, landslides, etc.
Hydrometeorological	Tropical cyclones, floods, drought, heatwaves, cold spells, coastal storm surges, etc.
Technological	Industrial pollution, nuclear radiation, toxic wastes, transport accidents, factory explosions, fires, etc.
Political	Pandemic lockdowns, trade wars, military confrontations, etc.

Notes: Examples of the upper five hazard types are summarized from the UNISDR website (https://www.undrr.org/terminology/hazard). The political hazard is added here to include pandemic lockdowns, trade restrictions, etc., which is an additional hazard type compared to the UNISDR classification.

On a broader scale, there is another type of hazards - political hazards - in addition to the above five hazard types. Political hazards usually stem from factors related to policy instability or geopolitical tensions. For instance, the lockdown measures to contain virus transmission could severely disrupt productive activities and lead to extensive economic impacts (Guan et al., 2020). Other examples are trade wars and even military confrontations (including terrorist attacks) between nations or regions, which may ultimately cause terrible humanitarian crises and paralyze the economies at risk (Itakura, 2020; Pant, 2022).

Several hazardous events can lead to a disaster, which is “a serious disruption of the functioning of a community or a society at any scale due to hazardous events interacting with conditions of exposure, vulnerability and capacity, leading to one or more of the following: human, material, economic and environmental losses and impacts” (UNISDR, 2017, https://www.undrr.org/terminology/hazard). It can be inferred,

by definitions, that the consequences of a disaster are more severe than a hazard. Despite the differences in severity, hazards and disasters are essentially disruptive events that have manifold negative impacts to the human society. As this thesis evaluates these events from an economic perspective, the hazards hereinafter cover all kinds of disruptive events causing negative shocks to the economic system.

2.1.1.2. What are compound hazards?

Hazards may be single, sequential, or combined in their origin and effects. For example, during the 2017 Atlantic Hurricane Season, Hurricane Harvey, Irma, and Maria hit successively the southeast coastal line of the United States within a month. Simultaneously, devastating wildfires in California have been burning for months[2]. UNISDR (2017) uses the term 'multi-hazard' to define "(1) the selection of multiple major hazards that the country faces, and (2) the specific contexts where hazardous events may occur simultaneously, cascadingly, or cumulatively over time, and taking into account the potential interrelated effects" (UNISDR, 2017, https://www.undrr.org/terminology/hazard).

Although 'multi-hazard' describes the co-occurrence of multiple hazardous events, another term 'compound event' has become more popular in climate research for underscoring the compound or combined effects of multiple hazards. The concept of compound events was first introduced in the Intergovernmental Panel on Climate Change (IPCC) special report on climate extremes to briefly describe "(1) two or more extreme events occurring simultaneously or successively, (2) combinations of extreme events with underlying conditions that amplify the impact of the events, or (3) combinations of events that are not themselves extremes but lead to an extreme event or impact when combined" (Seneviratne et al., 2012, p. 118)(IPCC, 2012). The

[2] Source: https://www.ncei.noaa.gov/access/monitoring/monthly-report/national/201713 (accessed on 30 May 2022).

contributing events can be of similar (clustered multiple events) or different type(s). Leonard et al. (2014, p. 115) further developed a more general notion of compound events as "an extreme impact that depends on multiple statistically dependent variables or events". This concept refers only to extreme-impact events with dependent drivers. Zscheischler et al. (2018, p. 470) ultimately formalized the definition of compound events as "the combination of multiple drivers and/or hazards that contribute to societal or environmental risk". This definition highlights that compound events may not necessarily result from dependent drivers and has been embedded within the latest risk framework by the 6th Assessment Report (AR6) of IPCC (Seneviratne et al., 2021).

Zscheischler et al. (2020) classified compound events into four types: (1) preconditioned, where a weather-driven or climate-driven precondition aggravates the impacts of a hazard; (2) multivariate, where multiple drivers and/or hazards lead to an impact; (3) temporally compounding, where a succession of hazards leads to an impact; and (4) spatially compounding, where hazards in multiple connected locations cause an aggregated impact. Table 2-2 lists some examples of compound events according to these four categories.

Table 2-2: Examples of compound events according to their categories.

Types of compound events	Examples
Preconditioned	Heavy precipitation on saturated soil, rain on snow, False spring, etc.
Multivariate	Compound flooding, compound drought and heat, humid heatwave, compound precipitation and wind extremes, etc.
Temporally compounding	Temporal clustering of precipitation events, temporal clustering of storms, sequences of heatwaves, etc.
Spatially compounding	Spatially concurrent precipitation extremes/floods at regional scale, spatially co-occurring climate extremes at global scale, etc.

Notes: summarised from Zscheischler et al. (2020).

Current definitions of compound events are mainly focused on climatic hazards. It was

not until the unprecedent COVID-19 pandemic prevails the world that researchers started to consider incorporating biological hazards into the compound event framework (Collins et al., 2021; Phillips et al., 2020; Shen et al., 2021). In addition, political hazards, such as trade wars and deglobalisation, can also be compounded in a hazard mix to generate convoluted economic consequences (Brenton and Chemutai, 2021; Hu et al., 2021). Yet there has not been a standard term for the combination of hazards beyond the climatic context. This thesis extends the concept of 'compound event' to 'compound hazard' to describe "the compounding of multiple hazards, in a wide range beyond climatic hazards, that causes interconnected shocks to the economic system".

2.1.2. Disaster Footprint

Hazardous events can cause massive socio-economic costs directly to the affected regions. For instance, in 2021, twenty weather/climate extreme events with direct costs exceeding $1 billion each were sustained in the United States. The total direct costs of these events were estimated at $148 billion with 724 deaths[3]. Examples of direct impacts include (tangible) physical damage to residential, commercial, and municipal buildings; productive capital; transport and electrical infrastructure; agricultural assets including crops and livestock; as well as intangible damage to human health and work productivity or capacity[4].

These tangible and intangible direct impacts resulting from hazards can lead to indirect economic impacts that propagate through the production supply chain to other initially non-affected sectors and regions (Botzen et al., 2019; Koks and Thissen, 2016). These

[3] Source of data: NOAA National Centres for Environmental Information (NCEI). (2022). U.S. Billion-Dollar Weather and Climate Disaster. https://www.ncei.noaa.gov/access/billions/, DOI: 10.25921/stkw-7w73.

[4] This thesis classifies hazard-related health impairment (e.g., casualties, mortality, or morbidity) and work productivity loss as intangible direct impacts because they are due to direct exposure to hazardous factors (e.g., extreme heat and air pollution) by population at risk or workers in the workplace.

indirect impacts include interruption losses of economic activities, costs of recovery processes, and any positive spillover effects due to the substitution of production and the demand for reconstruction. The indirect impacts may sometimes account for a large proportion of the total impacts during a hazard and its aftermath. For example, the indirect losses caused by the 2009 Central European flood event were estimated to reach 65% of the total economic impacts (Mendoza-Tinoco et al., 2020). Similarly, the cascading effects amplified the flood losses by up to 1.97 times during the 2013 heavy flooding in Germany (Oosterhaven and Többen, 2017).

Mendoza-Tinoco et al. (2017) proposed the concept of 'flood footprint' to integrate the direct and indirect economic impacts of a flood event in the affected region and wider economic systems. The direct 'flood footprint' is the economic impacts caused by direct contacts or exposure to flood events and refers to the short-term impacts on natural resources, human health, and tangible assets. It interprets the flood-induced direct damage into productive factor loss from the economic perspective. The indirect 'flood footprint' is the economic impacts resulting from supply shortage of productive factors (i.e., labour or capital loss), disruptions of economic activities along the production supply chain, and costs for physical capital reconstruction. It captures both short- and long-term changes in economic activities at sectoral and regional levels during the hazard and its aftermath. The concept of 'flood footprint' results especially relevant for the objective to provide differentiated information between direct and indirect impacts, considering the source of impacts in productive factors. It is not purely a measurement of the total economic impacts of a flood, but also describes the flow of impacts across economic sectors and regions, as well as the recovery dynamics over time (Mendoza-Tinoco et al., 2020). The concept was further developed by Zeng et al. (2019) to incorporate the roles of post-flood recovery management and process monitoring, and eventually extended to accommodate the compound event of sequencing floods (Zeng and Guan, 2020). Similar to the 'flood footprint', this thesis

adopts ‘disaster footprint’ to characterize the flow of economic impacts that are directly and indirectly caused by diverse hazards beyond flooding, as well as the recovery dynamics in the disaster aftermath.

‘Footprint’ is a concept commonly used in studies on human-nature relationships (Hoekstra and Hung, 2002; Rees, 1992; Wiedmann and Minx, 2008). It is first used in the concept of ecological footprint (Rees, 1992), which is most widely known in the field of ecological economics. It measures the total impacts of human activities, like the production of a car, on the Earth’s ecosystem. It involves the whole lifecycle of the product, not just the product itself, but also materials that it needs during the production. This concept is followed by carbon footprint (Wright et al., 2011), and water footprint (Hoekstra et al., 2011). They refer to the total amount of carbon/water that are emitted or consumed along the entire processes of production activities. Like car production, it considers processes from the production of each part of the car, to the transportation, and to the assembly processes. All these concepts evaluate the impacts of human activities on the natural environment and eco-systems. By contrast, ‘disaster footprint’ looks in the reverse direction from nature to humans. As mentioned above, this concept demonstrates a dynamic process, and thus is suitable for describing the dynamics of economic disruption and recovery during a certain affected period. ‘Disaster footprint’ is an ideal concept to describe how the impact of a single or compound hazard spreads across economic sectors, how it evolves over the time of economic recovery, and how it spills over to other economically interrelated regions. It is aimed to reveal the total economic costs that could be saved if governments take active disaster risk reduction and adaptation strategies, which is vital for decision planning.

2.2. Conventional Methods for Hazard Impact Analysis

Efforts have been made, in the engineering and economic communities, to analyse the

direct and indirect impacts resulting from hazardous events, but each of them is often focused on a single hazard at a time. One of the common approaches for hazard impact analysis relies on primary data collection (Zeng, 2018). Although this method is good at providing direct or immediate damage information on human lives and physical assets, it can hardly present a full picture of the indirect or intangible impacts to the economic system. Moreover, the hazard impacts are not always well-recorded due to the lack of effective observations on historically low-probability hazards (Botzen et al., 2019). Therefore, computational models are developed to account for the potential hazard impacts. Direct impacts are usually estimated using the so-called catastrophe models, which are specific to hazard types; while indirect impact assessment is often based on a macroeconomic modelling framework, such as IO and CGE models. On top of that, econometric models are also used to provide empirical findings on the economic impacts of hazardous events, which can sometimes complement the simulating results from computational models.

2.2.1. Catastrophe Models for Direct Impact Assessment

2.2.1.1. Methods and Applications

Catastrophe models refer to a class of models that relate the physical characteristics of a hazard to the expected damage to the exposed population or property according to specific vulnerability curves or functions (ibid.). The development of a catastrophe model is highly dependent on the type of the targeted hazard, as each hazard type has quite distinct physical characteristics and impacting mechanisms. According to the time scale of a hazard influencing the human society, hazards can be divided into two categories, that is, rapid and slow onset hazards (Nelson, 2018). The former hazards develop with little warning and strike rapidly, such as flash floods, hurricanes, earthquakes, etc; while the latter hazards take longer times to develop, such as droughts, heatwaves, air pollution, disease epidemics, etc. Rapid onset hazards usually generate substantial damage to physical assets, such as buildings, roads, and bridges, and hence

the main target of their impact assessment (Charvet et al., 2017; de Ruiter et al., 2017; Merz et al., 2010). By contrast, slow onset hazards tend to cause relatively persistent impacts on human health and little damage to physical capital, and thus their impact assessment is generally focused on health impairment and related labour productivity loss[5] (Burnett et al., 2014; Walker Patrick et al., 2020; Zhao, Lee, et al., 2021). In an economic system, physical and human assets usually constitute the main sources of two important production factors, namely capital and labour, respectively. Therefore, rapid and slow onset hazards can also be referred to as capital- and labour-shocked hazards, respectively, according to the type of production factors initially affected by hazards. The difference in the initial hazard shocks would inevitably require distinct methodology for direct impact assessment.

Table 2-3 presents an overview of specific methods or models for estimating the direct impacts of hazards, as well as existing applications or examples.

For flood hazards, direct damage is commonly calculated by depth-damage functions, which relates flood depth to the resulting monetary damage of the submerged/exposed building- or land-use type (de Moel et al., 2015; Jongman, Kreibich, et al., 2012). Sometimes other flood characteristics, such as flow velocity and duration, are added (FEMA, 2009; Kreibich et al., 2010; Zhai et al., 2005). The damage can be expressed as either a percentage of a pre-defined maximum damage value (relative damage), or absolute monetary value (absolute damage). Applications are mostly from the local to national scale, including the FLEMO model for Germany (Kreibich et al., 2010), the Damage Scanner model for the Netherlands (Klijn et al., 2007), the HAZUS-MH Flood model for the US (FEMA, 2009), and the Multi-Coloured Manual (MCM) for the UK (Penning-Rowsell et al., 2013). Recently, a globally consistent database of

[5] Labour or work productivity loss and capacity loss are considered as interchangeable in this thesis, which both refer to the reduction in effective working hours under adverse working conditions.

depth-damage functions has been developed by Huizinga et al. (2017). This database adopted a consistent approach to develop a set of relative depth-damage curves for each continent and maximum damage values for each country. It also incorporated a wider range of building- or land-use types, including residential, commercial, and industrial buildings, and transport, infrastructure (roads), and agriculture use of land. Such country- and sector-specific functions can greatly advance the development of an integrated modelling framework (Alfieri et al., 2017; Dottori et al., 2018; Yin et al., 2021).

For seismic hazards (e.g., earthquakes), direct damage assessment, which is quite similar with that of flood hazards, traditionally uses fragility or vulnerability curves to translate hazard characteristics such as ground motion intensity into probable damage to a physical or capital asset at risk (Douglas, 2007; Hosseinpour et al., 2021). Fragility and vulnerability curves represent the likelihood of exceeding a certain damage state and the mean damage ratio (also known as loss ratio), respectively, conditioned on a set of seismic motion intensities. The development of fragility or vulnerability functions is generally through empirical, expert judgement, analytical, or hybrid approaches (de Ruiter et al., 2017; Hosseinpour et al., 2021; Kalakonas et al., 2020; Rossetto et al., 2014). Method selection often depends on the quality of available data, expert's knowledge, and the research scope (Hosseinpour et al., 2021). Like flood hazards, most of seismic loss estimation is conducted for a specific region considering their own seismotectonic settings and construction practices (ibid.). These include the HAZUS Earthquake model for the US (Kircher et al., 2006), SELENA for Norway (Molina and Lindholm, 2005), EQRM for Australia (Robinson et al., 2007), and InaSAFE for Indonesia (AIFDR, 2022). Beyond the regional scale, a global modelling tool named OpenQuake has been collaboratively developed as a part of the Global Earthquake Model (GEM) project aiming to establish uniform and open standards for calculating and communicating earthquake risk worldwide (Silva et al., 2014).

For heat-related hazards (e.g., heat stress), direct impacts intangibly occur to human assets rather than capital assets, which is different from the above two hazard types, mainly by causing health impairment and labour productivity loss (Orlov et al., 2020). Epidemiological studies confirmed that excessive heat exposure increases the mortality and morbidity rates of certain diseases, such as cardiovascular and respiratory diseases (Basu and Samet, 2002; Turner et al., 2012). Nonlinear or linear exposure-response functions (ERFs) have been constructed to account for the heat-induced mortality (Curriero, 2002; Honda et al., 2014; Yang et al., 2019) and morbidity (Bayentin et al., 2010; Liang et al., 2008). These ERFs typically estimate the relative risk (RR), which is represented by excess deaths or hospital admissions in mortality or morbidity assessment respectively, during days with extreme temperature compared to days with normal temperature. Such heat-induced health impairment is often translated into a type of direct economic costs by calculating the monetised value of Years of Life Lost (YLL) based on the estimated Value of Statistical Life (VSL) (OECD, 2012).

Beyond those, studies also found apparent declines in work productivity (also known as workability) among employees under heat stress (Kjellstrom et al., 2009). Yet, little attention has been given to this type of heat-related direct impacts until recently. A novel ERF was derived by Kjellstrom et al. (2018) and further used in studies of heat stress affecting labour productivity (Bröde et al., 2018; Liu et al., 2021; Orlov et al., 2020). This ERF is also named as the Hothaps function because it is developed for the 'High Occupational Temperature Health and Productivity Suppression' (Hothaps) programme. The Hothaps function is a two-parameter logistic function, which describes the relationship between the heat stress index Wet Bulb Globe Temperature (WBGT) and the Work Loss Factor (WLF, namely the fraction of work hours lost) for three different levels of work intensity (quantified by the metabolic rate). Such heat-induced workability loss would directly reduce the work output and possibly affect

income if workers are paid by the unit produced (Cai et al., 2018). The relevant income loss is then often calculated by the product of total working hours lost and local average hourly wage (Romanello et al., 2021).

For air pollution hazards, which are similar with heat stress as labour-shocked hazards, their direct impacts are typically evaluated by calculating the short-term or long-term excess morbidity and premature mortality induced by air pollution (Atkinson et al., 2014). Fine Particulate Matter ($PM_{2.5}$) is most commonly used as the proxy indicator of exposure to air pollution among other air pollutants including NOx, ozone, carbon monoxide and sulphur dioxide (WHO, 2016). Epidemiological studies on $PM_{2.5}$-induced health outcomes have linked $PM_{2.5}$ concentration levels with various disease endpoints (such as ischemic heart disease, stroke, chronic obstructive pulmonary disease, and lung cancer) using ERFs, and RRs for $PM_{2.5}$-induced mortality, hospital admissions and outpatient visits are derived from them (Burnett et al., 2014; Xia, Guan, et al., 2018; Xu et al., 1995). The collaboration of Global Burden of Disease (GBD) studies, which have been updated to 2019, have developed a standardised framework to estimate the particulate matter risk curves for over 200 countries and territories and selected subnational locations (Murray et al., 2020). These risk curves have been widely used for studies on $PM_{2.5}$-induced adverse health impacts from local to global scales (Hekmatpour and Leslie, 2022; Pandey et al., 2021; Romanello et al., 2021; Zhou et al., 2016).

For epidemic/pandemic hazards, the transmission of a certain virus, such as COVID-19, is commonly simulated by the Susceptible-Exposed-Infected-Recovered (SEIR) model, which divides the disease life cycle into four stages: susceptibility, exposure, infectivity, and recovery (Efimov and Ushirobira, 2021; He et al., 2020; Huang et al., 2021; Keeling et al., 2020; Linka et al., 2020; Walker et al., 2020). The effective reproductive number (R) at each stage and the size of exposed population at the starting

point are key parameters of the model. From these parameters, the daily rates of new infections, hospitalizations, and fatalities are calculated as a time series during the epidemic dynamics. Infection with an epidemic virus can cause a range of health problems, from acute illness to lasting symptoms and even premature deaths. Burden of disease studies usually estimate a disease impact on human health by measuring how many years of life are lost to death and illness from a disease in a single metric called disability-adjusted life years (DALYs) (Cuschieri et al., 2021; Wyper et al., 2021). This metric combines the health outcomes of mortality (translated into estimates of years of life lost (YLL)) and morbidity (translated into estimates of years lived with disability (YLD)) due to a disease to track its direct impacts on the population. Except for health impairment, the non-pharmaceutical interventions (NPIs), such as lockdown restrictions, to contain the spread of the virus can also negatively affect labour mobility, personal income, and household consumption, expanding the direct impacts of the epidemic/pandemic (Bonaccorsi et al., 2020; Martin et al., 2020; Sweeney et al., 2021).

Table 2-3: Direct impact analysis - methods and applications.

Types	Hazards	Specific methods	Model inputs	Model outputs	Examples
Rapid onset (capital-shocked)	Flood	Depth-damage functions	Flood depth, flow velocity, duration	Relative or absolute damage to capital assets	Regional models of FLEMO (Kreibich et al., 2010), Damage Scanner (Klijn et al., 2007), HAZUS-MH Flood (FEMA, 2009), MCM (Penning-Rowsell et al., 2013); a global database by Huizinga et al. (2017)
	Seismic	Fragility or vulnerability curves	Ground motion intensity	Probability of damage or mean damage ratio to capital assets	Regional models of HAZUS Earthquake (Kircher et al., 2006), SELENA (Molina and Lindholm, 2005), EQRM (Robinson et al., 2007), InaSAFE (AIFDR, 2022); a global model of OpenQuake (Silva et al., 2014)
Slow onset (labour-shocked)	Heat stress	ERFs	Ambient temperature; WBGT	Relative or excess risks of mortality and morbidity; fraction of work hours lost	Assessment of heat-induced mortality (Curriero, 2002; Yang et al., 2019), morbidity (Bayentin et al., 2010; Liang et al., 2008), and labour productivity loss (Bröde et al., 2018; Kjellstrom et al., 2018)
	Air pollution	ERFs	Ambient air pollutant concentration	Relative risks of mortality and morbidity	A global dataset of particulate matter risk curves (Global Burden of Disease Collaborative Network, 2021) and its applications from the local scale (Pandey et al., 2021; Zhou et al., 2016) to global scale (Hekmatpour and Leslie, 2022; Romanello et al., 2021)
	Epidemic/pandemic	SEIR models	Effective reproductive number	Daily rates of new infections, hospitalizations, and fatalities	On the subnational scale (He et al., 2020; Huang et al., 2021); on the national scale (Efimov and Ushirobira, 2021; Keeling et al., 2020); on the regional scale (Linka et al., 2020); on the global scale (Walker et al., 2020)

Catastrophe models for various hazards have been developed in different ways pertaining to hazard characteristics. Still, there are some similarities in these models, particularly for hazards within the same group (i.e., capital- or labour-shocked). For capital-shocked hazards, the direct impacts are usually assessed using the fragility or vulnerability curves which relate hazard intensity to physical damage according to land use or building types. For labour-shocked hazards, the direct impacts are typically evaluated by ERFs which link hazard exposure to excess risk of health impairment specific to related diseases or all causes. Numerous studies have applied these catastrophe models to assess the direct impacts of hazards on geographical scales ranging from local to global.

2.2.1.2. Uncertainty and Validation

Uncertainty in hazard (direct) damage assessment is generally associated to three modelling processes: (1) hazard characteristic simulation; (2) exposure assessment; and (3) vulnerability assessment (de Moel and Aerts, 2011; Jongman, Kreibich, et al., 2012; Kalakonas et al., 2020; Merz and Thieken, 2009).

First, the quality of hazard models and data used to simulate hazard characteristics can influence the formation of hazard risk, which is defined as hazard damage exceeded by a given probability (Merz and Thieken, 2009). For instance, studies have shown that the simulation results for flood volumes and/or inundation depths at different locations are sensitive to the type of hydraulic/flood models and/or climate data used, as well as different modelling parameterization and assumptions (Apel et al., 2009; Ward et al., 2013; Yamazaki et al., 2011). Similar results are also found for seismic hazards (Crowley et al., 2005; Kalakonas et al., 2020), heat stress (Zhao, Lee, et al., 2021), air pollution (WHO, 2016), among others. When predicting hazard damage under future scenarios, increased uncertainty occurs in relation to the choice of Global Climate Models (GCMs) used to drive the hazard models (Alfieri et al., 2017;

Kjellstrom et al., 2018; Orlov et al., 2020; Winsemius et al., 2016).

Second, there is also notable uncertainty in hazard exposure for direct damage assessment. For flood hazards, this is mainly related to land-use data and asset values (Jongman, Kreibich, et al., 2012; Wagenaar et al., 2016), whereby the latter has a larger effect than the former (de Moel and Aerts, 2011). The spatial resolution of the available exposure datasets is also an essential source of uncertainty, particularly for the seismic hazards (Kalakonas et al., 2020). A coarse resolution may result in misrepresentation of the distance between the assets and the seismic sources, and thus implicit correlation in the ground motion for all assets at a given location (ibid.). For hazards mainly affecting human assets, such as heat stress and air pollution, simulated or projected demographics of the researched population and values of statistical life may also contribute to the heterogeneity of modelling results (Romanello et al., 2021; Turner et al., 2012; Zhao, Lee, et al., 2021).

Third, hazard vulnerability sometimes accounts for the largest part of variation in direct damage estimates (Apel et al., 2009; Crowley et al., 2005; Jongman, Kreibich, et al., 2012), highlighting the importance of customizing vulnerability parameters according to regional or sectoral features. For flood hazards, the vulnerability is embodied in the construction of depth-damage functions, which are country- and sector-specific in Huizinga et al. (2017); while for hazards like heat stress and air pollution, the precision of vulnerability assessment is dependent on how to properly quantify the exposure-response relationships, which could differ among regions and age or gender groups (Martiello and Giacchi, 2010; Orlov et al., 2020; WHO, 2016). Rossetto et al. (2014) proposed an evaluation framework to choose the suitable fragility curves for seismic hazards based on relevance and overall quality, which can be generalized to other types of hazards. A few studies also considered the effects of adaptative factors, such as flood protection (Ward et al., 2013) and air conditioning

(Liu et al., 2021), on the robustness or reliability of vulnerability assessment.

Validation of catastrophe models is relatively rare due to the limited number of observations of hazardous events in history. Sparse validations would harm the credibility of catastrophe models. However, it is necessary as uncertainties in hazard damage estimates are generally found to be quite large (Molinari et al., 2019; Xie et al., 2016; Zhao, Lee, et al., 2021). Global disaster databases, such as NatCatSERVICE from Munich Re (www.munichre.com) and EM-DAT database (http://www.emdat.be/), that compile historic extreme hazards across countries and hazard observations and/or damage investigations led by local governments can provide valuable information for assessing the external validity of catastrophe models.

Modelled damage can differ substantially from observed damage, notably for assessments at larger scales (de Moel et al., 2015). Apel et al. (2009) compared the modelling results with the reported flood damage for the August 2002 flood in East Germany, Eilenburg, under combinations of hydraulic and flood loss models. They found that all hydraulic models were able to simulate the maximum water levels of the flood within certain accuracy levels. However, the flood loss models (i.e., exposure and vulnerability assessments) generate larger variability and biases in modelling results than hydraulic models (i.e., hazard simulation). On top of that, direct estimates at larger scales tend to show higher discrepancies from the observed damage of hazards, mainly due to a lack of high-resolution data that provides an appropriate level of details. Bouwer et al. (2009) showed that flood damage estimated based on coarse inundation maps can lead to 22% overestimation and 100% underestimation for the categories of high-density urban areas and infrastructure, respectively. Consistent findings are found for seismic hazards, where the loss estimates become accurate and stable with a certain (fine) spatial resolution (Bal et al., 2010; Kalakonas et al., 2020). Studies on heat stress and air pollution sometimes calibrate the applied ERFs based on limited field research

only, which may impair the model validities when regional characteristics are averaged out on the global scale (Orlov et al., 2020).

2.2.1.3. Refinements and Limitations

Due to an increased computing power, globally consistent datasets with a high spatial resolution on exposure, such as land use and population, are becoming more available in recent years (Chambers, 2020; ESA, 2017). Alternative approaches with the use of night-time lights or satellite imagery are also developed to improve the detail of exposure information (Dabbeek and Silva, 2020; van Donkelaar et al., 2015). Vulnerability curves, which depict the relations between hazard exposure and direct damage or health response, have also been refined based on an increasing number of empirical studies. A typical example here was the development of a global database of depth-damage functions by Huizinga et al. (2017), which makes it possible to use country- and sector-specific vulnerability curves to estimate flood damage. The ERFs for heat- or air pollution-related impact assessment have also been improved by incorporating the lag effect, socio-economic conditions and adaptive factors (Yang et al., 2019; Zhao, Lee, et al., 2021), or by providing more detailed location- or age-specific estimates (Murray et al., 2020). Nevertheless, catastrophe models continue to be featured by large uncertainties and deviations from reported results, notably in the assessment of vulnerability as mentioned above.

Moreover, despite of increasing spatial resolution, few improvements have been made for catastrophe models to understand impacts at the sector level. Flood depth-damage functions, for instance, are generally constructed for up to six sectors, that is, residential, commercial, industrial, transport, infrastructure, and agriculture sectors (Huizinga et al., 2017). Methods for seismic vulnerability assessment are also focused on specific buildings and infrastructure classes, thereby limiting their wider applicability (Hosseinpour et al., 2021). The heat-related labour productivity loss is

only assessed for three types of working groups with different work intensity (Kjellstrom et al., 2018). The health outcomes of air pollution are usually sourced from specific emission sectors (e.g., agriculture, transport, households, power plants, etc.) for specific air pollutants (Cai et al., 2021; Romanello et al., 2021). The mapping of land-use sectors, building classes, working groups and emission sectors to specific economic sectors in the economic system is inevitably required for a comprehensive hazard impact analysis (Mendoza-Tinoco et al., 2020); yet, this has been beyond the scope of catastrophe models.

Thirdly, it is still difficult for catastrophe models to anticipate the evolution of hazard vulnerability, particularly for long-term assessment of direct impacts under future climate change and socio-economic development scenarios (Botzen et al., 2019; de Ruiter et al., 2017; Yin et al., 2021). Most of these studies simply assume that vulnerability and socio-economic condition are constant over time. However, vulnerability is a dynamic process. Adaptation measures, such as flood dikes and air conditioning devices, may be enhanced by stakeholders at risk, to reduce vulnerability and thus increase resilience (Hallegatte et al., 2011; Zhao, Lee, et al., 2021). Some socio-economic changes like urbanization and ageing, which are rarely considered in direct impact modelling, may also affect the vulnerability of diverse hazards (Garschagen and Romero-Lankao, 2015; Park et al., 2020).

Finally, catastrophe models for diverse hazards are almost always developed in isolation. Direct impact assessment is mostly conducted for a single event at a time, and studies on the direct impacts of compound hazards are rare or at an early stage. A few studies have found a short-term synergistic effect of heat and air pollution on premature mortality in specific regions, despite high uncertainty in the results (Pascal et al., 2021; Scortichini et al., 2018). There has also been emerging attention to the health impacts of changes in ambient and indoor air pollution due to COVID-19

lockdowns (Giani et al., 2020; Zhang et al., 2022). However, these studies do not reveal whether there are long-term combined health impacts. The drivers and mechanisms behind the reported interactions are still poorly understood (Sillmann et al., 2021). More importantly, such communications are most likely to happen within modelling communities for hazards that share a certain level of similarity in their direct impact characteristics (e.g., the flood and seismic hazards in the group of capital-shocked hazards, or the heat-related and air pollution hazards in the group of labour-shocked hazards); while exchanges between the capital-shocked and labour-shocked hazard groups are relatively fewer or even non-existent, and methods used in these two hazard groups substantially differ (ibid.).

2.2.2. Macroeconomic Models for Indirect Impact Assessment

Direct impacts of hazards on either capital or labour can further disrupt economic activities, break the market equilibrium along the production supply chain, and thus lead to changes in economic output or value added in sectors and regions which are not initially affected by the hazards. The trail of these propagation effects across the economic network has been termed as indirect disaster footprint in Section 2.1.2, and is typically estimated by macroeconomic models, including IO models, CGE models and hybrid models (Eckhardt et al., 2019). It should be noted that researchers have not reached a consensus on which model is better yet, and the choice of model is dependent on the specific research aims, data availability, etc. (Greenberg et al., 2007; Koks et al., 2016; Okuyama, 2007).

2.2.2.1. IO Models

The IO approach is perhaps the most widely used methodological framework for indirect disaster impact analysis (Okuyama, 2008). The IO models, which are based on IO matrices/tables that capture the trade flows of production inputs and outputs across sectors in an economic equilibrium, consider the economy as a sectoral-

interdependent system and track down the cascading effects of an external shock through inter-industrial and inter-regional linkages (Miller and Blair, 2009). Studies using IO models have investigated various types of disruptive events, ranging from natural hazards (e.g., earthquakes (Cho et al., 2001), heatwaves (Xia, Li, et al., 2018), and pandemics (Orsi and Santos, 2010)) to man-made ones (e.g., air pollution (Xia et al., 2016), power outages (Crowther and Haimes, 2005), and terrorist attacks (Santos and Haimes, 2004)). An early version of the standard IO model was the so-called supply-driven Ghosh model (Ghosh, 1958; Miller and Blair, 2009), which expresses production output as a function of primary inputs like labour and capital and can measure the impacts of constrained supply due to a disruption. However, this model has been criticized for the restrictive assumption that supply generates demand and ignoring the possible perturbations in the demand side of the economy (Oosterhaven, 1988).

Around demand-related risks and how they propagate through interdependencies between sectors within the economic system, Santos and Haimes (2004) proposed an extension of the IO framework, namely the inoperability input-output model (IIM), and applied it to assess the impacts of a terrorism-induced perturbation in demand for air transportation. It adopts the inoperability index - a dimension number ranging from 0 (ideal system state) to 1 (total failure state) to indicate the extent of degradation in final demand in the directly affected sector. Later, Crowther and Haimes (2005) combined the supply-side and demand-side calculations in IIM and found that the national power outage would cause economic losses in both sectors providing power and sectors requiring power for essential operations.

The simplicity of the IO framework has made it easy to understand and integrate with engineering models and/or data, taking advantage of the inclusion of sectoral details, in order to account for higher-order effects that are more sensitive to capacity

destruction (Botzen et al., 2019; Greenberg et al., 2007; Okuyama, 2008). However, this simplicity of the IO approach has been subjected to a set of limitations. First, the technology and productivity are assumed to follow a constant linear structure that relates production outputs proportionally to production inputs during the disruption and its aftermath. This excludes the possibility of input and import substitutions which may affect the economic resilience against disasters. Second, the market price mechanism that adjusts the supply and demand for final and intermediate products towards a new equilibrium after the disruption is ignored in most IO models. Third, there are also no individual-, firm- or sectoral-level adaptive behaviours (such as recapturing lost production by working overtime, maintaining inventories, or rerouting trade shipments) to mitigate the negative impacts during the post-disaster recovery.

Refinements and extensions of the IO framework have sought to overcome these limitations. For instance, Lian and Haimes (2006) proposed a dynamic IIM to simulate the short-term recovery process of economic sectors in discrete-time form following disruptive events such as natural or man-made hazards. Two types of dynamics are incorporated in their model: 1) the demand-reduction dynamic which describes the dynamic behaviours of sectors adjusting themselves in face of final demand reduction; and 2) the dynamic recovery associated with the production outputs of interdependent sectors. In contrast to most traditional dynamic IO models, the dynamic IIM introduced sectoral resilience coefficients, which are affected by adaptive or response policies, to measure the efficacy of risk management options in disaster impact mitigation. On top of that, several studies have combined the dynamic IIM with other models to incorporate adaptive factors such as sector-level inventory adjustment (Barker and Santos, 2010) and substitution of different inputs (MacKenzie and Barker, 2011). Still, these extensions have inherent deficiencies as the resilience coefficients on which the modelling results depend are difficult to estimate (MacKenzie et al., 2012). Dietzenbacher and Miller (2015) noted that the IIM and its extensions are at best a

mild variation of the supply-side Ghosh model, and in a similar vein, Oosterhaven (2017) pointed out other shortcomings including the inability of these models to handle supply constraints.

Advances have been made in incorporating uncertainty into the IO framework to estimate the indirect economic impacts of natural or manmade hazards (Rose and Wei, 2013), and most of these uncertainties are associated with diverse settings of resilient measures and recovery paths (Botzen et al., 2019). The effects of several resilience measures, including ship rerouting, export diversion, use of inventories, conservation of inputs, putting unused capacity to work, input and import substitution and production recapturing (rescheduling), have been examined in a port shutdown case study by Rose and Wei (2013). Over two-thirds of the total indirect economic losses can be reduced by all the resilience tactics, among which shipping rerouting and production rescheduling have the greatest effects in mitigating the regional output losses. Jonkeren and Giannopoulos (2014) argued that recovery paths vary according to the kinds of disasters and sectors. Directly impacted sectors, which suffer from enormous physical damage, may initially recover slowly and then faster afterward when repair activities and logistics are coordinated, while indirectly impacted sectors may follow the opposite recovery path. They have shown that the size of the economic losses differs considerably with the assumed shape of the recovery path (a difference of a factor 4.5) by a numerical example. In addition, inventories which can be used to make up for sector inoperability have also been found to reduce economic losses by 31% in a Dutch winter storm case study (ibid.).

2.2.2.2. CGE Models

The CGE approach, although developed from the IO approach, provides a more flexible model framework than the IO approach as it allows for changes in prices, non-linear production functions, and possibilities of input and import substitutions (Botzen

et al., 2019; Greenberg et al., 2007; Okuyama, 2007). It is essentially a multi-market simulation model based on the simultaneous optimizing behaviour of individual consumers and firms in response to price signals, subject to economic account balances and resource constraints (Shoven and Whalley, 1992; Tsuchiya et al., 2007). In addition to maintaining the main advantage of the IO models, which is the inclusion of sectoral and regional interconnections at various levels of detail, the CGE models have another major advantage of being able to explicitly reflect resilience by the adoption of some elasticities (e.g., price and substitution elasticities) in the equation structure (Greenberg et al., 2007; Okuyama and Santos, 2014). Unlike the IO models that use extreme price elasticity values of either 0 or ∞, the CGE models can respond to price changes with finite price elasticities (Oosterhaven, 2017; Rose and Liao, 2005). Moreover, they also use substitution elasticities to account for the possibilities of substitution between different inputs or regions.

The CGE models have been widely applied to estimate the indirect economic impact of various types of hazards on spatial scales ranging from local to global. Some of these studies have established a model cascade that combines a CGE model with a catastrophe model to estimate the overall disaster impacts (including both direct and indirect ones) (Carrera et al., 2015; Pauw et al., 2011) and/or with climate models to project future economic losses under global warming (Bosello et al., 2012; Darwin and Tol, 2001; Orlov et al., 2020). On the subnational or national scale, Tatano and Tsuchiya (2008) formulated a spatial CGE model to assess the multi-regional economic losses incurred due to transportation network disruption after the 2004 Niigata-Chuetsu earthquake in Japan. The results showed that 20% of the indirect losses occurred in the Niigata region directly affected by the earthquake, whereas 40% of the total losses were experienced in the Kanto region and non-negligible losses reached rather remote zones of the country such as Okinawa. A similar approach was later used by Kajitani and Tatano (2018) with different elasticity values that had been

validated by the observed estimates for the case of the 2011 Great East Japan Earthquake. In a previous work of Pauw et al. (2011), the higher-order economic impacts of crop yield losses due to droughts and floods in Malawi were estimated under an integrated analytical framework that combines a hydrometeorological crop-loss model with a regionalized CGE model. They found that an average of 1.7% of national GDP was lost annually due to the combined effects of droughts and floods on agricultural production. They also validated the model by comparing the model results with observed ones, which demonstrated a broad consistency as least in the direction of changes and a likely underestimation of the actual hazard impacts. Another example is provided by Carrera et al. (2015) who integrated a spatially explicit catastrophe model into a regionally calibrated CGE model to assess the direct and indirect economic impacts caused by the 2000 Po river flood in three Italian regions. The total direct impacts ranged between 3.3 and 8.8 billion Euro depending on water depth assumptions, while the total indirect impacts fell between 0.64 and 1.95 billion Euro depending on the controlled flexibility of substitution and mobility and the length of productivity disruption. The approximated indirect losses, though could be partly offset by the economic gains from substitution effects in areas not directly affected by the floods, still amounted to a significant share (19%-22%) of the direct losses.

On the broader continental or global scale, CGE models have been used to examine large-scale problems such as heat stress, sea level rise and related flood risks. For example, Orlov et al. (2020) assessed the global economic costs of heat-induced reductions in labour productivity under two Representative Concentration Pathways (i.e., RCP2.6 and RCP8.5) for climate change scenarios by employing a recursive-dynamic multi-region, multi-sector CGE model from 2011 to 2100. The dynamic CGE model was calibrated and run under the projected pathways of GDP and population growth associated with a range of Shared Socioeconomic Pathways (i.e., SSP1, SSP4 and SSP5). They found that heat-induced worker productivity losses would result in

an average decline of 1.4% in GDP relative to the reference scenario with no climate change under RCP8.5 by 2100. Adaptation measures, such as an autonomous penetration of air conditioners and mechanisation of outdoor work, could significantly diminish the economic costs from heat stress. Countries in Africa, South-East Asia, and South Asia would be the worst affected by heat stress. However, the average reduction in global GDP was estimated to be only 0.5% under RCP2.6, implying that economic costs could be substantially alleviated if a 2°C climate change target is achieved.

As for the impacts of sea level rise, Darwin and Tol (2001) applied a static global CGE model to assess the economic costs of land and capital submergence due to sea-level rise without coastal protection and with optimal coastal protection. The annuitized total costs of a 0.5-m sea level rise in 2100 were projected to reach $66 billion for the world, which could be reduced to $4.4 billion if optimal coastal protection is implemented. A more recent study was conducted by Bosello et al. (2012), who used the combination of the Dynamic Interactive Vulnerability Assessment (DIVA) model (a catastrophe model for sea level rise driven by GCMs) and the GTAP-EF mode (a CGE model for European countries based on Global Trade Analysis Project (GTAP)) to examine the direct and indirect costs of sea level rise and related flood risks for Europe under a range of sea level rise scenarios in the 2020s and 2080s. They found that the loss of land as a production factor due to the sea level rise would ultimately result in reductions in GDP by a percent ranging from 0.0003% in the Netherlands to 0.08% in Malta. The indirect impacts were not confined to the coastal zone but also landlocked countries (Austria would lose 0.003% of its GDP for instance) due to inter-regional dependencies. Some positive effects, which could offset parts of the negative impacts, were detected notably in developed countries with relatively higher input substitution possibilities. Moreover, coastal protection could be very effective in reducing the negative economic impacts of sea level rise.

CGE models have also been used to investigate the effects of resilience measures in disaster impact mitigation, which is one of their major advantages. For example, Rose and Liao (2005) developed a CGE model with recalibrated production function parameters to reflect resilience for a case study of a water supply disruption during the 1994 Northridge earthquake in the Portland Metropolitan Area. The production function parameters, which represent the elasticity of substitution and productivity, were linked to various types of producer adaptations in emergencies (e.g., conservation of water and other inputs, increased substitutability of production inputs, the use of backup water supplies, and long-run changes in production technologies) to account for both inherent and adaptive resilience. Their results showed that water conservation and substitution could substantially reduce the economic losses from the disruption of water supply and a mitigation strategy that replaces vulnerable pipes could diminish the total losses by nearly half. A similar approach was used in two other studies to assess the effects of resilience during an electricity blackout caused by a terrorist attack in Los Angeles (Rose et al., 2005) and during a port disruption caused by a tsunami in Southern California (Rose et al., 2016). Both studies concluded with similar findings that resilience measures, such as input conservation and substitution and rescheduling (recapture) of production, could greatly reduce the potential disruption impacts.

Still, CGE models have been questioned when applied to hazard impact analysis. A major shortcoming of CGE models lies in the assumption of the agents' optimizing behaviour in an economic equilibrium, which may not be perfectly grounded for a post-disaster situation where imbalances and behavioural changes occur (Kajitani and Tatano, 2018; Okuyama, 2007; Rose and Liao, 2005; Tsuchiya et al., 2007). Rose and Liao (2005) argued that CGE models tend to be overly optimistic about market flexibility (or adjustment capability) and thus underestimate the potential disaster impacts, particularly during a short time of response. Therefore, most CGE models are

intended for a long-run disaster impact analysis due to this market flexibility, except a recent work by Kajitani and Tatano (2018) who validated the CGE simulations with different elasticities of substitution of interregional trade for the short-term impacts of the 2011 Great East Japan Earthquake on monthly industrial production. They found that smaller elasticities of substitution, which indicate relatively rigid settings with low substitutability as in the IO models, were deemed 'best' for the short-run analysis. CGE models, in their description, are perceived as 'black boxes' that require further calibration and validation for parameters used on various time scales after disasters (ibid.). This also relates to another weakness of CGE models, that is, the use of many parameters which rely on external sources for calibration (Greenberg et al., 2007). The empirical values of price and substitution elasticities and specific forms of sectoral production functions are difficult to derive, especially for regional models (ibid.). More extensive data are needed for CGE modelling than IO modelling, creating obstacles for its application in hazard impact analysis (Okuyama, 2007). Oosterhaven (2017) also suggested that CGE models are complex, time consuming and rather costly to estimate, even if the essential data, such as interregional social accounting matrices and various elasticities, are available.

2.2.2.3. Hybrid Models

Hybrid models usually refer to combinations of IO and CGE models that address a number of IO disadvantages and, similar to CGE, allow more flexibility (Koks et al., 2015; Koks et al., 2016). Oosterhaven (2017) has described these models as 'combining the simplicity of the IO model with the greater plausibility of the CGE approach'. Two different types of hybrid models have been developed regarding the decision rationale of economic agents (i.e., producers and consumers). Otto et al. (2017) noted that economic agents have to make two kinds of decisions during the post-disaster economic cycles: 1) rationing decisions of producers on their output if the demand they receive outnumbers their production capacity; and 2) distributing

decisions of consumers on their demand among available suppliers in the disaster aftermath. Correspondingly, the first type of hybrid models assumes that producers and consumers make these decisions by ad-hoc behavioural rules, while the second type of hybrid models assumes that these decisions are governed by local or global optimization principles using linear or non-linear programming techniques. A detailed review of these two types of hybrid models is presented below.

One of the most well-known hybrid IO models with CGE characteristics is the adaptive regional input-output (ARIO) model developed by Hallegatte (2008), which belongs to the first type of hybrid models mentioned above. The ARIO model is built on the linear Leontief production technique as in traditional IO models but with an overproduction capacity when production is insufficient to satisfy the demand. It can accommodate supply constraints as well as demand changes within a macroeconomic framework and trace the propagations of a hazardous shock through both backward and forward linkages along the production supply chain. That is, in addition to reducing consumption in the 'upstream' sectors that supply inputs, constraints in a sector's production could also affect those 'downstream' sectors, to whom it sells its outputs.

The model introduces a prioritized-proportional rationing scheme to determine the deliveries of products to different types of demand when the available production cannot satisfy the total demand. This process is interpreted as a form of substitution by Hallegatte (2008), which, however, is different from the type of substitution considered in CGE models. In this process, the ARIO model only substitutes between outputs, whereas CGE models specifically substitute between inputs (Koks et al., 2016).

On the demand side, new demand occurs in relevant sectors due to the reconstruction needs of damaged capital. Consumers (including final customers and local businesses)

in the disaster area can adjust their final and intermediate demand between local and external suppliers with a certain characteristic time according to the production capacity of local suppliers. Such adaptation behaviours are only allowed for transportable products and, to some extent, reflect the possibility of import substitution.

Moreover, it specifically incorporates price responses to increase the flexibility of economic agents tackling disaster consequences. The model is dynamic and reproduces the whole reconstruction pathway, assuming that the economy will eventually return to the pre-disaster equilibrium state without considering structural changes in the economy that may occur due to a disaster.

Later, an extension to the ARIO-inventory model was proposed by Hallegatte (2014) to account for the effects of inventory dynamics and input heterogeneity in the production system. This improvement has led to a more realistic simulation of the production process and a lower estimate of the indirect economic losses than the previous version when applied to the landfall of the 2005 Hurricane Katrina in Louisiana, the US. Using the ARIO model, the estimated indirect losses (from the economic rippling effects) were found to increase nonlinearly with the direct losses (mainly from capital damage during the hurricane) and even surpass them under extreme scenarios. The model outcomes were highly sensitive to some production and behavioural parameters, with overproduction capacity, characteristic times of adaptation and inventory restoration, and scale of heterogeneity being the most important. However, like CGE models, the parameters of the ARIO model are highly uncertain due to limited available data and approximations have to be made based on observations during other similar disasters or ad-hoc assumptions of values (Botzen et al., 2019).

Still, the ARIO model has provided enlightening experience in overcoming the rigidity

of IO modelling, as well as avoiding falling into the intricacy of CGE modelling. It has been widely used, sometimes with slight modifications (e.g., to include labour constraints), to assess the single- or multi-regional indirect economic impacts of various (types of) hazardous events such as coastal floods in the city of Copenhagen, Denmark (Hallegatte et al., 2011), the 2008 Wenchuan Earthquake in the Sichuan province, China (Wu et al., 2012), and climate change-induced direct shocks (including crop yield loss, energy demand increase, and labour productivity loss) in the US (Zhang, Li, Xu, et al., 2018).

Drawing on the ARIO model, Bierkandt et al. (2014) developed a dynamic damage propagation model using a multi-regional IO table on the global scale, called Acclimate. The first version of Acclimate is focused on the downstream or forward propagation of supply failures in a global supply network considering inventory buffers and transport-related time delay. The model was then extended by Wenz et al. (2014) to examine the backward dynamics of disaster-induced production breakdowns by incorporating the possibility of production extension (i.e., raising the maximum production capacity to satisfy an increased demand) and demand redistribution (i.e., readdressing the demand to nonaffected suppliers). During a stylised disaster which was designed and used as a numerical example in their studies, the production capacity of directly affected sectors is destroyed for days; whereas after the disaster duration, the full production capacity of these sectors is restored immediately, and then the actual output of all sectors (including those indirectly affected due to economic connections) is gradually recovered through the inventory and demand dynamics. This is a quite restrictive assumption as it disregards the rebuilding process of damaged capital and the resulting capital constraint on production capacity before the full reconstruction, as well as the potential increase in final demand due to capital reconstruction and repair efforts. The negative impact of capital constraint and the stimulus effect of capital reconstruction tend to influence the economic output in opposite directions (Hallegatte,

2014). Hence, the neglect of capital dynamics implies a potential over- or underestimation of the disaster impacts and has been identified as one of the major limitations of the Acclimate model (Wenz et al., 2014).

Another recent example of the first type of hybrid models is the so-called Flood Footprint model, which was initially proposed by Mendoza-Tinoco et al. (2017) as an extension of the ARIO model and later improved by Zeng et al. (2019) to include the assurance of basic demand (i.e., necessities of life such as food, clothes, medicines, etc.) and an endogenized capital reconstruction process. The first version of the Flood Footprint model extends the ARIO model by incorporating labour availability and a series of dynamic inequalities, such as the imbalance between capital production capacity and labour production capacity, on the basis of the Basic Dynamic Inequalities (BDI) model developed by Li et al. (2013). However, a major limitation of the model is that it treats import capacity as an exogenous variable by simply adding available imports to the actual production to satisfy both intermediate and final demands. This drawback has been addressed in the second version of the Flood Footprint model. Noting that capital reconstruction is usually constrained by external investment or imports in the previous ARIO, BDI and Flood Footprint models, Zeng et al. (2019) endogenized capital recovery dynamics into post-disaster economic simulations by calculating the amount of capital restored from the satisfied reconstruction demand at each time step. The reconstruction demand is satisfied following a prioritized-proportional rationing rule, which is similar with that of the ARIO model except that the basic and reconstruction demands are prioritized following the intermediate demand. Although the capital recovery process is endogenized, the labour recovery pathway is still an exogenous factor in the model. The sensitivity analysis on alternative labour recovery paths indicates that the indirect flood impacts under different labour recovery scenarios roughly show the same pattern among sectors over recovery periods, but absolute values may widely differ. Other

limitations of the Flood Footprint model include not considering sector substitutability, technology changes and market mechanisms (ibid.).

Among these hybrid models belonging to the first type, which use ad-hoc behavioural rules, the Flood Footprint model appears to outperform the ARIO and Acclimate models in endogenizing the capital recovery process, but it does not consider the presence of inventories and the possibility of substitution between available suppliers as in the two latter models. Further improvement is then required to integrate the advantages of these models, as capital stock, inventory levels, and demand changes are all important factors that could impose binding constraints on the actual production in the disaster aftermath (Hallegatte, 2014).

The second type of hybrid models combines the IO approach with linear or non-linear programming techniques which are commonly used in CGE models. A typical example of this type is the multi-regional impact assessment (MRIA) model developed by Koks and Thissen (2016). The MRIA model shares certain features of the ARIO, such as the modelling of both backward and forward rippling effects of a hazard and the accounting for supply-side constraints, but demand adaptation, inventory dynamics and price changes in ARIO are not included in MRIA. Instead of the well-designed rationing scheme in ARIO, MRIA models the flow of products following the objective function to minimize the total costs of production over all regions given demand, available technologies, and the maximum production capacity. It also includes interregional trade-offs via trade links between regions. Although the possibility of intraregional input substitution in CGE models is ignored, the MRIA model allows for the substitution of production between regions, which is viewed as a resilience measure. This will cause positive interregional spillover effects to firms outside the disaster area taking over production from firms with damaged capacity, which partly offsets the negative disaster impacts to the economic system. Moreover, the recovery

process in the MRIA model is driven by reconstruction demand and determined by exogenous parameters such as the recovery duration and specific paths. By examining the results for floods in Rotterdam, the Netherlands, the authors found that the indirect losses as estimated by the MRIA model were significantly smaller than the direct losses and more comparable to a CGE approach than the ARIO model. They have attributed this to the inter-regional substitution effects which are ignored in the ARIO model. Sensitivity analyses showed that the recovery duration has a large influence on the model results, with substantially larger indirect losses for longer recovery periods. The MRIA model was also well equipped to applications on broader scales such as towards future flood risks on the pan-European scale (Koks et al., 2019).

Similar to the MRIA model, Oosterhaven and Bouwmeester (2016) proposed to combine the IO framework with a non-linear programming model to estimate the interregional and intersectoral rippling impacts of disruptive events. Assuming that economic agents attempt to stick to their usual activities, as closely as possible, the objective function in the model is designed to minimize the information gain between the pre- and post-disaster pattern of economic transactions of the economy at hand. The resulting nonlinear program should therefore be able to reproduce the recovery towards the pre-disaster economic equilibrium. Spatial substitution effects are also accounted by allowing firms to find different suppliers when faced with a supply shortage. However, this is a partial substitution as domestic supply supplements the foreign supply and the drop in supply is not fully compensated. The model was later applied to simulate the inter-regional impacts of natural gas flow disruptions between Russia and the EU (Bouwmeester and Oosterhaven, 2017) and the 2013 heavy flooding in Germany (Oosterhaven and Többen, 2017). In the latter study, the empirical outcomes indicated that the assumption about partial substitution between regions can substantially reduce the estimates of indirect disaster losses by a factor of about six, compared to the assumption about fixed trade and market shares in

traditional multiregional IO models.

Faturay et al. (2019) pointed out that hybrid IO models with linear or non-linear programming approaches can adopt many alternative objective functions depending on the behaviours of economic actors or the goals of policy makers under various disaster-induced or economically inherent constraints. The selected objective function may also be normative and based on political viewpoints. Some examples of possible objective functions, in addition to the ones already mentioned above, include: 1) to keep the post-disaster outputs closest to the pre-disaster outputs by minimizing the sum of squares of deviations between post- and pre-disaster sectoral outputs; 2) to maintain the post-disaster welfare as much as possible by maximizing the sum of (weighted) consumption for basic and luxury goods; and 3) to avoid the disaster losses as much as possible by maximizing the sum of sectoral outputs or value-added after the disaster. Note that these objective functions are all global ones aiming at the total costs, outputs, value added, or consumption of all sectors and regions within the economy, leading to the lack of microeconomic foundations to ensure the realisation of a targeted aggregate economic outcome (Oosterhaven, 2017). To address this problem, Otto et al. (2017) adapted the Acclimate model with local optimization principles. In the model setting, a producer determines its actual production level by maximizing its profit and a consumer distributes its demand requests among its suppliers by minimizing the expected purchase costs under production, delivery, and demand constraints at each time step. Price mechanisms are introduced to address the disequilibrium between supply and demand that arises after a disaster strikes. Still, like the previous two versions of the Acclimate model, this version of the Acclimate model does not consider the dynamic process of capital reconstruction. It was later applied by Willner et al. (2018) to project the indirect losses of river floods within the global economic network under the context of climate change. Their results showed that uncertainties quickly accumulate not only with the ensemble of climate projections,

but also with the assumptions made for the socio-economic factors, particularly for the recovery and response dynamics in modelling the loss propagation.

Comparing the two types of hybrid models, although the second type with optimization principles usually allows for more market flexibilities and resembles more of the CGE approach by using linear or nonlinear programming techniques than the first type with ad-hoc behavioural rules, it has an inherent weakness in reproducing the pre-disaster economic state. The assumptions made for simulating the optimal behavioural decisions of economic agents in the post-disaster disequilibrium may not hold in the pre-disaster economy, and therefore the disrupted economy may eventually recover to a new equilibrium that deviates from the pre-disaster state. Note that this new equilibrium does not arise from technology replacements or structural changes which may take place after a disaster, but simply from problematic assumptions about real-world economic agents. Faturay et al. (2019) also noted that the objective functions in the second type of hybrid models could be manipulative depending on the question(s) one would like to answer and should be chosen with caution. In addition, the mathematical solving process of an optimization problem appears like a 'black box' masking the details on how different parts of the economic system interact to reach a specific target, especially for targets at the global or aggregate level, under complex constraints during the post-disaster disequilibrium. Finally, the optimization principles adopted in the second type of hybrid models may even become invalid when considering the existence of irrational agents with limited or asymmetric information that is likely to happen during the short time after a disaster. By contrast, the first type of hybrid models usually uses ad-hoc behavioural rules (regarding production, rationing, and demand) based on real-world observations, and therefore is more intuitive and better able to reproduce the post-disaster recovery path towards the initial economic state, which is the most common recovery target without considering structural changes in existing case studies.

2.2.2.4. Summary

Overall, all these three categories of methods can reflect the ripple effects of an external hazardous shock through economic interdependencies along the supply chain at various levels of sectoral and regional details. A summary of them is presented in Table 2-4. The main differences between them lie in the assumptions of production techniques and flexibility of market responses (including input and import substitution and price adjustment). The IO approach typically adopts a linear production structure without input substitutability and a rather rigid setting without market responses, while the CGE approach uses a non-linear production structure which allows for a certain degree of input substitutability and a quite flexible setting with market responses which are usually over-optimal for the time scale of the hazardous shock. Because of these features, researchers have reached a consensus that the IO approach is suitable for short-term analysis and provides an upper-bound estimate of disaster impacts while the CGE approach fits for long-term analysis and offers a lower-bound estimate of disaster impacts (Botzen et al., 2019; Hallegatte, 2014; Koks et al., 2016; Okuyama, 2007, 2008; Okuyama and Santos, 2014; Pauw et al., 2011; Rose and Liao, 2005; Rose and Wei, 2013). Hallegatte (2014, p. 154) argued that 'IO models are pessimistic in their assessment of disaster output losses because there is flexibility even over the short term (for instance, maintenance can be postponed; workers can do more hours to cope with the shock; production can be rescheduled); while CGE models are optimistic, even in the long run, because prices cannot adjust perfectly and instantaneously, and because technical limits to substitution are not adequately represented in production functions'.

By comparison, the hybrid approach often tries to find a common ground between the IO and CGE approaches. It combines the simplicity of the IO approach with some characteristics of the CGE approach in terms of flexibility by considering production

bottlenecks, overproduction capacity, inventory adjustment, input and import substitution, demand adaptation, recovery dynamics, etc. It is thus suitable for medium-term analysis and offers a middle estimate of disaster impacts between the IO and CGE approach (Hallegatte, 2014; Koks et al., 2016; Otto et al., 2017). This has given the hybrid approach an edge in disaster impact analysis as most disasters and their recovery phases are medium-term events, spanning from the first hours of the shock to years of reconstruction after large-scale events (Hallegatte, 2014).

Correspondingly, the IO studies usually derive higher ratios of indirect to direct disaster losses than the CGE studies. For example, the indirect economic losses from a 10% reduction in demand for air transport due to terrorist attacks in New York were approximated to be 1.5-2.6 times of the direct losses by Santos and Haimes (2004) using the IIM model. The assessment of economic costs resulting from air pollution-induced labour time loss in China provided an indirect cost of 200 billion Yuan in 2007, which was 1.4 times of the direct cost, by Xia et al. (2016) using the Ghosh model. By comparison, the ratio between indirect and direct losses from the 2000 Po River flood in Italy was estimated to range between 0.19-0.22 by Carrera et al. (2015) using a regionalized CGE model. As for the hybrid approach, results from empirical studies show that the ratio usually falls between the IO and CGE simulations. For instance, the ARIO model elicited a ratio of 0.39 for the case study of Hurricane Katrina in Louisiana by Hallegatte (2008) and the MRIA model derived ratios between 0.64-0.87 for three flood events with different return periods (probabilities of occurrence) in Rotterdam, the Netherlands, in a previous study of Koks and Thissen (2016). Though providing a rough comparison between the outcomes of different models, the above differences in the estimated ratios of indirect to direct loses may be ascribed to the varying economic resilience in areas affected by diverging hazardous shocks other than the different modelling approaches. Instead, Koks et al. (2016) compared the results of two hybrid models (i.e., ARIO and MRIA) and a regional CGE model in a

systematic way for two specific flood scenarios in the same geographical area - the Po River area in the Northern Italy with similar input data. They found that the calculations with the ARIO model resulted in the highest indirect losses for the whole of Italy for both floods and for each recovery paths, while the CGE model had the lowest indirect losses in almost every model set-up. This is consistent with expectations, as the ARIO model fails to capture the potential substitution effects in production and trade and thus all other initially non-affected regions will suffer economic losses, while the CGE model is featured by perfect substitution across sectors of labour and capital and therefore some initially non-affected regions can yield economic gains by taking over from regions with damaged production capacity. The outcomes of the MRIA model were close to but still higher than those of the CGE model in most flood and recovery scenarios, as the MRIA model was built to allow for a certain degree of substitution effects in their study.

Table 2-4: Indirect impact analysis - methods and applications.

Methods	Features	Strengths	Weaknesses	Applications
IO approach	Linear production structure via fixed technical coefficients; ripple effects through sectoral interdependencies	Simple and easily compatible with other models; suitable for short-term analysis	Rigidity on market responses (without inputs or import substitution and price adjustment); overestimation of disaster impacts	Ghosh model for heatwaves (Xia, Li, et al., 2018) and air pollution (Xia et al., 2016); IIM for terrorist attacks (Santos and Haimes, 2004), pandemics (Orsi and Santos, 2010) and power outages (Crowther and Haimes, 2005)
CGE approach	General equilibrium analysis; non-linear inter-sectoral deliveries; ripple effects through sectoral interdependencies	Flexible market responses with input and import substitution and price changes; fit for long-term analysis	Incapability to reflect post-disaster imbalance between supply and demand; complex and overmuch parameters involved; overly optimistic about market responses and underestimation of disaster impacts	Regional models for earthquakes (Kajitani and Tatano, 2018; Tatano and Tsuchiya, 2008), droughts and floods (Carrera et al., 2015; Pauw et al., 2011); global models for heat stress (Orlov et al., 2020) and sea level rise (Darwin and Tol, 2001)
Hybrid approach	Hybrid IO analysis with CGE characteristics by considering supply constraints, overproduction capacity, production bottlenecks, inventory dynamics, input heterogeneity, input and import substitution, and flexibility in recovery, etc.	Realistic post-disaster recovery and response mechanisms emphasizing economic imbalances; increased flexibility on market responses than IO models; suitable for mid-term analysis	Uncertainty in assumptions about the decision rationale of economic agents (ad-hoc behavioural rules or optimization principles)	ARIO model for hurricanes (Hallegatte, 2008, 2014), coastal floods (Hallegatte et al., 2011) and earthquakes (Wu et al., 2012); MRIA model for floods (Koks and Thissen, 2016; Koks et al., 2019); Flood Footprint model for floods (Mendoza-Tinoco et al., 2017); Acclimate model for river floods (Willner et al., 2018)

The methodology of this thesis is based on the hybrid approach because it not only emphasizes a series of important imbalances or inequalities that may occur in the disaster aftermath and are neglected in traditional IO modelling, but also captures the step-by-step process of an economy recovering from the disaster-induced disequilibrium back to the initial equilibrium, rather than implying an immediate market clearing equilibrium at each time step as in CGE modelling (Li et al., 2013; Otto et al., 2017; Zeng et al., 2019). Using hybrid models can easily bridge the gap between IO and CGE literature by creating a setting less rigid than IO models and at the same time less flexible than CGE models. The hybrid approach is therefore suited best for the timescale of months following a disaster - too short for the economy to restructure and substitute perfectly, but long enough to make a few production and consumption adaptations. More specifically, this thesis acknowledges that the type of hybrid models using ad-hoc behavioural rules, which is represented by the ARIO model and subsequent extensions, has more advantages over the other type using optimization principles (e.g., the MRIA model and the third version of the Acclimate model) in disaster-induced economic impact analysis due to the incorporation of more realistic recovery and response mechanisms on the basis of microeconomic foundations. However, an integrative hybrid model that accommodates all important dynamic constraints and adaptive factors (such as capital recovery, inventory adjustment, and demand redistribution) is still lacking.

Moreover, similar with most studies on direct impact analysis, studies on indirect impact analysis usually focus one (type of) disaster at a time. Although Pauw et al. (2011) used a CGE model to examine the economic losses for the full distribution of possible weather events including floods and droughts in Malawi, calculations of flood- and drought-induced economic losses were carried out separately and interactions between the impacts of different events within the economic system were ignored. Only recently, Zeng and Guan (2020) proposed an adaptation of the Flood

Footprint model to explore the compound economic effects of two successive floods. They found that the combined losses resulting from sequencing floods can be higher than the sum of losses resulting from separate floods. This is because the economy tends to spend longer time to recover from the new flood when it has not been fully taken back after the previous flood, and the recovery resources are more limited for each flood when multiple floods happen closely. However, their analysis is based on hypothetical flooding and economic scenarios and limited to sequencing events of the same hazard type. Further extensions and applications to compound events comprising of different hazard types are therefore still in need to enhance current understanding of the complex economic consequences we are facing ahead as global warming continues.

2.2.3. Empirical Evidence from Econometric Models

In addition to computational models for the evaluation of direct and indirect disaster footprint, there are a large number of empirical studies based on econometric methods which provide parallel evidence for the results about disaster-induced economic impacts and influencing factors. These studies usually use time-series, cross-sectional, or panel regressions to correlate economic outcomes (such as GDP, GDP growth rates, consumption, trade flows, death counts, employment, and per capita income) to disaster measures (such as disaster occurrence, frequency, intensity, damage, and fatalities), while controlling for other potential determinants of the economic outcomes (such as population, land area, income inequality, average education, political regimes, financial development, trade openness, and foreign direct investment) (Botzen et al., 2019; Kousky, 2014). In general, these studies can be mainly categorized into three strands, that is, the estimation of 1) direct effects, 2) short-run indirect effects, and 3) long-run effects of hazardous events on the macroeconomy, which will be reviewed in turn in the following sections.

2.2.3.1. Direct Effects of Hazardous Events

Direct effects of hazardous events are usually measured by fatalities and physical damage. For instance, Kahn (2005) used cross-national data for 73 countries to examine the determinants of annual deaths from disasters over 1980-2002. Death counts of five types of disasters (i.e., earthquakes, extreme temperature, floods, landslides, and windstorms) were obtained from the EM-DAT database (https://www.emdat.be/). The study found that, though richer countries (with higher GDP per capita) do not experience fewer or weaker disaster shocks than poorer countries, the former indeed suffers less deaths from disasters than the latter. Other factors such as geography and institutions also play a role in determining the annual disaster-induced fatalities. Lower income inequality (Gini index), more democratic regime, and stronger institutions could all help reduce the death toll in the sampling countries. In addition to direct losses of human lives, disasters can also cause direct damage to physical assets. Regressing on a similar dataset for 151 countries over 1960-2003, Toya and Skidmore (2007) found that countries with higher income, higher educational attainment, greater openness, more complete financial systems, and smaller government would experience less damage (in relative terms of GDP) from disasters.

Yet, follow-up studies tend to discover non-linear relationships, either U-shaped (Raschky, 2008) or invertedly U-shaped (Kellenberg and Mobarak, 2008), between disaster-induced direct impacts and per capita income. Schumacher and Strobl (2011) showed that the non-linear relationship between disasters and wealth depends on the exposure to disaster hazard. According to their regression results using the panel data for 181 countries over 1980-2004, low hazard countries are likely to experience first increasing disaster damage and then decreasing one with the increasing wealth (i.e., invertedly U-shaped relationship), while high hazard countries tend to see first decreasing damage and then increasing one as the per capita income increases (i.e., U-

shaped relationship). Their findings were supported by a recent study of Patri et al. (2022) who examined the potential determinants of a broad range of direct impacts caused by floods, including people affected, crop losses, house damage, damage to public properties, and the total economic damage, in 21 major Indian states from 1981 to 2019. All these flood-induced direct impacts were found to be significantly correlated with the real per capita state GDP following a U-shaped pattern, as India is a high-risk country of climate change and natural disasters. The study also suggested that increasing the urbanization rate and expenditure under the Disaster Risk Reduction program can reduce the flood damage, while a rise in population density, more flooded areas, and heavy rainfall enhance the damage risk of floods.

2.2.3.2. Short-run Indirect Impacts of Hazardous Events

Much more attention has been given to the indirect impacts than direct ones in the empirical literature on hazardous events. The short-run indirect impacts are often referred to as the impacts on the macroeconomy (mostly measured by GDP or GDP growth rates) in the struck region within one to five years after the events. In a widely cited study of Noy (2009), the GDP growth rate is regressed on standardized measures of a disaster and a set of controls using the EM-DAT data on rapid-onset disasters for a panel of 109 countries over 1970-2003. The disaster measures included casualties divided by population and direct costs divided by the previous year's GDP, weighted by the month of occurrence. The study found that natural disasters have a significant adverse impact on economic development in the short run when they are measured by the amount of property damage incurred. Developing countries and smaller economies face larger output declines after a disaster of similar relative magnitude than developed countries or bigger economies. Moreover, countries with a higher literacy rate, better institution, higher per capita income, higher level of government spending, and higher degree of trade openness are better able to withstand the initial disaster shock and prevent further spillover effects into the macroeconomy. Financial conditions also

seem to matter. Countries with less open capital accounts, more foreign exchange reserves, and higher levels of domestic credit appear more robust and better able to endure natural disasters with less adverse spillover to domestic production.

However, some scholars noted that using monetary direct damage recorded by EM-DAT or other similar databases such as NatCatSERVICE and Sigma as a measure of disaster magnitude may cause endogeneity bias when examining the relationship between disasters and economic development (Felbermayr and Gröschl, 2014). Such a disaster measure is likely to be correlated with GDP per capita, which is the main dependent variable in the literature, as the disaster damage is greater and better recorded for developed countries in these databases. To overcome this data issue, Felbermayr and Gröschl (2014) built a new database called GeoMet based on physical measures for the magnitude of natural disasters including earthquakes, volcanic eruptions, storms, floods, droughts, and temperature extremes from 1979 to 2010 for more than hundred countries in the world. Using this database, the authors constructed an aggregate disaster intensity index for each country in each year and investigated the immediate disaster impacts on national GDP per capita. They discovered that natural disasters do indeed lower GDP per capita in the short run and the marginal reduction increases with the disaster magnitude (i.e., non-linear relationship). Specifically, a disaster in the top 1-percentile of the disaster index distribution reduces GDP per capita by at least 6.83%, while the top 5-percentile disasters cause per capita income to drop by at least 0.33%. Low- and middle-income countries tend to experience the highest losses, and better institutional quality, higher openness to trade, and higher financial openness can significantly reduce the adverse effect of a disaster on per capita income.

Similarly, Anttila-Hughes and Hsiang (2013) looked at a specific type of disaster - tropical cyclones in the Philippines linking physical storm data with household survey data into a difference-in-difference approach. They demonstrated that the physical

measure of typhoon exposure, i.e., wind speed, is a good predictor of damage and deaths at both the national and household levels. They estimated that the annual household income (net of public and private transfers) is reduced by 6.6% in the short run given the average annual exposure of typhoons in the country. Such income loss could persist for several years following the typhoon, particularly for poorer households, and cause a nearly one-for-one reduction in household expenditures, mostly in the categories of human capital investment.

While most of the literature focuses on rapid-onset disasters like earthquakes and cyclones, there have been some studies on the economic impacts of slow-onset disasters like extreme heat and epidemics/pandemics. Dell et al. (2012) examined the historical relationship between temperature fluctuations and economic growth using a panel dataset for 125 countries over the period from 1950 to 2003. Their estimates showed that a 1°C rise in temperature in a certain year is likely to reduce the economic growth in that year by about 1.3 percentage points in poor countries, while having no significant effect on the economic growth in rich countries. Higher temperatures also have broader impacts outside of agriculture, leading to reductions in industrial output and political stability. Similar impacts on the aggregate and industrial output were also documented in an earlier study of Hsiang (2010) on temperature shocks in 28 Caribbean countries, in which the response of economic output to increased temperatures was found to be structurally similar to the response of labour productivity to thermal stress.

Wang et al. (2022) used a panel vector autoregressive model to examine the impact of COVID-19 on the daily economic resilience in 286 cities in China during a very short time (roughly the first month after the onset of the pandemic). A comprehensive indicator system was constructed to measure economic resilience, consisting of five socio-economic aspects of economic performance, public opinion, public health,

management policies, and population inflows, based on macro and big data. They found that the surge in confirmed cases shows a significant negative effect on economic resilience, which usually persists for the following five days and then converges in later days. Additionally, a longer pandemic tends to have a greater negative impact on economic resilience. The macroeconomy may also be affected by lockdown restrictions implemented to control the spread of an epidemic/pandemic. Bonaccorsi et al. (2020) used a massive near-real-time dataset of human mobility provided by Facebook to analyse how mobility restrictions affect economic conditions of individuals and local governments in Italy. Their results showed that low-income individuals tend to be more affected by the economic consequences of the lockdown, making poor municipalities, as well as rich ones but with high income inequality (i.e., a greater number of low-income individuals), suffer more pronounced mobility contractions and sharper reductions of the fiscal revenues generated by their tax bases. This would pose a greater fiscal challenge at the municipal level in sustainably supporting the recovery of the weaker fraction of the population and probably induce a further increase in poverty and inequality.

Besides, there are some studies focusing on the effects of hazardous events on finer scales, i.e., on the sectoral or even firm levels. For example, Guimaraes et al. (1993) used a multi-sector regional econometric model to examine the impacts of Hurricane Hugo, which hit South Carolina in 1989, and found that, though the overall economic impacts were neutral, these impacts were distributional among sectors. The construction sector witnessed a short-term boom due to the rebuilding efforts in the post-disaster recovery, while forestry and agriculture sustained large losses. Retail trade, transportation, and public utility income declined immediately after the hurricane and then rose above baseline for more than a year. Focusing instead on firm-level variables, Leiter et al. (2009) examined the impacts of floods on capital accumulation, employment growth, and productivity of European firms using a

difference-in-difference approach. They found that floods result in significant increases in asset and employment growth, while productivity is not significantly affected. This indicates that damaged production capabilities can be offset by increased investment in assets and increased labour following a flood. Two recent studies leveraged the same panel dataset of Chinese manufacturing firms from 1998 to 2007 to investigate the effects of temperature on industrial output (Chen and Yang, 2019; Zhang, Deschenes, et al., 2018). Both discovered a non-linear relationship between temperature and industrial output, though identifying diverging mechanisms through which temperature affects output. While Zhang, Deschenes, et al. (2018) found that output losses mainly arise from the negative response of total factor productivity (TFP) to high temperatures, Chen and Yang (2019) illustrated that declines in firms' investment and expansion in inventories in response to high temperatures are two other drivers of output reductions. In both studies, timber and rubber are the two sectors more affected by higher temperatures.

Although most of these empirical studies focus on one type of hazard at a time, Hsiang (2010) presents one of the few studies of the impacts of two different hazards, i.e., increased temperatures and tropical cyclones, in various sectors of 28 Caribbean countries during 1970-2006. Because sea surface temperatures in the tropical Atlantic have been correlated with basin cyclone activities since 1950, the economic impacts of tropical cyclones should be estimated and separated from the impacts of temperature, the main purpose of the paper. Differences were found in the sectoral distribution of the impacts of these two hazards. Increased surface temperatures exert much larger negative impacts on the output of non-agriculture sectors than the agriculture sector, while tropical cyclones cause output losses most strongly distributed in the agriculture, tourism, and mining sectors and output booms in the construction sectors probably due to its role in reconstruction. The author also found that the impacts of a cyclone could persist for several years after the initial event, especially in the tourism sector due to

reductions in tourist visits.

In general, empirical studies suggest that hazardous events tend to significantly lower economic growth in the short run, notably in low-income countries. On the sectoral scale, extreme temperatures not only reduce crop yield in the agriculture sector but also cause wider and even larger effects to other economic sectors, while capital-struck disasters (such as cyclones and hurricanes) may also trigger temporary increases in the construction income due to the reconstruction efforts in the disaster aftermath.

2.2.3.3. Long-run Effects of Hazardous Events

The current literature remains inconclusive about the long-run effects of hazardous events on the macroeconomy. Theoretically, the standard Solow model, a representative model of exogenous growth, would suggest that even though a hazardous event can cause short-run reductions in production and income due to capital or labour destruction, the economy will eventually return to its initial steady-state or balanced growth path, leading to no significant long-run effects (Solow, 1957). However, Aghion and Howitt (1990) proposed a model of endogenous growth through creative destruction and argued that the disaster-induced destruction of both physical and human capital might have a positive effect on the long-term growth through increased marginal returns and reconstruction investment. The theoretical debates regarding whether a catastrophic event pushes the economy away from its initial path temporarily or permanently have motivated empirical studies to investigate the long-term effects of such an event.

However, fewer empirical studies, compared to the number of studies on the short-run impacts, have been carried out for examining the long-run effects of disasters on economic growth, due to the large data requirements and complex causality considerations associated to the long-run temporal scale (Botzen et al., 2019; Loayza

et al., 2012; Okuyama and Santos, 2014). In an influential study, Skidmore and Toya (2002) investigated the long-run relationships between natural disasters, capital accumulation, TFP, and economic growth using the cross-sectional regression with EM-DAT data for 89 countries. Their analysis related the average annual growth rate of per capita GDP over the 1960-1990 period to the total number of natural disasters occurring in a country over the same period. They found that climatic disasters (mainly floods, cyclones, and storms) are positively correlated with economic growth, human capital investment, and TFP growth, while geological disasters (mainly volcanic eruptions, landslides, and earthquakes) are negatively correlated with growth. The response of TFP towards natural disasters appears to be the primary driver behind changes in economic growth. However, this study has a major limitation for the possibility of omitted variable bias which is inherent in the cross-sectional method.

Dell et al. (2012), discussed above, also conducted a first-differenced regression on the long-run relationship between temperature changes and growth changes from the early period (1970-1985) to the late period (1986-2000) across countries. Their results showed that the warming temperature tends to exhibit substantial and significant negative effects on the economic growth of poor countries, while having no significant effects on that of rich countries. Their analysis on the long-run scale provides evidence that the negative temperature effects seen in the annual growth may persist over a 15-year time horizon.

A more comprehensive study of the long-term effects of tropical cyclones was carried out by Hsiang and Jina (2014). They related the economic growth rate (measured by the first difference of the logarithm of GDP) to both contemporaneous and historical area-averaged tropical cyclone exposure (measured by wind speed and energy dissipation), using a difference-in-difference approach, for almost all countries over the 1950-2008 period. They found that tropical cyclones can cause persistent and

negative effects on GDP growth rates for over a decade after the initial strike, leading to even longer and severer cumulative impacts on national income. Their conclusion is robust in rich and poor countries or in response to large and small cyclones. Interestingly, countries where cyclones are more frequent tend to experience less economic losses, indicating a higher level of investment in adaptation to shield their economy from cyclones.

2.2.3.4. Summary

Overall, the empirical literature on disaster impacts generally suggest negative direct and short-run indirect economic effects of hazardous events, while the long-run economic effects are ambiguous and sometimes contradictory when examined using different methods or focusing on different hazard types.

Factors such as the income level, quality of institution, democratic regime, geographic features, education attainment, degree of trade openness, urbanization, infrastructure, financial conditions, early warning system, and protection levels can also influence the severity of disaster impacts (Felbermayr and Gröschl, 2014; Hsiang and Jina, 2014; Kahn, 2005; Loayza et al., 2012; Noy, 2009; Patri et al., 2022; Toya and Skidmore, 2007). Moreover, some studies demonstrate that regions highly exposed to a certain hazard in the past, such as countries repeatedly hit by cyclones (Hsiang and Jina, 2014) and historically high-temperature regions in China (Chen and Yang, 2019), tend to suffer less economic losses from the hazard than other regions in the study sample, suggesting an active role of human adaptation in mitigating the hazard impacts. In summary, ‘a developed, diversified, and open economy with sound institutions’ tend to display a stronger resilience towards various hazards. This is to some extent consistent with the results from computational models (i.e., IO and CGE models), which emphasize the mitigating effects of substitutability (mainly through trade) in offsetting the lost production of sectors caused by a hazardous event (Botzen et al.,

2019).

More importantly, empirical studies on the sectoral level have found the presence of linkages transmitting shocks across sectors (Loayza et al., 2012), which, however, has to rely on IO or CGE models to more closely trace and isolate these propagations among the cumulative economic impacts. Meanwhile, these studies have also found statistically significant positive effects of hazardous events (mainly hurricanes and cyclones) on the output of the construction sector due to its role in capital reconstruction (Guimaraes et al., 1993; Hsiang, 2010). This is also in support of results of some hybrid computational models, particularly the Flood Footprint model, that considers the post-disaster reconstruction need as an endogenous driving factor behind the economic recovery.

2.3. Emerging Concerns for Compound Hazards and Their Economic Implications

As discussed in Section 2.1.1.2, a compound hazard in this thesis refers to "the compounding of multiple hazards, in a wide range beyond climatic hazards, that causes interconnected shocks to the economic system". This concept stems from the notion of 'compound events' in the field of climate science, which mainly focuses on the co-occurrence of multiple climatic hazards, and is then extended to include collisions with biological, political, and other hazards against the diversified and complex background of intensifying climate change, continuing COVID-19 pandemic, and escalating geopolitical tensions. Research on compound hazards is still at an early stage, giving most attention to the physical characteristics (e.g., drivers, intensity, frequency, distributions, and impacts) while with inadequate understanding on the associated socio-economic implications.

2.3.1. Increasing Risk of Compound Hazards

In the 6th (also latest) IPCC annual report, climate scientists have reached a consensus that compound hazards will become more common as global temperatures continue to rise (IPCC, 2021). This report provides the first evaluation on changes in compound hazards by summarizing the research progress since the concept was initially introduced in the IPCC 2012 special report on climate extremes (IPCC, 2012). Many major climate catastrophes are inherently of a compound nature, including but not limited to coastal extremes, floods, heatwaves, droughts, and wildfires (AghaKouchak et al., 2020; Ridder et al., 2020; Zscheischler et al., 2018). The IPCC report takes a special look at two types of mostly studied compound events in literature, i.e., compound floods and concurrent droughts and heatwaves. Recognizing that flood occurrence may be caused by the interaction between storm surge, heavy precipitation, and high river flow, as well as by sea level rise and astronomical tides and waves, floods with multiple drivers are often defined as compound floods (Bevacqua et al., 2020; Moftakhari et al., 2017; Wahl et al., 2015). For another, due to land-atmosphere feedbacks, temperature and precipitation are strongly negatively correlated during summer over most land regions, leading to a compound hot and dry condition, which is also a climate feature of many other weather-related disasters like wildfires and tree mortality (Brando et al., 2014; Zscheischler and Seneviratne, 2017). The IPCC report has concluded that the probability of compound flooding has increased in some regions (including the US coasts) over the past century (medium confidence) and will continue to increase in the future due to both sea level rise and increases in heavy precipitation (medium confidence) (Seneviratne et al., 2021). The frequency of concurrent heatwaves and droughts has also showed or will show an upward trend at the global scale in the history due to human influence or in the future as global temperature increases (high confidence), which may further cause more frequent wildfires (fire weathers) in some regions (ibid.).

Temperature and precipitation anomalies can also create another type of compound event, i.e., the so called compound flood-hot hazards (Gu et al., 2022), where a flood event and an extreme heat event hit the same region in close succession. By examining the historical data over the period from 1979 to 2017 across the central United States, Zhang and Villarini (2020) showed that heat stress can set the stage for subsequent flooding by preparing an extremely hot and humid condition. As global warming continues, heat stress will become more frequent in the future, so will be this type of compound event in the central US. Alternatively, a heatwave may also closely follow a flood, exacerbating the hazard damage. A typical example is the consecutive flood-hot extreme event that struck Japan in July 2018, during which the flood-induced electricity outages left many people without air conditioning in the subsequent record-breaking heatwave (Wang et al., 2019). Although a compound flood-hot event like this has not happened in the history of China, it is projected to be more possible in the future as temperature rises, particularly in the Southern China (Liao et al., 2021). Very recently, Gu et al. (2022) presented the first global assessment of projected changes in compound river flood-hot extremes. They found that an increasing fraction of floods will be accompanied by hot extremes under global warming, with tropical regions being the new global hotspot of such compound flood-hot extreme events. Moreover, the exacerbation of this global compound hazard is mainly dominated by changes in hot extremes, especially in tropical regions.

Except for the concurrence of different climatic hazards, hazardous climatic events can also intersect with high air pollution episodes, as a results of their shared underlying meteorological drivers, such as low wind speeds, high temperatures, and low precipitations (Schnell and Prather, 2017; Sillmann et al., 2021). For example, the 2017 December wildfires in Southern California have significantly raised the ambient $PM_{2.5}$ concentration to the level above the national standard (i.e., 35 $\mu g/m^3$) for 5 to 13 days in the nearby and downwind regions, leading to adverse health impacts (Shi et al.,

2019). Besides, the co-occurring O_3 pollution during the 2003 European heatwave has caused high levels of excess deaths in European countries (e.g., France and the Netherlands) and the United Kingdom (Dear et al., 2005; Vautard et al., 2005), representing another type of air pollution-related compound hazards. Heatwaves are often accompanied by increased levels of air pollutants released during wildfires or produced by photochemical reactions. Other unfavourable weather conditions like stagnant air can further aggravate the severity of air pollution by negatively affecting the transportation or diffusion of harmful aerosols (Jacob and Winner, 2009; Schnell and Prather, 2017). Such effects of climate change in deteriorating air quality has been termed a 'climate change penalty' in literature (Fu and Tian, 2019, p. 160). On the other hand, air pollution, especially associated with elevated emissions of sulphates and black carbon, can also affect climate conditions such as regional temperature and precipitation patterns (Falloon and Betts, 2010; Ramanathan et al., 2005; Sillmann et al., 2017). These interactions between climate conditions and air quality will enhance the risks of compound hazards comprising of extreme weathers and air pollution episodes, which may become more frequent, longer lasting, and more intense as the climate keeps warming (Fiore et al., 2015; Horton et al., 2014).

Since the onset of the COVID-19 pandemic, there has been a concerning body of evidence indicating that the pandemic outbreaks and associated public health responses may collide with climatic hazards, which are increasing in frequency and intensity under climate change (Phillips et al., 2020). According to the report released by the International Federation of Red Cross and Red Crescent Societies (IFRC), hundreds of extreme weather events (mostly storms, floods, heatwaves, and droughts) have intersected with the COVID-19 pandemic globally (not only in low-income countries but also in medium- and high-income countries), leaving millions of people simultaneously exposed to multiple hazards (Walton et al., 2021). For instance, a severe hurricane made landfall in the state of Louisiana in June 2020 during a surge of

COVID-19 cases due to the ease of physical distancing restrictions there (Salas et al., 2020). In Zimbabwe, drought has left millions of people without access to clean water and at risk of acute food insecurity during June to September 2020, which affected the country's response to the virus (FEWS NET, 2020). Sometimes the double threats of climate and COVID-19 may even overlap with other shocks, such as trade frictions between China and US and military conflicts in Afghanistan, generating increasingly complex and challenging circumstances (Shahid, 2020; Walton et al., 2021).

In summary, individual or interrelated hazards are compounding with each other due to the combined effects of the warming climate, ongoing COVID-19 pandemic, and intensifying geopolitical tensions, etc. Multiple climate hazards will occur simultaneously, and multiple climatic and non-climatic hazards will interact, posing severe challenges to sustaining human society (IPCC, 2022). The occurrence of these compound hazards will increase in the future as the mixed situation continues.

2.3.2. Economic Implications of Compound Hazards

The enhanced socio-economic impacts of compound hazards are increasingly recognized, but only rarely estimated. The combination of multiple hazards, each of which is not necessarily extreme, can result in higher economic losses and death tolls than the sum of the impacts of isolated hazards, for overwhelming the coping capacity of natural and human systems more quickly (Hao and Singh, 2020; Ridder et al., 2020; Seneviratne et al., 2021; Zscheischler et al., 2018). AghaKouchak et al. (2020) highlighted in their review of literature that temporal clustering of extreme events can markedly amplify the disaster damage and slow down the recovery process. This viewpoint has also been quantitively confirmed by one of the few studies modelling the cumulative impacts of two successive floods to a hypothetical economy (Zeng and Guan, 2020). An empirical study of the interaction between heat and air pollution found that higher PM_{10} concentration levels can non-linearly increase the risk of heat-

related mortality, leaving the single-living elderly people (above 85 years old) at the highest risk (Willers et al., 2016). Zscheischler et al. (2020) has ascribed the augmented impacts to: 1) interactions between multiple hazards occurring at the same time (e.g., heatwaves and air pollution); 2) previously adverse conditions increasing the system's vulnerability to a subsequent event (e.g., successive floods); or 3) spatially concurrent events resulting in regionally or globally overlapping effects (e.g., globally synchronized heatwaves influencing global food production).

Notably, there has been a growing concern that pandemic outbreaks (including COVID-19) and associated public health responses may have a potential for aggravating the socio-economic impacts of climatic hazards (IPCC, 2021). Communities appear to be more vulnerable to extreme events during a pandemic, as physical distancing regulations reduce the capacity of temporary shelters (Salas et al., 2020). The use of personal protective equipment (PPE) against the pandemic also makes health care personnel suffer more intense heat strain during hot extremes (Bose-O'Reilly et al., 2021). Countermeasures against one crisis may jeopardize the efforts to confront another crisis, which then exacerbates the negative impacts of both and slow down the recovery (Ishiwatari et al., 2020; Salas et al., 2020; Selby and Kagawa, 2020). However, few studies have actually estimated the extent to which these compounding effects of pandemic and climate shocks may influence an economy. Dunz et al. (2021) carried out the first evaluation on the quantitative impacts of overlapping COVID-19 and hurricanes on Mexican real GDP using a macro-economic model considering the roles of bank credit and public finance. Their results showed that the combination of COVID-19 and extreme weather events generates non-linear effects that can amplify the magnitude and persistence of economic losses (e.g., measured in terms of GDP) over time. In some extreme cases where strong hurricanes coincide with the COVID-19 shock, the compound impacts can be 50% larger than the sum of the individual shocks, preventing GDP from returning to its initial path in the

short- to mid-term. Yet, this study does not consider the cascading effects of compound shocks across sectors and regions. The integration of these supply chain effects in the model would rely on more detailed input-output based information and techniques.

International trade also plays an important role in affecting price volatility, food security, and supply chain stability disrupted by climate and pandemic shocks (Bezner Kerr et al., 2022; Verschuur et al., 2021). The border restrictions on imported goods and foreign workers to prevent virus transmission may impede the production restoration following a destructive climate disaster (Mahul and Signer, 2020). Export restrictions imposed on critical supplies (such as food, vaccines, and other essential goods) can prolong the global supply chain disruptions caused by pandemic lockdowns, generating myriad consequences including shortages of production inputs, raw material and shipping cost rises, abnormal demand changes, and logistic and capacity bottlenecks (Dickinson and Zemaityte, 2021; Eaton, 2021; Espitia et al., 2020).

In summary, compound hazards may aggravate the socio-economic consequences of isolated hazards, highlighting the importance of holistic risk assessment and integrated solutions for enhancing compound resilience of an economy (IPCC, 2022). There is an emerging literature calling for analysis on interactions between individual and interrelated hazards (AghaKouchak et al., 2020; Phillips et al., 2020; Zscheischler et al., 2018) and their risk transmission channels within the economic network (Dunz et al., 2021). Existing knowledge and frameworks should be extended to address the complex impacts of compound hazards and inform financial investment and public policies in future risk preparedness (Kruczkiewicz et al., 2021; Mahul and Signer, 2020).

2.4. Research Gaps

This chapter has reviewed the growing literature on the direct and indirect economic impacts of individual and compound hazards and synthesized the key definitions, computational methods, and empirical evidence to extract the main findings. The review has shown that a hazardous event causes not only significantly negative direct economic consequences (e.g., casualties and property damage), but also generally negative indirect economic impacts through interdependencies between sectors and regions (e.g., production and trade losses). Sectors involved in capital construction may sometimes experience a temporary boom in the disaster aftermath due to the surges in demand for reconstruction. More developed and diversified economies tend to suffer less disaster impacts due to their higher building codes and stronger capacity to compensate for lost production with increased production elsewhere. Compound hazards, particularly in combination with pandemic shocks such as COVID-19, may amplify the negative economic impacts of isolated hazards due to their interactions in risk transmission within the economic system. However, there still exist three major research gaps that should be bridged:

1) **There is a lack of universally applicable methodology to assess the hazard-induced indirect economic impacts.**

Despite the growing awareness of the potentially large scale of indirect hazard impacts (sometimes even exceeding the direct ones), there has not been a universally applicable accounting method in the literature. Most of the models developed for indirect hazard impact assessment (including IO, CGE, and hybrid models) are intended for specific hazard scenarios with distinctive features (see Section 2.2.2.4).

Standard IO models adopt a relatively rigid setting without input substitution or other market responses, thus suitable for the short-run impact assessment. By contrast, CGE

models establish equations on long-run economic equilibrium and tend to be overly optimistic about market flexibility, leading to underestimation of the disaster impacts.

Though hybrid models are built on the middle ground of IO and CGE models and fit best for a medium-term timescale on which most disasters and their recovery phases last, these models are usually developed from limited economic angles, such as the incorporation of adaptive demand and price responses (Hallegatte, 2008), post-disaster inequalities and/or imbalances (Li et al., 2013), inventory dynamics and constraints (Hallegatte, 2014), demand redistribution through substitution of suppliers (Wenz et al., 2014), and endogenous capital recovery process and reconstruction demand (Zeng et al., 2019). Though important for determining disaster impacts and economic resilience, none of the existing studies has fully considered all these factors in their modelling framework. Previous models also tend to ignore the crowding-out effect of reconstruction costs on household consumption by assuming that these costs are largely funded by insurance companies (Hallegatte, 2008). However, as mentioned by Cochrane (2004), household demand decreases temporarily when the recovery is financed by local savings and borrowing, which thus should be considered in disaster impact analysis. Moreover, previous studies in this regard are either at the theoretical stage or case specific, with unverified applicability to a wider range of hazardous events. An integrated hybrid model that can reflect all possible constraints (such as capital restoration, inventory dynamics, and demand redistribution) and accommodate a multitude of hazard types in a broad context (including climate, pandemic, and political hazards) is still lacking.

This research gap, specifically the establishment of an improved hybrid model for indirect hazard impact assessment, is addressed in Chapter 3 of this thesis.

2) Studies on economic impacts of compound hazards are accumulating but still

limited.

Previous analysis on disaster impacts is often carried out for a single hazard at a time. Considering the increasing likelihood of compound hazards under climate change and ongoing COVID-19 pandemic, an emerging literature has advocated for analysis on the combined effects of multiple or interrelated hazards on socio-economic systems. However, many of these studies are in conceptual stages and qualitative manners. Quantitative analysis of the overall economic impacts resulting from compound hazards is still scarce.

Though some empirical studies have discovered the short-term synergistic health effects of heat and air pollution (Pascal et al., 2021; Scortichini et al., 2018) and of air pollution and COVID-19 lockdowns (Giani et al., 2020; Zhang et al., 2022), the drivers and mechanisms behind the reported interactions are still poorly understood (Sillmann et al., 2021).

Beyond that, even less attention has been paid to the indirect economic losses caused by compound hazards. An early study of Pauw et al. (2011) used a CGE model to estimate the annual production (or GDP) losses due to historical floods and droughts in Malawi. The study has emphasized the importance of considering all possible extreme weather events when evaluating the climate impacts, but it calculates the production loss for each individual event independently and ignores the chance of possible interactions between compound shocks to the economic system.

A more holistic assessment that considers the interactions between two successive floods was carried out by Zeng and Guan (2020). Their results confirmed that the economy would suffer larger losses than the sum of each induvial flood and take longer to return to its initial state, if the subsequent flood disrupts the recovery of capital damaged by the first flood. However, their analysis is limited to sequential flood

shocks for a hypothetical economy in a single region, and the applicability of their model to a wider range of compound hazards has yet to be verified.

In a post-pandemic world where climate and pandemic hazards are more likely to collide, most climate hazards such as floods are rapid-onset events which require immediate responses, while pandemic hazards such as COVID-19 last for longer periods and the corresponding control measures could be of various durations and intersect with different developing periods of climate hazards. Therefore, compound climate and pandemic hazards require a different way of accounting for the cumulative hazard impacts on the economic system. The very recent study of Dunz et al. (2021) takes a meaningful first step to embed these compound shocks within a macro-financial risk assessment framework, but their model only indirectly includes global supply chain shocks and thus cannot fully capture the cascading effects of individual or compound shocks across sectors and regions. The integration of IO based information, which can reveal how compound shocks are transmitted interactively through the economic network, is still required in future research to enhance understanding of the potential indirect economic impacts of compound hazards in complex scenarios.

This research gap, specifically the establishment of a compound hazard economic impact assessment model and its applications to case studies of various compound hazard crises, is addressed in Chapter 3, Chapter 6, and Chapter 7 of this thesis.

3) **There is an absence of integrated assessment on both direct and indirect economic impacts of future hazards in combination with climate change and socio-economic projections.**

Despite the rapid development of indirect hazard impact modelling, most of these models have only been applied to historical extreme events. Projections on future

changes have largely focused on population exposed and direct damage (usually to urban areas) (Alfieri et al., 2017; Ward et al., 2017; Winsemius et al., 2016). Integrated assessment on joint direct and indirect economic impacts of future hazards is relatively rare (Sieg et al., 2019). This is usually because the inclusion of indirect impact accounting would increase the model complexity and introduce more uncertainties.

Dottori et al. (2018) carried out a global fluvial flood risk assessment by estimating human losses, and direct and indirect economic impacts under a range of temperature and socio-economic scenarios. Nevertheless, they only considered welfare or consumption losses as a proxy of indirect impacts, ignoring changes in sectoral outputs.

Some other studies have evaluated the indirect economic consequences of future flood risks at the sectoral level for countries/regions including China, the US, and the EU, but with fixed socio-economic conditions (Koks et al., 2019; Willner et al., 2018). Given the long time-window (usually 30 years) adopted in most standard climate change studies, the time scale in hazard impact analysis should also be adjusted from the short term to the long term. However, most of previous studies only calculated the economic impacts shortly after the event with constant socio-economic conditions, which is not suitable for a long-term study. The evolution of demographic and economic indicators over the study periods should be incorporated into the impact analysis against the backdrop of climate change.

This research gap, specifically the comprehensive projection of direct and indirect economic impacts of future hazards considering changing climate and socio-economic conditions, is addressed in Chapter 5 of this thesis.

Chapter 3 Methodology: From Single-Hazard to Compound-Hazard Economic Impact Modelling

The purpose of this chapter is to fulfil Research Objectives 3 and 4, which are the improvement of single-hazard economic impact accounting and the development of the Compound-Hazard Economic Footprint Assessment (CHEFA) model. This contributes to Research Questions 2 and 3 raised in Section 1.4.1. As the CHEFA model draws on previous modelling experience for single-hazard analysis and uses the estimated direct impacts as inputs to assess the indirect impacts, this chapter starts with a detailed description of the accounting methods for both direct and indirect economic impacts under the single-hazard analytical framework (Section 3.1). More specifically, methods of direct impact assessment are introduced in Section 3.1.1 with a separate focus on three types of hazards (i.e., flooding, heat stress, and air pollution), which could represent a full range of possible shocks on production factors (i.e., capital and labour) and correspond to the applications in following chapters. Then for indirect impact assessment, the Disaster Footprint model, which is compatible with various single-hazard event settings, is established at the end of Section 3.1.2 following a methodological review on its theoretical origins and modelling grounds. This chapter culminates in a full picture of the CHEFA model for compound-hazard impact analysis, which integrates hazard interactions with other important factors such as recovery dynamics, inventory adjustment and cross-regional substitution (Section 3.2).

It should be noted that two versions of the Disaster Footprint model (i.e., DF-growth and DF-substitution) have been developed for single-hazard indirect impact analysis in Section 3.1.2.3. These two versions mainly differ in the assumptions about the decision rationale of economic sectors and the economic recovery target. The first

version, namely the DF-growth model, assumes that economic sectors make their production decisions based on optimization principles (i.e., output maximization) and thus belongs to the second type of hybrid models reviewed in Section 2.2.2.3. It also allows for economic growth and a recovery target above the initial economic state, which is suitable for the long-term analysis. By comparison, the second version, namely the DF-substitution model, assumes that the production, delivery, and consumption decisions are governed by ad-hoc behavioural rules (i.e., production extension, rationing scheme, and demand adaptation) and thus belongs to the first type of hybrid models reviewed in Section 2.2.2.3. It also assumes constant economic conditions and a recovery target at the pre-disaster level, which is suitable for the short-term analysis. The CHEFA model is then built on the DF-substitution model, as this version reflects more realistic recovery and response mechanisms in the short run and could be easily extended to accommodate hazard interactions.

The DF-growth model was constructed for an early work on projecting the economic impacts of fluvial floods in six vulnerable countries in the context of climate change and socio-economic development. In this study, estimations of indirect impacts were carried out at the single-national level over the 30-year baseline and future periods. Analysis on such broad spatial and temporal scales implies higher flexibility and more optimization behaviours, as well as the necessity of including economic growth, hence the application of the DF-growth model. Its detailed description is extracted from the paper:

Yin, Z.[#], **Hu, Y.**[#], Jenkins, K., …, Guan, D*. (2021). Assessing the economic impacts of future fluvial flooding in six countries under climate change and socio-economic development. *Climatic Change, 166*(3), 38. https://doi.org/10.1007/s10584-021-03059-3

The DF-substitution model was developed with increasing micro-foundations after full

consideration of important factors which may affect the economic recovery pathway in the disaster aftermath. These factors include dynamic production constraints, endogenized capital recovery, substitution between regions, overproduction capacity, inventory adjustment, etc. This version could be applied for analysis on finer spatial and temporal scales, such as a multi-regional analysis allowing for cross-regional substitution. It was applied for the assessment of economic impacts resulting from heat stress, air pollution, and extreme weather events in Chinese provinces, which has been or is to be published as parts of the China reports of the Lancet Countdown on health and climate change. The detailed model settings are presented in this chapter by integrating relevant contents from the supplemental materials of the reports listed below:

1) Cai, W.[#], Zhang, C.[#], Zhang, S.[#], …, **Hu, Y.**, …, Gong, P*. (2022). The 2022 China report of the Lancet Countdown on health and climate change: leveraging climate actions for healthy ageing. *The Lancet Public Health*. https://doi.org/10.1016/s2468-2667(22)00224-9

2) Cai, W.[#], Zhang, C.[#], Zhang, S.[#], …, **Hu, Y.**, …, Gong, P*. (2021). The 2021 China report of the Lancet Countdown on health and climate change: seizing the window of opportunity. *The Lancet Public Health,* *6*(12), e932-e947. https://doi.org/10.1016/S2468-2667(21)00209-7

Finally, the CHEFA model was developed for a work program of the World Bank on trade and climate change, in which a hypothetical perfect storm of flooding, pandemic control and export restrictions was used to illustrate the model applicability. The CHEFA model was then applied for the impact analysis of a real compound event of extreme floods and COVID-19 control in China, which has been published in the *China Journal of Econometrics*. This chapter describes the construct of the CHEFA model based on relevant contents from the following papers:

1) **Hu, Y.**, Wang, D., Huo, J., …, Chemutai, V. (2021). *Assessing the economic*

impacts of a 'perfect storm' of extreme weather, pandemic control and deglobalization: a methodological construct [Working Paper No. 160571]. World Bank. https://documents.worldbank.org/en/publication/744851623848784106

2) **Hu, Y.**, Yang, L., & Guan, D*. (2022). Assessing the economic impact of 'natural disaster-public health' major compound extreme events: a case study of the compound event of floods and COVID epidemic in Zhengzhou China (in Chinese). *China Journal of Econometrics, 2*(2), 257-290. https://doi.org/10.12012/CJoE2021-0090

Regarding the mathematical symbols and formulae, matrices are represented by bold uppercase letters (e.g., $\mathbf{X}$), vectors are represented by bold lowercase letters (e.g., $\mathbf{x}$), and scalars are represented by italic letters (e.g., x or X). Vectors are column vectors by default and the transposition is denoted by an apostrophe (e.g., $\mathbf{x}'$). The conversion from a vector to a diagonal matrix is expressed as a bold lowercase letter with a 'hat' (e.g., $\hat{\mathbf{x}}$). The operators '.*' and './' are used to express the element-by-element multiplication and element-by-element division of two vectors, respectively.

3.1. Methodology for Single-Hazard Economic Impact Assessment

3.1.1. Assessing the Direct Impacts

As defined in Section 2.1.2, this thesis uses 'direct disaster footprint' to denote the economic impacts caused by direct contact or exposure to hazards. These impacts include tangible or intangible damages to 1) physical assets, such as buildings, factories, machinery and equipment, infrastructure, land, and crops; and 2) human assets, such as human health and workability. Different types of hazards cause damages to different elements, either capital or labour, in the economic system. For

example, floods mainly result in capital inundation and destruction, while heat stress and air pollution only impair human health or labour productivity. These direct impacts are usually estimated using hazard-specific catastrophe models, which will be presented in the following sections.

3.1.1.1. Flood Events

For flood events, this thesis mainly illustrates the method of assessing the direct damage to capital assets. Although the labour supply, another key productive factor, may also be disrupted by flood events, data on flood-induced labour constraints is scarce or coarsely recorded. Therefore, the labour loss and recovery curves are usually developed exogenously using proxy variables (e.g., transport damage) and assumed influence and resilience parameters (Mendoza-Tinoco et al., 2020; Yin et al., 2021; Zeng et al., 2019). In addition, empirical evidence also shows that compared to the percentage reduction in capital stock, the relative losses of labour are often much lower, so that they have little effect on the final estimates of economic impacts resulting from a flood hazard (ibid.). On the other hand, capital damage is calculated for agricultural, residential, commercial and industrial land-use classes/sectors by linking the gridded flood data (mainly inundation depths and extent) with country- and sector-specific depth-damage functions and maximum damage values from Huizinga et al. (2017) based on the land cover map of the flooded region. The depth-damage functions provide estimates of the fractional damage (damage as a percentage of the associated maximum damage value) for a given flood depth per land-use class.

Key assumptions made in calculation of flood-related direct damage are listed below:

- Flood vulnerability (expressed by depth-damage functions and maximum damage values) of each country and sector is constant over the study period.
- Sub-national regions/grids within the same country share the same set of depth-damage functions and maximum damage values.

In particular, the direct damage to capital assets for each land-use sector or class in a grid cell can be calculated as below:

$$D_k^c = f_k\left(d^c\right) \times D_k^{\max} \times A_k^c . \quad (1)$$

Here D_k^m is the direct damage to land-use sector k in the grid cell c in monetary terms. $f_k\left(d^c\right)$ is the depth-damage function that expresses the fractional damage given the gridded flood depth d^c for land-use class k. $D_k^{\max}$ is the maximum damage value for land-use class k per square metre. A_k^c is the inundated area of land-use sector k within the grid cell c.

Then, the gridded direct damage is aggregated at the region level to obtain the total direct damage per land-use sector within the entire flooded region, as below:

$$D_k = \sum_c D_k^c . \quad (2)$$

Here D_k is total direct damage to capital assets for land-use sector k in monetary terms.

Note that this thesis does not include the transport and infrastructure (roads) sectors, which were considered in two studies (Alfieri et al., 2017; Dottori et al., 2018). This is mainly because the database does not provide depth-damage functions of these sectors for most of the regions (mainly developing countries) involved in the case studies in this thesis (Huizinga et al., 2017). Besides, the direct damage to the transport and infrastructure sectors in developing countries could be very low compared to other sectors (ibid.).

3.1.1.2. Heat Stress

Extensive literature has identified that heat stress can directly affect an economy through two channels: (1) by causing health impairment, and (2) by generating labour productivity loss (see Section 2.2.1.1). The former generally refers to the impacts of heat on mortality and morbidity from all-cause or a specific disease. Most research concentrates on heat-related mortality rather than morbidity mainly due to data limitations (Martiello and Giacchi, 2010; Turner et al., 2012), so does this thesis. Apart from health impairment, heat stress can also reduce labour productivity among workers and lead to wage or income loss. However, this type of heat impact has been given relatively little attention in hazard analysis to date. Drawing on the methodology from Yang et al. (2019) and Kjellstrom et al. (2018), this thesis incorporates both types of heat-induced direct impacts into analysis for a case study in China.

1) Heat-related mortality

This thesis estimates non-accidental heatwave-related deaths with special consideration of the impacts on the elderly by using age-specific exposure-response relationships. Here a heatwave event is defined as a period of three or more days where the daily maximum temperature is higher than the reference (92.5th percentile of daily maximum temperature between 1986 and 2005) in China. This definition is chosen among various heatwave definitions to best capture the health effects of heat events in China (Ma et al., 2014; Yang et al., 2019). The days of a heatwave are defined as the number of days within the heatwave event.

Several key assumptions are used as below:

- The exposure-response relationship between heatwave and mortality for each age group and region is constant during the study period.
- Sub-provincial regions/grids within the same province in China share the same set of exposure-response relationships, which are represented by the capital city of

that province.

- Different regions/grids in China have the same baseline annual non-accidental mortality rate.

The deaths attributable to the heatwave (AN) are first calculated at the grid level as below:

$$AN^c = Pop^c \times Mort \times HW^c \times AF^c . \quad (3)$$

Here Pop^c refers to the grid-level population size in the grid cell c. $Mort$ is the baseline daily non-accidental mortality rate. For the case of China, the mortality rate is obtained from China Statistical Yearbook, which is an annual statistic and adopts the same value for different grids in mainland China. Considering the fact that mortality has seasonal patterns with a marked excess of deaths in winter (Huang and Barnett, 2014), the mortality rate is multiplied by monthly mortality proportion and then divided by days per month as a pre-process in this thesis. HW^c is the grid-level heatwave days in the grid cell c within a year. AF^c denotes the attributable fraction, which is calculated as:

$$AF^c = \frac{\left(RR^c - 1\right)}{RR^c} . \quad (4)$$

Here RR is short for 'relative risk' indicating the increase in the risk of mortality during heatwave days compared to non-heatwave days. RR^c refers to the gridded RR by matching climate division-specific RR to the grid. The original RR values are derived from the exposure-response relationship between heatwave and mortality according to a previous work of Yang et al. (2019). Based on the general trend that risks are homogeneous in the same climate regions and higher in the north of China than those in the south (Chen et al., 2018), this thesis combines risks through meta-analysis according to the climate zones based on the basic risk distribution pattern.

By multiplying the baseline daily non-accidental mortality rate $Mort$ by the heatwave days within a year HW^c and an attribution fraction AF^c for each grid, the combination of the last three items on the right-hand side of Equation (3) derives the gridded annual mortality rate attributable to heatwaves. This is then multiplied by the grid-level population size Pop^c to finally obtain the gridded annual deaths due to heatwaves.

Then the gridded annual deaths due to heatwaves are aggregated at provincial and national levels to calculate the total heat-related deaths (AN) in the study regions. It should be noted that the above calculation is limited to the warm season, which is between May and September, in each year within the study period, as a previous study has shown that approximately 90% of deaths attributable to heatwaves occurred during these months of the year (Vaidyanathan et al., 2020).

In addition, this thesis also investigates the heat-related mortality by age group using the same method as mentioned above, except that the age-specific RR and population of a specific age group are used to replace the whole-age RR and whole population for calculation. The formula for subgroup analysis is as below:

$$AN_k^c = Pop_k^c \times Mort_k \times AgeP_k^c \times HW^c \times AF_k^c \,. \tag{5}$$

Here k is a categorical variable denoting one of the age groups. The case study in China is particularly focused on the vulnerability of the elderly in a changing climate, and thus divides the population into two groups, that is, people under and above 65 years. $AgeP_k^c$ is the proportion of people in the age group k among the total population.

2) Heat-related labour productivity loss

Firstly, several assumptions are used in the calculation of heat-related labour productivity loss as below:

- The exposure-response relationship between heat stress and work performance for each sector is constant over the study period.
- The agriculture and construction sectors involve outdoor high intensity work (at a metabolic rate of 400W), the manufacturing sector involves indoor medium intensity work (300W), and the service sector involves indoor low intensity work (200W).
- Different regions/grids within China share the same set of exposure-response relationships between heat stress and work performance, which are equivalent to the global levels.
- The sectoral employment rates in each grid are equivalent to the levels of the province where the grid is located.
- A labourer works 8 hours a day in China.

Then, the Wet Bulb Globe Temperature (WBGT), which is a commonly used heat stress index to measure the exposure-response relationship between climate variables and work performance, is estimated based on gridded (0.5°×0.5°) climate data. For indoor (or outdoor in the shadow) activities, the hourly WBGT in the shade (WBGT_shade) is calculated using air temperature and dew point temperature; and for outdoor activities, the hourly WBGT in the sun (WBGT_sun) is calculated using air temperature, dew point temperature, solar radiation, and wind speed. More details on the iteration calculation method can be obtained from Kjellstrom et al. (2018).

Thirdly, the fraction of work hours lost (WHL) in each sector is derived from the hourly WBGT level according to the cumulative normal distribution loss function (ERF) as below:

$$loss\ fraction = \frac{1}{2} \times \left(1 + \mathrm{ERF}\left(\frac{WBGT_{hourly} - Prod_{mean}}{\sqrt{2} \times Prod_{sd}} \right) \right). \quad (6)$$

Here $WBGT_{hourly}$ is the hourly WBGT_shade or WBGT_sun estimated in the first step. Then $Prod_{mean}$ and $Prod_{sd}$ indicate the fixed parameters for labourers working with different intensities, which are quantified by the thermal metabolic rates (see Table 3-1). For each cell grid, labours (also referred to as the working age population between 15-64 years old) are divided into four sectors: agriculture, construction, manufacturing, and service sectors. This study assumes that labours in the agriculture and construction sectors work at a metabolic rate of 400W, those in the manufacturing sector work at 300W and those in the service sector work at 200W. For the agriculture and construction sectors, which mainly involve outdoor work, the WBGT_sun is used to calculate the hourly work time loss caused by heat stress; while for the manufacturing and service sectors, which mainly involve indoor work, the WBGT_shade is used. It should be noted that the above loss function is originally developed on the global scale and whether it is appropriate for estimating WHL at the provincial level in China is still unknown. However, region-specific loss functions for China are not available so far.

Table 3-1: Input values for labour loss fraction calculation.

Metabolic rate	$Prod_{mean}$	$Prod_{sd}$
200W	35.53	3.94
300W	33.49	3.94
400W	32.47	4.16

Notes: W represents the unit of watts.

Fourthly, the grid-level population is multiplied by sectoral employment rates to calculate the working population in the four sectors in each grid cell during the study period. The sectoral employment rates in each grid cell are assumed to be equivalent

to the levels of the province where this grid cell is located.

Finally, it is assumed that a labourer works 8 hours a day (typically from 8 am to 5pm with an hour break from 12pm to 1pm), which is the legal working time stipulated by the Labour Law of China. For each sector in each cell grid, the hourly work time loss per worker in the third step is first multiplied by the number of labourers in the fourth step and then aggregated over all working hours within a year to calculate the total annual WHL caused by heat stress. The grid-level results can be summed up over all grid locations in each province (or in the country) to obtain the results at provincial or national levels.

3.1.1.3. Air Pollution

Numerous studies have shown that air pollution can directly affect an economy by causing increased mortality and morbidity (see Section 2.2.1.1). However, like heat stress, most research have focused on air pollution-related mortality rather than morbidity due to data limitations, and so does this thesis. In particular, this thesis quantifies the number of premature deaths attributable to long-term ambient fine particulate matter ($PM_{2.5}$) exposure by sectoral sources for each province in China as a case study. $PM_{2.5}$ is selected here as it is an air pollutant that has been most closely studied and is most commonly used as a proxy indicator of exposure to air pollution (WHO, 2005, 2016).

Several assumptions are used in the calculation of pre-mature deaths caused by $PM_{2.5}$ exposure as below:

- The concentration-response relationship between air pollution and premature mortality for each disease endpoint is constant over the study period.
- Different regions/provinces in China adopt the same set of concentration-response relationships between air pollution and premature mortality.

Premature deaths from total ambient $PM_{2.5}$ by province and sector in China are estimated following the methodology of the Global Burden of Disease (GBD) 2019 study (Murray et al., 2020), which relies on cause-specific concentration-response functions (ERFs) to calculate the relative risks (RRs) of mortality for six causes of deaths.

The meta-regressed Bayesian regularized trimmed (MR-BRT) curves are obtained from the public release site (IHME, 2021) and RRs for six diseases: ischaemic heart disease; chronic obstructive pulmonary disease; stroke; lung cancer; acute lower respiratory infection; and type II diabetes are calculated from them. 1000 draws of the MR-BRT curve for each disease and age group (where age specific) are used and scaled to have RR=1 at the theoretical minimum-risk exposure level (TMREL, taken from 1000 corresponding draws, average 4.15μgm^{-3}). Exposure levels below the TMREL level are assigned RR=1.

The concentration-response functions and RRs are based on the MR-BRT functions from the GBD 2019 study across the full range of $PM_{2.5}$ concentrations, as below:

$$RR_{IER}(C) = \begin{cases} 1, & \text{if } C < C_0 \\ 1 + \alpha \times \left\{ 1 - \exp\left[-\gamma \times (C - C_0)^{\delta} \right] \right\}, & \text{if } C \geq C_0 \end{cases}. \quad (7)$$

Here $RR_{IER}(C)$ represents the RRs in the $PM_{2.5}$ exposure concentration of C (in micrograms per meter cubed); C_0 indicates the counterfactual concentration below which it is assumed there is no additional risk. For very large C, $RR_{IER}(Z)$ approximates $1+\alpha$. A power of $PM_{2.5}$ (δ) is included to predict risk over a very large range of concentrations.

Then the $PM_{2.5}$-related premature mortality for each disease in each province of China can be calculated based on the above estimated RRs at different $PM_{2.5}$ concentration levels, as below:

$$M_{i,j} = P_i \times \hat{I}_j \times \left(RR_j\left(C_i\right) - 1\right), \quad \text{where } \hat{I}_j = \frac{I_j}{\overline{RR_j}}. \tag{8}$$

Here $M_{i,j}$ is the premature mortality of disease endpoint j attributable to ambient $PM_{2.5}$ in province i. $\hat{I}_j$ represents the hypothetical 'underlying incidence' (i.e., cause-specific mortality) rate of endpoint j that would remain if the $PM_{2.5}$ concentration levels are reduced to the TMREL level. P_i refers to the population size of province i. I_j is the reported regional average annual disease incidence (mortality) rate for endpoint j. C_i represents the annual average $PM_{2.5}$ concentration in province i. $RR_j\left(C_i\right)$ is the relative risk for endpoint j at $PM_{2.5}$ concentration C_i and $\overline{RR_j}$ denotes the average population-weighted relative risk for endpoint j.

It should be noted that the same ERF is used for all provinces in China due to a lack of evidence to identify more location-specific ERFs between air pollution and premature mortality. Besides, the above calculation is performed at the provincial level rather than the grid level as for floods and heat stress.

3.1.2. Assessing the Indirect Impacts

As defined in Section 2.1.2, this thesis uses 'indirect disaster footprint' to imply the subsequent economic impacts induced by direct consequences of hazards. These impacts include the business interruption of directly affected sectors and regions, the

propagation of initial disruptions along the production supply chain towards wider economic systems, and the costs of recovery processes. As the assessment of indirect disaster footprint is carried out at various levels of sectoral and regional details, the above estimated results of direct disaster footprint are aggregated or disaggregated into the corresponding sectors and regions before being fed into indirect disaster footprint accounting models. The main methodology used in this thesis to assess the indirect disaster footprint of a single-hazard event is the Disaster Footprint model, which is originated from the IO analytical framework and improved on the ARIO model following a hybrid approach. A full description of the development of the Disaster Footprint model, together with a methodological review on its theoretical origins and modelling grounds, is presented below.

3.1.2.1. IO Analysis for Disaster Events

IO analysis is a macroeconomic analytical framework developed by Wassily Leontief in the 1930s, considering the economic system as a circular flow of income and output among economic sectors through the production, distribution, and consumption processes (Miller and Blair, 2009). The fundamental purpose of the IO framework is to analyse the interdependence of economic sectors/industries in an economy using an IO table which contains basic information on interindustry transactions (ibid.). Due to its simplicity and capability to interpret sectoral interrelationships and economic structures, IO analysis has been widely used as a powerful tool for socio-economic analysis and extended to accommodate energy and environmental accounts or integrated with catastrophe models for interdisciplinary analysis on various geographical scales from local to global (ibid.).

The basic framework of IO analysis is built on the IO table/matrix, which records the flows of products from each industrial sector, considered as a producer, to each of the sectors, itself and others, considered as consumers, in monetary values, within an

economy during a given period, usually a year. Formulation of a basic IO table often uses socio-economic data assembled in the form of a system of national (or regional) economic accounts which is often routinely collected by means of a periodic census or some other surveys (Miller and Blair, 2009) (Chapter 4). These data include interindustry transactions, household income and expenditures, governmental taxes and purchases, savings and investment, imports and exports, etc. Details of interindustry transactions are usually obtained through a census or survey of all economic activities of firms involved in the economy.

Fundamental assumptions used in IO analysis are listed as below:

- Each sector makes only one unique product that cannot be substituted by the products of other sectors.
- Each sector uses inputs in fixed proportions to make its product, which is characterized as the Leontief production function.
- The units of inputs required from all other sectors to make one unit of product in each sector is constant over time.
- Primary inputs (e.g., labour and capital) are fully employed by sectors to carry out production in the pre-disaster equilibrium.
- The total output of each sector is equal to the total input used to make that amount of output during each period for an economy in the equilibrium.

As shown in Figure 3-1 below, the general structure of a basic Leontief IO table consists of four blocks of 1) intermediate transactions; 2) final demand; 3) primary input; and 4) gross domestic product. First, the intermediate transaction block (shaded in grey) describes the sales and purchases of products (denoted as $z_{i,j}$) from each industrial sector (e.g., sector i) to another industrial sector (e.g., sector j) for production. For the former sector i, $z_{i,j}$ is the units of outputs allocated to sector j

to satisfy the intermediate demand from sector j; while for the latter sector j, $z_{i,j}$ is the units of inputs received from sector i as intermediate inputs necessary for production. Second, the final demand block (shaded in green) records the units of outputs of each industrial sector directly purchased and consumed by various types of final users. In general, there are four types of final demand in an open economy, that is, household consumption expenditures, governmental purchase expenditures, capital formation or investment, and net exports (i.e., exports minus imports). Third, the primary input block (shaded in blue) represents the added values of each industrial sector from the primary (or non-industrial) inputs necessary for production. Labour and capital are two most important primary inputs for production, while sometimes other inputs such as land and entrepreneurship are also included. This block also implies the income received by owners of primary inputs from payments of industrial sectors, i.e., payments for employee compensation (labour services), governmental services (paid for in taxes), capital (interest payments), land (rental payments), entrepreneurship (profit), etc. Fourth, the gross domestic product block (shaded in yellow) indicates the total GDP in the economy by summing up all sources of income or expenditure of economic agents. Finally, the last row and column of the IO table refer to the total input and output of each industrial sector, respectively. The total input x_j of sector j equals to the total intermediate input $\sum_i z_{i,j}$ plus the total primary input $\sum_{q\in\{l,k\}} v_{q,j}$; the total output x_i of sector i is the sum of products allocated to satisfy the intermediate demand $\sum_j z_{i,j}$ and final demand $\sum_{p\in\{hc,gc,inv,ex\}} f_{i,p}$. For an economy in its equilibrium, the total input of each industrial sector should be equal to its total output.

		Producers as consumers (intermediate demand)					Final demand				Total output
	Sectors	*1*	…	*j*	…	*n*	Hous. purchases	Govt. purchases	Capital formation	Net Exports	
Producers (intermediate input)	*1*	$z_{1,1}$	…	$z_{1,j}$	…	$z_{1,n}$	$f_{1,hc}$	$f_{1,gc}$	$f_{1,inv}$	$f_{1,ex}$	x_1
	…	…	…	…	…	…	…	…	…	…	…
	i	$z_{i,1}$	…	$z_{i,j}$	…	$z_{i,1}$	$f_{i,hc}$	$f_{i,gc}$	$f_{i,inv}$	$f_{i,ex}$	x_i
	…	…	…	…	…	…	…	…	…	…	…
	n	$z_{n,1}$	…	$z_{n,j}$	…	$z_{n,n}$	$f_{n,hc}$	$f_{n,gc}$	$f_{n,inv}$	$f_{n,ex}$	x_n
Value added (primary input)	Labour	$v_{l,1}$	…	$v_{l,j}$	…	$v_{l,n}$	Gross domestic product				
	Capital	$v_{k,1}$	…	$v_{k,j}$	…	$v_{k,n}$					
Total input		x_1	…	x_j	…	x_n					

Figure 3-1: General structure of an IO table (in monetary values).

It should be noted that, in this basic form of the IO table, products used or consumed by industrial production (e.g., $z_{i,j}$) and final users (e.g., $f_{i,hc}$) contain not only domestic but also imported ones. The imports are subtracted from GDP by turning the export column into a net export column (i.e., exports minus imports). Another approach to record these imports is to add an import row above the total input row while keeping the original export column in the final demand block. In this way, intermediate use and final consumption of domestic products are distinguished from those of imported products, leading to an expanded IO table as illustrated in the book of Miller and Blair (2009) (p. 14). The choice of different forms of IO tables depends on specific research questions.

1) Technical coefficients and demand-driven Leontief IO model

In a balanced economy with n industrial sectors and a structure as shown in Figure 3-1, each row vector illustrates the allocation of output from a certain sector to the corresponding intermediate demand and final demand. The output of sector i can be expressed as:

$$x_1 = z_{1,1} + \ldots + z_{1,n} + f_{1,hc} + f_{1,gc} + f_{1,inv} + f_{1,ex} = \sum_{j=1}^{n} z_{1,j} + \sum_{p=1}^{4} f_{1,p}$$

$$\ldots$$

$$x_i = z_{i,1} + \ldots + z_{i,n} + f_{i,hc} + f_{i,gc} + f_{i,inv} + f_{i,ex} = \sum_{j=1}^{n} z_{i,j} + \sum_{p=1}^{4} f_{i,p} \quad . \tag{9}$$

$$\ldots$$

$$x_n = z_{n,1} + \ldots + z_{n,n} + f_{n,hc} + f_{n,gc} + f_{n,inv} + f_{n,ex} = \sum_{j=1}^{n} z_{n,j} + \sum_{p=1}^{4} f_{n,p}$$

Here, $f_{i,p}$ refers to the final demand for sector i's product by the p-th type of final consumers: $p=1$ is for household consumption, $p=2$ is for governmental expenditures, $p=3$ is for investment in capital formation, and $p=4$ is for net exports (i.e., exports minus imports).

The ratio of input of sector i's product to output of sector j's product can be derived by dividing $z_{i,j}$ by x_j. This ratio is called the technical coefficient or direct input coefficient, denoted by $a_{i,j}$, representing the units of product i required as the intermediate input to make one unit of product j. Mathematically, it is expressed as:

$$a_{i,j} = \frac{z_{i,j}}{x_j}. \tag{10}$$

Similarly, the ratio representing the units of primary input q (labour or capital) required to make one unit of product j is denoted by $d_{q,j}$ and expressed as:

$$d_{q,j} = \frac{v_{q,j}}{x_j}. \tag{11}$$

A basic assumption for IO analysis is that a sector uses inputs in fixed proportions. In other words, a proportional change in the output of a sector will result in the same proportional change in the use of all necessary inputs. Since technical coefficients are

fixed using an IO table for a given period, then the input proportions are fixed for all industrial sectors.

Corresponding to this basic assumption, the production function embodied in IO analysis for each sector is:

$$x_j = \min\left\{\text{for all } j \in \{1,...,n\},\ \frac{z_{i,j}}{a_{i,j}};\ \text{for all } q \in \{l,k\},\ \frac{v_{q,j}}{d_{q,j}}\right\}. \tag{12}$$

This is the so-called Leontief production function, which requires inputs in fixed proportions where a fixed amount of each input is required to produce one unit of output.

With the introduction of a set of fixed technical coefficients, Equation (9) can be rewritten by replacing each $z_{i,j}$ on the right by $a_{i,j} \times x_j$:

$$\begin{aligned}
x_1 &= a_{1,1} \times x_1 + ... + a_{1,n} \times x_n + f_{1,hc} + f_{1,gc} + f_{1,inv} + f_{1,ex} = \sum_{j=1}^{n} a_{1,j} \times x_j + \sum_{p=1}^{4} f_{1,p} \\
&... \\
x_i &= a_{i,1} \times x_1 + ... + a_{i,n} \times x_n + f_{i,hc} + f_{i,gc} + f_{i,inv} + f_{i,ex} = \sum_{j=1}^{n} a_{i,j} \times x_j + \sum_{p=1}^{4} f_{i,p} \\
&... \\
x_n &= a_{n,1} \times x_1 + ... + a_{n,n} \times x_n + f_{n,hc} + f_{n,gc} + f_{n,inv} + f_{n,ex} = \sum_{j=1}^{n} a_{n,j} \times x_j + \sum_{p=1}^{4} f_{n,p}
\end{aligned} \tag{13}$$

Further, these relationships can be represented compactly in matrix form:

$$\mathbf{x} = \mathbf{A} \times \mathbf{x} + \mathbf{f}\,. \tag{14}$$

Here $\mathbf{x}$ is the output vector of dimension $n \times 1$ denoting the output of each sector in the economy. $\mathbf{A}$ is the technical coefficient matrix of dimension $n \times n$ using $a_{i,j}$ as the i-th row and j-th column element. $\mathbf{f}$ is the final demand vector of dimension $n \times 1$ denoting the total final demand for each sector's product, i.e.,

$\sum_{p=1}^{4} f_{i,p}$.

Let $\mathbf{I}$ be the $n \times n$ identity matrix - ones on the main diagonal and zeros elsewhere, then Equation (14) can be further rewritten as:

$$\mathbf{x} = \left(\mathbf{I} - \mathbf{A}\right)^{-1} \times \mathbf{f} = \mathbf{L} \times \mathbf{f} \cdot \tag{15}$$

Here $\left(\mathbf{I} - \mathbf{A}\right)^{-1} = \mathbf{L} = \left[l_{i,j}\right]$ is the famous Leontief inverse or the total requirements matrix. The Leontief inverse is an economic multiplier measuring the spillover effects that arise between economic sectors. It shows explicitly the dependence of each of the gross outputs on the values of each of the final demands, or in other words, the gross outputs that are required to meet a certain set of final demands.

In the demand-driven Leontief IO model, the overall changes in sectoral output $\Delta\mathbf{x}$ due to an external shock to final demand $\Delta\mathbf{f}$ (e.g., an increase in final demand) can be easily derived from Equation (15) with the Leontief inverse:

$$\Delta\mathbf{x} = \mathbf{L} \times \Delta\mathbf{f} \cdot \tag{16}$$

Noting that the Taylor expansion of the Leontief inverse is $\mathbf{L} = \left(\mathbf{I} - \mathbf{A}\right)^{-1} = \left(\mathbf{I} + \mathbf{A} + \mathbf{A}^2 + \mathbf{A}^3 + ...\right)$, Equation (16) can be found as:

$$\Delta\mathbf{x} = \left(\mathbf{I} + \mathbf{A} + \mathbf{A}^2 + \mathbf{A}^3 + ...\right) \times \Delta\mathbf{f} = \Delta\mathbf{f} + \mathbf{A} \times \Delta\mathbf{f} + \mathbf{A}^2 \times \Delta\mathbf{f} + \mathbf{A}^3 \times \Delta\mathbf{f} + ... \cdot \tag{17}$$

Initially, an increase in final demand for the product of a sector will directly cause that sector to increase its output by the same amount. This is the ‘first round’ of effects or the direct impacts of a final demand shock, as found in the first item of the rightmost side of Equation (17), namely $\Delta\mathbf{f}$ itself. Then, these increased outputs would generate a need for additional inputs from ‘upstream’ sectors, causing a ‘second round’

of increase in sectoral output, as found in the second item $\mathbf{A} \times \Delta \mathbf{f}$; and so forth. As a result, these 'round-by-round' effects accumulate through backward linkages between sectors and the cumulative effects after the first round are called the indirect impacts of the shock. The indirect impacts are caused by higher-order industrial inter-dependencies and measured by $\left(\mathbf{A} \times \Delta \mathbf{f} + \mathbf{A}^2 \times \Delta \mathbf{f} + \mathbf{A}^3 \times \Delta \mathbf{f} + ...\right)$.

This standard Leontief IO model is called a demand-driven model as it mainly considers disruptions in final demand and examines the backward rippling effects through the production supply chain. However, it has been criticized for its inability to handle supply constraints or shortages which are more likely to happen during a disaster (Hallegatte, 2008; Okuyama, 2007; Okuyama and Santos, 2014).

2) Allocation coefficients and supply-driven Ghosh model

By contrast, Ghosh (1958) presented an alternative IO model with a focus on the supply-side of the economy. This model is used to calculate sectoral gross production changes caused by disruptions in primary inputs. Recalling the economic structure as shown in Figure 3-1, each column vector represents the intermediate input and primary input used to support the production of a certain sector. The total input, which in a balanced economy is equal to the total output, of sector j can be expressed as:

$$\begin{aligned} x_1 &= z_{1,1} + ... + z_{n,1} + v_{l,1} + v_{k,1} = \sum_{i=1}^{n} z_{i,1} + \sum_{q=1}^{2} v_{q,1} \\ &... \\ x_j &= z_{1,j} + ... + z_{n,j} + v_{l,j} + v_{k,j} = \sum_{i=1}^{n} z_{i,j} + \sum_{q=1}^{2} v_{q,j} \\ &... \\ x_n &= z_{1,n} + ... + z_{n,n} + v_{l,n} + v_{k,n} = \sum_{i=1}^{n} z_{i,n} + \sum_{q=1}^{2} v_{q,n} \end{aligned} \quad . \tag{18}$$

Here $v_{q,j}$ refers to the q-th type of primary inputs consumed by the production of sector j: $q = 1$ is for labour input and $q = 2$ is for capital input.

By diving $z_{i,j}$ by x_i, a set of allocation coefficients or direct output coefficients, denoted by $b_{i,j}$, are derived:

$$b_{i,j} = \frac{z_{i,j}}{x_i}. \tag{19}$$

These $b_{i,j}$ coefficients stand for the distribution of sector i's outputs across sectors j that purchase intermediate inputs from sector i. Comparing the demand-driven Leontief IO model which uses technical coefficients by dividing each column of the intermediate transaction matrix by the gross output of the sector associated with that column, the supply-driven Ghosh model takes a rotated or transposed view from vertical to horizontal and uses allocation coefficients by dividing each row of the intermediate transaction matrix by the gross output of the sector associated with that row.

On the notion of allocation coefficients, Equation (18) can be rewritten by replacing each $z_{i,j}$ on the right by $b_{i,j} \times x_i$:

$$\begin{aligned}
x_1 &= b_{1,1} \times x_1 + \ldots + b_{n,1} \times x_n + v_{l,1} + v_{k,1} = \sum_{i=1}^{n} b_{i,1} \times x_i + \sum_{q=1}^{2} v_{q,1} \\
&\ldots \\
x_j &= b_{1,j} \times x_1 + \ldots + b_{n,j} \times x_n + v_{l,j} + v_{k,j} = \sum_{i=1}^{n} b_{i,j} \times x_i + \sum_{q=1}^{2} v_{q,j}. \\
&\ldots \\
x_n &= b_{1,n} \times x_1 + \ldots + b_{n,n} \times x_n + v_{l,n} + v_{k,n} = \sum_{i=1}^{n} b_{i,n} \times x_i + \sum_{q=1}^{2} v_{q,n}
\end{aligned} \tag{20}$$

Further, these relationships can be represented compactly in matrix form:

$$\mathbf{x}' = \mathbf{x}' \times \mathbf{B} + \mathbf{v}'. \tag{21}$$

Here $\mathbf{B}$ is the allocation coefficient matrix of dimension $n \times n$ using $b_{i,j}$ as the i -th row and j -th column element. $\mathbf{v}'$ is the transposed value added or primary input vector of dimension $1 \times n$ denoting the total value added of each sector, i.e., $\sum_{q=1}^{2} v_{q,j}$.

Following simple transformations, Equation (21) can be found as:

$$\mathbf{x}' = \mathbf{v}' \times \left(\mathbf{I} - \mathbf{B}\right)^{-1} \cdot \tag{22}$$

Defining $\mathbf{G} = \left(\mathbf{I} - \mathbf{B}\right)^{-1}$ with elements $g_{i,j}$, which has been called the output inverse, in contrast to the usual Leontief inverse or input inverse $\mathbf{L} = \left(\mathbf{I} - \mathbf{A}\right)^{-1} = \left[l_{i,j}\right]$, Equation (22) can be rewritten with the resulting vector of gross output in a row as:

$$\mathbf{x}' = \mathbf{v}' \times \mathbf{G}\,, \tag{23}$$

or in a column as:

$$\mathbf{x} = \mathbf{G}' \times \mathbf{v} \cdot \tag{24}$$

The element $g_{i,j}$ indicates the total value of production that comes about in sector j from each unit of primary input in sector i.

Then, an external shock to primary input, i.e., changes in $\mathbf{v}$, would cause associated changes in sectoral gross output as:

$$\Delta\mathbf{x} = \mathbf{G}' \times \Delta\mathbf{v} \cdot \tag{25}$$

Similar with the Leontief inverse, the Taylor expansion of the output inverse is:

$$\mathbf{G} = \left(\mathbf{I} - \mathbf{B}\right)^{-1} = \mathbf{I} + \mathbf{B} + \mathbf{B}^2 + \mathbf{B}^3 + \ldots \cdot \tag{26}$$

And the overall changes of sectoral gross output resulting from a primary input

disruption can be expressed as:

$$\Delta \mathbf{x} = \left(\mathbf{I} + \mathbf{B} + \mathbf{B}^2 + \mathbf{B}^3 + ...\right)' \times \Delta \mathbf{v} = \Delta \mathbf{v} + \mathbf{B}' \times \Delta \mathbf{v} + \mathbf{B}'^2 \times \Delta \mathbf{v} + \mathbf{B}'^3 \times \Delta \mathbf{v} + ... \cdot \quad (27)$$

In the supply-driven Ghosh model, the direct impact of a primary input disruption, say a decrease in primary input of sector j, refers to the 'first-round' or initial reduction in sector j's output by the same amount, as found in the first item of the rightmost side of Equation (27), i.e., $\Delta \mathbf{v}$ itself. However, the reduced output of sector j will cause a shortage of supply to 'downstream' sectors that purchase sector j's product as an intermediate input for production, leading to a 'second round' of decrease in sectoral output, as found in the second item $\mathbf{B}' \times \Delta \mathbf{v}$; and so forth. The cumulative reductions in sectoral output after the first round (i.e., $\mathbf{B}' \times \Delta \mathbf{v} + \mathbf{B}'^2 \times \Delta \mathbf{v} + \mathbf{B}'^3 \times \Delta \mathbf{v} + ...$) are called the indirect or higher-order impacts of this primary input disruption.

The Ghosh model is derived following similar mathematical procedures with the Leontief IO model, except that it takes a rotated view of the IO table and introduces the concept of allocation coefficients. It is a supply-driven model as it is focused on disruptions in the primary input or supply-side of the economy and traces the forward rippling effects along the production supply chain. However, it ignores the possibility of final demand changes during a disaster and the backward rippling effects as described in the Leontief model.

The basic assumption of the Ghosh model is that the allocation coefficients $b_{i,j}$, rather than the technical coefficients $a_{i,j}$ as in the Leontief IO model, are fixed during the disruption and its aftermath. In other words, the output distribution among downstream customers is stable and proportional to the total output for each sector in the economic system. To explain this assumption, Ghosh (1958) proposed a planned economy experiencing severe supply shortages or excess demand, with government-imposed

restrictions on supply patterns. This assumption may be not a very general situation in much of the modern economy, but supply shortages can still happen during special times after a disaster. Giarratani (1981) suggested a possibly broader context where voluntary supply decisions occur given supply shortages or the disruption of some basic commodity. Firms may try to maintain their existing markets by allocating available products based on deliveries in normal times.

However, the assumption of constant allocation coefficients has caused another problem which makes the Ghosh model subjected to criticisms for its plausibility in the impact analysis. Oosterhaven (1988) pointed out that "the essential notion of production requirements, i.e., the production function, is actually abandoned", and that "input ratios vary arbitrarily and may, in principle, assume any value depending upon (again) the availability of supply". Considering an external shock that reduces the primary input only in sector j, Equation (25) in the Ghosh model implies that such a primary input reduction in sector j will be transmitted forward along the supply chain and cause output reductions in all sectors that purchase intermediate input from sector j, without any corresponding decreases in their use of primary input. This violates the notion of sectoral production functions where intermediate and primary inputs are used in fixed proportions.

In fact, this raises the issue of 'joint stability' as discussed by Rose and Allison (1989) and Miller and Blair (2009). Given the proven similarity between the technical coefficient matrix $\mathbf{A}$ and the allocation coefficient matrix $\mathbf{B}$, which is found as $\mathbf{A} = \hat{\mathbf{x}} \times \mathbf{B} \times \hat{\mathbf{x}}^{-1}$, inconsistency arises between the requirements of the supply-driven Ghosh model and the demand-driven Leontief model. More specifically, when the supply-driven Ghosh model is used for impact analysis, the allocation coefficient matrix $\mathbf{B}$ and the corresponding output inverse $\mathbf{G}$ are assumed to be constant, and then in general the technical coefficient matrix $\mathbf{A}$ and the corresponding Leontief

inverse $\mathbf{L}$ cannot remain constant due to their connections (unless each sector's output changes at the same rate); on the other hand, when the demand-driven Leontief model is used, the requirements of constant $\mathbf{A}$ and $\mathbf{L}$ generally imply non-constant $\mathbf{B}$ and $\mathbf{G}$ in the related supply-driven Ghosh model. However, several studies concluded that such instability in actual empirical applications was not a major issue, as changes in the corresponding technical coefficients were well within conventional tolerance levels when applying the supply-driven Ghosh model to a representative region (Rose and Allison, 1989), particularly for small supply-side shocks (Gruver, 1989).

3.1.2.2. The Adaptive Regional Input-Output (ARIO) Model

Traditional IO models, such as the Leontief IO model and the Ghosh model presented in the previous section, are typically focused on disruptions to one side (either the demand side or the supply side) of the economy and their rippling effects in one direction (either backward or forward) along the supply chain, whereas losing the perspective from the other side or direction. Another limitation of traditional IO models is their rigid assumptions about economic responses towards disasters. For instance, economic agents cannot respond to supply shortages by switching to alternative suppliers that are not affected by the disaster. To overcome these limitations, Hallegatte (2008) developed an Adaptive Regional Input-Output (ARIO) model to investigate the economic costs of natural disasters by taking into account sectoral production capacities and both backward and forward propagations within the economic system, as well as adaptive behaviours in the disaster aftermath. This original ARIO model was later improved by Hallegatte (2014) to incorporate inventory effects in the production system. Overall, the ARIO model adopts a hybrid modelling approach and has been widely used in disaster impact analysis as it can well represent production processes and supply-demand interactions at the inter-industrial level (Guan et al., 2020; Hallegatte et al., 2013; Hallegatte et al., 2011; Liu et al., 2021; Wu

et al., 2012; Zhang, Li, Xu, et al., 2018).

Key assumptions made for the original ARIO model (first version) and the ARIO-inventory model (second version) are listed in Table 3-2.

Below is the basic framework of the ARIO model, integrated from the two versions developed by Hallegatte (2008, 2014). The ARIO model is based on local IO tables where productions and demands are linked through the relationships as:

$$\overline{Y}(i) = \sum_j \overline{A}(i,j) \times \overline{Y}(j) + \overline{TFD}(i). \quad (28)$$

This is similar with Equation (13) for the conventional Leontief IO model, describing flows of the output of each sector (e.g., sector i) to its downstream customers. $j = 1,...,N$ for all industrial sectors in the economy. The local IO table used here is different from traditional IO tables as imports are removed to distinguish between inputs produced locally – and therefore potentially impacted by a disaster – and inputs produced outside the region and imported. Correspondingly, $\overline{A}(i,j)$ is the technical coefficient implying the intermediate consumption of local product i by sector j to make one unit of its product before the disaster. Besides, sector j also needs to import $\overline{I}(j)$ units of an aggregate product to make one unit of its product before the disaster. $\overline{Y}(i)$ and $\overline{TFD}(i)$ are the output and total final demand of sector i, respectively, in the pre-disaster economic equilibrium where supply matches demand. The overbars are used to indicate values at the pre-disaster levels.

Table 3-2: Key assumptions used in the original ARIO model and the ARIO-inventory model respectively.

Assumptions	Original ARIO model	ARIO-inventory model
Common assumptions	• The economy consists of many households that have a fixed bundle of consumption and N industrial sectors which exchange intermediate consumption products, import products from outside the region, make final consumption products for local demand, and export products outside the region. • Each industrial sector makes a unique product with inputs from all other sectors necessary for its production. • The Leontief production function is adopted, that is, each sector uses inputs in fixed proportions to make its product. • Imports are not constrained by the disaster. • Approximately four units of capital are needed to produce one unit of annual value-added in each sector. • Reconstruction expenditures are largely funded by insurance claims, which do not have a crowding-out effect on other consumption. • If the production of a sector is insufficient to satisfy all its demand, it can increase the production capacity towards the maximum in a certain time.	
Special assumptions	• If a sector cannot produce enough to satisfy the demand, its production goes first to intermediate consumption from other sectors and is then proportionally rationed among various final demands including local final demand, exports, and reconstruction demand (prioritized-proportional rationing scheme). • Local final demand/exports depend on price dynamics, which respond linearly to the level of underproduction, and the adapted local final demand/exports in the disaster aftermath. • If a sector cannot produce enough to satisfy the demand, and if the product made by this sector is substitutable, then its customers shift away regularly to other producers in a certain time.	• The production of a sector is distributed to intermediate demand and various final demands proportionally (proportional rationing scheme). • There are stockable and non-stockable products; and the inventory of a non-stockable product is not larger than the amound required to sustain three days of production. • The characteristic time of inventory restoration is identical in all sectors (except for non-stockable products). • Disaster impacts are heterogeneous among production units (firms) within each sector.

Normally, the total final demand is equal to the sum of final demand from both local and foreign consumers (i.e., local final demand $LFD(i)$ and exports $E(i)$); however, following a disaster, the reconstruction demand for repairing damaged capital is added to the total final demand, and thus the supply-demand relationships become:

$$Y(i) = \sum_j A(i,j) \times Y(j) + \overbrace{LFD(i) + E(i) + HD(i) + \sum_j RD(j,i)}^{\text{Total Final Demand } (TFD(i))}. \quad (29)$$

Considering a disaster that hits the economy at $t = 0$ and destroys both household physical assets and industry productive capital, then the need for repairing these damages requires additional inputs from industrial sectors, especially those involved in the reconstruction process. The reconstruction demand of sector j for inputs from sector i is represented by $RD(j,i)$, and the reconstruction demand of households for inputs from sector i is represented by $HD(i)$. Labour constraint is not considered here.

1) The original ARIO model (first version)

On the production side, the first-guess production of each sector $Y^1(i)$ is based on the minimum of the production capacity $Y^{\max}(i)$ and the first-guess total demand $TD^0(i)$ at each time step t[6] (Equation (30)). The first-guess total demand $TD^0(i)$ can be derived by solving Equation (29), which is $\mathbf{Y} = \mathbf{A} \times \mathbf{Y} + \mathbf{TFD}$ in the matrix form, to obtain the required production to satisfy the total demand (Equation (31)). The production capacity $Y^{\max}(i)$ is determined by the pre-disaster output level, disaster damages $TRD(i)$, and an overproduction capacity $\alpha(i)$, as in Equation (32).

[6] For equations in this section, variables depend on the time step t, which is omitted for simplicity.

Before the disaster, the amount of capital in each sector is approximately $\overline{K}(i) \approx 4 \times \overline{VA}(i)$, where $\overline{VA}(i)$ is the pre-disaster annual value-added of that sector. $TRD(i)$ is the total amount of capital damaged by the disaster in sector i, which is equal to $\sum_j RD(i,j)$. Therefore, the second item of the right-hand side of Equation (32) measures the percentage of remaining capital stock and thus remaining production capacity in sector i following the disaster. This is due to the assumption of the Leontief production function, where the production capacity is proportional to the available capital input. $\alpha(i)$ is the capacity to overproduce, if necessary, which will be described in the adaptation part (Equations (54) and (55)).

$$Y^1(i) = \min\left\{Y^{\max}(i); TD^0(i)\right\}, \tag{30}$$

$$\left\{TD^0(i)\right\} = \mathbf{TD^0} = \mathbf{Y^0} = (\mathbf{I} - \mathbf{A})^{-1} \times \mathbf{TFD}, \tag{31}$$

$$Y^{\max}(i) = \overline{Y}(i) \times \left[1 - \frac{TRD(i)}{4 \times \overline{VA}(i)}\right] \times \alpha(i). \tag{32}$$

However, production bottlenecks may occur in the disaster aftermath when the first-guess output, affected by capital input constraints and final demand changes, cannot provide sufficient intermediate inputs to support the whole economic system to produce that output. Given that sectors need to purchase the necessary intermediate inputs to carry out their production, the first-guess orders for product i from all the upstream clients $O^1(i)$ are therefore calculated as Equation (33). Two possible scenarios are then considered to cope with the issue of production bottlenecks. First, if $Y^1(i) \geq O^1(i)$, this means that sector i can provide enough products to satisfy the intermediate demand from all its buying sectors and the production of these upstream sectors is not affected. Second, if $Y^1(i) < O^1(i)$, then sector i cannot provide enough products to satisfy the intermediate demand from its buying sectors and the

production of these upstream sectors will be limited by the availability of product i. In the second case, the first-guess output of sector i will be rationed among its buyers in proportions to the orders they have placed and the production of each buying sector j is bounded by $\frac{Y^1(i)}{O^1(i)} \times Y^1(j)$. Therefore, the second-guess production of each sector $Y^2(i)$ is given by Equation (34).

$$O^1(i) = \sum_j A(i,j) \times Y^1(j), \tag{33}$$

$$Y^2(i) = \min\left\{ Y^1(i);\ \text{for all } j,\ \frac{Y^1(j)}{O^1(j)} \times Y^1(i) \right\}. \tag{34}$$

Here imports are assumed to be never constrained. If the second-guess output vector of all sectors ($\mathbf{Y}^2 = \{Y^2(i)\}$) is equal to the first-guess output vector ($\mathbf{Y}^1 = \{Y^1(i)\}$), then there is no production bottleneck and $\mathbf{Y}^2$ is the actual production. Otherwise, the production bottleneck occurs, and a new total demand is generated as:

$$TD^1(i) = TFD(i) + \sum_j A(i,j) \times Y^2(j). \tag{35}$$

This bottleneck calculation is iterated by repeating Equations (30)-(35) with $\{TD^1(i)\}$ instead of $\{TD^0(i)\}$ until convergence of the output vector $\mathbf{Y}^k$. This convergence will eventually occur, as productions of all sectors decline at each iteration and are bounded by zero.

The final values for total demand and output will be denoted as $TD^\infty(i)$ and $Y^\infty(i)$, respectively. $Y^\infty(i)$ is then the actual output of each sector after solving the issue of production bottleneck, which means all intermediate demand could be satisfied with $Y^\infty(i) \geq O^\infty(i)$. Yet, according to Equation (30), $Y^\infty(i)$ may be still less than or

equal to $TD^{\infty}(i)$. If $Y^{\infty}(i) = TD^{\infty}(i)$, then sector i can satisfy both the intermediate and final demands it faces. However, if $Y^{\infty}(i) < TD^{\infty}(i)$, then a mixed rationing scheme is adopted by sector i regarding the distribution of its outputs among different types of demands. Hallegatte (2008) has described this rationing scheme as "a mix of priority system and proportional rationing", in which intermediate demands from other sectors are satisfied with priority and then the remaining outputs are rationed proportionally among various final demands including local final demand, exports, and reconstruction demand (Equations (36)-(40)). This rationing scheme is designed based on the observed fact that "business-to business relationships are most of the time deeper than business-to-household relationships and a business would often favour business clients over household clients".

$$O^{\infty}(i) = \sum_{i} A(i,j) \times Y^{\infty}(j), \tag{36}$$

$$LFD^{\infty}(i) = LFD(i) \times \frac{Y^{\infty}(i) - O^{\infty}(i)}{Y^{0}(i) - O^{0}(i)}, \tag{37}$$

$$E^{\infty}(i) = E(i) \times \frac{Y^{\infty}(i) - O^{\infty}(i)}{Y^{0}(i) - O^{0}(i)}, \tag{38}$$

$$\Delta HD(i) = HD(i) \times \frac{Y^{\infty}(i) - O^{\infty}(i)}{Y^{0}(i) - O^{0}(i)}, \tag{39}$$

$$\Delta RD(j,i) = RD(j,i) \times \frac{Y^{\infty}(i) - O^{\infty}(i)}{Y^{0}(i) - O^{0}(i)}. \tag{40}$$

Then the damaged household physical assets and industry productive capital can be restored at each time step through the satisfaction of reconstruction demand, as below:

$$HD(i) - \Delta HD(i) \times \Delta t \xrightarrow{\Delta t} HD(i), \tag{41}$$

$$RD(j,i) - \Delta RD(j,i) \times \Delta t \xrightarrow{\Delta t} RD(j,i). \tag{42}$$

Here Δt is the time step of the model.

On the final demand side, local final demand $LFD(i)$ is assumed to depend on price dynamics $p(i)$ and the adapted local final demand $\widetilde{LFD}(i)$, as in Equation (43). The adapted local final demand $\widetilde{LFD}(i)$ is the adapted final consumption by local consumers if prices remain at the pre-disaster levels, which will be described in the adaptation part (Equations (46) and (50)). Price dynamics $p(i)$ is given by the simple relationship where the price of product i, which is normalized at one before the disaster ($p_0(i)=1$), is positively and linearly correlated to the excess demand over the production capacity, with a price elasticity γ_p (Equation (44)). The macroeconomic indicator M is measured by the ratio of total earnings (profit plus wages) in the disaster aftermath to total earnings in the pre-disaster situation. ξ is the elasticity of local final demand with respect to the product price for all sectors.

$$LFD(i) = M \times \widetilde{LFD}(i) \times \left[1 - \xi \times \left(p(i) - 1\right)\right], \tag{43}$$

$$p(i) = p_0(i) \times \left(1 + \gamma_p \times \frac{TD^{\infty}(i) - Y^{\infty}(i)}{Y^{\infty}(i)}\right). \tag{44}$$

Exportations are calculated in the similar way, except that there is no influence of the local macroeconomic indicator M :

$$E(i) = \widetilde{E}(i) \times \left[1 - \xi \times \left(p(i) - 1\right)\right]. \tag{45}$$

Here $\widetilde{E}(i)$ is the adapted exportations as defined in the adaptation part (Equations (47) and (51)).

Reconstruction demands are raised by industrial sectors and households as they need inputs from the reconstruction sectors (e.g., the construction sector and the

manufacturing sector) to restore their productive capital or other physical assets destroyed by the disaster. As such, these demands will decrease gradually with the accumulation of recovered capital, as described in Equations (41) and (42) above. The model assumes that reconstruction expenditures do not have a crowding-out effect on other types of consumption as they are largely funded by insurance claims, government spending, borrowing, or the use of savings. Reconstruction demand is also insensitive to price changes and the microeconomic situation.

Finally, the ARIO model considers three kinds of adaptation behaviours of economic agents in the disaster aftermath: final demand adaptation, intermediate-consumption adaptation, and production adaptation. These adaptations are assumed to be independent of price changes and only driven by quantities.

The first two types of adaptations are based on the ability of consumers to delay their orders or turn to external suppliers outside the disaster region when local suppliers cannot provide sufficient products in need. The model distinguishes between transportable products and non-transportable products, with only the former ones being able to be substituted by external sources. For a sector making a substitutable product i, if it cannot satisfy all the demand it faces, i.e., $Y^{\infty}(i) < TD^{\infty}(i)$, then the adapted local final demand $\widetilde{LFD}(i)$ and the adapted exports $\widetilde{E}(i)$ will decrease gradually to zero with characteristic times $\tau_{LFD}^{\downarrow}$ and $\tau_{E}^{\downarrow}$, respectively (Equations (46) and (47)). Similarly, the intermediate consumption by sector j of product i will decrease, and imports by sector j will increase by the corresponding amount, with a characteristic time $\tau_{A}^{\downarrow}$, for each unit of production in sector j (Equations (48) and (49)).

$$\widetilde{LFD}(i) - \frac{TD^{\infty}(i) - Y^{\infty}(i)}{TD^{\infty}(i)} \times \widetilde{LFD}(i) \times \frac{\Delta t}{\tau_{LFD}^{\downarrow}} \xrightarrow{\Delta t} \widetilde{LFD}(i), \tag{46}$$

$$\widetilde{E}(i)-\frac{TD^{\infty}(i)-Y^{\infty}(i)}{TD^{\infty}(i)}\times\widetilde{E}(i)\times\frac{\Delta t}{\tau_E^{\downarrow}}\xrightarrow{\Delta t}\widetilde{E}(i), \tag{47}$$

$$A(j,i)-\frac{TD^{\infty}(i)-Y^{\infty}(i)}{TD^{\infty}(i)}\times A(j,i)\times\frac{\Delta t}{\tau_A^{\downarrow}}\xrightarrow{\Delta t}A(j,i), \tag{48}$$

$$I(j)+\frac{TD^{\infty}(i)-Y^{\infty}(i)}{TD^{\infty}(i)}\times A(j,i)\times\frac{\Delta t}{\tau_A^{\downarrow}}\xrightarrow{\Delta t}I(j). \tag{49}$$

However, when the sector i is recovered from the disaster and can supply enough products in need, i.e., $Y^{\infty}(i)=TD^{\infty}(i)$, the shifted final and intermediate customers or demands will return to sector i with a different set of characteristic times (i.e., $\tau_{LFD}^{\uparrow}$, $\tau_E^{\uparrow}$, and $\tau_A^{\uparrow}$), and the imports of its upstream (buying) sectors will fall back to the pre-disaster level correspondingly, as below:

$$\widetilde{LFD}(i)+\left(\varepsilon+\frac{\widetilde{LFD}(i)}{\overline{LFD}(i)}\right)\times\left(\overline{LFD}(i)-\widetilde{LFD}(i)\right)\times\frac{\Delta t}{\tau_{LFD}^{\uparrow}}\xrightarrow{\Delta t}\widetilde{LFD}(i), \tag{50}$$

$$\widetilde{E}(i)+\left(\varepsilon+\frac{\widetilde{E}(i)}{\overline{E}(i)}\right)\times\left(\overline{E}(i)-\widetilde{E}(i)\right)\times\frac{\Delta t}{\tau_E^{\uparrow}}\xrightarrow{\Delta t}\widetilde{E}(i), \tag{51}$$

$$A(j,i)+\left(\varepsilon+\frac{A(j,i)}{\overline{A}(j,i)}\right)\times\left(\overline{A}(j,i)-A(j,i)\right)\times\frac{\Delta t}{\tau_A^{\uparrow}}\xrightarrow{\Delta t}A(j,i), \tag{52}$$

$$I(j)-\left(\varepsilon+\frac{A(j,i)}{\overline{A}(j,i)}\right)\times\left(\overline{A}(j,i)-A(j,i)\right)\times\frac{\Delta t}{\tau_A^{\uparrow}}\xrightarrow{\Delta t}I(j). \tag{53}$$

Here, ε is a small positive value (e.g., 0.01) ensuring that $\widetilde{LFD}(i)$ and $\widetilde{E}(i)$ could return to their pre-disaster levels, i.e., $\overline{LFD}(i)$ and $\overline{E}(i)$, respectively, even if they have decreased to zero. The exact value of ε has no significant impact on the results. The two different sets of characteristic times ($\tau^{\downarrow}$ and $\tau^{\uparrow}$) specify how fast consumers shift away from and back to the initial suppliers according to the dynamic relationship between supply and demand.

The third type of adaptation is associated with sectors' capacity to overproduce in response to demand surges or production shortages. The fact that sectors are rarely at full employment of their production capacities makes instantaneous overproduction possible during crisis. This process is modelled with the introduction of an overproduction capacity variable $\alpha(i)$. When the production of a sector cannot satisfy its total demand, i.e., $Y^{\infty}(i) < TD^{\infty}(i)$, $\alpha(i)$ will increase up to a maximum value $\alpha^{\max}$ in a time delay τ_{α} (Equation (54)). When the situation is back to normal, i.e., $Y^{\infty}(i) = TD^{\infty}(i)$, this overproduction capacity will go back to its pre-disaster level $\overline{\alpha}$, which is usually set at 100% (i.e., no extra capacity), also in the time delay τ_{α} (Equation (55)).

$$\alpha(i) + \left(\alpha^{\max} - \alpha(i)\right) \times \frac{TD^{\infty}(i) - Y^{\infty}(i)}{TD^{\infty}(i)} \times \frac{\Delta t}{\tau_{\alpha}} \xrightarrow{\Delta t} \alpha(i), \tag{54}$$

$$\alpha(i) + \left(\overline{\alpha} - \alpha(i)\right) \times \frac{\Delta t}{\tau_{\alpha}} \xrightarrow{\Delta t} \alpha(i). \tag{55}$$

2) The ARIO-inventory model (second version)

Hallegatte (2014) proposed a modified version of the ARIO model to take into account the inventory effects in the production system. Inventories matter as they can buffer the production disturbance caused by input shortages and thus increase the flexibility or robustness of the system during crisis. The introduction of inventory dynamics has made this version "more satisfying than the previous version in the way it models production bottlenecks and the impact of input scarcity on the production system". Besides, price responses, which were previously included, have been removed from this version, as little change in prices has been observed in the disaster aftermath due to socioeconomic inertia, transaction costs and antigouging legislation (ibid.). Below

is a description of the ARIO-inventory model with a focus on changes from the previous version.

To model inventory dynamics, a new variable $S(i,j)$ is introduced to indicate the inventory level of product j held by sector i at time step t (where t is omitted for simplicity). Inventories are consumed during the production of each sector, and then refilled by supplies from upstream supplying sectors. Each sector i has a target inventory level for each of its production inputs (e.g., product j), which is equal to a given number of days n_j^i of intermediate consumption at the production level needed to satisfy total demand (or the maximum production, considering existing production capacity). This target inventory level is expressed as:

$$S^t(i,j) = n_j^i \times \min\left\{Y^{\max}(i), TD(i)\right\} \times A(j,i). \tag{56}$$

The model has distinguished between stockable products (e.g., manufacturing products) and non-stockable products (e.g., electricity). The inventory of a non-stockable product is assumed to be not larger than the amount required to sustain three days of production. $Y^{\max}(i)$ is the maximum production determined by the production capacity constrained by capital availability and the capacity to overproduce, which is calculated in the same way as the previous version (see Equation (32)). Again, labour is not considered as a possible constraint here. $TD(i)$ is the total demand for the product of sector i, including intermediate demand, local final demand, exports, and reconstruction demand following a disaster. However, the calculation, particularly for intermediate demand, changes with respect to the previous version as the production bottleneck is addressed by inventory dynamics, which is not previously considered, and the intermediate demand now arises from the business-to-business orders to restore the exhausted inventories (see Equations (57) and (58) below).

The orders $O(i,j)$ from sector i to sector j in the next time step $t+1$ are given by:

$$O(i,j) = A(j,i) \times Y^a(i) + \frac{\Delta t}{\tau_s^i} \times \left(S^t(i,j) - S(i,j) \right). \quad (57)$$

Here $Y^a(i)$ is the actual production of sector i (see Equation (62)). So, the first item on the right-hand side of Equation (57) is the units of product j that have been used during the production of sector i at the current time step t. This indicates the orders needed to make up for the current consumption of inventory input j by sector i. The second item on the right-hand side of Equation (57) represents the orders that make the inventory converge towards its target value $S^t(i,j)$, with a characteristic time of inventory restoration τ_s^i. τ_s^i is assumed to be identical for all sectors, except for those making non-stockable products.

Then the total demand for product j in the next time step $t+1$ can be derived by summing up all intermediate demands from industrial sectors, local final demand, exports, and reconstruction demand:

$$TD(j) = \sum_i O(i,j) + LFD(j) + E(j) + HD(j) + \sum_i RD(i,j). \quad (58)$$

Here $LFD(j)$, $E(j)$, $HD(j)$ and $\sum_i RD(i,j)$ are modelled in the same ways as the previous version. This modelling of demands can well reflect backward ripple effects as Equation (57) shows that less production would lead to less demand for intermediate inputs and thus less production in the upstream supplying sectors.

The production process is also considered differently compared to the previous version. With the presence of inventories, production in each sector is not only dependent on

the minimum between observed demand $TD(i)$ and the maximum production capacity constrained by productive capital $Y^{\max}(i)$, but also on input availability (i.e., inventory levels).

First, in the absence of inventory constraints, the production in sector i would be:

$$Y^{opt}(i) = \min\left\{Y^{\max}(i), TD(i)\right\}. \tag{59}$$

Second, production can also be limited by insufficient inventories. The model introduces a required inventory level $S^r(i,j)$ to represent the amount of input necessary for production, which is given by:

$$S^r(i,j) = n_j^i \times Y^a(i) \times A(j,i). \tag{60}$$

Here $Y^a(i) \times A(j,i)$ is the required intermediate consumption of product j to produce the output level at the previous time step. The required inventory level $S^r(i,j)$ is different from the target inventory level $S^t(i,j)$, as the former represents the amount of input necessary for production and incorporates the constraints on other supplies, while the latter simply represents the orders to replenish inventories.

The model assumes that if the inventory of input j held by sector i is lower than a share φ of the required level $S^r(i,j)$, i.e., $S(i,j) < \varphi \times S^r(i,j)$, then the production of sector i will be reduced to:

$$Y^j(i) = \begin{cases} Y^{opt}(i), & \text{if } S(i,j) \geq \varphi \times S^r(i,j) \\ Y^{opt}(i) \times \min\left\{1, \dfrac{S(i,j)}{\varphi \times S^r(i,j)}\right\}, & \text{if } S(i,j) < \varphi \times S^r(i,j) \end{cases}. \tag{61}$$

Then the actual production $Y^a(i)$ is eventually determined by the minimum of

inventory constraints from all supplying sectors:

$$Y^a(i) = \min\left\{Y^j(i),\ \text{for all } j = 1,...,N\right\}. \tag{62}$$

In this modelling of production, the parameter φ represents the degree of heterogeneity in the economic system and in disaster direct impacts. When the inventory of a sector is lower than its required level, it is likely that some firms in that sector have their inventories at extremely low levels and have to largely reduce or even stop production, while other firms still have enough inventories and can keep producing normally. The model uses φ to describe how production is reduced when inventories are insufficient and sets $0 \le \varphi \le 1$. $\varphi = 0$ implies the scenario that disaster impacts are completely homogeneous and all firms in a sector make substitutable products. In this situation, a reduction by $x\%$ in a sector's inventory relative to the required inventory level represents that all firms in that sector have an inventory reduced by $x\%$ and can keep producing until the sector inventory $S(i,j)$ is empty. In other words, an inventory shortage by $x\%$ leads to no production reduction unless $x = 100\%$; in the latter case, production has to stop. On the other hand, $\varphi = 1$ refers to the scenario that disaster impacts are completely heterogenous (i.e., a few firms suffer most of the disaster damage) and firms make products that cannot be mutually substituted even within the sector. In this situation, a reduction by $x\%$ in a sector's inventory relative to the required inventory level represents that $x\%$ of the firms in that sector have an empty inventory and stop producing, while other firms have an inventory at or above the required level and can keep producing normally. In other words, an inventory shortage by $x\%$ leads to a reduction in production by $x\%$. The actual value of φ may be relevant to the economic size and structure. It would be low for a small economy which is entirely affected by the disaster or for a highly interconnected economy in which all firms are mutually connected, but high for a large economy in which only one of its regions is affected by the disaster or for a less interconnected economy in which firms only have one supplier in each other sector.

Both capacity and inventory constraints on production will then cascade into the production supply chain. If a sector cannot produce enough to fulfil the total demand it faces, it will ration its outputs among the downstream clients (forward rippling effect) and meanwhile demand less to its upstream suppliers (backward rippling effect). These are the two major effects that cause indirect disaster impacts to the entire economy.

The overproduction capacity is modelled in the same way as the previous version, except that the scarcity index $\frac{TD^{\infty}(i)-Y^{\infty}(i)}{TD^{\infty}(i)}$ in Equation (54) is replaced by $\frac{TD(i)-Y^{a}(i)}{TD(i)}$.

The second version of the ARIO model also considers a different rationing scheme with respect to the previous version, when the actual production is insufficient to satisfy the total demand. This version no longer prioritizes business-to-business orders but instead simply introduces a proportional rationing scheme that distributes the sectoral output to all intermediate and final demands proportionally:

$$O^{*}(j,i)=O(j,i)\times\frac{Y^{a}(i)}{TD(i)}, \tag{63}$$

$$LFD^{*}(i)=LFD(i)\times\frac{Y^{a}(i)}{TD(i)}, \tag{64}$$

$$E^{*}(i)=E(i)\times\frac{Y^{a}(i)}{TD(i)}, \tag{65}$$

$$HD^{*}(i)=HD(i)\times\frac{Y^{a}(i)}{TD(i)}, \tag{66}$$

$$RD^{*}(j,i)=RD(j,i)\times\frac{Y^{a}(i)}{TD(i)}. \tag{67}$$

Here $O^*(j,i)$ is the actual purchases of product i by sector j to refill its inventory. $LFD^*(i)$ and $E^*(i)$ are the actual purchases of product i by local and foreign final consumers, respectively, to satisfy their consumption needs. $HD^*(i)$ and $RD^*(j,i)$ are the actual purchases of product i by local households and sector j, respectively, to restore their damaged physical assets and productive capital.

Thus, with the satisfaction of intermediate orders $O^*(i,j)$, the dynamics of inventory in sector i can be expressed as:

$$S(i,j)(t+1) = S(i,j)(t) + O^*(i,j)(t) - A(j,i) \times Y^a(i)(t). \quad (68)$$

Here the second item on the right-hand side of the equation indicates the increase in inventory through purchases from supplier j, while the last item shows the decrease in inventory due to the consumption of input j during the production process.

The rest of the model is the same with the previous version, except that the adaptations of technical and import coefficients and of final demand, together with price responses, are no longer included. This is because the flexibility of the economic system is modelled by inventory dynamics in the current ARIO-inventory model. Other flexibilities brought about by import substitution, delay maintenance, production rescheduling, etc., essentially affect a sector's ability to keep production during a crisis, which has already been represented by inventory indicators, such as the inventory size and restoration characteristic time.

Although widely used in disaster impact analysis, both versions of the ARIO models have drawbacks, particularly in their modelling of production bottlenecks and/or

constraints. To address the issue of production bottlenecks, the first version of the ARIO model proposes an iterative process to reduce productions of all sectors until the associated intermediate orders are small enough to be satisfied by the productions (see Equations (30)-(35)). However, as the production bottleneck is resolved entirely on production cuts, ignoring other possible flexibilities in production rearrangement, this approach may result in very low production levels and thus increase the economic impacts. On the other hand, the second version of the ARIO model has allowed more flexibility with the introduction of inventory dynamics, which appears to be "more satisfying than the previous version in the way it models production bottlenecks and the impact of input scarcity on the production system" (Hallegatte, 2014). Still, the way it models inventory constraints needs to be improved. The assumption of the Leontief production function, which is embodied in the use of IO tables, treats inventories from other sectors and productive capital as equally important inputs for production. Inventory availability and capital availability should affect production capacity simultaneously, but they are considered separately and inconsistently in the ARIO-inventory model. Inventory constraints take effect only after the optimal production has been determined by capital constraints and total demand (see Equation (59)). A parameter φ is introduced to specify how production is further affected by insufficient inventories, which, however, is not present in the modelling of capital constraints. Besides, the setting of this parameter in Equation (61) is to some extent far-fetched to reflect the heterogeneity in disaster impacts as intended. For instance, setting $\varphi = 0$ simply amounts to assuming that inventory shortages have completely no influence on production, which is very unlikely and not a homogenous situation as described above. In that homogeneous situation, if the inventory level of a sector is reduced below what is needed to maintain the current period of production, not necessarily a 100% reduction, the sectoral production will be reduced proportionally. Meanwhile, for a large economy suffering quite heterogenous disaster impacts, a multi-regional approach would be more effective to model such heterogeneity than

relying on an exogenously given value of this parameter. In fact, both versions of the ARIO models were intended for single-regional analysis using a local IO table and thus did not consider the possibility of substitution between regions. Substitution of suppliers of the same product from different regions may largely mitigate the shock waves in an economic network and should be incorporated when extending the ARIO model for multi-regional analysis (Guan et al., 2020; Wenz et al., 2014).

3.1.2.3. The Disaster Footprint Model

In this thesis, the Disaster Footprint model is developed drawing on the ARIO model and to overcome some of its drawbacks, mainly by improving the modelling of production bottlenecks (the first version) and extending to a multi-regional approach with the inclusion of the substitution effects between regions (the second version). The concept of 'disaster footprint' is an extension of 'flood footprint' proposed and improved by Mendoza-Tinoco et al. (2017) and Zeng et al. (2019), respectively, to describe the cascading economic impacts of a disaster event through the production supply chain (see Section 2.1.2). Starting from the direct damage to productive factors (e.g., labours and capital), the model seeks to measure the indirect effects that ripple through all interdependent sectors and accumulate over time until the full recovery of the affected economy.

There are two versions of the Disaster Footprint model developed for different research purposes and contexts. The first version is called the DF-growth model, which is intended to account for the effects of economic growth on the long-term disaster impacts under the context of climate change. Growth elements like capital accruement, population growth and technical progress are added into the model to realise an economic recovery to higher levels than the pre-disaster state, which marks a major improvement for disaster impact analysis, given that most studies usually assume that the economy can only recover to the pre-disaster level shortly after a disaster. Besides,

the model adopts a linear programming technique to optimize the supply (i.e., output plus imports) decisions under the disaster-induced capacity constraints, which represents a better-case scenario in addressing the potential supply bottlenecks compared to the iterative process described in Hallegatte (2008). The inclusion of economic growth and supply optimization has introduced more flexibility based on the first version of the ARIO model, making the model more suitable for the long-term disaster impact analysis, notably in the context of climate change. On the other hand, the second version is called the DF-substitution model, which is developed for a multi-regional analysis considering the effects of cross-regional substitution in buffering the propagations of disaster shocks along the production supply chain. This version also incorporates the role of inventories based on the ARIO-inventory model (Hallegatte, 2014), but improves on the modelling of inventory dynamics with the combination of supply constraints and demand redistribution. In addition, both versions have extended the ARIO model by incorporating disaster-induced labour constraints, which, together with the existing capital constraints, presents a complete picture of disaster impacts on the production system. Below is a full description of these two versions of the Disaster Footprint model.

Key assumptions used in the DF-growth model and DF-substitution model are listed in Table 3-3.

Table 3-3: Key assumptions used in the DF-growth model and DF-substitution model respectively.

Assumptions	DF-growth model	DF-substitution model
Common assumptions	• The economy consists of N production sectors, each of which makes only one unique product that cannot be substituted by a different sector. • Primary inputs (e.g., labour and capital), which are not mutually substitutable, are fully employed by sectors to carry out production in the pre-disaster economic equilibrium. • The input-output relationship (i.e., economic structure) is constant over the study period. • Post-disaster labour dynamics follow an exogenous process, reflecting labour losses from casualties, labour recovery at certain rates, and lost working hours due to transport disruptions. • Labour force flows freely across sectors. • The prioritized-proportional rationing scheme is adopted, in which the output of each sector goes first to intermediate use and/or basic consumption before proportionally allocated to other categories of final demands and reconstruction demand. • Inputs from other sectors required by each unit of capital formation are identical across sectors in the region.	
Special assumptions	• A modified Leontief production function is adopted, which considers labour-side technical change in the long run. • The rate of labour-side technical progress is identical across sectors. • The growth rates of final demands and capital stock are equal to that of GDP. • The economy can recover to a higher level than the pre-disaster state based on its growth potential. • Imports are constrained by the surviving capacity of the transport sector during and after the disaster. • Sectors simultaneously decide their optimal production and imports to maximize the total supply of the economy under disaster-induced capacity constraints at each time step. • Damaged capital needs a certain time to be fully recovered	• There are R regions in the economy, each of which has N production sectors. • A modified Leontief production function is adopted, which allows for substitution of inputs from the same sector in different regions. • Sectors can gradually increase their production capacity up to the maximum in response to demand surges or supply shortages. • Imports from outside the economy are never constrained by the disaster. • Sectors are always expecting to receive as many orders as in the previous period. • Customers can redistribute their orders among suppliers from different regions according to the production capacity of suppliers.

	before which it is under construction and cannot be employed in production.	• Sectors aim to keep a certain level of inventory to sustain a given number of weeks of production at the pre-disaster level. • Final demands do not shift significantly in the short run after the disaster. • Reconstruction expenditures are largely funded by insurance claims, which do not have a crowding-out effect on other consumption. • The economy is targeted to recover to the pre-disaster level in the short run after the disaster.

1) DF-growth model (first version)

The DF-growth model starts from an economy in equilibrium before the disaster events. The total supply and demand of the economy are initially kept in balance:

$$\bar{x}_i + \overline{im}_i = \sum_{j=1}^{N} a_{i,j} \times \bar{x}_j + \overline{fd}_i, \tag{69}$$

$$\overline{fd}_i = \overline{hc}_i + \overline{gc}_i + \overline{inv}_i + \overline{ex}_i. \tag{70}$$

Here $\bar{x}_i$, $\overline{im}_i$, $\overline{fd}_i$ are the output, imports and final demand of products in sector i in the pre-disaster equilibrium ($t = 0$). The overbars are used to indicate values at the pre-disaster levels. $a_{i,j}$ is the i-th row and j-th column element of the technical coefficient matrix, which refers to the units of product i that are required to produce one unit of product j. N represents the number of industrial sectors and it is assumed that each industrial sector makes only one unique product[7]. The supply of each sector is equal to its domestic production plus imports from outside the region. The demand of each sector is categorized into two major groups: intermediate demand and final demand. Intermediate demand is the use of products by other industrial sectors in the middle of their production, i.e., $\sum_{j=1}^{N} a_{i,j} \times \bar{x}_j$. Final demand refers to the consumption of products by end users, i.e., $\overline{fd}_i$. According to the types of final users, final demand is further classified into four sub-groups: 1) household consumption $\overline{hc}_i$, divided into basic demand ($\overline{bd}_i$) and other consumption ($\overline{ohc}_i$): $\overline{hc}_i = \overline{bd}_i + \overline{ohc}_i$; 2) governmental expenditures ($\overline{gc}_i$); 3) fixed capital formation or investment ($\overline{inv}_i$); and 4) exports ($\overline{ex}_i$) (Equation (70)). Thus, the left-hand side of Equation (69) represents the total supply of product i, while the right-hand side denotes its total demand.

[7] Apart from industrial sectors, the residential sector may be also damaged by disaster events. Unless specifically mentioned, 'sectors' in this section only refer to industrial sectors.

Inherent in the IO framework, the productive factors are invested in fixed proportions during the production process. That means the output of each sector is determined by the minimum of capital and labour inputs. In addition, for the long run analysis, a labour-augmenting technical progress is assumed to simulate endogenous economic growth. This is a standard approach in macroeconomics with an observation that most economies tend to have a labour-biased growth (Acemoglu, 2003). This modified Leontief production function with technical change is expressed as:

$$\bar{x}_i = \min\left\{\frac{\bar{c}\times\bar{v}_{l,i}}{d_{l,i}}, \frac{\bar{v}_{k,i}}{d_{k,i}}\right\}. \tag{71}$$

Here 'min' means the minimum of the two values in the bracket. $\bar{v}_{l,i}$ and $\bar{v}_{k,i}$ denote the primary inputs of labour and capital in sector i before the disaster, respectively; while $d_{l,i}$ and $d_{k,i}$ are the technical labour and capital coefficients showing the amount of labour and capital required to produce one unit of product in sector i. As the economic structure is assumed to be stable during the study period, the values of $a_{i,j}$ (in Equation (69)), $d_{l,i}$ and $d_{k,i}$ are kept constant before and after the disaster, and can be derived from the IO tables used. The model only considers technical shift through the effect of $c(t)$, which represents the labour-augmenting technical change, varying with time. The value of $c(t)$ is assumed to be the same across all industrial sectors and is measured by the percentage increase in GDP per capita relative to the pre-disaster level; so for $t = 0$, it has $\bar{c} = 1$.

Following a disaster, the above equilibrium (in Equation (69)) would break up with imbalanced supply and demand. On the supply side, physical assets, such as buildings and equipment, are damaged and out of operation. Casualties occur during the disaster

events, and people spend more time commuting to and from work due to traffic disruptions. Capital and labours are directly damaged by the disaster events, with a further shrink in production capacity. Importation would also be limited due to traffic constraints. On the demand side, the households and governments may cut off some unnecessary expenditures to live with the shortage of supply, while damaged assets create greater demand for investment to support reconstruction. Inequalities arise between the capacity to supply and the actual demand after the disruptions.

On the supply side, the direct disaster damage to industry productive capital and labour reduces the production capacity of affected sectors. The industry productive capital available for production at the beginning of each time step $K_i(t)$ depends on two factors: the disaster-induced capital damage at that time and the recovered capital during the last period:

$$K_i(t) = \left(1 - \delta_i^K(t)\right) \times \left(K_i(t-1) + K_i^{rec}(t-1)\right). \tag{72}$$

Here $\delta_i^K(t)$ is the proportion of damaged capital in sector i at time step t (estimated with methods in Section 3.1.1.1). $K_i^{rec}(t-1)$ is the recovered capital in sector i during the last period (see Equation (90)).

Due to the linear relationship between input factors and industrial output, capital production capacity $x_i^K(t)$ is proportional to available capital $K_i(t)$, at each time step, relative to the pre-disaster level:

$$x_i^K(t) = \frac{K_i(t)}{\overline{K_i}} \times \overline{x_i}. \tag{73}$$

Damaged physical capital includes industry productive and residential capital. The

amount of residential capital at the beginning of each time step $K_{res}(t)$ is calculated in the same manner as for industry productive capital (Equation (74)). However, damages to residential capital have no effects on production capacity, as it is not involved in the production processes[8].

$$K_{res}(t) = \left(1 - \delta_{res}^{K}(t)\right) \times \left(K_{res}(t-1) + K_{res}^{rec}(t-1)\right). \tag{74}$$

Here the subscript 'res' refers to the residential sector.

Similarly, labour availability also changes after a disaster. This model is mainly intended for capital-shocked disasters like floods. There is usually little reported information on flood-induced labour damage and recovery, therefore labour dynamics are assumed to follow an exogenous process, reflecting labour losses from casualties and labour recovery from the previous period, as well as transport disruptions which may delay or impede travel to work:

$$L(t) = \left[\left(1 + r_n\right) \times L(t-1) + \sum_q L_q^{rec}(t-1) - \sum_q L_q^{dam}(t) \right] \times \frac{wh(t)}{\overline{wh}}. \tag{75}$$

Here $L(t)$ represents the total supply of labour in the economy at time step t, and r_n denotes the natural growth rate of population. $L_q^{dam}(t)$ denotes the three types of labour unable to attend work due to casualties, namely the dead, the heavily injured and the slightly injured, $q = 1, 2, 3$. $L_q^{rec}(t-1)$ corresponds to the recovery of each affected labour type during the previous period. Apart from casualties, other labour may be delayed for work due to transport disruptions. $wh(t)$ and $\overline{wh}$ denote total working hours during time t and normal times before the disaster, respectively,

[8] However, damages to residential capital have indirect effects on the production process, as its recovery results in a non-negligible part of the total reconstruction demand, competing with industry productive capital for reconstruction resources.

which are related to traffic conditions. As labour recovery is considered exogenously, a few assumptions are made here: 1) labour affected by transport disruptions are delayed for work for one hour per day during the first period after the disaster; 2) the disaster shocks begin to subside within 6 months, which means that the working hours increase linearly to the pre-disaster level in 6 months; 3) slightly injured labour comes back to work after half a month; 4) 23% of the heavily injured labour recovers health at each time step after the disaster. These assumptions are made due to data limitations.

It is assumed that the labour force flows freely across different industrial sectors, so that during each period the labour production capacity in each sector experiences the same percentage change as the total labour supply. Therefore, the labour production capacity $x_i^L(t)$ is given by the equation below considering a labour-augmenting technical change $c(t)$:

$$x_i^L(t) = \frac{c(t) \times L(t)}{\overline{L}} \times \overline{x}_i . \tag{76}$$

Considering both constraints, the maximum production capacity $x_i^{\max}(t)$ is determined by the minimum capacity of labour and capital at that time, as shown below:

$$x_i^{\max}(t) = \min\left\{x_i^K(t), x_i^L(t)\right\}. \tag{77}$$

Therefore, the output of each sector at time step t, $x_i(t)$, should be non-negative and no larger than the maximum production capacity:

$$0 \le x_i(t) \le x_i^{\max}(t). \tag{78}$$

On the other hand, the imports are related to the capacity of sectors that are involved in transporting and delivering goods. Therefore, the maximum import capacity

$im_i^{\max}(t)$ is constrained by the surviving capacity of the transport sector $x_{tran}^{\max}(t)$, that is, if the remaining capacity of the transport sector 'tran' is declined by $x\%$ at time t, then the imports will contract by the same percentage relative to the pre-disaster level $\overline{im}_i$:

$$im_i^{\max}(t) = \frac{x_{tran}^{\max}(t)}{\overline{x}_{tran}} \times \overline{im}_i . \tag{79}$$

Similar with the output constraint, the imports at time t, $im_i(t)$, should be non-negative and no larger than the maximum import capacity:

$$0 \le im_i(t) \le im_i^{\max}(t). \tag{80}$$

On the demand side, a new kind of final demand to support the reconstruction and replacement of damaged physical capital arises after the disaster. The final use of products in sectors that are involved in the reconstruction process increases. The formation of demand from the reconstruction of industry productive capital is:

$$rd_{i,j}(t) = \max\left\{\left[(1+r_s)\times K_j(t-1) - K_j(t) - K_j^{cons}(t-1)\right]\times \eta_i, 0\right\}. \tag{81}$$

Here $rd_{i,j}(t)$ is the element of an $N \times N$ reconstruction demand matrix $\mathbf{RD}(t)$, which denotes the investment that is needed for sector i to support the capital reconstruction of industrial sector j. 'Max' means the maximum. r_s is the targeted growth rate of capital stock. $K_j^{cons}(t-1)$ is the cumulative capital under construction before time t (see Equation (92)). Capital under construction does not contribute to productivity increase until it is fully recovered. Therefore, the demand for capital reconstruction in sector j comes from the gap between the capital target $(1+r_s)\times K_j(t-1)$ and the actual amount of capital at time t, $K_j(t)$, subtracting the

capital already under construction $K_j^{cons}(t-1)$. Then a proportion of this demand is allocated to sector i, according to the contribution of sector i to capital reconstruction, namely η_i. If sector i is involved in capital reconstruction (e.g., machinery, equipment, vehicle, and construction), $0 < \eta_i \leq 1$; otherwise, $\eta_i = 0$. The sum of η_i is equal to one ($\sum_{i=1}^{N} \eta_i = 1$).

Similarly, the reconstruction demand of the residential sector for products in sector i at time t is:

$$rd_{i,res}(t) = \max\left\{\left[\left(1+r_s\right)\times K_{res}(t-1) - K_{res}(t) - K_{res}^{cons}(t-1)\right]\times \eta_i, 0\right\}. \quad (82)$$

Finally, the total reconstruction demand for sector i, $frec_i(t)$, is the sum of investment required by all other industrial and residential sectors to support their reconstruction activities.

$$frec_i(t) = rd_{i,res}(t) + \sum_{j=1}^{N} rd_{i,j}(t). \quad (83)$$

On the other hand, it has been noted that strategic adaptive behaviour in the aftermath of the disaster would drive people to ensure their continued consumption of basic commodities, such as food, clothes and medical services (Mendoza-Tinoco et al., 2017). The coexistence of reconstruction and basic demand delimits the boundary of final demand. That is, the final use of products in sector i at time t, $fd_i(t)$, after satisfying its intermediate demand, should be at least larger than the basic demand $bd_i(t)$, but do not exceed the aggregate demand of all other final users (including the reconstruction use).

$$bd_i(t) \leq fd_i(t) \leq \left(1+r_g\right)^t \times \overline{fd}_i + frec_i(t). \quad (84)$$

Here $fd_i(t) = x_i(t) + im_i(t) - \sum_{j=1}^{N} a_{i,j} \times x_j(t)$ according to Equation (69). r_g is the targeted growth rate of national GDP. It is simply assumed that the growth rate of final demand equals that of GDP. Basic demand $bd_i(t)$ is usually a fraction (5% in this analysis) of the domestic final demand at time t, i.e., $(1+r_g)^t \times (\overline{fd}_i - \overline{ex}_i)$.

Given the above production, import, and consumption constraints (see Equations (78), (80), and (84)), industrial sectors choose their optimal production $x_i(t)$ and imports $im_i(t)$ to maximize the total economic supply at each time step. This is a linear objective that entails the most efficient economic recovery in the disaster aftermath. The optimization problem is given by:

$$\begin{aligned} \max \quad & \sum_{i=1}^{N} \left(x_i(t) + im_i(t) \right) \\ s.t. \quad & 0 \le x_i(t) \le x_i^{\max}(t) \\ & 0 \le im_i(t) \le im_i^{\max}(t) \\ & bd_i(t) \le x_i(t) + im_i(t) - \sum_{j=1}^{N} a_{i,j} \times x_j(t) \le (1+r_g)^t \times \overline{fd}_i + frec_i(t) \end{aligned} \quad . \quad (85)$$

Using the linprog function in MATLAB solves this optimization problem and derives the optimal production $x_i^a(t)$ and imports $im_i^a(t)$ for each time step t, which in turn determines the remaining final products $x_i^{rem}(t)$ after satisfying the intermediate demand $\sum_{j=1}^{N} a_{i,j} \times x_j^a(t)$ and the basic demand $bd_i(t)$:

$$x_i^{rem}(t) = x_i^a(t) + im_i^a(t) - \sum_{j=1}^{N} a_{i,j} \times x_j^a(t) - bd_i(t) . \quad (86)$$

The remaining final products are then proportionally allocated to the reconstruction

demand and other categories of final demand, as below:

$$rc_{i,j}(t) = x_i^{rem}(t) \times \frac{rd_{i,j}(t)}{(1+r_g)^t \times (\overline{fd}_i - \overline{bd}_i) + rd_{i,res}(t) + \sum_{j=1}^{N} rd_{i,j}(t)}, \tag{87}$$

$$rc_{i,res}(t) = x_i^{rem}(t) \times \frac{rd_{i,res}(t)}{(1+r_g)^t \times (\overline{fd}_i - \overline{bd}_i) + rd_{i,res}(t) + \sum_{j=1}^{N} rd_{i,j}(t)}, \tag{88}$$

$$fc_{i,p}(t) = x_i^{rem}(t) \times \frac{fd_{i,p}(t)}{(1+r_g)^t \times (\overline{fd}_i - \overline{bd}_i) + rd_{i,res}(t) + \sum_{j=1}^{N} rd_{i,j}(t)}. \tag{89}$$

Here $rc_{i,j}(t)$, $rc_{i,res}(t)$, and $fc_{i,p}(t)$ are the units of products in sector i allocated to satisfy the reconstruction demand of the industrial sector j, the reconstruction demand of the residential sector and the p-th type of final demand (i.e., household consumption, governmental expenditures, fixed capital formation and exports), respectively, at time t.

On satisfaction of reconstruction demand, damaged capital becomes under construction. This stage usually last 1-7 months for various types of capital according to their physical characteristics and empirical evidence. Damaged capital is fully recovered and put into production after its construction is completed. Therefore, at time t, the recovered capital in the industrial sector i and in the residential sector by investment from all other industrial sectors, $K_i^{rec}(t)$ and $K_{res}^{rec}(t)$, are calculated as:

$$K_i^{rec}(t) = \sum_{m=1}^{7} \left(\omega(m) \times \sum_{j=1}^{N} rc_{j,i}(t-m+1) \right), \tag{90}$$

$$K_{res}^{rec}(t) = \sum_{m=1}^{7} \left(\omega(m) \times \sum_{j=1}^{N} rc_{j,res}(t-m+1) \right). \tag{91}$$

Here $\omega(m)$ is the proportion of capital that completes its construction in m time steps, where $m = 1, 2, ..., 7$ and $\sum_{m=1}^{7} \omega(m) = 1$.

Correspondingly, the cumulative amount of industry productive and residential capital under construction before the next period $(t+1)$ are given by:

$$K_i^{cons}(t) = \sum_{m=1}^{7} \left[\left(1 - \sum_{s=1}^{m} \omega(s) \right) \times \sum_{j=1}^{N} rc_{j,i}(t-m+1) \right], \tag{92}$$

$$K_{res}^{cons}(t) = \sum_{m=1}^{7} \left[\left(1 - \sum_{s=1}^{m} \omega(s) \right) \times \sum_{j=1}^{N} rc_{j,res}(t-m+1) \right]. \tag{93}$$

The recovered capital $K_i^{rec}(t)$ will increase the capital availability for the next time period $K_i(t+1)$ and boost capital production capacity $x_i^K(t+1)$, as in Equations (72) and (73). On the other hand, labour recovery $\sum_q L_q^{rec}(t)$ is exogenously determined as mentioned above, as well as labour availability $L(t+1)$ and labour production capacity $x_i^L(t+1)$, as in Equations (75) and (76). This iterative process continues until the supply and demand of the economy reach an equilibrium. During this process, the economic output can recover to a higher level than the initial level, converging towards a targeted growth trajectory which is exogenously determined by the values of capital growth rate r_s, population growth rate r_n, GDP growth rate r_g, and technical change factor $c(t)$ (i.e., labour productivity growth rate). Still, the model can be applied to a no-growth scenario with additional constraints on these growth parameters, i.e., $r_s = r_n = r_g = 0$ and $c(t) \equiv 1$.

Finally, the indirect disaster footprint is calculated as the cumulative losses of regional

GDP compared to its potential during the whole study period.

$$IndirectFootprint = \sum_{t}\left[\left(1+r_g\right)^t \times \sum_{i=1}^{N}\overline{va}_i - \sum_{i=1}^{N} va_i^a\left(t\right)\right]. \quad (94)$$

Here $va_i^a\left(t\right)$ refers to the value added of sector i at time t, which is the extra value of final products created above intermediate inputs, i.e., $va_i^a\left(t\right) = x_i^a\left(t\right) - \sum_{j=1}^{N} a_{j,i} \times x_i^a\left(t\right)$. $\overline{va}_i$ is the value added at the pre-disaster level. Summation of value added in all sectors $\sum_{i=1}^{N} va_i^a\left(t\right)$ constitutes the regional GDP during the time t.

2) DF-substitution model (second version)

The DF-substitution model extends the previous version to a multi-regional analysis by considering inventory dynamics and substitution of suppliers from different regions. The model starts from a similar pre-disaster economic equilibrium as in the previous version (see Equations (69) and (70)), except that there are R regions in the economy and each of them has N industrial sectors. Each industrial sector in each region makes only one product which cannot be substituted by the product of a different sector but can be substituted by the product of the same sector from a different region.

On the production side of the economy, each sector rent capital and employ labour to process natural resources and intermediate inputs produced by other sectors into a specific product. Traditionally, the Leontief production function is adopted where different inputs are used in fixed proportions during production and not mutually substitutable (Miller and Blair, 2009). This may overestimate the economic losses from negative shocks (Okuyama and Santos, 2014). However, in this multi-regional modelling, the product of a sector in a region can be substituted by that of the same

sector from a different region, and the production function for each sector in each region is given by:

$$x_{ir} = \min\left\{\text{for all } j,\ \frac{z_{j,ir}}{a_{j,ir}};\ \text{for all } q,\ \frac{v_{q,ir}}{b_{q,ir}}\right\}. \tag{95}$$

Here x_{ir} demotes the output of sector i in region r in monetary values. $z_{j,ir}$ are the intermediate input made by sector j from all regions and used in the production of sector i in region r. $v_{q,ir}$ are the value-added/primary input q (i.e., capital and labour) used by this sector. $a_{j,ir}$ and $b_{q,ir}$ are the technical coefficients which indicate the amount of intermediate input j and primary input q required to produce one unit of product i in region r, respectively:

$$a_{j,ir} = \frac{\bar{z}_{j,ir}}{\bar{x}_{ir}}, \tag{96}$$

$$b_{q,ir} = \frac{\bar{v}_{q,ir}}{\bar{x}_{ir}}. \tag{97}$$

Here the overbars indicate the values of variables in the pre-disaster equilibrium state, which can be obtained from the IO tables. Equation (95) is still a Leontief-type production function but slightly different from the traditional Leontief production function. It does not allow substitution between different types of inputs, as economic agents do not have enough time to adjust other inputs to replace temporary shortages. However, it allows for the substitution between products of the same sector from different regions. As in Equations (95)-(97), the model does not distinguish between intermediate input j from different regions, considering products of the same sector from different regions are completely mutual substitutable, and therefore $z_{j,ir} = \sum_{s=1}^{R} z_{js,ir}$.

In an equilibrium state, industrial sectors use intermediate products and primary inputs to produce goods and services to satisfy demand from their clients. However, after a disaster event, output will decrease due to the capital, labour, and inventory constraints.

First, the productive capital in sector i and residential capital in region r at time t are expressed as:

$$K_{ir}(t) = K_{ir}(t-1) - K_{ir}^{dam}(t) + K_{ir}^{rec}(t-1), \tag{98}$$

$$K_{res,r}(t) = K_{res,r}(t-1) - K_{res,r}^{dam}(t) + K_{res,r}^{rec}(t-1). \tag{99}$$

Here $K_{ir}(t)$ and $K_{res,r}(t)$ are the surviving capital stock held by industrial sector i and the residential sector in region r at time t, respectively. $K_{ir}^{dam}(t)$ and $K_{res,r}^{dam}(t)$ refer to the amount of capital damaged/destroyed by the disaster (estimated with methods in Section 3.1.1.1). $K_{ir}^{rec}(t-1)$ and $K_{res,r}^{rec}(t-1)$ represent the recovered capital during the last period $t-1$ (see Equations (115) and (116)). The modelling of capital dynamics here is more explicit than the previous version (see Equations (72) and (74)), as it uses absolute (rather than relative) values of capital damage estimated from the catastrophe models.

Then at each time step following the disaster, the percentage reduction in productive capital of sector i in region r, relative to the pre-disaster level, is:

$$\gamma_{ir}^{K}(t) = \frac{\overline{K}_{ir} - K_{ir}(t)}{\overline{K}_{ir}}. \tag{100}$$

Here $\overline{K}_{ir}$ is the capital stock of sector i in region r in the pre-disaster equilibrium.

The capital production capacity of sector i in region r, $x_{ir}^{K}(t)$, is assumed to be constrained by the proportion of the available capital relative to the pre-disaster level. This assumption is hard-coded through the Leontief-type production function and its restricted substitution. That is, as capital and labour are considered perfectly complementary as well as the main factors of production, and the full employment of those factors in the economy is also assumed, then damage in capital assets is linearly related with production level and therefore, value added level. Besides, in this version, an overproduction capacity $\alpha_{ir}^{q}(t)$ of the primary input q (i.e., capital or labour, $q=\{K,L\}$) is incorporated to reflect the production adaptation in response to demand surges or production shortages (detailed modelling processes are described in Equations (126) and (127)). Then, the remaining production capacity of the industry productive capital at each time step is:

$$x_{ir}^{K}(t)=\alpha_{ir}^{K}(t)\times\left(1-\gamma_{ir}^{K}(t)\right)\times\overline{x}_{ir}. \tag{101}$$

Second and similarly, the remaining production capacity of labour in each sector at time t, $x_{ir}^{L}(t)$, is given by:

$$x_{ir}^{L}(t)=\alpha_{ir}^{L}(t)\times\left(1-\gamma_{ir}^{L}(t)\right)\times\overline{x}_{ir}, \tag{102}$$

$$\gamma_{ir}^{L}(t)=\frac{\overline{L}_{ir}-L_{ir}(t)}{\overline{L}_{ir}}. \tag{103}$$

Here $L_{ir}(t)$ and $\overline{L}_{ir}$ are the employment of labours by sector i in region r at time t and before the disaster, respectively. $\gamma_{ir}^{L}(t)$ is the percentage reduction in labour supply of sector i in region r at time t. For capital-shocked disasters like floods and earthquakes, the modelling of labour dynamics $L(t)$ is similar with the previous version, except that there is no population growth shortly after the disaster

(i.e., $r_n = 0$) (see Equation (75)); while for labour-shocked disasters like heatwaves and air pollution, labour damage $\gamma_{ir}^{L}(t)$ is usually well estimated with methods in Sections 3.1.1.2 and 3.1.1.3, and can be directly fed into Equation (102).

Third, insufficient inventory of intermediate products will create a bottleneck for production activities. The potential production level, $x_{ir}^{j}(t)$, that the inventory of the intermediate product j can support is:

$$x_{ir}^{j}(t) = \frac{S_{ir}^{j}(t)}{a_{j,ir}}. \tag{104}$$

Here $S_{ir}^{j}(t)$ refers to the units of intermediate product j held by sector i in region r at the beginning of time t.

Considering all these constraints, the maximum production capacity, $x_{ir}^{\max}(t)$, of sector i in region r can be expressed as:

$$x_{ir}^{\max}(t) = \min\left\{x_{ir}^{K}(t);\ x_{ir}^{L}(t);\ \text{for all}\, j,\ x_{ir}^{j}(t)\right\}. \tag{105}$$

Here imports of a sector from outside the studied regions are assumed to be never constrained, as this model mainly focuses on substitution between regions within the economy instead of substitution between local and external regions.

It is worth noting that some disasters only cause damage to one of labour or capital. For instance, only labour availability is reduced during heatwaves due to the associated health impairment and labour productivity loss. Under such circumstances, capital no longer poses a further constraint on production and the maximum production capacity $x_{ir}^{\max}(t)$ is equivalent to the minimum level of production that can be sustained by the

available labour and inventories of intermediate inputs respectively. This is also true for the DF-growth model (the first version) and the CHEFA model (the compound hazard version in Section 3.2).

The actual production of sector i in region r depends on both its maximum production capacity and the total orders it expects to receive from the clients:

$$x_{ir}^{a}(t) = \min\left\{x_{ir}^{\max}(t);\ TD_{ir}(t-1)\right\}. \tag{106}$$

Here it is assumed that the sector always expects to receive the same quantities of orders as the previous period, that is, $TD_{ir}(t-1)$ (see Equation (125)).

Then, the inventory of product j held by sector i in region r will be consumed during the production process. The model uses $S_{ir}^{j,used}(t)$ to denote the units of intermediate product j used in the production of sector i in region r at time t, which is:

$$S_{ir}^{j,used}(t) = a_{j,ir} \times x_{ir}^{a}(t). \tag{107}$$

After production, suppliers then deliver their products to the clients according to the orders they have received. Considering that probably not all demands can be met by outputs under constraints, a prioritized-proportional rationing scheme is adopted to simulate the resource allocation process during the disequilibrium period. Under this scheme, a sector first allocates its products to address the intermediate demand and then proportionally allocates the remaining products to other categories of demands. This assumption is based on the observation that business-to-business relationships are stronger than business-to-client relationships and therefore should be prioritized (Hallegatte, 2008).

First, products of sector i in region r is allocated to sector j in region s in quantities $ic_{js}^{ir}(t)$:

$$ic_{js}^{ir}(t)=\begin{cases}\dfrac{id_{js}^{ir}(t-1)}{\sum_{j=1}^{N}\sum_{s=1}^{R}id_{js}^{ir}(t-1)}\times x_{ir}^{a}(t), & \text{if } x_{ir}^{a}(t)<\sum_{j=1}^{N}\sum_{s=1}^{R}id_{js}^{ir}(t-1)\\ id_{js}^{ir}(t-1), & \text{if } x_{ir}^{a}(t)\geq\sum_{j=1}^{N}\sum_{s=1}^{R}id_{js}^{ir}(t-1)\end{cases}. \quad (108)$$

Here $id_{js}^{ir}(t-1)$ refers to the orders issued by sector j in region s to the supplying sector i in region r at time $t-1$. If the actual output of sector i in region r is smaller than its expected total orders from other sectors $\sum_{j=1}^{N}\sum_{s=1}^{R}id_{js}^{ir}(t-1)$, it will ration all its products to the business clients in proportion to the orders. Otherwise, it will allocate just enough products to satisfy the expected intermediate demand.

Recalling the previous version, the production bottleneck is addressed by a linear programming technique, in which the sectoral production and importation are optimized to ensure that the associated intermediate demands can be fully satisfied (see Equation (85)). By contrast, in this version, the complete satisfaction of intermediate demand is no longer a requirement to proceed production (see Equation (108)). This is because a sector now employs the remaining inventories to make its products, rather than relying on the instant inputs from other sectors. The supply of inputs from other sectors mainly contributes to a replenishment of inventories that are consumed in production.

The remaining products of sector i in region r, after (partly or fully) satisfying the intermediate demand, at time step t, is equal to:

$$x_{ir}^{rem}(t)=x_{ir}^{a}(t)-\sum_{j=1}^{N}\sum_{s=1}^{R}ic_{js}^{ir}(t). \quad (109)$$

Then, the remaining products will be proportionally allocated to the final demand and reconstruction demand. The final demand mainly consists of four types, that is, household consumption, government expenditures, fixed capital formation and exports. The reconstruction demand refers to the demand for capital goods to restore both the industry productive and residential capital damaged by the disaster. The quantities of products of sector i in region r allocated to satisfy the p-th type of final demand in region h, $fc_{ph}^{ir}(t)$, are expressed as:

$$fc_{ph}^{ir}(t) = x_{ir}^{rem}(t) \times \frac{fd_{ph}^{ir}(t-1)}{\sum_{p=1}^{4}\sum_{h=1}^{R} fd_{ph}^{ir}(t-1) + \sum_{j=1}^{N}\sum_{s=1}^{R} rd_{js}^{ir}(t-1) + \sum_{h=1}^{R} rd_{res,h}^{ir}(t-1)}. \quad (110)$$

Here $fd_{ph}^{ir}(t-1)$ refers to the orders issued by the p-th type of final consumers in region h to the supplying sector i in region r during the previous period. $rd_{js}^{ir}(t-1)$ and $rd_{res,h}^{ir}(t-1)$ are the orders issued to support the reconstruction of damaged capital of sector j in region s and of the residential sector in region h, respectively.

Similarly, the quantities of products of sector i in region r allocated to satisfy the reconstruction demand of productive capital of sector j in region s, $rc_{js}^{ir}(t)$, and residential capital of the residential sector in region h, $rc_{res,h}^{ir}(t)$, are:

$$rc_{js}^{ir}(t) = x_{ir}^{rem}(t) \times \frac{rd_{js}^{ir}(t-1)}{\sum_{p=1}^{4}\sum_{h=1}^{R} fd_{ph}^{ir}(t-1) + \sum_{j=1}^{N}\sum_{s=1}^{R} rd_{js}^{ir}(t-1) + \sum_{h=1}^{R} rd_{res,h}^{ir}(t-1)}, \quad (111)$$

$$rc_{res,h}^{ir}(t) = x_{ir}^{rem}(t) \times \frac{rd_{res,h}^{ir}(t-1)}{\sum_{p=1}^{4}\sum_{h=1}^{R} fd_{ph}^{ir}(t-1) + \sum_{j=1}^{N}\sum_{s=1}^{R} rd_{js}^{ir}(t-1) + \sum_{h=1}^{R} rd_{res,h}^{ir}(t-1)}. \quad (112)$$

Then, sector j in region s receives intermediates from all regions to restore its inventories of product i at time step t, as below:

$$S_{js}^{i,restored}(t)=\sum_{r=1}^{R} ic_{js}^{ir}(t). \tag{113}$$

Therefore, the available inventory level of intermediate product i held by sector j in region s at the beginning of the next period $t+1$ is:

$$S_{js}^{i}(t+1)=S_{js}^{i}(t)-S_{js}^{i,used}(t)+S_{js}^{i,restored}(t). \tag{114}$$

This equation describes the inventory dynamics of sector j in region s after a disaster. The second item on the right-hand side denotes the inventory used at each time step, which is directly determined by the production level of that sector at that time (Equation (107)). The third item on the right-hand side refers to the inventory restored at each time step, which is associated with both the intermediate orders placed by that sector at last time and the supplying capacity of other sectors at that time (Equation (108)). If the use of an inventory is faster than its restoration, the remaining level of this inventory will continue to decrease and eventually generate a binding constraint on the production capacity, which in turn limits or reduces the subsequent production and the inventory usage until the remaining inventory level increases again. This self-limiting mechanism of inventory dynamics may be observed during a rapid production expansion, which leads to a temporary slowdown of post-disaster economic recovery (see the illustrative results of Chapter 6).

Similarly, the recovered capital of sector j in region s and the residential sector in region h during the period t are equal to:

$$K_{js}^{rec}(t)=\sum_{i=1}^{N}\sum_{r=1}^{R} rc_{js}^{ir}(t), \tag{115}$$

$$K_{res,h}^{rec}(t)=\sum_{i=1}^{N}\sum_{r=1}^{R}rc_{res,h}^{ir}(t). \tag{116}$$

Then on the demand side of the economy, downstream sectors and households issue orders to their suppliers at the end of each period according to their production, consumption, and reconstruction plans for the next period. When a product comes from multiple suppliers, the orders are redistributed among suppliers from different regions according to their production capacities.

First, a sector issues orders to its suppliers because of the need to restore its intermediate product inventory. The model assumes that sector j in region s has a specific targeted inventory level of product i, $S_{js}^{i,G}$, which is equal to a given number of weeks n_{js}^{i} of intermediate consumption of product i based on its production capacity at the pre-disaster level:

$$S_{js}^{i,G}=n_{js}^{i}\times a_{i,js}\times\bar{x}_{js}. \tag{117}$$

To fill the gap between the targeted and the actual inventory levels of intermediate product i at the end of time t (i.e., at the beginning of time $t+1$), sector j in region s will allocate its orders among the suppliers of product i from different regions based on their production capacities. Then the order issued by sector j in region s to the supplying sector i in region r is equal to:

$$id_{js}^{ir}(t)=\begin{cases}\left(S_{js}^{i,G}-S_{js}^{i}(t+1)\right)\times\dfrac{\overline{id}_{js}^{ir}\times x_{ir}^{a}(t)}{\sum_{r=1}^{R}\overline{id}_{js}^{ir}\times x_{ir}^{a}(t)}, & \text{if } S_{js}^{i,G}>S_{js}^{i}(t+1)\\ 0, & \text{if } S_{js}^{i,G}\le S_{js}^{i}(t+1)\end{cases}. \tag{118}$$

Here $\overline{id}_{js}^{ir}$ is the intermediate demand of sector j in region s for products of sector i in region r at the pre-disaster level. Instead of a complete substitution, this

model assumes a partial substitution of suppliers in the same sector from different regions by setting the possibility of substitution on the basis of suppliers' production capacity. This is due to the fact that not all products can be easily substituted between regions. For instance, a car manufacturing sector in Japan may use screws from Chinese auto parts manufacturing sector and engines from German auto parts manufacturing sector, then the products of the supplying sectors in these two regions cannot be substituted. In an economic system with diverse products, an overly optimistic assumption about cross-regional substitutability may lead to an underestimation of production losses. Therefore, this model takes a middle way between zero substitutability and full substitutability to alleviate the evaluation deviations.

Furthermore, this modelling of intermediate demand is also different from the previous version of the Disaster Footprint model, as the intermediate demand of a sector no longer depends on its production level (Equation (86)), but on the gap between the remaining inventory level and a targeted level (Equation (118)).

Second and similarly, final users (i.e., domestic households, governments, investors, and foreign consumers) allocate orders among their suppliers from different regions based on their demand and the production capacities of their suppliers. The p-th type of final demand in region h for product i at time t, $\widetilde{fd}^{i}_{ph}(t)$, is obtained by adding up the demand from different regions, as below:

$$\widetilde{fd}^{i}_{ph}(t) = \sum_{r=1}^{R} \overline{fd}^{ir}_{ph} . \tag{119}$$

Here $\overline{fd}^{ir}_{ph}$ is the p-th type of final demand in region h for product i in region r at the pre-disaster level. This model simply assumes that final demands do not shift significantly in the short run after the extreme event.

Then, the orders issued by the p-th type of final users in region h to the supplying sector of product i in region r is:

$$fd_{ph}^{ir}(t) = \widetilde{fd}_{ph}^{i}(t) \times \frac{\overline{fd}_{ph}^{ir} \times x_{ir}^{a}(t)}{\sum_{r=1}^{R} \overline{fd}_{ph}^{ir} \times x_{ir}^{a}(t)}. \tag{120}$$

Third, an industrial sector or the residential sector (the households) in a region also issues orders to its suppliers because of the reconstruction demand to recover its capital damaged by the disaster. Here the model adopts the assumption in Hallegatte (2008) that capital damage will all be repaired and that insurance companies will pay the whole repair costs, so that the reconstruction expenditures do not have a crowding-out effect on other types of consumption. Sector j in region s and the households in region h set their targeted level of capital stock at the pre-disaster level, $\overline{K}_{js}$ and $\overline{K}_{res,h}$, respectively. The model uses the capital matrix coefficients η_s^{ir} to express the units of product i in region r that are invested to form one unit of capital in region s. Different sectors in the same region are assumed to share the same capital matrix coefficients. Therefore, the total demand for product i to support reconstruction of sector j in region s and the residential sector in region h at time step t, $\widetilde{rd}_{js}^{i}(t)$ and $\widetilde{rd}_{res,h}^{i}(t)$, are calculated as:

$$\widetilde{rd}_{js}^{i}(t) = \max\left\{\sum_{r=1}^{R}\left(\overline{K}_{js} - K_{js}(t)\right) \times \eta_s^{ir}; 0\right\}, \tag{121}$$

$$\widetilde{rd}_{res,h}^{i}(t) = \max\left\{\sum_{r=1}^{R}\left(\overline{K}_{res,h} - K_{res,h}(t)\right) \times \eta_h^{ir}; 0\right\}. \tag{122}$$

Here $K_{js}(t)$ and $K_{res,h}(t)$ are the capital stock held by sector j in region s and the residential sector in region h at time t, respectively, which are derived from

Equations (98) and (99).

Then the orders issued by the reconstruction agents of j in region s and the residential sector in region h to the supplying sector of product i in region r are:

$$rd_{js}^{ir}(t) = \widetilde{rd}_{js}^{i}(t) \times \frac{\eta_{s}^{ir} \times x_{ir}^{a}(t)}{\sum_{r=1}^{R} \eta_{s}^{ir} \times x_{ir}^{a}(t)}, \tag{123}$$

$$rd_{res,h}^{ir}(t) = \widetilde{rd}_{res,h}^{ir}(t) \times \frac{\eta_{h}^{ir} \times x_{ir}^{a}(t)}{\sum_{r=1}^{R} \eta_{h}^{ir} \times x_{ir}^{a}(t)}. \tag{124}$$

Therefore, the total order received by sector i in region r is:

$$TD_{ir}(t) = \sum_{j=1}^{N}\sum_{s=1}^{R} id_{js}^{ir}(t) + \sum_{p=1}^{4}\sum_{h=1}^{R} fd_{ph}^{ir}(t) + \sum_{j=1}^{N}\sum_{s=1}^{R} rd_{js}^{ir}(t) + \sum_{h=1}^{R} rd_{res,h}^{ir}(t). \tag{125}$$

Finally, the model assumes that sectors can overproduce with primary inputs (i.e., capital and labour) in response to demand surges or production shortages[9]. The modelling of overproduction capacity is similar with Hallegatte (2008), except of a different trigger condition considering the presence of inventory constraints and a distinction between the two primary inputs. The overproduction capacity of primary input q in each sector and region at time t is denoted by $\alpha_{ir}^{q}(t)$, where $q = \{K, L\}$ representing capital or labour input. $\alpha_{ir}^{q}(t)$ can increase up to a maximum value $\alpha_{ir}^{\max}$ in a time delay τ_{α} when capital or labour production capacity is smaller than both the total demand and inventory capacities, i.e., $x_{ir}^{q}(t) < \min\left\{TD_{ir}(t);\ \text{for all}\, j,\ x_{ir}^{j}(t)\right\}$; it can also drop back to the pre-disaster level

[9] The overproduction capacity is imposed on primary inputs, such as labour and capital, but not on intermediate inputs (i.e., inventories), considering that idle equipment can be employed and workers can increase their productivity during crisis.

$\overline{\alpha}_{ir}$ (normalized at 100%) in the same time delay τ_{α} when capital or labour production capacity is larger than any one of the total demand and inventory capacities, i.e., $x_{ir}^{q}(t) > \min\left\{TD_{ir}(t);\ \text{for all}\, j,\ x_{ir}^{j}(t)\right\}$; otherwise, that is, if $x_{ir}^{q}(t) = \min\left\{TD_{ir}(t);\ \text{for all}\, j,\ x_{ir}^{j}(t)\right\}$, it will remain unchanged. Here an indicator function $\Omega(q,t)$ is used to summarize the direction of changes in the overproduction capacity, as below:

$$\Omega(q,t) = \begin{cases} 1, & \text{if } x_{ir}^{q}(t) < \min\left\{TD_{ir}(t);\ \text{for all}\, j,\ x_{ir}^{j}(t)\right\} \\ -1, & \text{if } x_{ir}^{q}(t) > \min\left\{TD_{ir}(t);\ \text{for all}\, j,\ x_{ir}^{j}(t)\right\} \\ 0, & \text{if } x_{ir}^{q}(t) = \min\left\{TD_{ir}(t);\ \text{for all}\, j,\ x_{ir}^{j}(t)\right\} \end{cases}. \tag{126}$$

Then the dynamics of this overproduction capacity, which is bounded by $\left[\overline{\alpha}_{ir},\ \alpha_{ir}^{\max}\right]$, can be expressed as:

$$\alpha_{ir}^{q}(t+1) = \min\left\{\max\left\{\alpha_{ir}^{q}(t) + \frac{\alpha_{ir}^{\max} - \overline{\alpha}_{ir}}{\tau_{\alpha}} \times \frac{\left|TD_{ir}(t) - x_{ir}^{q}(t)\right|}{\overline{x}_{ir}} \times \Omega(q,t);\ \overline{\alpha}_{ir}\right\};\ \alpha_{ir}^{\max}\right\} . \tag{127}$$

Here $\dfrac{\left|TD_{ir}(t) - x_{ir}^{q}(t)\right|}{\overline{x}_{ir}}$ represents the absolute gap between production capacity and total demand, relative to the pre-disaster level of sectoral output. This term determines the size of movement in $\alpha_{ir}^{q}(t)$ at each time step, which decreases to zero as the gap is narrowed to zero during the post-disaster recovery. This mechanism ensures the convergence of the overproduction capacity towards the pre-disaster level over time.

Following a disaster, the economic agents on the supply and demand sides go through the above production, allocation, recovery, and demand adjustment procedures recursively, until a full economic recovery to the pre-disaster level after all constraints

are lifted (i.e., damaged productive capital is fully recovered, all labour constraints are lifted, and all business linkages are repaired). Socio-economic development is not considered in this version. This discrete-time dynamic procedure can reproduce the economic equilibrium and simulate the propagation of exogenous shocks in the economic network. During a disaster, if the supply of a sector is constrained by capital or labour damage, this will have two effects. On the one hand, the decrease in output of this sector means that the orders of its clients cannot be fulfilled. This will result in a decrease in inventory of these clients, which will constrain their production. This is the so-called forward or downstream effect. Reversely, less output in this sector also means less use of intermediate products from its suppliers. This will reduce the production level of its suppliers. This is the so-called backward or upstream effect.

These impacts continuously propagate through the production supply chain, from one sector to another and one region to another, leaving footprint in the economic network. The model defines the value-added decrease of all sectors during these process as the indirect disaster footprint, which is calculated as:

$$IndirectFootprint = \sum_{t} \sum_{i=1}^{N} \sum_{r=1}^{R} \left(\overline{va}_{ir} - va_{ir}(t) \right). \tag{128}$$

Here $\overline{va}_{ir}$ and $va_{ir}(t)$ are the value added of sector i in region r at the pre-disaster level and at time t, respectively. The value added of a sector is equal to the value of output minus the value of intermediate input used to produce that output, i.e., $va_{ir}(t) = x_{ir}^{a}(t) - \sum_{j=1}^{N} \sum_{s=1}^{R} a_{js,ir} \times x_{ir}^{a}(t)$. $a_{js,ir}$ is the technical coefficient derived from the IO table used indicating the input of product j in region s required to produce one unit of product i in region r.

3.2. A Compound-Hazard Economic Footprint Assessment (CHEFA) Model for Disaster Analysis

The Compound-Hazard Economic Footprint Assessment (CHEFA) model is built on the second version of the Disaster Footprint model (i.e., the DF-substitution model) to evaluate the overall economic impacts of a compound hazard along the production supply chain. The DF-substitution model is characterised by the incorporation of inventory dynamics and cross-regional substitutability of suppliers at a multi-regional level, which can better reproduce the post-disaster recovery process, particularly for large-scale disruptive events, than other models. A comparison between the two versions of the Disaster Footprint model, as well as other models in similar veins, is presented in Appendix Table A1 and Appendix Table A2. The CHEFA model further extends the DF-substitution model to the case of compound hazards (say a perfect storm comprising of flooding, pandemic control, and export restrictions in the complex context of climate change, pandemic outbreaks, and deglobalisation), with three improvements: 1) it analyses the interaction between climate and pandemic responses, that is, the negative externality of pandemic control on the recovery of capital destructed by natural disasters and the stimulus effects of capital reconstruction to offset the negative impacts of pandemic control; 2) it considers the roles of export restriction and production specialization in exacerbating the economic consequences of compound events. Export restriction is a common trade policy signalling deglobalization, while production specialization reduces the substitutability of regional products and may increase the economic vulnerability for negative shocks (Boehm et al., 2019); and 3) it incorporates the effects of external subsidies, reconstruction expenditures, and intertemporal consumption preferences on post-disaster production and consumption adaptations. Previous models usually ignores the crowding-out effect of reconstruction costs on household consumption by assuming that these costs are largely funded by insurance companies (Hallegatte, 2008).

However, as mentioned by Cochrane (2004), household demand decreases temporarily when the recovery is financed by local savings and borrowing, which should therefore be considered in disaster impact analysis.

It should be noted that the pandemic impact mentioned here does not mean the impact of pandemic itself, but the shock of its control measures, mainly referred to as the lockdowns, to the economy. The total impacts (including the health impacts) of a pandemic such as COVID-19 might be huge (Cutler and Summers, 2020), but this thesis only focuses on the economic impacts of pandemic control, which is characterised into different combinations of duration and strictness of regional lockdowns[10]. The monetarized values of premature deaths and health impairment caused by virus infections are not within the research scope. It is also recognized that differences exist in many aspects between the pandemic control, flooding, and export restrictions, and it is unrealistic to cover all these differences in the CHEFA model. As the model is mainly aimed for the economic impact assessment, it only extracts features that are of economic relevance and parameterizes them with different values (such as different durations, intensities, and spatial spreads) for different events. To keep it simple, the model does not distinguish the specific warning, impact, and response phases of different events, instead it considers them as a whole in the scenario settings.

In the CHEFA model, the three types of events enter the economic system in different ways given their different characteristics, but they all cause indirect impacts, which sometimes intertwines, through both backward and forward propagations along the supply chain. First, the flood impacts start with the direct damage to labours and capital stock and the increasing reconstruction needs. The labour/capital damage limits the

[10] Strictness represents the percentage by which transportation capacity is reduced relative to the pre-pandemic level.

production and supply of the flooded sectors, which propagates forward to the production of downstream sectors because of an input shortage. There are also large backward propagations to upstream sectors through reduced demands (when the flooded sectors have lower production capacities) or increased demands (due to reconstruction needs). Second, the pandemic control affects the economy by restricting the transportation capacity and labour availability, which is different from flood impact. This is also accompanied with forward and backward propagations due to delivery failures of intermediate inputs and reduced demand at a low production capacity. Meanwhile, the transport restriction impedes the process of flood-related reconstruction, which exacerbates the indirect impacts. Third, as for deglobalization, trade restrictions are used as a proxy to measure its economic impacts. A trade restriction limits the maximum export of specific products from a region to another region below a certain percentage of the previous level. It causes both forward propagations (when the importing sectors in the latter region produce less due to a shortage of imported input) and backward propagations (as the exporting sectors in the former region also produce less due to a reduced export demand), which is similar and entangled with flood and pandemic impacts. This is how the model packages the three types of hazards into a macro-economic risk assessment. Although these events are different in many aspects, they have similar and intertwined risk transmission channels within the economic system.

Figure 3-2 presents the framework of the CHEFA model, which is driven by four modules, that is, a compound shock module, a production module, an allocation module, and a demand module. The compound shock module refers to the negative compound shocks of flooding, pandemic control, and export restriction on various aspects of the economy. The production module describes the sectors' production activities under production, transport and import capacity constraints. The allocation module explains how sectors allocate output to their clients, including downstream

sectors and households, to satisfy the intermediate demand for inventory refilling and final demand for consumption and reconstruction. Finally, the demand module portrays how clients issue orders to their suppliers, which iterates into the next round of production until the economy recovers to the pre-disaster state.

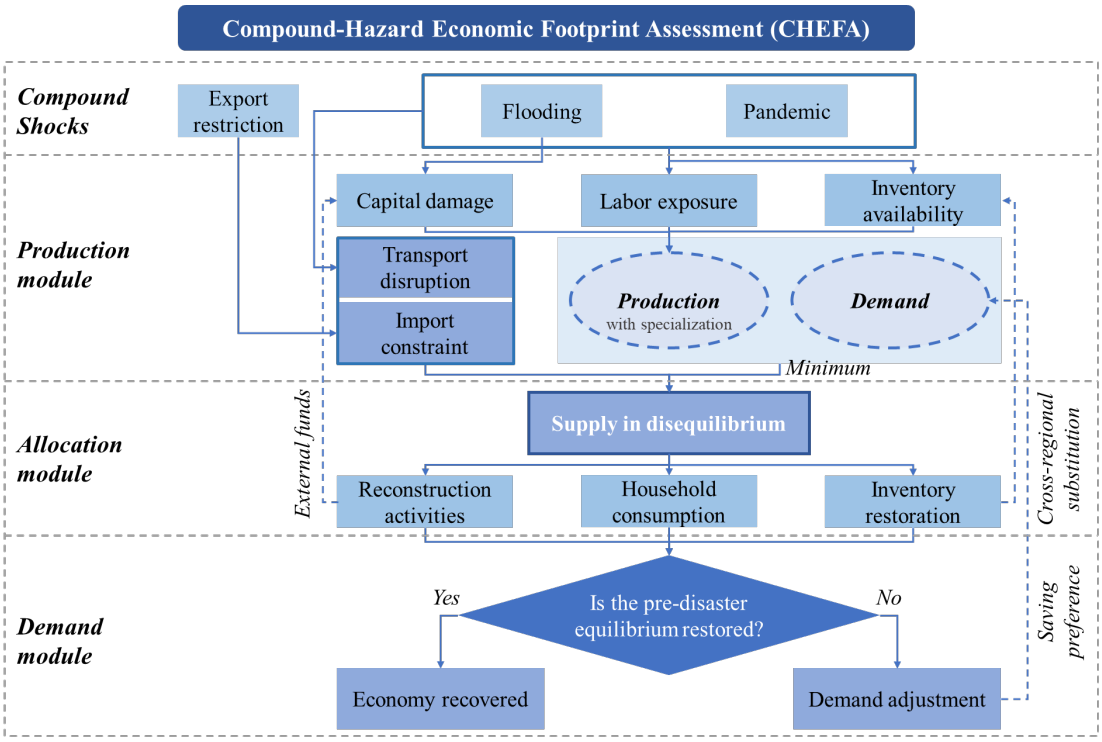

Figure 3-2: Framework of the CHEFA model.

The CHEFA model starts with a multi-regional economy in equilibrium. It defines two types of economic agents, namely industrial/production sectors and households, distributed in R regions. Sectors make products which can be consumed by either downstream sectors or households. There is a total of N types of products, one-to-one corresponding to N production sectors, therefore there are up to $R \times N$ sectors in the economy. For simplification purposes, the model uses a representative household which consumes multiple types of products to represent all the households in a region. The total number of representative households in the economy is equal to R. A brief description of key variables used in the model is listed in Appendix Table A3.

Key assumptions used in the CHEFA model are listed below:

- There are R regions in the economy, each of which has N production sectors.
- Each sector makes only one product with inputs from other sectors necessary for its production.
- There are specialized and non-specialized products in the economy. The specialized products cannot be substituted by the products from different sectors or regions, while the non-specialized products can be substituted by the products from the same sector in different regions.
- A modified Leontief production function is adopted, which distinguishes between specialized and non-specialized intermediate inputs.
- Primary inputs (e.g., labour and capital), which are not mutually substitutable, are fully employed by sectors to carry out production in the pre-disaster economic equilibrium.
- The input-output relationship (i.e., economic structure) is constant over the study period.
- Post-disaster labour dynamics follow an exogenous process, reflecting labour losses from casualties, labour recovery at certain rates, and lost working hours due to transport disruptions.
- The impacts of a specific transport disruption on the operation of sectors are different according to sectoral characteristics.
- The transportation capacity between two regions is mainly constrained by the transport condition of the place of origin.
- The transportation capacity is recovered exogenously at a given rate according to the duration of disease control and the repairing progress of inundated transport infrastructure.
- The maximum export volume of a product in a region is reduced by the export restriction imposed on that product.

- Local consumption, import and export of the accommodation, food and recreation services decline in the epidemic and flooded regions, while the local consumption and import of medical services and emergency products increase in these regions.
- A prioritized-proportional rationing scheme under export restriction is adopted, in which each sector first allocates its output to address intermediate demand and then proportionally allocates the remaining output to other categories of demands without violating the export restriction imposed on that sector's product.
- The reconstruction costs are paid by household savings, which has a crowding-out effect on other consumption.
- A change in household income affects not only current but also future consumption, which is related to the specific intertemporal consumption/saving preference of the households in that region.
- Inputs from other sectors required by each unit of capital formation are identical across sectors in the region.
- Sectors can gradually increase their production capacity up to the maximum in response to demand surges or supply shortages.
- Imports from outside the economy are never constrained by the disaster.
- Sectors are always expecting to receive as many orders as in the previous period.
- Customers can redistribute their orders among suppliers from different regions according to the production, transportation, and exportation capacities of suppliers.
- Sectors aim to keep a certain level of inventory to sustain a given number of weeks of production at the pre-disaster level, but with a control of adjustment rate to prevent dynamic instabilities.
- The economy is targeted to recover to the pre-disaster level in the short run after the disaster.

3.2.1. Compound Exogenous Shocks

Considering a compound hazard comprising of flooding, pandemic control, and trade

frictions, there are mainly four categories of direct shocks introduced to the affected multi-regional economy, that is, damages to production factors (e.g., capital and labour), transport disruptions, export restrictions, and final consumption disruption.

3.2.1.1. Capital Damage

Both industry productive and residential capital can be inundated or destroyed by flooding. Industry productive capital is the capital invested in production by industrial sectors, including factories, machines, equipment, etc. Residential capital mainly refers to houses or residential buildings that are owned by households in the region. The damaged capital can also be recovered by the post-disaster reconstruction activities. Residential capital is not involved in production processes, but its restoration after the disaster could compete resources with that of productive capital, and therefore affect the recovery of production. The model assumes that all capital damage is caused by flooding, while pandemic control and trade frictions have no direct impact on these physical assets. Then, the capital dynamics (including capital damage and recovery) are modelled in the same way as the DF-substitution model (see Equations (98)-(100)).

3.2.1.2. Labour Damage

Labour supply is damaged by both flooding and pandemic crises. First, fewer employees can work because of injury, illness or death from flooding and virus infection. Second, healthy employees spend more time commuting to and from work due to transport disruptions, which results in working time losses. The shortage or malfunction of production factors will reduce the sectors' production capacity. In this model, labour damage, $\gamma_{ir}^{L}(t)$, is expressed as the fraction of working hour loss in each sector and region during each time step:

$$\gamma_{ir}^{L}(t)=\frac{\left(L_{ir}^{dam,C}(t)+L_{ir}^{dam,F}(t)\right)\times\overline{wh}_{ir}+\left(\overline{L}_{ir}-L_{ir}^{dam,C}(t)-L_{ir}^{dam,F}(t)\right)\times\Delta wh_{ir}(t)}{\overline{L}_{ir}\times\overline{wh}_{ir}} \quad (129)$$

Here $\overline{L}_{ir}$ and $\overline{wh}_{ir}$ represents the number of employees and working hours per worker in sector i and region r at the pre-disaster levels. $L_{ir}^{dam,C}(t)$ and $L_{ir}^{dam,F}(t)$ are the numbers of workers unable to work due to virus infection and flooding at time t, respectively. $\Delta wh_{ir}(t)$ is the loss of working hours per worker in sector i and region r at time t. It is determined by the degree of transport disruption $\gamma_r^Z(t)$ in region r (see Equation (133)) and a sector-specific impact multiplier ρ_i:

$$\Delta wh_{ir}(t) = \rho_i \times \gamma_r^Z(t) \times \overline{wh}_{ir}. \tag{130}$$

Here ρ_i captures the impact of transport disruption on the operation of sector i. It is based on three factors: the degree of exposure of the sector (e.g., the extent of in-person interactions), whether it is the lifeline sector (e.g., electricity) and the possibility for work at home (Guan et al., 2020). For example, the multiplier for the education sector could be low (e.g., 0.1) because of the development of online learning.

Due to data limitations, the model assumes that the affected labours are recovered following an exogenous rate β_L, defined as the proportion by which the affected labours are reduced per next period ($0 < \beta_L < 1$). Then the affected labour at each time step can be expressed as:

$$L_{ir}^{dam,F}(t) = (1-\beta_L) \times L_{ir}^{dam,F}(t-1), \tag{131}$$

$$L_{ir}^{dam,C}(t) = (1-\beta_L) \times L_{ir}^{dam,C}(t-1). \tag{132}$$

3.2.1.3. Transport Disruption

Transport disruptions come from two aspects during the compound hazard. First, public transport restrictions are placed in the pandemic-hit regions to contain virus

transmission. Those restrictions may include reducing the number of passengers to keep social distance and suspending international flights from pandemic-hit areas. The model uses $\gamma_r^{Z,C}(t)$ to denote the percentage by which transportation capacity are reduced by lockdown measures relative to the initial equilibrium levels in region r at time t. This is also a metric measuring the strictness of pandemic control (see Footnote 10). Second, the transport infrastructure (e.g., roads, railways, and airports) could also be inundated and out of operation in the flooded regions. The model uses $\gamma_r^{Z,F}(t)$ to represent the percentage of submerged transport infrastructure during flooding. It is assumed that the transportation capacity from region r to other regions is simply constrained by the transport conditions in region r, which is further determined by the severer one between pandemic and flooding constraints in that region. Therefore, the relative reduction of transport capacity from region r to other regions at time t, $\gamma_r^Z(t)$, is calculated as:

$$\gamma_r^Z(t) = \max\left\{\gamma_r^{Z,C}(t); \gamma_r^{Z,F}(t)\right\}. \tag{133}$$

Transport disruptions not only affect labour supply (as mentioned above), but also increase the difficulty in delivering the intermediate and final products to downstream sectors and households. Similar with the labour constraint, the model calculates the connectivity loss of the supplying sector i in region r to its business and household clients in other regions as below:

$$\gamma_{ir}^Z(t) = \rho_i \times \gamma_r^Z(t). \tag{134}$$

Here the connectivity loss $\gamma_{ir}^Z(t)$ is defined as the reduction in the capacity of transporting the product of sector i in region r to the demanding sectors and households in other regions, relative to the pre-disaster level, at each time step.

As for transport recovery, the pandemic-induced transport constraint $\gamma_r^{Z,C}(t)$ is lifted after the duration of lockdowns in that region, while the flood-induced transport constraint $\gamma_r^{Z,F}(t)$ is alleviated at an exogenous rate β_Z as below:

$$\gamma_r^{Z,F}(t) = (1-\beta_Z) \times \gamma_r^{Z,F}(t-1). \tag{135}$$

This is similar with the assumed process of labour recovery due to data limitations. β_Z is defined as the proportion by which the flood-related transport disruptions are alleviated per next period ($0 < \beta_Z < 1$), which usually depends on the repairing progress of transport infrastructure (e.g., roads and bridges) damaged by the flood.

3.2.1.4. Export Restrictions

With the ongoing process of deglobalization, particularly in the complex of pandemic and natural crises, countries/regions may impose export restrictions on critical goods (e.g., food and medical products) to secure domestic supply (Eaton, 2021; Espitia et al., 2020). Although the export restrictions applied by large exporters may in the short run increase domestic availability, the measures reduce the world's supply of the products concerned and the importing countries incapable of self-sufficiency will suffer when they cannot import as much as they need (World Trade Organization, 2020). The model uses $\gamma_{ir}^{E}(t)$ to denote the degree of export restrictions introduced by region r on product i at time t. It is measured by the percentage reduction of the maximum export volume of that product in region r relative to the initial level. The export restrictions would generate additional constraints on the delivery or allocation of produced commodities to downstream consumers, as modelled in Section 3.2.3.1.

3.2.1.5. Final Demand Disruption

Households might also adjust their consumption in response to the compound hazard. For example, they may spend less on restaurants, travelling and other outdoor recreational activities, while more on medical services and emergency products. The model assumes that the local consumption, import and export of the accommodation, food and recreation services decline by $\theta\%$ in the pandemic- and flood-hit regions, while the local consumption and import of medical services and emergency products increase by $\vartheta\%$ in these regions. These adjustments of final consumption can be summarised as:

$$\widetilde{\widetilde{fd}}_h^{ir}(t) = (1-\theta\%)^{I(i\in N_\theta)\times I(r,h\in R_C\cup R_F)} \times (1+\vartheta\%)^{I(i\in N_\vartheta)\times I(h\in R_C\cup R_F)} \times \overline{fd}_h^{ir}. \quad (136)$$

Here $\widetilde{\widetilde{fd}}_h^{ir}(t)$ refers to the adjusted final consumption of product i in region r by the households in region h at time t after the disaster. $\overline{fd}_h^{ir}$ is the final consumption at the pre-disaster level. $I(i\in N_\theta)$ is an indicator function which takes value 1 when product i belongs to the sector set of accommodation, food, and recreation services (N_θ), otherwise it takes value 0. $I(r,h\in R_C\cup R_F)$ is an indicator function which takes value 1 when region r or h is one of the pandemic-hit regions (R_C) or flooded regions (R_F), otherwise it takes value 0. Similarly, $I(i\in N_\vartheta)$ is the indicator function which takes value 1 when product i belongs to the sector set of medical services and emergency products (N_ϑ), otherwise it takes value 0. $I(h\in R_C\cup R_F)$ is the indicator function which takes value 1 when region h is one of the pandemic-hit or flooded regions, otherwise it takes value 0.

Besides, the model also accounts for the stimulus effects of external consumption subsidies and the crowding-out effects of reconstruction costs paid by household savings. Assuming that, at each time step t', households in region h receive an

external subsidy from public finance or social donations, which is denoted by $sub_h(t')$, and meanwhile pay an amount of $K_{res,h}^{rec}(t')$ for house repairs and reconstruction from their savings, then the change in their disposable income during that time is:

$$\Delta income_h(t') = sub_h(t') - K_{res,h}^{rec}(t'). \tag{137}$$

Here $K_{res,h}^{rec}(t')$ is the monetary value of residential capital recovered in region h during the period t', which is assumed to be paid by the households from their savings[11]. Its calculation depends on the recovery process of residential capital at each time step (see Equation (158) in Section 3.2.3.2). The income change is assumed to affect both current and future consumption with an intertemporal consumption or saving preference coefficient β_C, where $0 < \beta_C < 1$. This means that the impacts of current income change on future consumption will decrease by a fixed fraction $1-\beta_C$ over time. The smaller the value of β_C, the more households tend to consume at present and the lower the savings rate. Then the actual adaptive final demand for product i in region r by the households in region h at time t, $\widetilde{fd}_h^{ir}(t)$, is:

$$\widetilde{fd}_h^{ir}(t) = \widetilde{\widetilde{fd}}_h^{ir}(t) + \frac{\widetilde{\widetilde{fd}}_h^{ir}(t)}{\sum_{i=1}^{N}\sum_{r=1}^{R}\widetilde{\widetilde{fd}}_h^{ir}(t)} \times \sum_{t'=1}^{t} \beta_C^{(t-t')} \times (1-\beta_C) \times \Delta income_h(t'). \tag{138}$$

Here $\sum_{t'=1}^{t} \beta_C^{(t-t')} \times (1-\beta_C) \times \Delta income_h(t')$ calculates the current change in the overall willingness to consume due to the cumulative impacts of previous income changes in

[11] The price effects are not considered in the CHEFA model.

region h before time t, which is then multiplied by $\frac{\widetilde{\widetilde{fd}}_h^{ir}(t)}{\sum_{i=1}^{N}\sum_{r=1}^{R}\widetilde{\widetilde{fd}}_h^{ir}(t)}$ to indicate a proportional impact to the final demand for product i in region r.

Finally, different categories of direct impacts are not isolated. As have mentioned above, the unavailability of transportation may lead to labour constraints. The restoration of damaged capital, as well as export restrictions, will affect the structure of final demands in the disaster aftermath. The interactions between direct shocks lead to complex indirect impacts on the economic system. Therefore, a systematic assessment method is needed to address these issues.

3.2.2. Production System

3.2.2.1. Production with Cross-regional Substitution and Specialization

Previously, the DF-substitution model has adopted a Leontief-type production function which allows for substitution between suppliers of the same sector from different regions (Equation (95)). However, some products are less substitutable between regions, particularly when production specialization occurs. For example, Boehm et al. (2019) discovered that during the Japanese earthquake the economic losses in the US are highly concentrated among affiliates of Japanese multinationals, relative to non-Japanese firms, due to declines in imported intermediate inputs from Japan. This suggests that affiliates of Japanese firms in the US were unable to quickly substitute alternative inputs in the short run. Besides, the recent shortage of microchips, which is driven by the perfect storm of multiple factors, such as COVID-19 outbreaks, a fire in an automotive chip plant in Japan, the trade frictions between the US and China, etc., has greatly hampered automotive production in the US (McCarthy, 2021). Most of microchip production is dominated by two foundries in Asia, namely TSMC and Samsung, and their customers lack alternative suppliers who can quickly build a new

microchip fab or catch up with the leading-edge process technologies (Kuo, 2021).

The CHEFA model Improves on the DF-substitution model by incorporating non-substitutable specialized products. Although the possibility of cross-regional substitution is allowed, specialized products cannot be substituted elsewhere. There are two types of non-substitutability. The first one is non-substitutability between the N production sectors, that is, products of a sector cannot be substituted by products of a different sector, though can be substituted by products of the same sector from a different region. The second one is non-substitutability of specialized products which is different from and cannot be substituted by any products in any sectors or regions. It is assumed that there are M types of specialized products, each one belonging to one of the N production sectors in one of the R regions. Then sectors can use $N+M$ different types of mutually non-substitutable intermediate inputs to make their products. The production process is defined as:

$$x_{ir} = \min\left\{\text{for all } j,\ \frac{z_{j,ir}}{a_{j,ir}};\ \text{for all } q,\ \frac{v_{q,ir}}{b_{q,ir}}\right\},\quad j = 1,...,N+M\,. \tag{139}$$

Here x_{ir} demotes the output of sector i in region r in monetary values. $z_{j,ir}$ and $v_{q,ir}$ are the intermediate input j and primary input q (i.e., capital and labour), respectively, used to produce x_{ir} units of output by sector i in region r. $a_{j,ir}$ and $b_{q,ir}$ are the technical coefficients indicating the amount of intermediate input j and primary input q required to produce one unit of product i in region r, respectively, which are usually derived from the IO table used.

This production function is very similar with the one in the DF-substitution model (Equation (95)), except that it adds the M specialized products as non-substitutable intermediate inputs for production. The intermediate input j, if not specialized, can

be supplied by sector j from any regions in the economy; but if it is one of the M specialized inputs, it can only be supplied by sector j in the specific region that makes that specialized input. In other words, these specialized products are completely different from and irreplaceable with the product made by any other sector and region.

3.2.2.2. Production under Capital, Labour, and Inventory Constraints

After a compound-hazard event, sectoral production may be constrained by reduced productive capital, labour, and inventory availabilities. As described in Sections 3.2.1.1 and 3.2.1.2, both capital and labour are damaged by the co-existence of floods and pandemic lockdowns, which then reduces the available productive capital and labour that could be used for production. The remaining production capacity of productive capital and labour, $x_{ir}^{K}(t)$ and $x_{ir}^{L}(t)$, are modelled in the same way as the DF-substitution model with the inclusion of an overproduction capacity $\alpha_{ir}^{q}(t)$ (see Equations (101)-(103)). Besides, insufficient inventories will generate additional constraints on the production capacity. With the presence of production specialization, there are $N+M$ different types of inventories consumed in production. The potential production level, $x_{ir}^{j}(t)$, that the inventory of the intermediate product j can support is:

$$x_{ir}^{j}(t)=\frac{S_{ir}^{j}(t)}{a_{j,ir}},\quad j=1,...,N+M. \tag{140}$$

Here $S_{ir}^{j}(t)$ refers to the units of intermediate product j held by sector i in region r at the beginning of time t.

Then the maximum production capacity, $x_{ir}^{\max}(t)$, is calculated under all these constraints:

$$x_{ir}^{\max}(t)=\min\left\{x_{ir}^{K}(t);\ x_{ir}^{L}(t);\ \text{for all } j,\ x_{ir}^{j}(t)\right\},\quad j=1,...,N+M\ . \tag{141}$$

Therefore, the actual production of sector i in region r, $x_{ir}^{a}(t)$, should be the minimum of its maximum production capacity $x_{ir}^{\max}(t)$ and the total orders it receives from the clients during the last period $TD_{ir}(t-1)$:

$$x_{ir}^{a}(t)=\min\left\{x_{ir}^{\max}(t);\ TD_{ir}(t-1)\right\}. \tag{142}$$

And the units of inventory input j used to produce $x_{ir}^{a}(t)$ units of product by sector i in region r at time t is:

$$S_{ir}^{j,used}(t)=a_{j,ir}\times x_{ir}^{a}(t). \tag{143}$$

3.2.3. Allocation and Recovery

3.2.3.1. Prioritized-Proportional Rationing Scheme under Export Restrictions

The CHEFA model adopts the same prioritized-proportional rationing scheme as the DF-substitution model, in which a sector first allocates its output to address the intermediate demand and then proportionally allocates the remaining output to other categories of demand, except that this rationing process is constrained by export restrictions, that is, the total export of a sector at each time step should be no more than its maximum quota restricted by the trade policy:

$$\sum_{s\neq r}\sum_{j=1}^{N}ic_{js}^{ir}(t)+\sum_{h\neq r}fc_{h}^{ir}(t)+\sum_{s\neq r}\sum_{j=1}^{N}rc_{js}^{ir}(t)+\sum_{h\neq r}rc_{res,h}^{ir}(t)\leq\left(1-\gamma_{ir}^{E}(t)\right)\times\overline{ex}_{ir}\ . \tag{144}$$

Here $ic_{js}^{ir}(t)$, $fc_{h}^{ir}(t)$, $rc_{js}^{ir}(t)$, and $rc_{res,h}^{ir}(t)$ are the output that sector i in region r initially hopes to allocate to sector j in region s as intermediate use, to the households in region h as final consumption use, to sector j in region s as

productive capital reconstruction use, and to the households in region h as residential capital reconstruction use, respectively at time t, following the same prioritised-proportional rationing scheme as in the DF-substitution model (see Equations (108)-(112)). $\gamma_{ir}^{E}(t)$ is the degree of export restriction imposed on product i by region r at time t. It is measured by the percentage reduction of the maximum export volume of this product in region r relative to the pre-disaster level (see Section 3.2.1.4). $\overline{ex}_{ir}$ represents the export of this product from region r to other regions under the pre-disaster equilibrium state.

The model then adjusts the initially attempted exports of sector i in region r to downstream sectors, $ic_{js}^{ir}(t)$, to households, $fc_{h}^{ir}(t)$, and to reconstruction activities, $rc_{js}^{ir}(t)$ and $rc_{res,h}^{ir}(t)$, where $s,h \neq r$, to satisfy the constraint (144) according to a similar prioritized-proportional rationing scheme. Specifically, the output actually allocated to the downstream sector j in region s ($s \neq r$) after being adjusted to the export restriction, $ic_{js}^{ir,*}(t)$, is equal to:

$$ic_{js}^{ir,*}(t) = ic_{js}^{ir}(t) \times \min\left\{ \frac{\left(1-\gamma_{ir}^{E}(t)\right) \times \overline{ex}_{ir}}{\sum_{s \neq r}\sum_{j=1}^{N} ic_{js}^{ir}(t)} ; 1 \right\}. \tag{145}$$

Here the intermediate demands from business clients are still given the priority to be satisfied under export restrictions. The asterisk stands for the adjusted value according to the export restriction. If the restricted export quota of sector i in region r is larger than or equal to its initial delivery attempts to all business clients in other regions, i.e., $\left(1-\gamma_{ir}^{E}(t)\right) \times \overline{ex}_{ir} \geq \sum_{s \neq r}\sum_{j=1}^{N} ic_{js}^{ir}(t)$, then the export restriction is not a binding constraint on intermediate deliveries and $ic_{js}^{ir,*}(t) = ic_{js}^{ir}(t)$; otherwise, the initially

attempted intermediate deliveries are reduced proportionally by a factor of $\frac{\left(1-\gamma_{ir}^{E}\left(t\right)\right)\times\overline{ex}_{ir}}{\sum_{s\neq r}\sum_{j=1}^{N}ic_{js}^{ir}\left(t\right)}$ to not exceed the restricted export quota.

Afterwards, the remaining export quota, $exq_{ir}^{rem}\left(t\right)$, is:

$$exq_{ir}^{rem}\left(t\right)=\left(1-\gamma_{ir}^{E}\left(t\right)\right)\times\overline{ex}_{ir}-\sum_{s\neq r}\sum_{j=1}^{N}ic_{js}^{ir,*}\left(t\right). \quad (146)$$

Then similarly, the remaining export quota is allocated to the final and reconstruction demands in other regions ($s,h\neq r$), as below:

$$fc_{h}^{ir,*}\left(t\right)=fc_{h}^{ir}\left(t\right)\times\min\left\{\frac{exq_{ir}^{rem}\left(t\right)}{\sum_{h\neq r}fc_{h}^{ir}\left(t\right)+\sum_{s\neq r}\sum_{j=1}^{N}rc_{js}^{ir}\left(t\right)+\sum_{h\neq r}rc_{res,h}^{ir}\left(t\right)};1\right\}, \quad (147)$$

$$rc_{js}^{ir,*}\left(t\right)=rc_{js}^{ir}\left(t\right)\times\min\left\{\frac{exq_{ir}^{rem}\left(t\right)}{\sum_{h\neq r}fc_{h}^{ir}\left(t\right)+\sum_{s\neq r}\sum_{j=1}^{N}rc_{js}^{ir}\left(t\right)+\sum_{h\neq r}rc_{res,h}^{ir}\left(t\right)};1\right\}, \quad (148)$$

$$rc_{res,h}^{ir,*}\left(t\right)=rc_{res,h}^{ir}\left(t\right)\times\min\left\{\frac{exq_{ir}^{rem}\left(t\right)}{\sum_{h\neq r}fc_{h}^{ir}\left(t\right)+\sum_{s\neq r}\sum_{j=1}^{N}rc_{js}^{ir}\left(t\right)+\sum_{h\neq r}rc_{res,h}^{ir}\left(t\right)};1\right\}. \quad (149)$$

After the export adjustment, the remaining output of sector i in region r available for local clients, $x_{ir}^{loc}\left(t\right)$, is calculated as:

$$x_{ir}^{loc}\left(t\right)=x_{ir}^{a}\left(t\right)-\sum_{s\neq r}\sum_{j=1}^{N}ic_{js}^{ir,*}\left(t\right)-\sum_{h\neq r}fc_{h}^{ir,*}\left(t\right)-\sum_{s\neq r}\sum_{j=1}^{N}rc_{js}^{ir,*}\left(t\right)-\sum_{h\neq r}rc_{res,h}^{ir,*}\left(t\right). \quad (150)$$

Finally, the products of sector i in region r allocated to the local production sectors,

households and reconstruction agents are adjusted proportionally as below:

$$ic_{jr}^{ir,*}(t)=\frac{ic_{jr}^{ir}(t)}{ic_{jr}^{ir}(t)+fc_{r}^{ir}(t)+rc_{jr}^{ir}(t)+rc_{res,r}^{ir}(t)}\times x_{ir}^{loc}(t), \tag{151}$$

$$fc_{jr}^{ir,*}(t)=\frac{fc_{jr}^{ir}(t)}{ic_{jr}^{ir}(t)+fc_{r}^{ir}(t)+rc_{jr}^{ir}(t)+rc_{res,r}^{ir}(t)}\times x_{ir}^{loc}(t), \tag{152}$$

$$rc_{jr}^{ir,*}(t)=\frac{rc_{jr}^{ir}(t)}{ic_{jr}^{ir}(t)+fc_{r}^{ir}(t)+rc_{jr}^{ir}(t)+rc_{res,r}^{ir}(t)}\times x_{ir}^{loc}(t), \tag{153}$$

$$rc_{res,r}^{ir,*}(t)=\frac{rc_{res,r}^{ir}(t)}{ic_{jr}^{ir}(t)+fc_{r}^{ir}(t)+rc_{jr}^{ir}(t)+rc_{res,r}^{ir}(t)}\times x_{ir}^{loc}(t). \tag{154}$$

3.2.3.2. Recovery of Inventory and Capital Stock

Sector j in region s receives intermediates from all relevant regions to restore its inventories of product i at time step t:

$$S_{js}^{i,restored}(t)=\sum_{r\in R^{i}}ic_{js}^{ir,*}(t),\quad i=1,...,N+M. \tag{155}$$

Here R^{i} refers to the set of regions which supply product i. If product i is a specialized product of sector i in region r, then r is the only region making product i and $R^{i}=\{r\}$.

Therefore, the units of intermediates i held by sector j in region s at the beginning of the next period $t+1$ are:

$$S_{js}^{i}(t+1)=S_{js}^{i}(t)-S_{js}^{i,used}(t)+S_{js}^{i,restored}(t). \tag{156}$$

Similarly, the recovered productive capital of sector j in region s and the recovered residential capital in region h during the period t are equal to:

$$K_{js}^{rec}(t)=\sum_{i=1}^{N}\sum_{r=1}^{R}rc_{js}^{ir,*}(t), \tag{157}$$

$$K_{res,h}^{rec}(t) = \sum_{i=1}^{N}\sum_{r=1}^{R} rc_{res,h}^{ir,*}(t). \quad (158)$$

Here the reconstruction costs of residential capital are paid by the households from their savings, which will have a crowding-out effect on their other consumption, as described in Section 3.2.1.5.

Moreover, the recovery of labour availability and transport capacity is exogenously assumed to be associated with the duration of pandemic lockdowns and the repairing progress of flooded transport infrastructure, which has been described in Sections 3.2.1.2 and 3.2.1.3.

3.2.4. Demand Adjustment

At the end of each period downstream sectors and households issue orders to their suppliers according to their production, consumption, and reconstruction plans for the next period. When a product comes from multiple suppliers, the orders are redistributed among suppliers from different regions according to their production, transportation, and exportation capacities.

3.2.4.1. Intermediate Demand

Similar with the DF-substitution model, a sector issues orders to its suppliers because of the need to restore its intermediate product inventory. Each sector j in region s has a specific targeted inventory level of product i (including non-substitutable specialized ones), $S_{js}^{i,G}$, which is equal to a given number of weeks n_{js}^{i} of intermediate consumption of product i based on its production capacity at the pre-disaster level:

$$S_{js}^{i,G} = n_{js}^{i} \times a_{i,js} \times \bar{x}_{js}, \quad i = 1,...,N+M. \quad (159)$$

However, dynamic instabilities, or the so-called bullwhip effect, may sometimes set in when sectors try to restore their inventories too quickly. To address these instabilities, the CHEFA model introduces a new parameter τ_s to control the speed of inventory restoration. It describes the proportion of inventory losses that production sectors try to restore in the next time step. For instance, if they lose x unit of their inventory, compared to the pre-disaster level, then they will increase their intermediate orders by $\tau_s \times x$ unit right in the next time step, and $0 \le \tau_s \le 1$. Therefore, the order placed by sector j in region s for intermediate input of product i at the end of time t is calculated as:

$$\widetilde{id}^{i}_{js}(t) = \max\left\{\tau_s \times \left(S^{i,G}_{js} - S^{i}_{js}(t+1) - a_{i,js} \times \bar{x}_{js}\right) + a_{i,js} \times \bar{x}_{js}; 0\right\}. \tag{160}$$

Here $S^{i,G}_{js} - S^{i}_{js}(t+1)$ is the gap between the targeted and actual inventory levels at the end of time t (i.e., the beginning of time $t+1$), and $a_{i,js} \times \bar{x}_{js}$ is that gap at the pre-disaster level. The latter is also the intermediate order placed each time before the disaster. If $\tau_s = 1$, then $\widetilde{id}^{i}_{js}(t) = \max\left\{S^{i,G}_{js} - S^{i}_{js}(t+1); 0\right\}$, which is the case in the DF-substitution model.

Next, sector j in region s will redistribute its intermediate orders among suppliers of product i from different regions based on their transportation, exportation, and production capacities. Therefore, the intermediate order issued by sector j in region s to the supplying sector i in region r is:

$$id^{ir}_{js}(t) = \widetilde{id}^{i}_{js}(t) \times \frac{\overline{id}^{ir}_{js} \times \left(1 - \gamma^{Z}_{ir}(t)\right) \times \left(1 - \gamma^{E}_{ir}(t)\right) \times x^{a}_{ir}(t)}{\sum_{r \in R^i} \overline{id}^{ir}_{js} \times \left(1 - \gamma^{Z}_{ir}(t)\right) \times \left(1 - \gamma^{E}_{ir}(t)\right) \times x^{a}_{ir}(t)}. \tag{161}$$

Here $\overline{id}_{js}^{ir}$ refers to the intermediate demand of sector j in region s for products of sector i in region r at the pre-disaster level. This modelling of the redistribution of intermediate demand is different from Equation (118) in the DF-substitution model, as it considers not only the production capacity $x_{ir}^{a}(t)$ of suppliers in different regions, but also their transportation and exportation capacities, i.e., $1-\gamma_{ir}^{Z}(t)$ and $1-\gamma_{ir}^{E}(t)$, respectively (see Sections 3.2.1.3 and 3.2.1.4). And if $s=r$, $\gamma_{ir}^{E}(t)$ is temporarily equal to zero.

3.2.4.2. Final Demand

Similarly, the households redistribute orders among their suppliers from different regions based on their adaptive demand and the transportation, exportation, and production capacities of their suppliers. The total adaptive demand of the households in region h to final product i (including non-substitutable specialized ones) at time t can be calculated by adding up the adaptive demand from different regions:

$$\widetilde{fd}_{h}^{i}(t)=\sum_{r\in R^{i}}\widetilde{fd}_{h}^{ir}(t),\ \ i=1,...,N+M\,. \tag{162}$$

Here $\widetilde{fd}_{h}^{ir}(t)$ is the post-disaster adaptive demand for product i in region r by the households in region h, after considering the effects of emergency responses, external subsidies and extra expenditures for house repair (see Equation (138) in Section 3.2.1.5).

Then the order issued by the households in region h to the supplying sector of product i in region r is:

$$fd_{h}^{ir}(t)=\widetilde{fd}_{h}^{i}(t)\times\frac{\overline{fd}_{h}^{ir}\times\left(1-\gamma_{ir}^{Z}(t)\right)\times\left(1-\gamma_{ir}^{E}(t)\right)\times x_{ir}^{a}(t)}{\sum_{r\in R^{i}}\overline{fd}_{h}^{ir}\times\left(1-\gamma_{ir}^{Z}(t)\right)\times\left(1-\gamma_{ir}^{E}(t)\right)\times x_{ir}^{a}(t)}. \tag{163}$$

Here $\overline{fd}_h^{ir}$ refers to the final demand of the households in region h for product i in region r at the pre-disaster level. And if $h=r$, $\gamma_{ir}^E(t)$ is temporarily equal to zero.

3.2.4.3. Reconstruction Demand

A sector or a household also issues orders to its suppliers because of the reconstruction demand to recover its damaged productive or residential capital. The modelling of reconstruction demand and its redistribution is similar with the DF-substitution model, except that it considers the presence of non-substitutable specialized inputs for capital formation and that the demand redistribution is based on the suppliers' production, transportation, and exportation capacities simultaneously. Then the total demand for product i (including non-substitutable specialized ones) to support the reconstruction of sector j in region s and the residential sector in region h at time t, $\widetilde{rd}_{js}^i(t)$ and $\widetilde{rd}_{res,h}^i(t)$, are calculated as:

$$\widetilde{rd}_{js}^i(t)=\max\left\{\sum_{r\in R^i}\left(\overline{K}_{js}-K_{js}(t)\right)\times\eta_s^{ir};0\right\},\ i=1,...,N+M, \tag{164}$$

$$\widetilde{rd}_{res,h}^i(t)=\max\left\{\sum_{r\in R^i}\left(\overline{K}_{res,h}-K_{res,h}(t)\right)\times\eta_h^{ir};0\right\},\ i=1,...,N+M. \tag{165}$$

Here $K_{js}(t)$ and $K_{res,h}(t)$ are the capital stock held by sector j in region s and the residential sector in region h at time t, respectively. $\overline{K}_{js}$ and $\overline{K}_{res,h}$ are the capital stock at the pre-disaster level. Capital dynamics are modelled in the same way as the DF-substitution model (see Equations (98) and (99)) and the economy is assumed to recover to the pre-disaster level. η_s^{ir} is the capital matrix coefficient indicating the units of product i in region r that are required to form one unit of capital in region s.

And the orders issued by sector j in region s and the households in region h to the supplying sector of product i in region r, to support the reconstruction of damaged productive and residential capital, are:

$$rd_{js}^{ir}(t) = \widetilde{rd}_{js}^{i}(t) \times \frac{\eta_{s}^{ir} \times \left(1-\gamma_{ir}^{Z}(t)\right) \times \left(1-\gamma_{ir}^{E}(t)\right) \times x_{ir}^{a}(t)}{\sum_{r \in R^{i}} \eta_{s}^{ir} \times \left(1-\gamma_{ir}^{Z}(t)\right) \times \left(1-\gamma_{ir}^{E}(t)\right) \times x_{ir}^{a}(t)}, \tag{166}$$

$$rd_{res,h}^{ir}(t) = \widetilde{rd}_{res,h}^{i}(t) \times \frac{\eta_{h}^{ir} \times \left(1-\gamma_{ir}^{Z}(t)\right) \times \left(1-\gamma_{ir}^{E}(t)\right) \times x_{ir}^{a}(t)}{\sum_{r \in R^{i}} \eta_{h}^{ir} \times \left(1-\gamma_{ir}^{Z}(t)\right) \times \left(1-\gamma_{ir}^{E}(t)\right) \times x_{ir}^{a}(t)}. \tag{167}$$

Finally, the total orders received by sector i in region r, $TD_{ir}(t)$, can be calculated by adding up all categories of demands from all sectors and regions as Equation (125) in the DF-substitution model.

3.2.4.4. Overproduction Capacity

This module is modelled in the same way as the DF-substitution model, that is, the overproduction capacity of a primary input q (i.e., capital or labour) in sector i of region r, $\alpha_{ir}^{q}(t)$, can increase up to a maximum value $\alpha_{ir}^{\max}$ in a time delay τ_{α} in response to production shortages or demand surges, and also fall back to the pre-disaster level $\overline{\alpha}_{ir}$ (normalized at 100%) in the same time delay when the situation becomes normal. A detailed modelling process has been presented in Equations (126) and (127).

3.2.5. Direct and Indirect Disaster Footprint

Following a compound-hazard event, sectors and households in all regions go through the above production, allocation, recovery, and demand adjustment processes

recursively, until a full economic recovery to the pre-disaster level after all constraints are lifted (i.e., damaged productive capital is fully recovered, all labour constraints are lifted, and all business linkages are repaired). Here the CHEFA model defines the physical damage resulting from the natural disasters (e.g., floods) in the compound hazard as the direct disaster footprint, while the value-added changes[12] of all sectors and regions in the economy triggered by the supply chain (backward and forward) propagation effects of all external shocks in the compound hazard as the indirect disaster footprint, which are calculated as:

$$DirectFootprint = \sum_{t}\sum_{i=1}^{N}\sum_{r=1}^{R}\left(K_{ir}^{dam}(t)+K_{res,r}^{dam}(t)\right), \tag{168}$$

$$IndirectFootprint = \sum_{t}\sum_{i=1}^{N}\sum_{r=1}^{R}\left(\overline{va}_{ir}-va_{ir}(t)\right). \tag{169}$$

Here $K_{ir}^{dam}(t)$ and $K_{res,r}^{dam}(t)$ are the amount of industry productive and residential capital damaged by the flood disaster in region r at each time step, which are estimated with methods in Section 3.1.1.1 and fed into the CHEFA model during the calculation of capital constraints. $\overline{va}_{ir}$ and $va_{ir}(t)$ are the value added of sector i in region r at the pre-disaster level and at time t, respectively. The value added of a sector is the extra value of final products created above intermediate inputs, i.e., $va_{ir}(t)=x_{ir}^{a}(t)-\sum_{j=1}^{N}\sum_{s=1}^{R}a_{js,ir}\times x_{ir}^{a}(t)$. $a_{js,ir}$ is the technical coefficient derived from the IO table used indicating the input of product j in region s required to produce one unit of product i in region r.

[12] The value-added changes include both increases and decreases in the sectoral value added. Suppliers in the less affected regions can replace the suppliers of the same product in the more severely affected regions through the mechanism of demand redistribution, and the increasing demand, as well as the demand for reconstruction, may drive these sectors to extend their production with an overproduction capacity above the initial level. These combined effects can thus result in value added increases in some sectors during the post-disaster recovery.

Chapter 4 Economic Costs of Heat Stress, Air Pollution and Extreme Weather Events in China over the Past Decades

The outcomes of this chapter have been integrated into the 2020-2022 China reports of the Lancet Countdown on health and climate change. The series of reports were aimed at tracking the health profile of climate change in China through 27 indicators across five sections: climate change impacts, exposures, and vulnerability; adaptation, planning, and resilience for health; mitigation actions and health co-benefits; economics and finance; and public and political engagement. Yixin Hu contributed 3 indicators on the economic costs of heat stress, air pollution and climate-related extreme events. The sections in this chapter have been reproduced under the permission of co-authors.

Cai, W.[#], Zhang, C.[#], Zhang, S.[#], …, **Hu, Y.**, …, Gong, P*. (2022). The 2022 China report of the Lancet Countdown on health and climate change: leveraging climate actions for healthy ageing. *The Lancet Public Health*. https://doi.org/10.1016/s2468-2667(22)00224-9

Cai, W.[#], Zhang, C.[#], Zhang, S.[#], …, **Hu, Y.**, …, Gong, P*. (2021). The 2021 China report of the Lancet Countdown on health and climate change: seizing the window of opportunity. *The Lancet Public Health, 6*(12), e932-e947. https://doi.org/10.1016/S2468-2667(21)00209-7

Cai, W.[#], Zhang, C.[#], Suen, H. P.[#], …, Hu, Y., …, Gong, P*. (2021). The 2020 China report of the Lancet Countdown on health and climate change. *The Lancet Public Health, 6*(1), e64-e81. https:/doi.org/10.1016/S2468-2667(20)30256-5

The purpose of this chapter is to fulfil Research Objective 5, which is the empirical application of the proposed Disaster Footprint model for the single-hazard impact analysis (see Section 3.1). This contributes to Research Question 2 raised in Section 1.4.1. The analysis is focused on historical patterns of hazards; heat stress, air pollution and climate-related extreme events in China are chosen as case studies. The selection of hazards ensures that both rapid and slow onset types with associated hazard shocks to capital and labour, respectively, are covered. Furthermore, this demonstrates a wide-ranging applicability of the proposed Disaster Footprint model (DF-substitution model in particular), which is possible whenever the direct impacts of a hazard can be translated into relative disruptions to either of the production factors, capital and labour, through vulnerability functions (such as depth-damage functions for floods and exposure-response functions for heat stress).

It is worth noting that all hazards studied in this chapter are considered to directly affect either labour or capital. Heat stress and air pollution only reduce labour availability, while climate-related extreme events (e.g., floods and storms) only cause capital damage. For the latter, direct labour impacts may also occur during climate-related extreme events, but they are rarely recorded in official documents and therefore neglected in this analysis due to data limitations.

A major innovation of this work is that the hazard-induced economic impacts are for the first time evaluated on a finer spatial scale in China (provincial scale). Besides, the method used for indirect impact assessment (i.e., the DF-substitution model) improves on the existing models by integrating inventory dynamics and cross-regional substitution of suppliers.

All economic values in this chapter are presented in 2020 US$ values.

4.1. Heat Stress

This section tracks the annual direct and indirect economic costs of heat stress in China since 2000. Heat stress can negatively affect the economy by bringing about productive working time loss resulting from 'absenteeism' (when an increasing number of employees are absent from work due to heat-related mortality and morbidity) and 'presenteeism' (when employees work more slowly due to reduced labour productivity under heat stress) (Schultz et al., 2009; Xia, Li, et al., 2018). To calculate the absenteeism- and presenteeism-related economic costs, heat-induced mortality and labour productivity loss are first estimated at the national and provincial levels, respectively, using the methods described in Section 3.1.1.2 and then fed into the DF-substitution model as in Section 3.1.2.3 for a systematic economic impact analysis. Again, heat-related morbidity is not included here due to data limitations, which has been explained in Section 3.1.1.2. Without capital damaged by heat stress, this thesis mainly considers the reduction in labour input (i.e., working time loss) and its rippling effect through the production supply chain. Therefore, the direct costs of each sector refer to the first-order losses of sectoral value added due to the reduced labour supply and the indirect costs are the higher-order losses of sectoral value added resulting from inter-dependencies between sectors and regions.

4.1.1. Absenteeism Costs

4.1.1.1. Heat-related Mortality

1) Methods and Data

As a type of direct impacts, the number of heat-induced non-accidental deaths is estimated for China and its provinces using the methods described in the first part of Section 3.1.1.2. The period during 1986-2005 is selected as the temperature reference

period for heatwave threshold, which is consistent with the global report of the Lancet Countdown (Romanello et al., 2021). The baseline non-accidental mortality rates and demographic data at national and provincial levels are derived from China Statistical Yearbooks (http://www.stats.gov.cn/tjsj./ndsj/). Gridded climate data is collected from the European Centre for Medium-Range Weather Forecasts (ECMWF) of the ERA5 project (Service(C3S) CCC, 2022). Gridded population data is obtained from a hybrid gridded demographic dataset for the world, which is provided by Chambers (2020). It should be noted that the ERFs, which describe the effects of heatwaves on mortality, are assumed to be constant without considering population adaptation in this analysis. This might create an estimation bias. In fact, along with the aging process, the increasing human adaptation ability, the popularity of air conditioning and other potential factors, the ERFs might also have changed over the past decades. However, due to limited investigation and data in this field, the ERFs are assumed to remain constant.

2) Results

Exposure to consecutive days of heat beyond threshold can lead to a notable increase in death risk (Xu et al., 2016). In 2021, heatwave exposure was 117% (or 7.85 days) higher than in the baseline (1986-2005) average, and the related deaths increased by 13,185, leading to an estimated 24,966 deaths. With China's population rapidly ageing, the proportion of deaths in people older than 65 years continues to increase from 61.1% in 1986-2005 to 78.4% in 2017-2021. Among all 31 mainland China provinces, heatwave-related deaths in the elderly were highest in Guangdong, followed by Henan, and Shandong, which accounted for 14.9%, 13.9%, and 10.7% of total deaths in 2021 respectively.

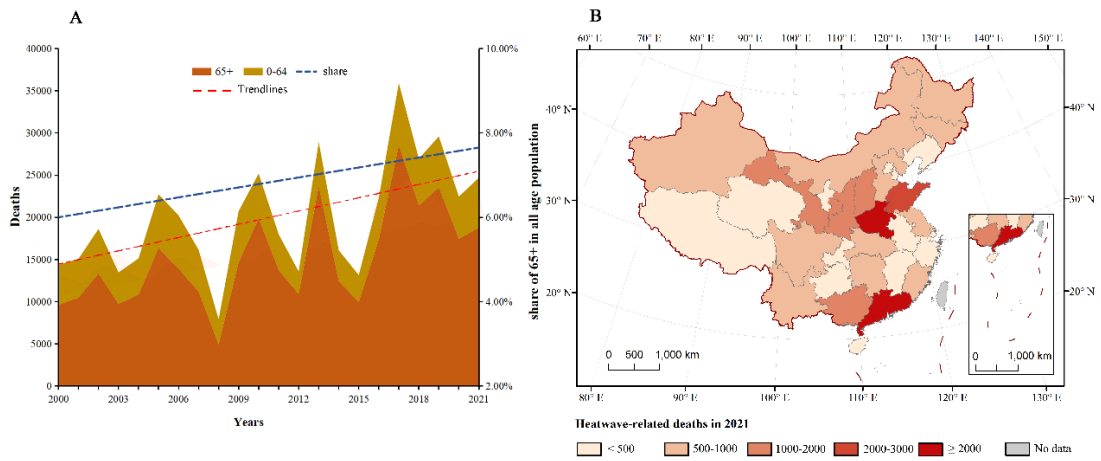

Figure 4-1: Heatwave-related mortality in China.

*(A) Trend of heatwave-related mortality in 2000–2021; (B) Heatwave-related mortality by province in 2021. The red dashed line shows the linear trend with the equation: heatwave-related deaths = 397*year – 785,447, P<0.05. The blue dashed line shows the share of people older than 65 years in the total population.*

4.1.1.2. Economic Costs of Heat-related Mortality

1) Methods and Data

First, the above results on heatwave-related working-age mortalities are divided by the sizes of industrial labour force in provinces (or the national labour force for the analysis on the national scale) to derive the percentage reduction in labour supply (or working time) caused by heat stress. The sizes of industrial labour force on the national and provincial scales are collected from China Statistical Yearbooks, which provide workforce data only for three major industry categories – primary, secondary, and tertiary. The primary industry refers to agricultural, forestry and fishing activities, the secondary industry includes mining, manufacturing, utilities, and construction, and the tertiary industry includes transport, trade, catering services, finance, real estate, and other services (see Table 4-1). For each province, the relative loss of labour supply in each industry category is further disaggregated into 20 subsectors, assuming sectors within the same industries share the same levels of labour loss.

Second, the relative reductions in labour supply by sector and province are delivered into the DF-substitution model as in the second part of Section 3.1.2.3 to estimate the

consequent economic costs nationwide. The model is run at a monthly time step. For direct costs, the calculated percentage reduction in industrial labour supply is expected to cause the same percentage reduction in industrial value added, as labour is a major component of the industrial value added. This assumption is drawn from the principle of the IO framework, which defines that proportional increase in industrial output can only be achieved by simultaneous increases in both capital and labour (Miller and Blair, 2009). In other words, the shortage of any input can directly constrain the industrial output capacity, with full employment of input factors. For indirect costs, the initial loss of industrial value added (i.e., direct costs) will have a knock-on effect disrupting the economic activities of other industries through the production and supply network characterised by the IO matrix, and the aggregate of value-added changes in all industries is counted as the total economic costs caused by heat stress. The increase from the direct to total costs indicates the indirect costs resulting from backward and forward interdependencies between industries and regions. At the time of writing, the Chinese national IO matrices were available for eight years (2002, 2005, 2007, 2010, 2012, 2015, 2017, 2018) from the website of the National Bureau of Statistics of China (https://data.stats.gov.cn/ifnormal.htm?u=/files/html/quickSearch/trcc/trcc01.html&h=740) and the Chinese multi-provincial IO matrices were updated to 2017 from the CEADs dataset (https://www.ceads.net/data/input_output_tables/). For other years without well-established IO matrices within the study period, the IO coefficients are derived from the existing IO matrices closest to those years, assuming a constant economic structure. Besides, the IO matrix used for each year are scaled to China's GDP of that year according to the annual updates from China Statistical Yearbooks and Bulletins (http://www.gov.cn/xinwen/2022-02/28/content_5676015.htm). These IO matrices, which are originally compiled for 42 economic sectors, are then aggregated to the 20 sectors as in Table 4-1, and divided by the number of months per year as the model is run on the monthly basis.

Third, all monetary values involved in the analysis are transformed into US$ at 2020 prices based on the US-China currency exchange rates of the relevant years, which are also obtained from China Statistical Yearbooks and Bulletins.

Table 4-1: Sector concordance.

Industries	**Subsectors**
Primary	Agriculture (including agricultural, forestry, and fishing activities)
Secondary	Mining
	Foods and tobacco
	Textiles
	Timbers and furniture
	Paper and printing
	Petroleum, coking, nuclear fuel
	Chemicals
	Non-metallic mineral products
	Metal products
	Ordinary machinery
	Transport equipment
	Electrical equipment
	Electronic equipment
	Other manufacturing industry
	Electricity, gas, water
	Construction
Tertiary	Transport
	Wholesale, retail, catering
	Other services (including finance, real estate, etc.)

2) Results

The overall economic costs of heatwave-related mortality of working-age people in 2021 were $109.4 million, about 5 times higher than the costs in 2002, and 14.4% up from those in 2020. About 74% of the overall costs were due to indirect impacts; the largest indirect costs were found in the secondary industry (52%), followed by the tertiary industry (38%). With provincial level data up to 2017, the three provinces with the greatest costs were Gansu (US$8.0 million) followed by Henan (US$7.6 million) and Inner Mongolia (US$6.7 million).

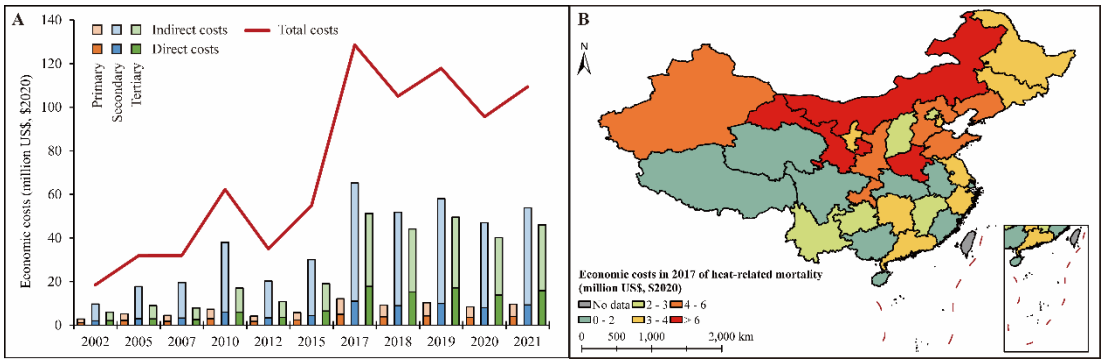

Figure 4-2: Economic costs of heatwave-related mortality (million US$, $2020).
(A) National direct and indirect economic costs by industry and year; (B) Provincial economic costs in 2017. Negative values indicate economic gains from inter-provincial trade.

4.1.2. Presenteeism Costs

4.1.2.1. Heat-related Labour Productivity Loss

1) Methods and Data

Another type of direct impact, the amount of heat-related labour productivity loss (i.e., work hours lost) is estimated for China and its provinces using the methods described in the second part of Section 3.1.1.2. Gridded climate and population data is collected from the same sources as those for heat-related mortality (see Section 4.1.1.1). Data on the percentage of people working in each sector is sorted from national and provincial statistical yearbooks of China. Here the economy is divided into four sectors - agriculture, manufacturing, construction, and service, which is consistent with the global report of Lancet Countdown (Romanello et al., 2021). Note that the loss function (ERF) used to estimate heat-related labour productivity loss in China is originally developed on the global scale, as more detailed loss functions specific to Chinese regions are not available so far.

2) Results

Heat stress can reduce labour capacity of working-age population and lead to losses in wage and economic outputs (Parsons et al., 2021). Compared with the average in

baseline years (1986-2005), potential work hours lost (PWHL) due to heat exposure increased by 2.2 billion hours (or 7.1%) in 2021, reaching 33 billion hours and representing 1.4% of the total national work hours. The PWHL in construction and manufacturing sectors continued to increase in 2021, which were 4.1 and 2.2 times higher than in baseline period. PWHL in the top 10 provinces accounted for 80% of total national losses in 2021, as a result of both rising temperature and concentration of labour-intensive sectors.

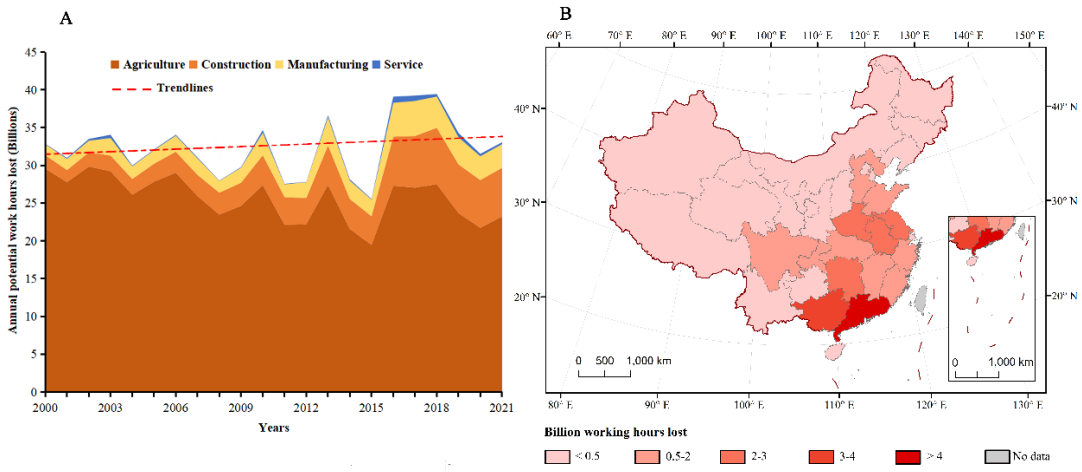

Figure 4-3: Heat-related work hours lost in China.

(A) Annual potential work hours lost due to heat in each industry from 2000 to 2021; (B) Total work hours lost in different provinces in 2021.

4.1.2.2. Economic Costs of Heat-related Labour Productivity Loss

1) Methods and Data

With inputs of the relative work hours lost for each sector and year between 2012-2021, the resulting direct and indirect economic costs due to heat stress can be estimated using the DF-substitution model described in the second part of Section 3.1.2.3. The model is run at a monthly time step. Detailed data sources and processing procedures are similar with those for the calculation of the economic costs of heat-related mortality (see Section 4.1.1.2).

2) Results

In China, the economic costs of heat-related labour productivity loss have increased by 2.3 times from US$122.9 billion (1.27% of GDP) to US$282.3 billion (1.97% of GDP) between 2012 and 2018. Afterwards, the national costs declined continuously to US$241.3 billion (1.64% of GDP) in 2020 before rebounding slightly to US$285.8 billion (1.68% of GDP) in 2021. The direct costs resulting from the reduced labour productivity mainly took place in the agriculture (32%) and construction (39%) sectors, while the indirect costs resulting from the cross-sector rippling effect concentrated in the service (49%) and manufacturing (48%) sectors in 2021. The three provinces that suffered the greatest economic costs in 2021, relative to their GDPs, were Hainan (4.75%), Guangxi (3.86%) and Jiangxi (3.33%).

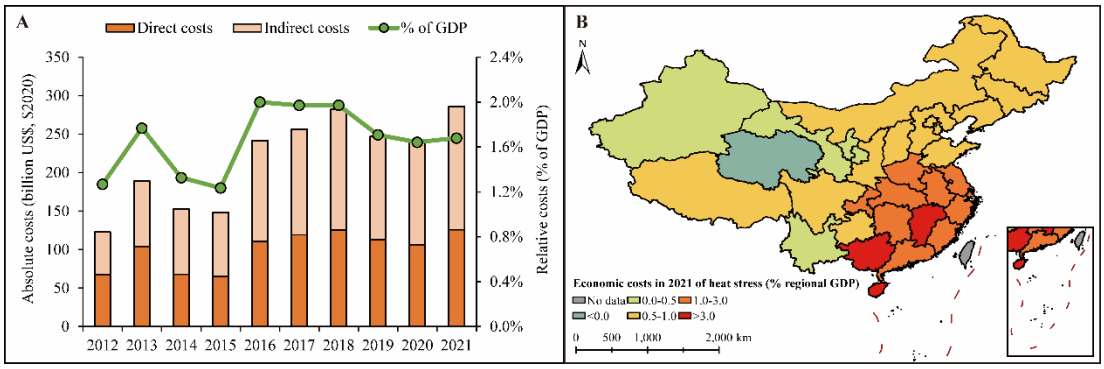

Figure 4-4: Economic costs of heat-related labour productivity loss.
(A) National-level results, by year, in billions of 2020 US$; (B) Provincial-level results in 2021, relative to provincial GDPs. Negative values indicate economic gains from inter-provincial trade.

4.2. Air Pollution

This section estimates the direct and indirect economic impacts caused by ambient air pollution (using $PM_{2.5}$ as a proxy indicator) in Chinese provinces between 2015 and 2020. First, the $PM_{2.5}$-related premature mortality by sector, which comprises the main source of direct economic impacts, is estimated for each province and year using the methods described in Section 3.1.1.3. Second, these mortality estimates are inputted

into the disaster footprint model as in Section 3.1.2.3 to systematically assess the resulting economic footprint impacts along the production supply chain, following similar procedures as for heat stress.

4.2.1. Premature Mortality from Ambient Air Pollution by Sector

1) Methods and Data

First, the ambient $PM_{2.5}$ concentration can be sourced from eight (emission) sectors: power plants, transport, industry, waste, natural, agriculture, other, and households. The sectoral contribution to ambient $PM_{2.5}$ is quantified using the greenhouse gas – air pollution interactions and synergies (GAINS) model (Amann et al., 2020). Data from the International Energy Agency (IEA) World Energy Outlook 2021 (IEA, 2021) and data from China Statistical Yearbook 2021 and China Energy Statistical Yearbook 2020 are integrated into GAINS to develop the provincial air pollution emission inventory by fuels and sectors. Ambient $PM_{2.5}$ concentrations are calculated from the region and sector specific emissions by applying atmospheric transfer coefficients, which are a linear approximation of full chemistry-transport models. Atmospheric transfer coefficients in GAINS are based on full year perturbation simulations with the European Monitoring and Evaluation Programme (EMEP) Chemistry Transport Model (Simpson et al., 2012) at 0.1°×0.1° resolution (for low-level sources) or 0.5°×0.5° resolution (for all other sources) using meteorology of 2015.

Second, the numbers of premature deaths resulting from ambient air pollution ($PM_{2.5}$) by sectoral sources for each province in China between 2015 and 2020 are estimated using the methods described in Section 3.1.1.3. Baseline mortality data and RR values are obtained from the results of the GBD 2019 study (Murray et al., 2020). Provincial demographic and mortality data is collected from Chinese Statistical Yearbooks for the relevant years.

It should be noted that the annual mean $PM_{2.5}$ concentration for each province is estimated from the GAINS model, rather than the observed data officially released, and the same concentration-response function and RR values are used for $PM_{2.5}$ from various sources, which may result in biased estimates deviating from the actual situation to some extent.

2) Results

As the most important global environmental risk factor for premature mortality (Watts et al., 2019), China has adopted an ambitious response to deliver cleaner air. The Three-Year Action Plan for Winning the Blue Sky Defence Battle (2018-2020) (State Council of China, 2018) has led to 14,600 fewer premature deaths from 2019 to 2020, continuing the downward trend (with 243,700 fewer deaths) between 2015 and 2019. 30% of the reduction in premature deaths occurred in South Central China, 28% in East China, and 16% in North China. Premature deaths attributable to air pollution from the household, industry and agriculture sectors had the most significant reduction, mainly because of the implementation of ultra-low air pollution emission standards and the Zero Growth of Chemical Fertilizer and Pesticide Use policy (MOA, 2017). However, the emissions from the waste sector caused more premature deaths in 2020 than in 2019, compared to the results of the 2021 China report (Cai et al., 2021). Despite the notable health benefits of cleaner air, progress towards improving air quality in China has been so far insufficient, with over 41% of the population being exposed to the annual average of $PM_{2.5}$ concentration above the WHO interim target-1 of 35 μg/m3 in 2021.

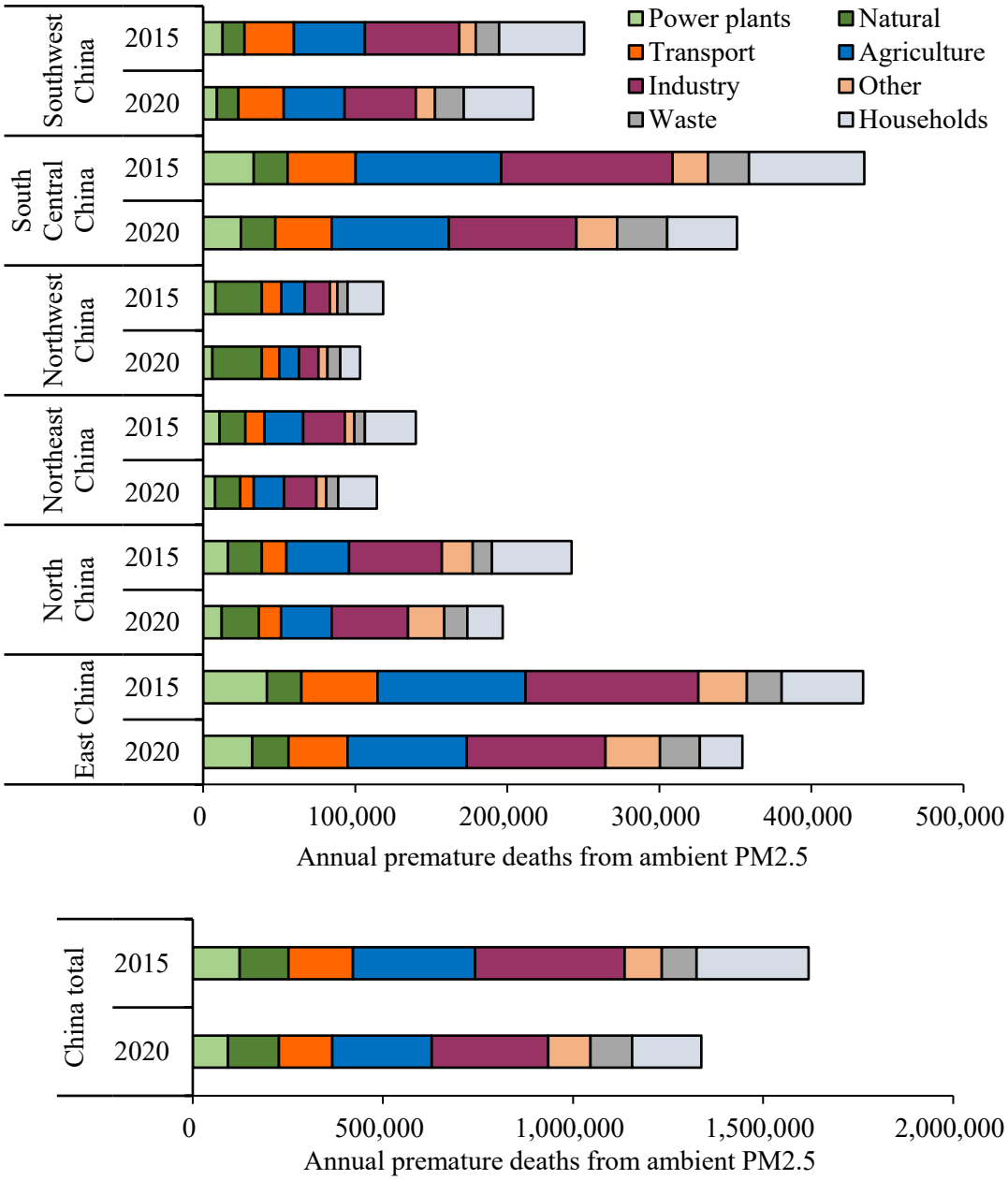

Figure 4-5: Annual premature deaths attributable to $PM_{2.5}$ by regions and sectors between 2015 and 2020.

4.2.2. Economic Costs of Air Pollution-related Premature Deaths

1) Methods and Data

First, the total numbers of $PM_{2.5}$-related deaths are multiplied by the 'labour force mortality rates' to calculate the absolute losses of labourers. Labour force mortality rates refer to the proportions of deaths at the working age (i.e., 15-64) among deaths

of all age groups. As $PM_{2.5}$-related labour force mortality rates are not available at present, the all-cause labour force mortality rates are used as reference, which are collected from the sixth national population census of China (National Bureau of Statistics of China, 2010). Different provinces have different labour force mortality rates.

Second, the absolute losses of labourers are disaggregated into the primary, secondary and tertiary industries according to the sectoral results of $PM_{2.5}$-related deaths, and then divided by the sizes of industrial labour force in provinces (or the national labour force for the analysis on the national scale) to obtain the relative losses of labourers. The numbers of national and provincial labourers by industry for the relevant years are sourced from China Statistical Yearbooks. It should be noted that the industrial labour losses are not derived directly from the sectoral results of $PM_{2.5}$-related deaths, as deaths attributable to a certain emission sector (e.g., the transport sector), do not necessarily mean deaths taking place within that sector. The breakdown of labour deaths into the three industries is weighted-proportional to the regional employment of the three industries. In other words, the three industries are first given specific weights against each of the eight emission sectors based on expert judgement (Appendix Table A4), and then the labour deaths attributable to each emission sector are disaggregated into the three industries in weighted proportion to the regional employment of the three industries. For example, it is assumed that most $PM_{2.5}$-related labour deaths attributable to the agriculture sector fall into the primary industry, while those attributable to the transport sector belong mainly to the secondary and tertiary industries. Therefore, the primary industry is given a larger weight than the secondary and tertiary industries when proportionally disaggregating the labour deaths with an agricultural cause into the three industries, while the secondary and tertiary industries are given larger weights for deaths attributable to the transport sector than the primary industry.

Finally, like heat stress, there is no capital loss resulting from $PM_{2.5}$ pollution. The relative losses of labourers by industry can be interpreted as the percentage reductions in industrial labour supply (i.e., working time), which are then fed into the DF-substitution model as in the second part of Section 3.1.2.3 to estimate the overall economic costs on both the national and provincial scales following similar procedures as for heat-related mortality in Section 4.1.1.2. The model is run at a monthly time step. The IO tables and economic data (e.g., GDPs) used in this analysis are also collected from the same sources and processed in similar ways as for heat-related mortality (see Section 4.1.1.2).

2) Results

Although the number of air pollution-related premature deaths decreased in 2020, with the increasing GDP of China, the absolute national economic costs increased slightly by 3% from $9.00 to $9.24 billion during 2015-2020. As a result, the relative costs as a percentage of China's GDP declined from 0.07% to 0.06%. Progress towards air pollution control seen in the previous year continued during 2020 (Cai et al., 2021). The secondary and tertiary industries still accounted for the majority (increased from 90% in 2015 to 92% in 2020) of total costs. Between 2015 and 2020, the share of the secondary industry in total costs increased from 47% to 53%, while the shares of the primary and tertiary industries decreased from 10% to 8% and from 44% to 39% respectively. The three provinces that suffered the greatest economic costs in 2020, relative to their GDPs, were Xinjiang (0.27%), Heilongjiang (0.26%) and Hebei (0.12%).

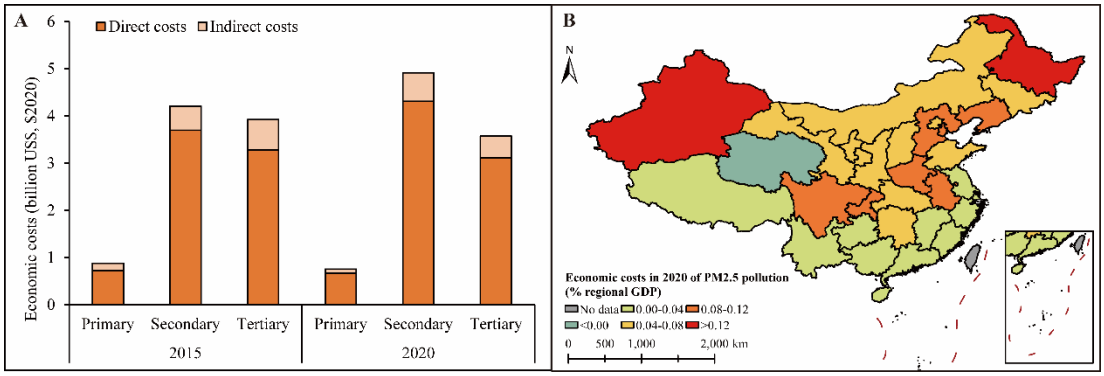

Figure 4-6: Economic costs of $PM_{2.5}$-related premature deaths.

(A) National-level results, by year and industry, in billions of 2020 US$; (B) Provincial-level results in 2020, relative to provincial GDPs. Negative values indicate economic gains from inter-provincial dependencies.

4.3. Extreme Weather Events

This section measures both the direct and indirect economic losses of climate-related extreme events that have occurred and been recorded in China during 2009-2021. Unlike heat stress and air pollution, most of these events mainly cause direct damage to capital assets rather than labour assets. Although casualties occur during climate-related extreme events, the direct labour impacts are rarely recorded and hard to calibrate. Therefore, the direct losses resulting from these events refer to the tangible damage to physical assets at risk, while indirect losses are the subsequent losses, including business interruption losses of affected economic sectors, and the spread of losses towards other initially non-affected economic sectors, and the costs of recovery processes.

1) Methods and Data

First, data on physical or direct damage of the climate-related extreme events during the study period is sourced from statistical yearbooks and reports released by Chinese authorities, including China Statistical Yearbooks on Environment, Yearbooks of Meteorological Disasters in China, and annual reports of Ministry of Emergency

Management of China. These statistics typically record the annual direct damage of five categories of climate-related extreme events (i.e., droughts, floods, hailstorms and thunderstorms, cyclones, blizzards and extreme low temperatures) in China on both the national and provincial scales.

Second, the annual direct damage due to climate-related extreme events is broken down into three industrial categories (i.e., primary, secondary, and tertiary) and a residential sector, according to the proportions based on empirical evidence of China's historical floods between 1961-1990 from a previous study (Yin et al., 2021), and damages in the three industrial categories are further disaggregated into 20 subsectors (see Table 4-1 in Section 4.1.1.2) in proportion to their value added. The annual direct damage of each sector is then divided into five months (from May to September), as the summer seasons are considered as highly risky with climate-related extreme events.

Third, assuming the capital stock held by each sector is around 4 times the sectoral value added, which is similar to previous studies (Hallegatte, 2008; Koks and Thissen, 2016), the percentage reductions in sectoral capital supply due to climate-related extreme events can be derived by dividing the annual direct damage by the capital stock for each year. These are then delivered into the DF-substitution model described in the second part of Section 3.1.2.3 to estimate the indirect economic impacts on both the national and provincial scales. The model is run at a monthly time step. The IO tables and economic data (e.g., GDPs) used in this section are collected from the same sources and processed in similar ways as for heat-related mortality (see Section 4.1.1.2).

2) Results

The absolute annual economic losses due to climate-related extreme events in China have been fluctuating around US$55 billion during 2009-2021, with significant

increases to US$109.5 billion in 2010, US$91.2 billion in 2013 and US$98.8 billion in 2016. However, the relative losses, as a percentage of China's GDP, generally demonstrated a downward trend from 0.88% in 2009 to 0.35% in 2021, again with notable rises to 1.52% in 2010, 0.99% in 2013 and 0.88% in 2016. The total losses, either in absolute or relative terms, have been kept at low levels since 2017. This indicates that China has been more economically resilient towards climate extremes, though the frequency and intensity of these events have been growing (IPCC, 2021). For each unit of direct damage caused by climate-related extreme events, 0.23-0.32 units of indirect losses occurred due to the rippling effects along the production supply chain. Most of the direct damage (~94%) took place in the secondary and tertiary industries and the residential sector, while the indirect losses (~60%) tended to accumulate in the primary industry. The primary industry was thus the most economically vulnerable towards climate extremes with higher indirect/direct loss ratios (1.95-2.79) than other industries. With provincial level data up to 2019, the three provinces that suffered the greatest economic losses, relative to their GDPs, were Jiangxi (2.61%), Heilongjiang (2.04%) and Zhejiang (1.19%).

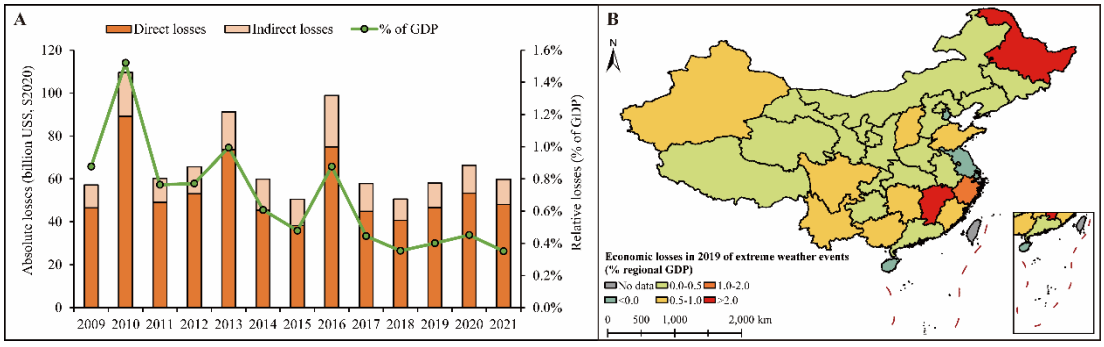

Figure 4-7: Economic losses due to climate-related extreme events.

(A) National-level results, by year, in billions of 2020 US$; (B) Provincial-level results in 2019, relative to provincial GDPs. Negative values indicate economic gains from the stimulus effects of post-disaster reconstruction and inter-provincial substitution.

4.4. Discussion and Conclusions

The total economic costs of heat stress, air pollution and climate extreme events in China have increased from US$207.9 billion (1.79% of GDP) in 2015 to US$317.1 billion (2.16% of GDP) in 2020. Despite the downward trend in the economic costs (particularly in relative terms as a percentage of China's GDP) of air pollution and climate extreme events, the economic costs resulting from heat-related health impacts have continued the concerning growing trend. Among the three types of hazards, the economic costs of heat stress were the biggest and accounted for an increasing proportion (from 71% in 2015 to 76% in 2020) of the total costs. This was followed by climate extreme events, which explained a declining share (from 24% to 21%) of the total costs. The economic costs of air pollution were the smallest and accounted for the rest of the total costs, which decreased from 4% to 3% during 2015-2020. Heat stress mainly negatively affected the economy by reducing labour productivity, as heat-related mortality only resulted in 0.03% of the total costs.

It should be noted that this chapter evaluates the economic impacts of heat stress, air pollution, and climate-related extreme events only separately over different years with accessible data. Still, comparisons of these single events can be made between 2015 and 2020, as data of these two years is available for all case studies.

For each unit of direct costs, heat stress was also inclined to cause more indirect supply chain costs than air pollution and climate extremes. The ratios between indirect and direct costs for heat-related labour productivity loss ranged between 0.81-1.28 during the study period, while those for air pollution and climate extremes were 0.14-0.17 and 0.23-0.32 respectively. For heat impacts, most of the direct costs occurred outdoors in the agriculture and construction sectors, while most of the indirect costs happened indoors in the manufacture and service sectors. This indicates that, in the next stage of

China's climate adaptation actions, more efforts should be made to enhance the adaptability of outdoor sectors to heat extreme, as well as to improve the supply chain resilience to mitigate the spillover effects of heat-related health impacts.

At the regional level, hotspot provinces with prominent economic risks from these hazards have been identified for China. Generally, southern provinces were more economically vulnerable to heat stress than northern provinces, while northern provinces tended to suffer larger economic costs from air pollution than southern provinces. By contrast, the economic impacts of climate extreme events were more spatially distributed in China than the other two types of hazards. Special attention should be paid to two provinces, namely Jiangxi in southern China and Heilongjiang in northern China. The former province suffered the third greatest economic costs from heat stress and the greatest losses from climate extreme events, in relative terms, while the latter province suffered the second greatest economic impacts from air pollution and climate extreme events, among all provinces in China. These location-specific economic impacts of climate change require location-specific response measures, including enhancing inter-departmental cooperation, strengthening climate emergency preparedness, supporting scientific research, raising public awareness, and promoting climate change mitigation and adaptation.

Chapter 5 Economic Impacts of Future Fluvial Flooding in Six Vulnerable Countries under Climate Change and Socio-economic Development

The outcomes of this chapter have been published in a paper co-authored by Zhiqiang Yin, Katie Jenkins, Yi He, Nicole Forstenhäusler, Rachel Warren, Lili Yang, Rhosanna Jenkins, and Dabo Guan. Yixin Hu is responsible for indirect impact modelling, result interpretation, and drafting. The sections in this chapter have been reproduced under the permission of co-authors.

Yin, Z.[#], **Hu, Y.**[#], Jenkins, K., …, Guan, D*. (2021). Assessing the economic impacts of future fluvial flooding in six countries under climate change and socio-economic development. *Climatic Change, 166*(3), 38. https://doi.org/10.1007/s10584-021-03059-3

The purpose of this chapter is to fulfil Research Objective 5, which is the empirical application of the proposed Disaster Footprint model for the single-hazard impact analysis (see Section 3.1). This contributes to Research Question 2 raised in Section 1.4.1. While Chapter 4 shows the economic impacts of several types of extreme events during the past years in China, this chapter extends the application to the projection of future economic risks due to climate change, taking fluvial flooding as an example, in six vulnerable countries. More specifically, this chapter presents an integrated flood risk analysis framework to calculate total (direct and indirect) economic damages, with and without socio-economic development, under a range of warming levels from <1.5°C to 4°C in Brazil, China, India, Egypt, Ethiopia, and Ghana. Direct damages are estimated by linking spatially explicit daily flood hazard data from the Catchment-

based Macro-scale Floodplain (CaMa-Flood) model with country and sector specific depth-damage functions. These values are fed into the Disaster Footprint model for the estimation of indirect losses. The results show that total fluvial flood losses are largest in China and India when expressed in absolute terms. When expressed as a share of national GDP, Egypt faces the largest total losses under both the climate change and climate change plus socio-economic development experiments. The magnitude of indirect losses also increased significantly when socio-economic development was modelled. The analysis highlights the importance of including socio-economic development when estimating direct and indirect flood losses, as well as the role of recovery dynamics, essential to provide a more comprehensive picture of potential losses that will be important for decision makers. All economic values in this chapter are expressed in 2010 US$ values.

5.1. Introduction

Floods are among the most frequent and costliest natural hazards. Globally, floods have affected more than 3.8 billion people and caused direct economic damages of ~826 billion US$ between 1960-2019, among which fluvial flooding accounts for two thirds, according to data from the EM-DAT database[13]. Economic damage from flood disasters has increased strongly over the past decades, reflecting increasing exposure of people and assets (IPCC, 2022; Jiménez Cisneros et al., 2014; Merz et al., 2021). The latest IPCC report has projected a 4-5 times increase in global flood impacts at 4°C compared to 1.5°C warming (Caretta et al., 2022). The impacts of fluvial floods are expected to increase in the future, predominantly driven by population and economic growth in flood-prone areas (Jongman, Ward, et al., 2012; Kinoshita et al., 2018; Tanoue et al., 2016). The intensification of the global hydrological cycle due to

[13] This is sourced from EM-DAT: the Emergency Events Database - Université catholique de Louvain (UCL) - CRED, D. Guha-Sapir - www.emdat.be, Brussels, Belgium (accessed 7 Feb 2020).

climate change will further increase future flood risks (Alfieri et al., 2017), exacerbating flood damages and posing a threat to future generations. Therefore, it is imperative to assess fluvial flood risks under scenarios of climate change and socio-economic development, to support decision-making regarding flood risk management and adaptation strategies.

Past efforts have largely focused on estimating future populations exposed to fluvial flooding (Arnell and Lloyd-Hughes, 2014; Hirabayashi and Kanae, 2009; Hirabayashi et al., 2013; Hirabayashi et al., 2021; Tellman et al., 2021) and the estimation of direct damages (usually to urban areas) (Alfieri et al., 2017; Kinoshita et al., 2018; Tanoue et al., 2021; Ward et al., 2017; Ward et al., 2013; Winsemius et al., 2016; Winsemius et al., 2013), under different scenarios of climate change and/or socio-economic development. Direct flood damages are typically assessed by linking physical properties of the hazard such as flood depth and area; exposure, in terms of the location of assets or land-use type; and vulnerability, derived from depth-damage functions that denote the damage that would occur at a given flood depth for a given asset or land-use type. Floods can also cause indirect damages, including reduced business production of affected economic sectors; the spread of these losses towards other initially non-affected sectors through inter-sectoral linkages; and the costs of recovery processes (Koks and Thissen, 2016; Taguchi et al., 2022; Tanoue et al., 2020). Indirect damages may continue to be felt after the flood event has ended, reflecting the full-time dimension of the event, as well as negatively and positively affecting regions outside of the original event (Carrera et al., 2015; Shughrue et al., 2020). Due to these factors, indirect losses can be high, or even exceed direct damages (Koks et al., 2015; Tanoue et al., 2020). The scale and duration of indirect losses will be dependent on the severity of the event, the pre-existing state of the economy, and the ability of individuals, businesses, and markets to adapt and recover. Yet, in terms of flood risks, indirect impacts and their wider macro-economic effects are still poorly understood

(Carrera et al., 2015; Tanoue et al., 2020), and detailed estimations of joint direct and indirect flood-induced economic impacts are relatively rare (Merz et al., 2021; Sieg et al., 2019).

Given the potential scale of indirect losses, it is important to consider them alongside direct damages to provide a more complete picture of the economic consequences of flood events (Koks et al., 2019). However, only a limited number of studies assess the total economic impacts of future fluvial flooding in combination with climate change and socio-economic projections. Dottori et al. (2018) carried out a global fluvial flood risk assessment by estimating human losses, and direct and indirect economic impacts under a range of temperature and socio-economic scenarios. However, they only considered welfare or consumption losses as a proxy of indirect impacts, ignoring changes in sectoral outputs. Willner et al. (2018) assessed the economic losses from climate change-related fluvial floods in the near future (2035), mainly in China, the US, and the European Union, but with fixed socio-economic conditions. Koks et al. (2019) evaluated the total economic consequences of future fluvial flooding at a sub-national scale for Europe, including indirect impacts and regional economic interdependencies for five aggregated sector groups. However, the authors noted the relatively simple approach to estimate the initial reduction in production capacity following a flood, from which indirect damages were calculated. This was based on the value of exposed assets per sector divided by the total asset value for each sector, assuming each sector needed a certain stock of assets to produce outputs. Furthermore, the study excluded damages to residential buildings, which are a significant part of direct flood impacts.

More recently, Taguchi et al. (2022) projected the flood-related indirect losses due to business interruption (BI loss) on the global scale by the end of the 21st century under Representative Concentration Pathway 8.5 (RCP8.5) and Shared Socioeconomic

Pathway 3 (SSP3) scenarios. However, they only calculated indirect losses for regions directly affected by floods and higher-order propagation effects to other regions were neglected, which resulted in smaller estimates than those from previous studies.

In addition, flood risk analysis is usually performed at a global, continental, or aggregated multi-country level. Single-country analysis is less common, particularly studies that consider both direct and indirect losses under future scenarios of climate change alongside scenarios of socio-economic development. This is particularly true for developing countries in Africa, Asia, and Latin America, where rapid growth in population and economic activities is forecast to take place, driving large increases in flood exposure and economic losses (Dottori et al., 2018; Jongman, Ward, et al., 2012). Developing countries are also found to suffer greater fluvial flood-induced growth losses in the long run (Krichene et al., 2021), implying the importance of in-depth investigation on fluvial flood risks for these countries. Where country level studies do exist, they often focus on specific cities or river basins only and are disparate, using different climate models, levels of global warming, economic and population data etc., hindering comparison (see Appendix C.1. Literature on Risks of Fluvial Flooding in the Study Countries of Chapter 5).

Lastly, existing flood risk projections do not always cover the plausible range of global warming, especially higher warming levels such as 3°C or above. Since the global mean temperature increase implied by countries' Nationally Determined Contributions (NDCs) under the Paris Agreement is estimated to be in the range of 2.7°C to 3.5°C by 2100 (Gütschow et al., 2018), it is important to examine a wide range of climate change impacts on flood risk. Likewise, an accurate understanding of the drivers of future fluvial flood risk is critical to help adopt effective risk reduction measures, but few studies have integrated both climate and socio-economic drivers (Kinoshita et al., 2018; Muis et al., 2015; Winsemius et al., 2016). Winsemius et al. (2016) performed

the first global fluvial flood risk assessment that separated the effects of climate change and socio-economic growth. This is followed by Kinoshita et al. (2018), who further included the effects of autonomous adaptation. However, both studies only estimated direct (urban) damages.

The study in this chapter is novel in that it presents an integrated flood risk analysis focused on direct and indirect economic damages caused by floods, both with and without the inclusion of socio-economic development. A broad range of warming levels from <1.5°C to 4°C are considered. The framework is applied to six developing countries: Brazil, China, India, Egypt, Ethiopia, and Ghana. This demonstrates the flexibility of the method to be applied to multiple countries, to facilitate regional comparison, and reflects a range of different climate impacts, geographies, and levels of development.

5.2. Experiment Design and Data

5.2.1. Model Experiment Design

Projected changes in average annual economic damage for the future period (2086-2115) are compared to the baseline period (1961-1990). Two sets of model experiments are conducted: a 'climate change only' experiment (CC), in which socio-economic conditions are kept constant at the baseline level for the six warming scenarios; and a 'climate change and socio-economic development' experiment (CC+SE), which considers both climate change and socio-economic growth in parallel. The differences between the estimates can reflect the effect of socio-economic development alone on future flood risks. Here, socio-economic development refers to each country's population, labour force, gross domestic product (GDP), capital stock, and land use changes. The flood hazard and socio-economic data used to calculate the direct and indirect losses for both the baseline and future scenarios are described below.

5.2.2. Climate Forcing and Flood Hazard Data

The daily streamflow and flood inundation depth are simulated at 0.25° spatial resolution by using a physical model cascade, the Hydrologiska Byråns Vattenbalansavdelning (HBV) model (Bergström, 1992) and the Catchment-based Macro-scale Floodplain (CaMa-Flood) model (Yamazaki et al., 2011). The WATCH daily bias-adjusted reanalysis dataset (Weedon et al., 2014) for 1961-1990 was used as the climate forcing data for the baseline period (1961-1990). The climate forcing data for the future period (2086-2115) were generated by combining monthly observations, daily reanalysis data, and projected changes in climate from GCMs. The projected changes in climate for the specific warming levels considered here are <1.5°C, <2°C (which denote aiming to stay below 1.5°C and 2°C in 2100, respectively, with 66% probability), exactly 2.5°C, 3°C, 3.5°C and 4°C relative to pre-industrial levels. The selection of warming levels is consistent with Warren et al. (2021), another work for the same project. To sample the uncertainty in regional climate change projections, this thesis uses patterns of change simulated by five GCMs obtained from the fifth phase of the Climate Model Intercomparison Project (CMIP5) (Taylor et al., 2012). A river discharge corresponding to a 1 in 100-year flood in the baseline period was selected as the hazard indicator, in line with several previous studies (Arnell and Gosling, 2016; Arnell and Lloyd-Hughes, 2014; Hirabayashi and Kanae, 2009; Hirabayashi et al., 2013). Whilst adaptation is not modelled, the 1 in 100-year event is often used as a hazard indicator given flood protection works are often designed for this return period (with some exceptions like the Netherlands). The time series of the simulated annual maximum daily river discharge in the baseline period for each grid, GCM and scenario were fitted respectively to a Gumbel distribution function using the maximum likelihood method. The magnitude of river discharge having a 100-year return period in the baseline was then calculated. The economic risks associated with the projected changes in flood hazard were calculated in the modelled inundation areas in which

annual maximum discharge in the future period exceeds the baseline 1 in 100-year threshold. Details of climate forcing and flood hazard data used in this study are described in He et al. (2022), also another work for the same project.

5.2.3. Socio-economic Data

Socio-economic data used for direct and indirect impact estimation includes information on national land use status, IO tables, GDP, capital stock and labour force (see Table 5-1 for an overview of data used to calculate the flood-induced economic impacts in the baseline and future periods for the CC and CC+SE experiments).

Table 5-1: Overview of data used for 'CC+SE' and 'CC' experiments.

Data used	**With socio-economic change (CC+SE)**	**Without socio-economic change (CC)**
Population exposure	Scale down/up to the relevant years	Scale down to the average level between 1961-1990
Capital damage	Scale down/up to the relevant years	Scale down to the average level between 1961-1990
IO Tables	Baseline: earliest available version (e.g., 2005 for Ghana) Future: latest available version (e.g., 2015 for Ghana) (See Appendix Table A5 for full details)	Same IO table as the baseline period
Land Cover	Baseline: 1992 Future: 2015	1992
GDP, labour, capital stock & other socio-economic indicators	Baseline: growing from 1961 using reported data Future: growing from 2086, according to SSP2 projections	Average between 1961-1990

The gridded land use data for each country is extracted from the European Space Agency Climate Change Initiative (ESA CCI) land cover product at 10-arcsec resolution (ESA, 2017). The land cover map of 1992, the earliest year available in the ESA CCI's product, is used for the baseline period. For the CC experiment, the same

land cover map is used for both the baseline and future periods. Under the CC+SE experiment, the map of 2015 is used for the future period, assuming a constant land cover after 2015. Employing two sets of land cover maps from the same data source means they are produced with the same approach and ensures consistency between estimates. Using different years can also account for the effect of land cover change, especially urban expansion, in the real world. This is beneficial as many studies do not allow for urban expansion (Rojas et al., 2013; Ward et al., 2017; Winsemius et al., 2016; Winsemius et al., 2013), which will be a key driver of increased future flood risks (Muis et al., 2015).

For each of the countries, IO tables are obtained from its national statistical website, providing information on intermediate demand, final demand, value-added, output, imports, and exports at the country level. For each country, the earliest version of the IO table available is used to approximate the economy during the baseline period. For the CC experiment, the same IO table is used for both the baseline and future periods. Under the CC+SE experiment the economic structure is assumed to vary in the future. This variance is represented by using the same IO table as used in the CC experiment in the baseline but the most recent version of the IO table available for each country in the future period (see Appendix Table A5 for country specific details on the IO tables used). This, to some extent, reflects the structural change from the baseline economy to the future one, given difficulties in projecting IO tables for 2100. The IO tables also provide data on the sectors involved in capital reconstruction from the investment column contained in the final demand block. The share of each sector investing in fixed capital formation indicates its contribution to the reconstruction process. The annual data in the IO table used is lastly divided by twelve to represent a monthly value.

Industry data from IO tables are aggregated to ten economic sector groups per country: Agriculture (AGR), Mining (MIN), Food Manufacturing (FDM), Other Manufacturing

(OTM), Utilities (UTL), Construction (CON), Trade (TRD), Transport (TRA), Public services (PUB) and Other Services (OTS) (see also Appendix Table A5). Where sectoral-level data is not available, such as for capital stock, it is disaggregated to the ten sector groups based on their proportional contribution to national GDP.

Data on GDP, population and labour force are derived from the World Bank World Development Indicators (World Bank, 2021). Data on capital stock is from the Investment and Capital Stock (ICSD) dataset from the IMF (IMF, 2015). Capital stock is divided into industry productive and residential capital based on land use from the land cover maps. Under the CC experiment data on GDP, population, labour force, and capital stock are set as constant to restrict any socio-economic change. In the CC+SE experiment these data are dynamic. For the baseline scenarios this reflects reported trends in data from 1961-1990. For the warming scenarios, trends in data are based on the SSP2 projections whereby social, economic, and technological trends do not shift markedly from historical patterns (Riahi et al., 2017).

The shock of the flood event Is represented by physical damage to capital assets and labour loss.

For the former, capital damage is calculated using the method described in Section 3.1.1.1. Three points are worthy of being noted here:

1) For the agricultural land-use sector, the cropland area is obtained directly from the ESA CCI land cover maps, then aggregated at the resolution of the flood hazard maps (0.25°). However, the global land cover data represents urban land as a single class and does not differentiate between residential, commercial, and industrial sectors. Therefore, the urban land class is disaggregated into these three sub-classes. In terms of the occupation of residential, commercial and industrial urban land-use sectors in cities, several previous studies assume uniform

percentages across the globe (Dottori et al., 2018), ignoring differences between individual countries. Huizinga et al. (2017) suggest that the percentages that commerce and industry contribute to national GDP could be used to downscale the single urban land class. However, the contribution of a sector to national GDP does not necessarily relate to the land surface it occupies. In this case, the population in a sector would be more relevant to the occupied land area. Therefore, in this study the residential population and employment in commercial and industrial sectors are used as proxies to downscale the single urban land class. It is assumed that the percentages of occupation of each sector within cities are equivalent to those of the population in each sector. Population data from the World Bank World Development Indicators are used (World Bank, 2021). To be consistent with the land cover maps, population data from 1992 and 2015 per country are used to calculate the country-specific percentages for the baseline and future scenarios respectively.

2) Since it is difficult to establish depth-damage functions for the future, this study uses the same set of functions for both the baseline and future periods as in other studies (Alfieri et al., 2017; Dottori et al., 2018), assuming that vulnerability is constant over time.
3) Capital damage is scaled based on the baseline and projected GDP per capita, according to the power law functions provided by Huizinga et al. (2017). Exponents in the power law functions are smaller than one, indicating that capital damage is not proportional to GDP per capita and grows slower than GDP per capita. The scaled capital damage in the four land-use sectors (i.e., agricultural, residential, commercial, and industrial sectors) is then disaggregated into the above-mentioned ten economic sectors in proportion to the capital stock held by these economic sectors.

For the latter, labour loss is calculated using data on population exposure to fluvial

flooding for each country provided by He et al. (2022) of this project. Affected labour is derived by multiplying the exposed population by the labour participation rate, from the World Bank (World Bank, 2021). The number of affected employees during each flood are divided into four categories: the dead, the heavily injured, the slightly injured, and others affected by flood-induced traffic disruptions. The ratios between these categories are determined based on the historical average of recorded floods for each country from the EM-DAT database (CRED, 1988).

Finally, the estimated capital damage and labour loss are fed into the DF-growth model (see the first part of Section 3.1.2.3) to track down the flood-induced indirect economic impacts for each country during the relevant periods. For the CC+SE experiment, the economy is allowed to recover to a target level above the initial level, converging to an exogenous growth trajectory; while for the CC experiment, the economy can only recover back to the initial state and additional constraints on growth parameters are set to exclude any growth potentials. The model is run at a monthly time step. All economic impacts are expressed in 2010 US$ values.

5.3. Results

5.3.1. Direct and Indirect Fluvial Flood Damages

Figure 5-1 presents estimates of direct and indirect economic damage for each country and climate scenario, under the CC and CC+SE experiments (results are plotted on the same axis to compare risk, see Appendix Figure B1 and Appendix Figure B2 for results plotted on separate axis per country for more details). The results reflect the underlying data provided from the flood hazard model, highlighting increasing economic damages, above the baseline, in line with the increasing warming scenarios. For Egypt, the largest increases in average damage occur up to Scenario 3: 2.5°C, after which damages continue to increase albeit at a smaller rate. This reflects the findings of He

et al. (2022), who noted that the proportional area of the Nile River Basin that experiences a decrease in the return period of a 1 in 100-year event (increase in flood frequency) changes little from Scenario 1: <1.5°C to 6: 4°C.

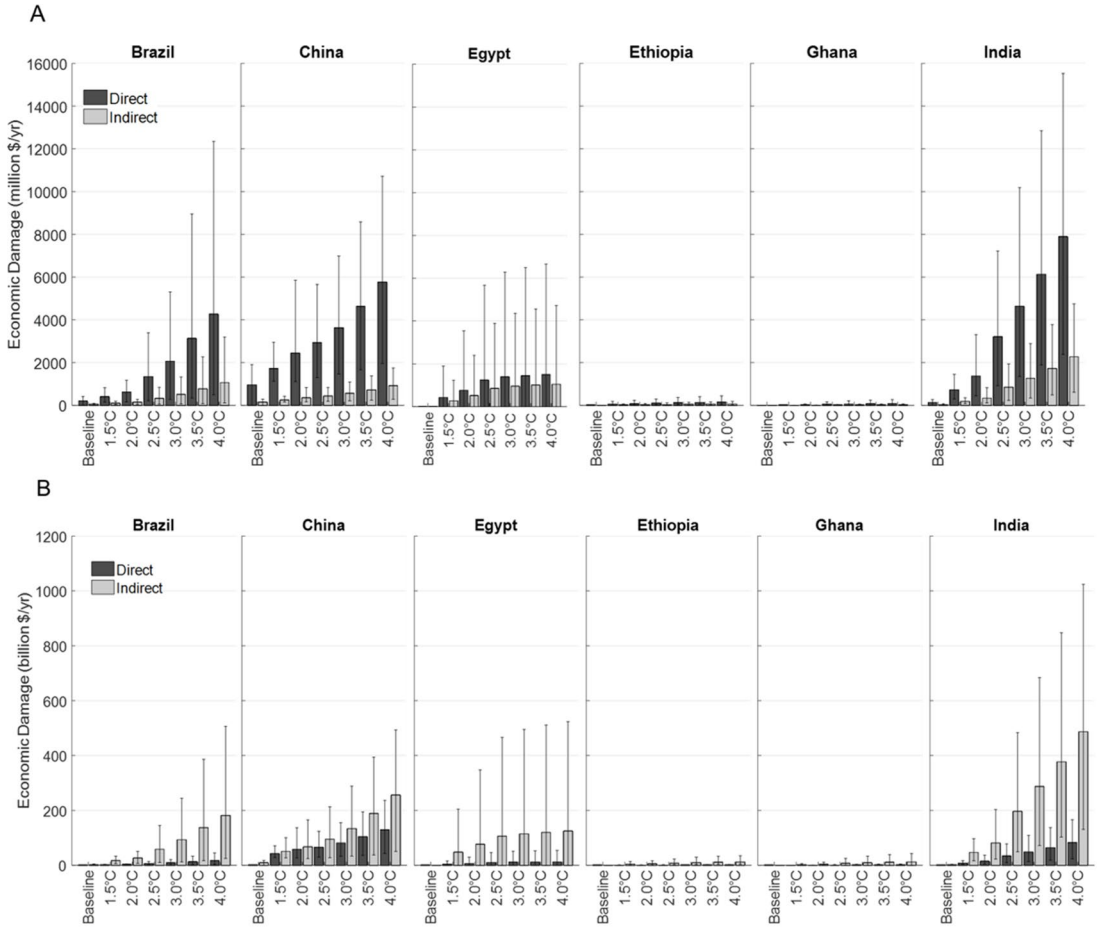

Figure 5-1: Average annual direct and indirect fluvial flood damages calculated across the 30-year time period for the baseline and six warming scenarios in each country.
Damages in panel A are expressed in million US$/year for the CC experiment and in panel B in billion US$/year for the CC+SE experiment. Bars represent the ensemble average of the five GCMs, with whiskers indicating the ensemble maximum and minimum.

Under the CC experiment, direct damages under Scenario 1: <1.5°C are 399 (+95%, relative to baseline, Brazil), 1,713 (+80%, China), 427 (+13,783%, Egypt), 54 (+341%, Ethiopia), 11 (+255%, Ghana) and 719 (+435%, India) million US$ per year. Direct damages increase to 4,267 (+1,979%, relative to baseline, Brazil), 5,759 (+506%, China), 1,495 (+48,508%, Egypt), 147 (+1,108%, Ethiopia), 79 (+2,401%, Ghana),

and 7,888 (+5,767%, India) million US$ per year under Scenario 6: 4°C. The indirect damages, though much lower than direct damages, display similar trends (Figure 5-1). The Economic Amplification Ratio (EAR), defined as the ratio of total costs to direct costs (Hallegatte et al., 2007), is relatively constant across the warming scenarios for each country. As an average across the warming scenarios, the EAR is 1.23 (Brazil), 1.15 (China), 1.61 (Egypt), 1.36 (Ethiopia), 1.22 (Ghana), and 1.26 (India).

Under the CC+SE experiment the magnitude of direct damage increases significantly for all countries, reflecting the increasing population and economic assets at risk. Under Scenario 1: <1.5°C direct damages range from 0.13 billion US$ per year (Ghana) to 42 billion US$ per year (China). Losses increase to 1.12 billion US$ per year (Ghana) and 129 billion US$ per year (China) under Scenario 6: 4°C. The magnitude of indirect damages not only increase but also surpass the direct damages (Figure 5-1). Indirect losses range from 1.7 billion US$ per year (Ghana) to 51 billion US$ per year (China) under Scenario 1: <1.5°C, increasing to 12 billion US$ per year (Ghana) and 256 billion US$ per year (China) under Scenario 6: 4°C. As an average across the warming scenarios, the EAR increases to 10.97 (Brazil), 2.36 (China), 16.21 (Egypt), 12.05 (Ethiopia), 12.94 (Ghana), and 6.62 (India).

The increase in direct damage under the CC+SE experiment reflects the steady growth in capital stock, population, and GDP under the SSP2 trajectories, resulting in larger flood exposure in the future period compared to the baseline. Indirect losses are significantly larger than direct losses as indirect losses in the CC+SE experiment accumulate over time and reflect the potential for a continuous slowdown in economic growth from the projected growth trajectory if no floods occurred. In other words, the indirect flood damages presented here not only result in a short-term impact on economic output, but also have the potential to restrict longer-term economic growth (discussed further in Section 5.3.4, Figure 5-5 and Figure 5-6). Thus, the inclusion of

socio-economic development results in large increases in total losses when compared to the equivalent CC experiment run; for example, under Scenario 6: 4°C, the total losses will increase by 3,613% (Brazil), 5,670% (China), 5,265% (Egypt), 6,095% (Ethiopia), 13,447% (Ghana), and 5,503% (India).

Figure 5-1 also illustrates that there is a large range in uncertainty, shown as the ensemble maximum and minimum values, which also increases under higher warming levels. This reflects the variance seen in the flood model outputs, representing differences in climate change patterns projected by the five GCMs.

5.3.2. Percentage Change to National GDP

Figure 5-2 presents the average annual indirect economic damage as a share of national GDP. Under both the CC and CC+SE experiments, Egypt suffers the largest reductions to national GDP, reaching 2.3% and 3.0% under Scenario 6: 4°C, respectively. This highlights the high population density and the fact that most economic activities, including agriculture, take place in the Nile Valley (Aliboni, 2012). While flood risk was low in the baseline period in Egypt, this increases in the future, driven by increased precipitation upstream in Sudan and Ethiopia which increases river flows and flood risk along the Nile (He et al., 2022).

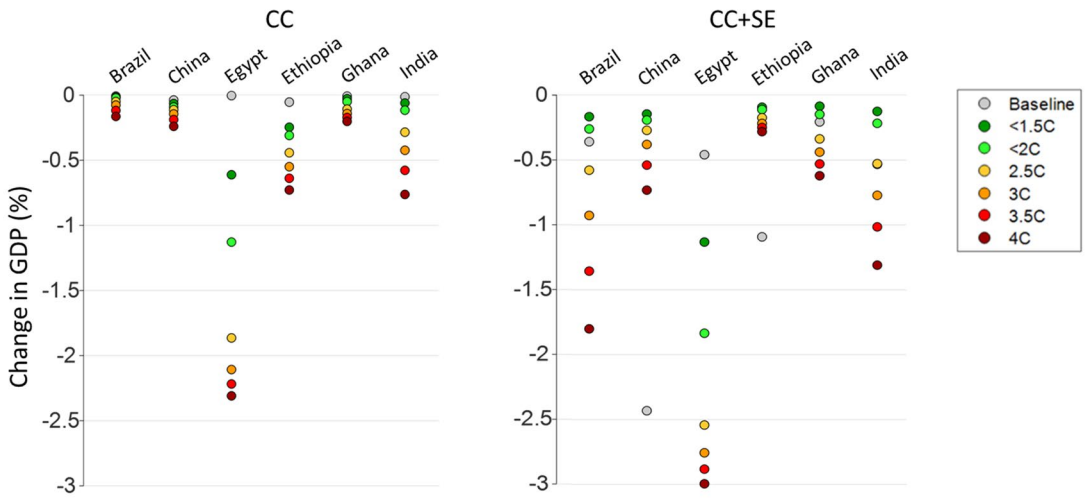

Figure 5-2: The average annual indirect economic damage as a share of national GDP (%) caused by fluvial flooding under the baseline and future scenarios with (CC+SE) and without (CC) socioeconomic change for the six countries.
The results are given by the ensemble average of the five GCMs.

Under the CC experiment, Ethiopia and India face the next largest impacts to GDP, after Egypt, equating to 0.73% and 0.76% of GDP respectively, under Scenario 6: 4.0°C. However, for Ethiopia losses decline from the baseline (1.09% of GDP) when socio-economic development is included, ranging from 0.09% to 0.28% of GDP under Scenarios 1 to 6. This reflects the different baseline and future projections of socio-economic growth in Ethiopia, which makes the country appear more resilient when viewed in relative terms, to the costs of fluvial floods under future projections of climate change (see also Appendix Figure B3 and Appendix Figure B4). A similar trend is seen in China when considering socio-economic development. Winsemius et al. (2016) also highlighted how socio-economic change can be a driver for reduced future flood risk, in relative terms, particularly in higher income countries.

Brazil faces the lowest indirect damages of all countries as a proportion of GDP under the CC experiment (0.16% under Scenario 6: 4°C), but the second largest losses under the CC+SE experiment (1.80% under Scenario 6: 4°C). Whilst losses as a proportion of GDP initially decline at lower warming levels, increases are seen from Scenario 3:

2.5°C onwards. A similar trend is seen for India and Ghana. For India, indirect losses as a proportion of GDP initially decline from the baseline at lower levels of warming, before increases are seen from Scenario 4: 3°C onwards, suggesting a tipping point where increasing flood risk outweighs any relative benefits of socio-economic development. Similar trends in direct flood damage were reported by Dottori et al. (2018) for several regions in the world, with damage as a share of GDP declining with warming, particularly for fast growing economies, although the trend was reversed when damages were reported in absolute terms (as in Figure 5-1 above). Hence, it is important to consider changing socio-economic characteristics such as population change, land-use change and economic growth trajectories, alongside climate change.

5.3.3. Sectoral Distribution of Fluvial Flood Damages

A further benefit of the methodology is that it allows sectoral disaggregation of flood damages. Figure 5-3 and Figure 5-4 show a subset of the results for the six countries, split by direct and indirect losses (see Appendix Figure B5 for full results). Direct and indirect losses to sectors increase in line with increasing warming scenarios. As above, they are significantly higher, with a greater share of indirect losses, under the CC+SE experiment.

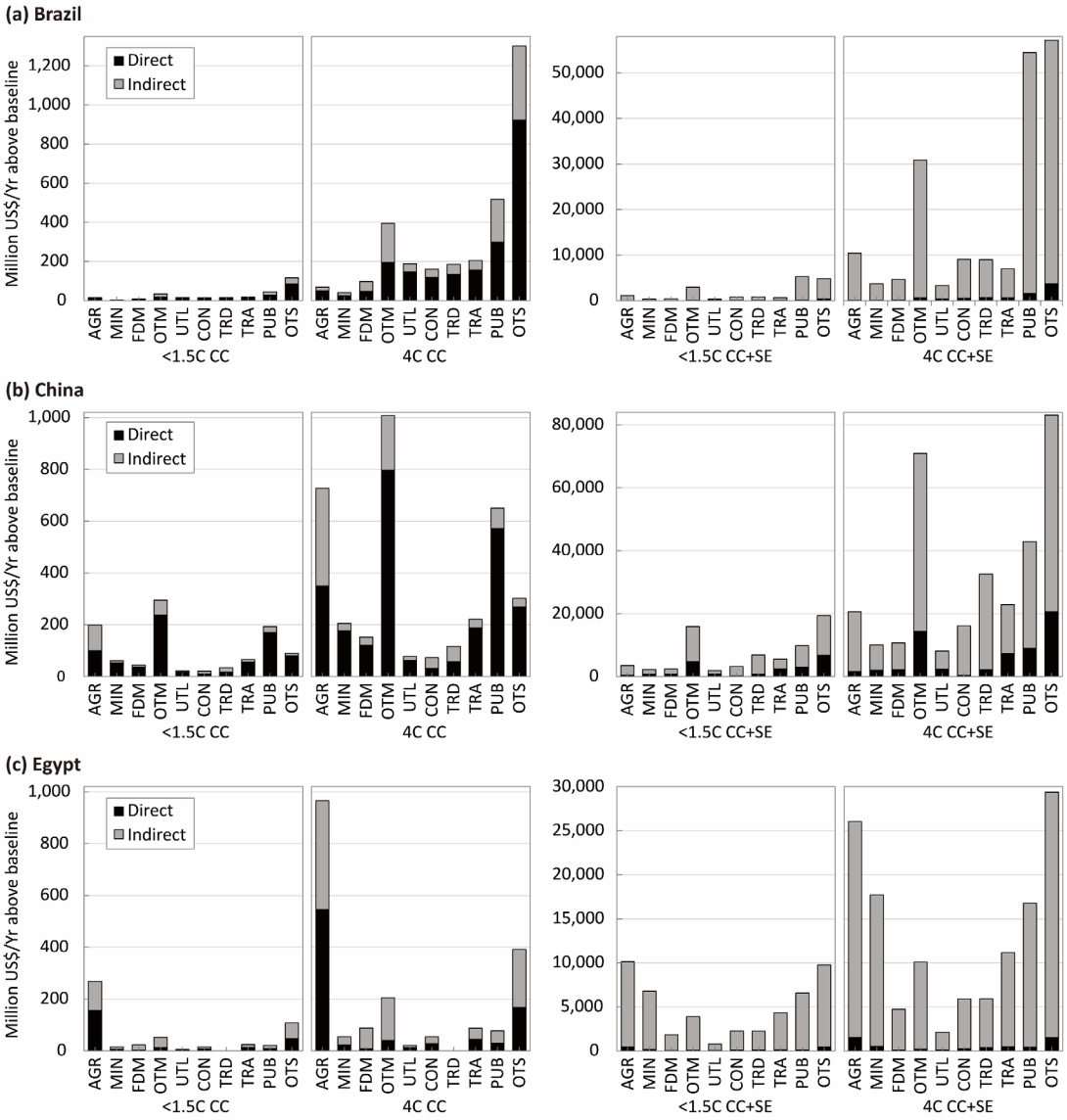

Figure 5-3: Sectoral losses in million US$/year, under the 1.5°C and 4°C climate scenarios with (CC+SE) and without (CC) socio-economic change for Brazil, China, and Egypt.

The bars represent total losses, with the share of direct and indirect losses indicated by the shading. Results are presented for ten sectors: agriculture (AGR); mining (MIN); food manufacturing (FDM); other manufacturing (OTM); utilities (UTL); construction (CON); trade (TRD); transport (TRA); public services (PUB); other services (OTS).

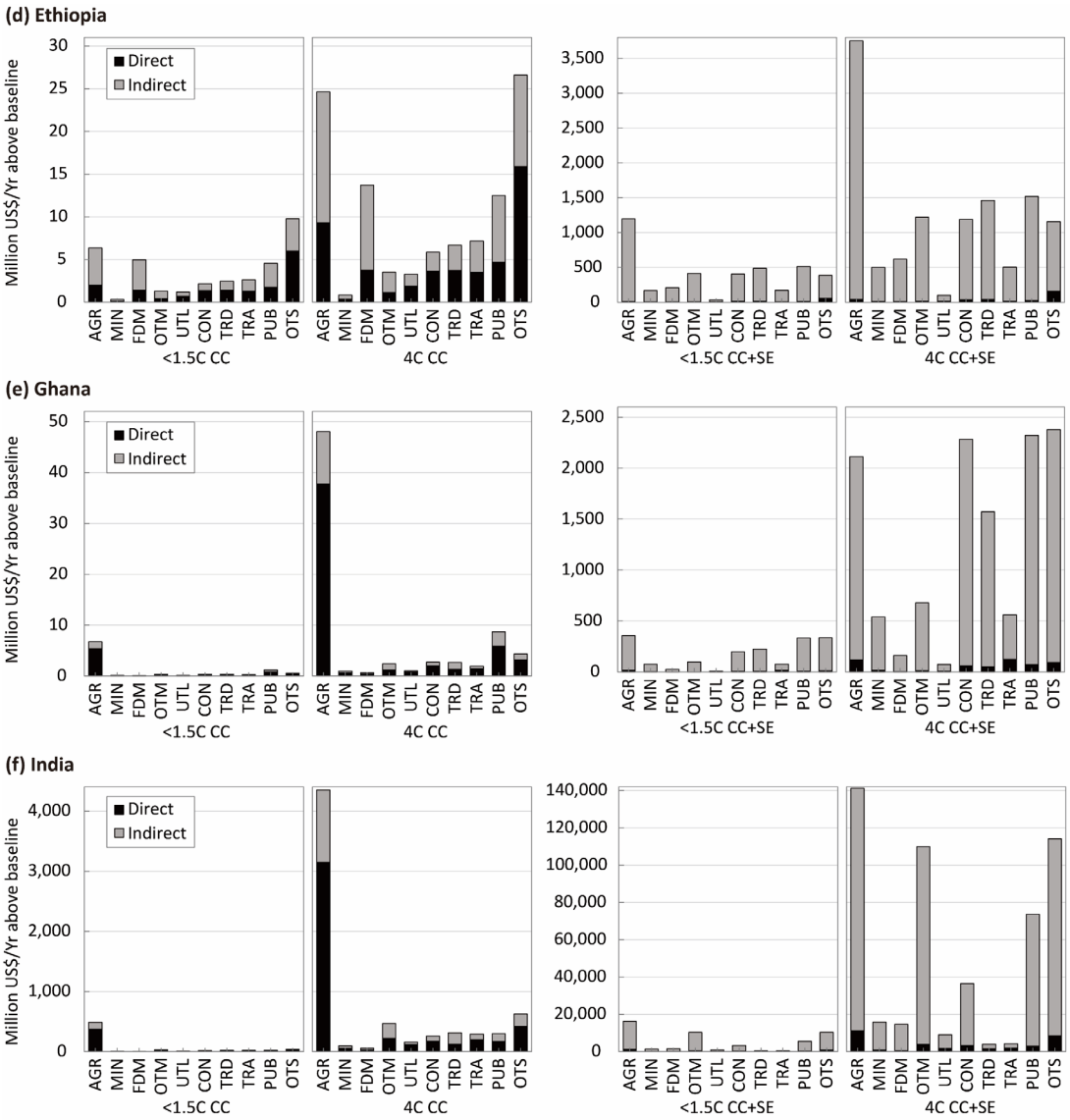

Figure 5-4: Sectoral losses in million US$/year, under the 1.5°C and 4°C climate scenarios with (CC+SE) and without (CC) socio-economic change for Ethiopia, Ghana, and India.
The bars represent total losses, with the share of direct and indirect losses indicated by the shading. Results are presented for ten sectors: agriculture (AGR); mining (MIN); food manufacturing (FDM); other manufacturing (OTM); utilities (UTL); construction (CON); trade (TRD); transport (TRA); public services (PUB); other services (OTS).

Under the CC experiment, the agricultural sector (AGR) faces some of the largest losses in China, Ethiopia, Egypt, Ghana, and India, as well as other manufacturing (OTM) and public (PUB) and other services (OTS). This is similar to findings of Dottori et al. (2018) who found pronounced agricultural losses in low-income regions with a higher share of agricultural GDP. In Brazil, the largest impacts are felt by other

manufacturing (OTM), public (PUB) and other services (OTS), whilst Ethiopia also sees large losses to its food manufacturing (FDM) sector. Whilst the losses increase from Scenario 1: <1.5°C to 6: 4°C, the sectoral distribution of losses in each country remains similar. However, under the CC+SE experiment, the results also reflect underlying changes in the economic structure of the countries, including the expansion of service sectors of the economy. For example, there are increasing losses to public services (PUB) and other services (OTS) under Scenario 6: 4°C for countries such as India and Ghana, who predominantly saw losses to the agricultural sector (AGR) under the CC experiment. Particularly for Ghana, the reduction in the share of agricultural losses from the CC to CC+SE experiment can be explained by the movement away from a primarily agricultural-based economy since the baseline period, which is embodied in a falling share of agriculture land use area (due to urban expansion) and a decreasing contribution of the agricultural sector (AGR) to Ghana's GDP.

5.3.4. Recovery Dynamics

When calculating indirect damages under the CC experiment, it is assumed that the economy recovers to the pre-flood level (Section 5.2.3). Figure 5-5 illustrates the dynamic percentage change of monthly GDP for each country, under the baseline and six warming scenarios, relative to the pre-flood level. The fluctuations highlight each occurrence of flooding and the post-flood recovery period. Fluvial flood losses to monthly GDP range from up to 2.9% in Ethiopia (baseline) and up to 15.2% in Egypt (Scenario 6: 4°C). For all countries, it usually takes several months for GDP to recover to pre-flood levels. The frequency of events, scale of losses, and recovery time increase in severity in line with the increasing warming levels.

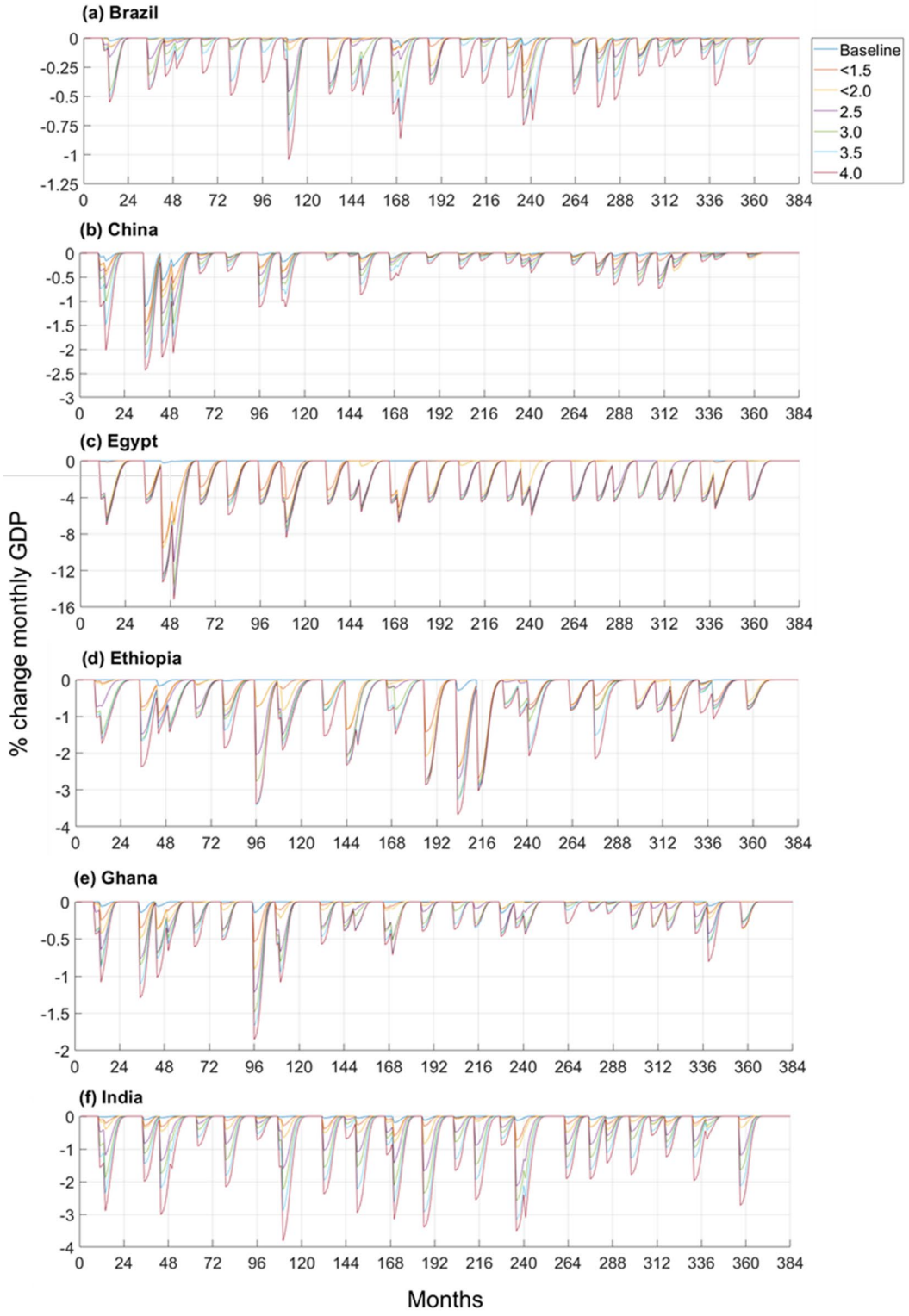

Figure 5-5: Percentage change in monthly GDP (%) due to fluvial flooding for the baseline and climate scenarios under the CC experiment.

Lines represent the ensemble average of the five GCMs. Calculations for the baseline scenario are based on actual exogenous growth data between 1960 and 1993, while those for the climate scenarios are based on projected exogenous growth data (SSP2) between 2085 and 2118.

In terms of flood frequency, it can be seen that during the 30-year baseline, in large countries which have some of the world's largest rivers (e.g., China, Brazil, and India), there will be more than 25 years with 1 in 100-year floods. Although flood-induced damages are aggregated to the national scale, these floods may occur in different areas of the country, particularly for countries with more than one major river. During the future period, a flood exceeding the baseline 1 in 100-year threshold will no longer be a 1 in 100-year flood, thus extreme flood events from the baseline perspective become more frequent in the future under the warming scenarios.

Focusing on the dynamics of individual flood events over time, and their indirect losses, is beneficial as it highlights the different magnitude of impacts between flood events. It also highlights the potential impact, in terms of the magnitude of losses and duration for recovery, of successive flood events that may occur while the country is still in a recovery period, as shown in China and Egypt around month 50.

Under the CC+SE experiment, the economy can recover to a level above the pre-flood economy based on the exogenous growth data used within the DF-growth model (2086-2115 for the climate scenarios and 1961-1990 for the baseline scenario). In this case, the level of recovery required to re-establish the pre-flood trajectory is larger (Figure 5-6). Consequently, indirect impacts can continue to accumulate over time as they also account for the overall slowdown in the growth rate of the economy from its potential trajectory, highlighted by the downward sloping trends in Figure 5-6. Fluvial flood losses to monthly GDP range from up to 1.5% in Egypt for Scenario 1: <1.5°C and up to 4.7% in Egypt for Scenario 6: 4°C. Indirect damage as a share of monthly GDP is generally lower than under the CC experiment given the future economic growth trajectories (see Appendix Figure B3). Yet, although the impact of individual flood events, in terms of the potential loss to monthly GDP, is more severe under the

CC experiment, when totalled over time the accumulated impacts are higher under the CC+SE experiment.

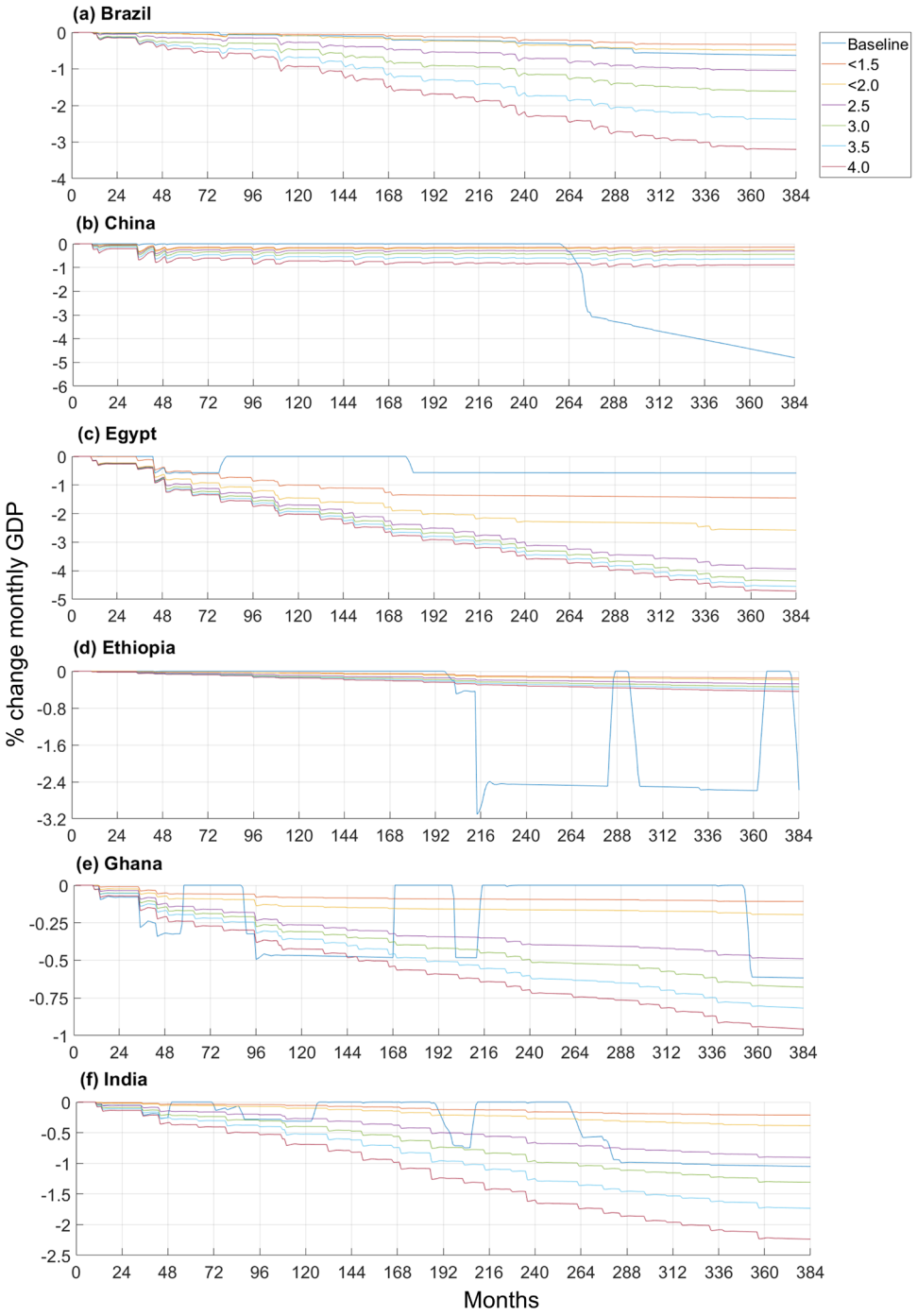

Figure 5-6: Percentage change in monthly GDP (%) due to fluvial flooding from the pre-flood economy for the baseline and climate scenarios under the CC+SE experiment.

Lines represent the ensemble average of the five GCMs. Calculations for the baseline scenario are based on actual exogenous growth data between 1960 and 1993, while those for the climate scenarios are based on projected exogenous growth data (SSP2) between 2085 and 2118.

Figure 5-6 also shows how the trajectory of trends under the baseline period (i.e., navy blue lines) differ to those of the climate scenarios, ranging from 0.6% in Egypt up to 4.8% in China. The differences reflect the different frequency and intensity of flood events, with the economy able to recover fully between events in many instances. Typically, when absolute economic growth continues over time, full economic recovery is impossible, as the growth continues at a slower rate than under the pre-flood economy. Full recovery usually occurs in periods of economic recessions (Appendix Figure B4) when other constraints (e.g., droughts and famine) become more severe than flood constraints and dominate economic trajectories. These deviations result in spikes, or downward trends, in Figure 5-6 when displayed as a percentage change in monthly GDP from the pre-flood economy. These periods of economic recession reflect that the baseline is based on historical growth data and these time series do not always follow a smooth trajectory. In contrast, the future scenarios are based on deviations from projected growth data between 2086-2115 from the SSP2 scenario. These trajectories do follow a smooth pathway, hence another reason for the difference in the baseline trajectories when compared to the climate scenarios in Figure 5-6. Thirdly, while absolute losses increase under the warming scenarios, in relative terms losses to GDP may appear smaller in the future given the level of projected economic growth, as seen in China when comparing the baseline to future scenarios (Figure 5-2). This is consistent with the results of Dottori et al. (2018), which implies that some economies grow faster than flood-induced direct damage with warming.

5.4. Discussion and Conclusions

The above analysis provides an assessment of the direct and indirect economic impacts of fluvial flooding in six countries under future scenarios of climate change and socio-economic development. It covers a range of climate scenarios reflecting ambitious

targets as well as higher levels of warming. The study demonstrates the importance of including socio-economic development when projecting direct and indirect flood losses, and the implications of this for damage estimates. Population change, land-use change, and economic growth can be just as, or more, important than climate change in terms of understanding the future dynamics of fluvial flood risk (Dottori et al., 2018). The methodology considers direct and indirect economic impacts, providing a more comprehensive assessment of total damages at the national level, while facilitating comparison across countries.

Results highlight the potential for large increases in flood related losses under future warming scenarios. Absolute fluvial flood losses are largest in China and India. However, as a share of national GDP, Egypt faces the most serious consequences, under both the CC and CC+SE experiments. The magnitude of indirect losses also varies largely when comparing between the CC and CC+SE experiments, becoming particularly severe in Egypt, Ghana, and Ethiopia under the CC+SE experiments.

The method enables the consideration of dynamic recovery. This provides valuable insights into the role of recovery dynamics in influencing losses and paves the way for further research in this area, particularly important given the past knowledge gap in considering such dynamics in traditional IO models (Meyer et al., 2013). The results highlight the potential opportunity costs, in terms of economic development, due to fluvial flooding in the future. The baseline CC+SE results also emphasise the importance of other exogenous constraints (such as droughts and famine) that may be felt in successive years or in combination with flooding constraints, causing different recovery dynamics and loss estimates. This provides a rationale for further research into compound hazards, with the development of the CHEFA model in this thesis, to present a more comprehensive picture of the economic impacts of all possibly co-occurring extreme events driven by climate change, and on a broader scale, by

anthropogenic instabilities (see Chapter 6 and Chapter 7 for further analysis).

In terms of validating results, the lack of empirical data on the dynamics of business recovery (Koks et al., 2019) and documented economic data on the indirect costs of flooding makes comparison difficult. Direct damage estimates for the baseline period under the CC+SE experiment can be compared with data from the EM-DAT database. Total direct damages for the baseline period modelled here are US$6,640 million in Brazil, US$25,123 million in China, US$87 million in Egypt, US$215 million in Ethiopia, US$86 million in Ghana, and US$4,050 million in India. Damages reported by EM-DAT during the same period are US$4,185 million in Brazil, US$10,219 million in China, US$14 million in Egypt, US$0.92 million in Ethiopia, US$75 million in Ghana, and US$5,744 million in India. For Brazil, Ghana, and India, the estimates are comparable to those reported by EM-DAT (around 15-60% difference). For the other three countries, the estimates are much larger than reported data. This likely reflects the underreporting of economic damages in the EM-DAT database, particularly for developing countries in past decades (Kundzewicz et al., 2014).

Regarding the percentage change in direct damages relative to the baseline, results can be compared with Alfieri et al. (2017). Their estimates were made under three warming scenarios (1.5°C, 2°C, and 4°C), assuming constant socio-economic conditions and using the same set of depth-damage functions as this study (Huizinga et al., 2017). Estimates presented here under the CC experiment for Brazil, China, and India are in good agreement with those reported by Alfieri et al. (2017). However, the estimates for the three African countries in this study are much larger. This discrepancy is also noted by He et al. (2022) when comparing population exposure to flooding with that of Alfieri et al. (2017). Consequently, the higher estimates for the three African countries in this study likely reflect higher increasing flood occurrences projected by the flood hazard model.

However, as with any economic impact study of climate change it is extremely challenging to capture all aspects of the subject within a single framework. Several studies highlight that flood risk assessments are sensitive to the choice of GCMs or climate driving datasets (Alfieri et al., 2015; Sperna Weiland et al., 2012; Ward et al., 2013). However, in this study, the overall patterns seen with increasing warming levels are consistent among the five GCMs, which sample a reasonable proportion of the overall uncertainty in modelled precipitation in the wider CMIP5 (He et al., 2022).

The study focuses on economic losses relating to floods whose magnitude exceeds a baseline 1 in 100-year return period. Smaller events, which may still have an economic effect, are not considered, leading to a potential underestimation of losses. Conversely, as the flood data from CaMa-Flood does not consider flood protection (He et al., 2022), focusing on a 1 in 100-year flood event can reduce the potential of overestimating risks given that many flood protection defences are designed at protection levels lower than the 100-year return period. While beyond the scope of this study, more recently available global flood defence data could be used to investigate the role of adaptation in the future (Scussolini et al., 2016). Winsemius et al. (2016) found that including improvement in flood protection levels over time would significantly reduce economic damages, although this extension to the modelling has its own limitations in terms of the availability and accuracy of data for this parameter (Tanoue et al., 2016).

There is also uncertainty associated with the depth-damage functions used. Dottori et al. (2018) employed the same set of functions in their study and claimed that the associated uncertainty would exceed ±50%, as also noted by Huizinga et al. (2017). Given there are no alternative, globally consistent databases available, it is not feasible to account for the effect of the depth-damage functions used in this study. Nevertheless, the database of depth-damage curves used in this study is beneficial as it accounts for

heterogeneity across the six countries as well as facilitating a country comparison.

This study also assumes a constant land cover after 2015 in the CC+SE experiment. When socio-economic growth is modelled with constant land cover, the exposure value per unit area increases more in the model than in reality where the area constructed on will grow. Though predicted future land cover maps exist (van Vuuren et al., 2017), they are often at a coarser resolution and subject to several assumptions (ibid), which can introduce further uncertainty into the economic calculations.

Lastly, there are uncertainties arising from the underlying data, parameterisation of the DF-growth model and assumptions on recovery dynamics used for the estimation of indirect losses, which would benefit from future research. For example, the IO tables used for the baseline and future analysis were dependent on the latest years of data available for each country, which differed, with the classification of certain sectors varying for some countries (see Appendix Table A5). However, modelling the future structure of an economy, particularly when applied to multiple countries, is always difficult (Koks et al., 2019).

Nonetheless, the analysis presented here is beneficial in many aspects as discussed at the start of this section. Going forwards, the provision of more comprehensive estimates of fluvial flood risk, that account for both the effects of climate change and uncertainty under a range of warming scenarios, and the role of socio-economic development, will provide important insights to support decision-making regarding flood risk management, and in terms of investment needs for adaptation (Mokrech et al., 2015). Being able to apply the analysis at a country level is important for future research as economic losses will be related to the level of development of the specific society, and could also capture any flood prevention measures in place which may differ regionally and overtime as income levels rise (Jongman et al., 2015). And, as

noted by other authors (Koks et al., 2019), the study also contributes to the objectives of the Sendai Framework for Disaster Risk Reduction to better understand disaster risk (UNISDR, 2015), essential to help inform and support the development of post-disaster recovery and adaptation strategies.

Chapter 6 CHEFA Model Illustration: A Perfect Storm of Flooding, Pandemic Control, and Deglobalization

The outcomes of this chapter are parts of the work program of the World Bank on trade and climate change, which were initially published online in a working paper of the World Bank and later revised into a journal paper under review. Yixin Hu is responsible for impact modelling, result interpretation, and drafting. The sections in this chapter have been reproduced under the permission of co-authors.

Hu, Y., Wang, D., Huo, J., …, Chemutai, V. (2021). *Assessing the economic impacts of a 'perfect storm' of extreme weather, pandemic control and deglobalization: a methodological construct* [Working Paper No. 160571]. World Bank. https://documents.worldbank.org/en/publication/744851623848784106

The purpose of this chapter is to fulfil Research Objectives 5 and 6, which are the empirical application of the proposed CHEFA model for the compound-hazard impact analysis (see Section 3.2) and providing policy enlightenment on the improvement of economic preparedness in complex scenarios. This contributes to Research Questions 3 and 4 raised in Section 1.4.1. As noted in the discussion of Chapter 5 (see Section 5.4), the co-occurrence of multiple extreme events, which is ignored in the single-hazard analytical framework, may cause different economic recovery dynamics and loss estimates and requires an integrated method for disaster footprint accounting. This is of particular importance in today's world with intensifying climate change, ongoing COVID-19 pandemic, and escalating deglobalization. With the development of the CHEFA model in previous sections, this chapter uses a hypothetical compound-hazard event in a global economy to illustrate the model's applicability and robustness.

Specifically, this chapter investigates the economic impacts of a multi-disaster mix comprising of extreme weathers, such as flooding, pandemic control and deglobalization, dubbed a 'perfect storm'. Scenarios are built to first examine the economic consequences when a flood and a pandemic lockdown collide and how these are affected by the timing, duration, and intensity/strictness of each shock. Subsequently, the outcomes of export restrictions during the compound of the pandemic and the flood are assessed, especially when there is specialization of production of key sectors. The results suggest that an immediate, stricter but shorter pandemic control policy would help to reduce the economic costs inflicted by a perfect storm, and regional or global cooperation is needed to address the spillover effects of such a compound event, especially in the context of the risks from deglobalization.

6.1. Introduction

During the past years, the ongoing COVID-19 pandemic appeared to have diverted attention away from the climate crisis (Selby and Kagawa, 2020; The Lancet Planetary Health, 2020), despite the fact that just a few years prior, the WHO had identified climate change as 'the greatest threat to global health in the 21st century' (WHO, 2015). The year 2020 saw a number of climate disasters. It was the hottest year on record (Gohd, 2021). The dry and hot conditions fuelled massive record-breaking wildfires across Australia, Siberia, and the United States. The 2020 Atlantic hurricane season was also the most active in recorded history (White, 2020). Devastating typhoons swamped the Indian subcontinent and south-east Asia while the Sahel and Greater Horn regions of Africa experienced severe droughts (Boyle, 2020) and devastation from locust swarms linked to climate change (UNEP, 2020). Early 2021 also saw the Swiss Alps develop an orange layer caused by heavy sandstorms from the Sahara Desert, the widest reach recorded in recent years (BBC News, 2021).

Several aspects signalling deglobalization have been at play in recent years. The 2020 World Development Report reports that growth in global value chains has flattened (World Bank, 2019). 2020 saw increasing trade tensions, especially in relations between the US and China, as well as the UK withdrawing from the EU, but also in some of the responses by governments to the COVID-19 pandemic. Indeed, some have argued that COVID-19 has further fuelled the process of deglobalization (Oxford Analytica, 2020; Shahid, 2020). A number of countries have responded by introducing export restrictions on critical medical equipment and food and even on vaccines (Eaton, 2021; Espitia et al., 2020). This raises the issue of whether restrictive trade policy measures can undermine effective responses when climate and pandemic crises collide to create a perfect storm (Mahul and Signer, 2020).

The collision of climate extremes, pandemic control and deglobalization creates a triple or compound event. The concept of 'compound event' was originally used in climatic research (AghaKouchak et al., 2020; Field et al., 2012; Hao et al., 2013; Leonard et al., 2014; Zscheischler et al., 2018) and defined as the 'combination of multiple drivers and/or hazards that contributes to societal or environmental risk' by Zscheischler et al. (2018, p. 470). Unable to foresee such a globally explosive outbreak of COVID-19, these studies were mainly focused on the co-occurrence of multiple dependent climatic hazards. Only very recently have researchers begun to incorporate the coexistence of biological hazards. As the COVID-19 pandemic and global warming continues, civil society will see a growing probability of collisions between COVID-19 surges and climate crises (Phillips et al., 2020), in tandem with other global issues, such as deglobalization, following recent trends. Countermeasures against one crisis may jeopardize the efforts to confront another crisis, which ultimately exacerbates the negative impacts of both (Ishiwatari et al., 2020; Salas et al., 2020; Selby and Kagawa, 2020). As a result, scholars have advocated for a comprehensive and holistic multi-hazard approach of disaster management that considers all possible

hazards together with compound ones in the post-pandemic world (Chondol et al., 2020). Hariri-Ardebili (2020) proposed a multi-risk assessment tool to qualitatively study the hybrid impacts of compound-hazard situations on healthcare systems, while Shen et al. (2021) provided a tool to assess the compound risk from flooding and COVID-19 at the county level across the United States. Beyond these, researchers also developed optimization models to study the effectiveness of evacuation strategies in risk control when floods intersect with the COVID-19 pandemic (Pei et al., 2020; Tripathy et al., 2021).

An important aspect of risk management is to assess the economic consequences of hazardous events (Laframboise and Loko, 2012), however, this has been rarely addressed in compound-hazard research. Typically, in single-hazard research, economic models, such as IO and CGE models, provide quantitative tools to evaluate the economic footprint of disruptive events (Botzen et al., 2019). Metrics related to disaster-induced economic damages, both direct and indirect ones, are developed to inform cost-benefit decisions in disaster preparedness investment (ESCAP, 2019). There are many studies that have focused on climate extremes (Hallegatte, 2008, 2014; Koks et al., 2015; Koks and Thissen, 2016; Lenzen et al., 2019; Mendoza-Tinoco et al., 2020; Oosterhaven and Többen, 2017; Willner et al., 2018; Xia, Li, et al., 2018; Zeng et al., 2019), but only a few have studied biological hazards like the COVID-19 pandemic (Guan et al., 2020; McKibbin and Fernando, 2020). Even fewer studies have looked into the economic aspects of compound events. Zeng and Guan (2020) employed the Flood Footprint model to quantify the combined indirect economic impacts of successive flood events. However, the interaction between pandemic control and flood responses is different from that between two flood events. Flood events are usually sudden or rapid onset events which require immediate emergency measures (Bubeck et al., 2017; Johnstone and Lence, 2009), while a pandemic such as COVID-19 lasts for longer periods and the corresponding control measures could be

of various durations and coincide with different flood periods. A focus on measures to prevent virus transmission can result in inadequate response towards flood disasters (Ishiwatari et al., 2020) and constrain the economic flows required by post-flood recovery, aggravating the impact of the flood. Similar perspectives are suggested by Swaisgood (2020) that the economic consequences of such compound events are underestimated if the interplay between individual hazards is not considered. The compound effects of natural and pandemic hazards increase the complexity of economic consequences, which cannot be addressed by traditional single-hazard assessment techniques.

Given these research gaps, this chapter uses the CHEFA model which is developed in Chapter 3 for compound-hazard impact analysis to assess the economic impacts resulting from triple shocks of pandemic control, flooding and deglobalization. The model, which is constructed under the ARIO-Inventory framework (Hallegatte, 2014), considers not only the economic-wise interplay between different types of negative shocks, but also the possibility of cross-regional substitution and production specialization. Scenarios are built on a hypothetical global economy consisting of four regions and five sectors where hazardous events with different durations and intensities collide at different spatial and temporal scales. Afterwards, specific scenarios are explored to understand the role of trade in disaster recovery during compound climate and health crises, with a special focus on how export restrictions and the extent of production specialization influence the magnitude of economic losses.

This study provides consistent and comparable loss metrics with single-hazard analysis and can be generalized to various types of compound events. This would support the formation of an integrated risk management strategy including compound hazards and the fulfilment of the mitigation and adaptation targets in the Paris Agreement and Sendai Framework for Disaster Risk Reduction (UNFCCC, 2015;

UNISDR, 2015).

6.2. Scenarios and Discussion

6.2.1. A Hypothetical Global Economy

Here a hypothetical global economy consisting of four regions and five sectors is assumed based on the multi-regional input-output (MRIO) table developed by Zheng et al. (2020) (see Appendix Table A6)[14]. The annual GDP of this hypothetical global economy is 9,613 units. The four regions are denoted by A, B, C and D, which account for 21%, 39%, 28% and 12% of the global economy, respectively. C is the only region hit by flooding, amid global pandemic control and deglobalization. B is the largest trade partner of C. More than half (52%) of C's total trade volume comes from region B, which is equivalent to 11% of C's output. This is followed by A and D, which accounts for 31% and 17% of C's total trade volume, respectively. There are five economic sectors, consisting of Agriculture (AGR), General Manufacturing (MANG), Capital Manufacturing (MANK), Construction (CON) and Other Services (OTH). 'MANK' and 'CON' are the two sectors that are involved in the reconstruction of capital damaged by flooding.

In this analysis, it is assumed that capital reconstruction largely relies on local inputs

[14] This MRIO table is adopted because of its open accessibility from the CEADs database (www.ceads.net). It is originally a Chinese MRIO table for 2015, covering 31 provinces and 42 socioeconomic sectors, and then aggregated into 4 major regions and 5 sectors to construct a virtual global economy with almost real and differentiated inter-regional or inter-sectoral linkages. Sector aggregation and disaggregation are common methods in IO analysis to deal with the mismatch in sector resolution of different databases used (Lenzen, 2011, 2019; Steen-Olsen et al., 2014; Weinzettel, 2022), and the current sector resolution of the five sectors are deliberately designed for the purpose of this study. Such a pre-process helps to simplify the analysis which is focused on the interaction mechanisms of compound shocks within the economic system instead of the sectoral details of disaster impact distribution. This chapter also examines the robustness of the analysis using a different GTAP-based MRIO matrix and finds consistent results on the economic interplay between flooding, pandemic control, and trade restrictions (see Appendix Table A7 and Section 6.3.5).

of capital goods and construction services and different sectors in the same region have the same capital matrix coefficients. For example, the 'CON' and 'MANK' sectors of C contribute to 68% and 20% of the reconstruction efforts in C, respectively, while the remaining 12% comes from the 'MANK' and 'CON' sectors of B and the 'MANK' sector of A. A full capital matrix indicating the sources of capital formation of each region is provided in Appendix Table A8.

Values of other parameters in the CHEFA model are presented in Table 6-1. While the values of $\alpha_{ir}^{\max}$ and τ_{α} are the same as in Hallegatte (2014), the value of n_{ir}^{j} is smaller than that in Hallegatte (2014). This is due to the assumption of a Just-In-Time (JIT) inventory management which is gaining popularity for its advantages in lowering inventory and related costs (Yang et al., 2021). In fact, some multinational corporates, such as Hyundai Motor in South Korea, threatened to suspend production in response to the inventory supply disruption around one month after the onset of COVID-19 in China (Reuters, 2020). The uncertainties in these values must be acknowledged and a sensitivity analysis on these parameters is provided in Section 6.3. The model is run on a weekly basis in this analysis.

Table 6-1: Parameter values of the CHEFA model applied in the case of a hypothetical perfect storm.

Parameters	Definitions	Values
n_{ir}^{j}	Weeks of intermediate use of inventory product j that sector i in region r wants to hold	4
τ_{s}	Proportion of inventory loss that a production sector tries to restore in the next time step	100%
$\alpha_{ir}^{\max}$	Maximum overproduction capacity of sector i in region r relative to the pre-disaster level	125%
τ_{α}	Weeks needed by a sector to achieve its maximum overproduction capacity	52

6.2.2. Interaction Between Pandemic Control and Flooding in the Free Trade Scenarios

This section first simulates the economic impacts of multi-scale floods and/or a global pandemic in a free trade world which consists of four regions: A, B, C and D. Three scales of floods are defined according to the severity of damages they cause directly to population and economic sectors (Table 6-2). All floods occur in week 5 and last for 2 weeks in region C. At the same time, a global pandemic is declared in all regions and measures are taken to bring its spread under control. The strictness of the control policy, which is measured by the percentage reduction of the transportation capacity due to lockdown measures relative to the pre-disaster level, is benchmarked at 30% for 24 weeks.

Table 6-2: Event settings of flooding and pandemic control.

	Scales	Direct damage (% losses)						Duration (weeks)	Spreads
		Labour	AGR	MANG	MANK	CON	OTH		
Flooding	Small	20%	20%	10%	10%	15%	15%	2	Region C
	Medium	40%	40%	20%	20%	30%	30%		
	Large	60%	60%	30%	30%	45%	45%		
Pandemic Control	**Strictness scenarios (%)** [30%, 60% of transportation capacity reduction]							[8, 24]	All regions

Notes: Direct damage of flooding refers to the percentage reduction in labour availability and capital stock in the five production sectors: AGR – Agriculture; MANG – Manufacture, general; MANK – Manufacture, capital; CON – Construction; OTH – Other services.

6.2.2.1. Economic Impacts of Flooding, Pandemic Control, and Their Collisions

There is a two-way interaction between the flooding and pandemic hazards in terms of economic losses, by comparing the 'flood-only', 'pandemic-only' and 'flood+pandemic' scenarios. First, the pandemic control aggravates the flood impacts by hampering the post-flood capital reconstruction, under all flood scales. As in Table 6-3, the recovery of capital stock damaged by multi-scales of flooding in region C is delayed by 8-10 weeks by the coincidence of a benchmarked global pandemic control.

The recovery of global GDP is consequently deferred by 3-7 weeks at different flood scales. Compared to the 'flood-only' scenario, the intervention of pandemic control increases the global economic losses by 1,040.6-1,144.1 units (10.82%-11.90% of global annual GDP) at different flood scales.

Consistent results are observed on the regional scale by comparing the first and third rows of Figure 6-1, as all regions suffer additional losses from the concurring pandemic control when they are already affected by flooding in C. For region C, which is the only flooded region, the post-flood recovery curves of its GDP (yellow lines) are significantly flattened and delayed by the intervention of pandemic control[15]. This makes the cumulative losses in region C increase by 176.0-268.3 units, which is equivalent to 6.51%-9.92% of its annual GDP at the pre-disaster level, at different flood scales. However, the greatest loss increases are found in region B, which accounts for nearly half (41-45%) of the increase in global losses, followed by region A (22-24%), under all flood scales. These two regions first experience slight GDP gains (by 0.21%-0.96% for B and 0.07%-0.34% for A) under the 'flood-only' scenarios (Figure 6-1a-c), but then suffer significant GDP losses (by 11.56%-12.49% for B and 12.00%-12.41% for A) under the 'flood+pandemic' scenarios (Figure 6-1g-i). Early economic gains come from the stimulus effect of the reconstruction demand to recover the capital damaged by flooding in C. This happens with the possibility of substitution between suppliers, which is also observed by Koks and Thissen (2016). When region C is flooded and unable to meet the increasing demand for reconstruction, clients will

[15] Taking the small flood as an example, delays in the recovery of region C could be seen from both Table 6-3 and Figure 6-1. In Table 6-3, capital recovery only takes place in region C which is hit by the flood. It takes 49 weeks during the compound crises of a small flood and pandemic control, which is 8 weeks more than in the 'flood-only' scenario. In Figure 6-1, the yellow lines depict the dynamics of GDP recovery in region C by weeks. Comparing with the yellow line in Figure 6-1a (flood-only), the yellow line in Figure 6-1g (pandemic+flood) is flattened by the intervention of the pandemic control. It takes about 38 weeks for region C to recover its GDP to the pre-disaster level in Figure 6-1g, which is around 12 weeks more than in Figure 6-1a. In addition, the yellow line in Figure 6-1g is similar with that in Figure 6-1d (pandemic-only), which is because that the flood impact is so small that the pandemic control has dominated the GDP recovery of region C.

choose suppliers in other regions to restore their damaged capital, which stimulates the economic performance there. Among all regions, B benefits most from flooding in C, as it accounts for the biggest part (52%) of C's trade volumes. Such stimulus effect expands with the flood scales. The gains in B's GDP from a small flood in C is 0.21%, which rises to 0.71% from medium flooding and further to 0.96% in large flooding (Figure 6-1a-c).

Second, flood response may sometimes alleviate some of the negative impacts of pandemic control due to the stimulus effect of post-flood reconstruction. It only exacerbates the negative pandemic impacts when the flood damage is large enough to exceed such stimulus effect. On the global scale (Table 6-3), the concurrence of a small or medium flood in region C reduces the supply-chain/indirect losses by 48.6 or 21.0 units, respectively, when the global economy is already burdened by the pandemic. The reduction of losses comes from the stimulus effect of post-flood reconstruction as mentioned above. However, a large flood leads to large direct damage and widespread supply chain losses which surpass the stimulus effect of reconstruction activities, and therefore increases the global pandemic impacts by 86.9 units.

On the regional scale, the flood-related alleviation effects of negative pandemic impacts are mainly found in the three non-flooded regions (i.e., A, B, and D), comparing the second and third rows of Figure 6-1. Taking region B, which benefits most from the stimulus effect of post-flood reconstruction, as an example, its relative GDP losses fall from 12.87% (pandemic-only) to 12.49% (small flood+pandemic), then to 12.12% (medium flood+pandemic), and finally to 11.56% (large flood+pandemic). The alleviation effect becomes more significant as the pandemic control intersects with a larger flood. The bottom row of Figure 6-1 zooms in on the GDP dynamics of regions A, B, and D in subplots f and i to take a close look at the regional differences between the 'pandemic-only' and 'large flood+pandemic'

scenarios. On the one hand, the post-flood reconstruction demand has buffered the negative impact of the pandemic control in the first place for all the three regions and accelerated the GDP recovery of at least region B afterwards, which is because that region B is the most involved in region C's capital reconstruction. On the other hand, however, the intervention of flooding also makes the three regions go through earlier and longer shortages of intermediate inputs, which is signalled by further drops of GDPs between weeks 24-30, as the pandemic-related transport constraint continues.

By contrast, flood damage aggravates the pandemic impacts in the flooded region C when the flood is above and equal to the medium scale. The region suffers GDP losses of 13.20% from the pandemic control alone, while 13.80% from the combination with a medium flood and 18.75% with a large flood. These regional results are in consistency with the global results in revealing the role of the stimulus effect associated with post-flood reconstruction.

A further discussion on the direct and indirect economic consequences caused by flooding, pandemic control, and their collisions, respectively, without trade restrictions, is provided in Appendix C.2. Direct and Indirect Impacts of a Perfect Storm under Free Trade Scenarios.

In addition, it is worth noting that the continued pandemic control may have a secondary negative impact on regional GDPs by restricting the transport and delivery of intermediate inputs needed to recover production. For example, the second falls in regional GDPs around week 28-29 in Figure 6-1d-f are due to the shortage of intermediate inputs arising from delivery failures under persistent transport constraints during the pandemic control. As mentioned above, the inventory shortage may appear earlier due to the intervention of flooding and last longer as the flood scale increases (Figure 6-1g-i). On the contrary, it could be avoided by a shorter but stricter pandemic

control (Figure 6-2g-h). Its occurrence is also linked with the size of inventories held by economic sectors. A large inventory size could improve the inventory resilience and reduce the risk of inventory shortage. As in Section 6.3.1 and Figure 6-5, the second GDP decline resulting from an inventory shortage in each region is delayed by weeks as the inventory size increases and finally disappears as the inventory size is large enough.

Table 6-3: Global economic footprint under the 'flood-only', 'pandemic-only' and 'flood+pandemic' scenarios without trade restrictions.

Scenarios		Direct Damage[a]	Indirect Losses[b]	Total Impacts	% of Global Annual GDP	Capital Recovery Weeks[c]	GDP Recovery Weeks[c]
Pandemic-Only		0.0	1,242.6	1,242.6	12.9%	-	42
Small	Flood-Only	317.2	50.0	367.2	3.8%	41	40
	Flood+Pandemic	317.2	1,194.1	1,511.2	15.7%	49	44
Medium	Flood-Only	634.3	142.1	776.5	8.1%	51	44
	Flood+Pandemic	634.3	1,221.6	1,856.0	19.3%	61	47
Large	Flood-Only	951.5	288.9	1,240.4	12.9%	60	46
	Flood+Pandemic	951.5	1,329.5	2,281.0	23.7%	70	53

Notes:

[a] The direct damage refers to the capital damage due to inundation of physical assets and occurs only in the flooded region C.

[b] The indirect losses are the GDP losses along the global supply chain caused by the compound event. They start from the directly affected regions and spill over to other regions through inter-sectoral and inter-regional dependencies.

[c] Full recovery is achieved when the amount of capital or global GDP in the disaster aftermath is within ±0.1% of the pre-disaster level.

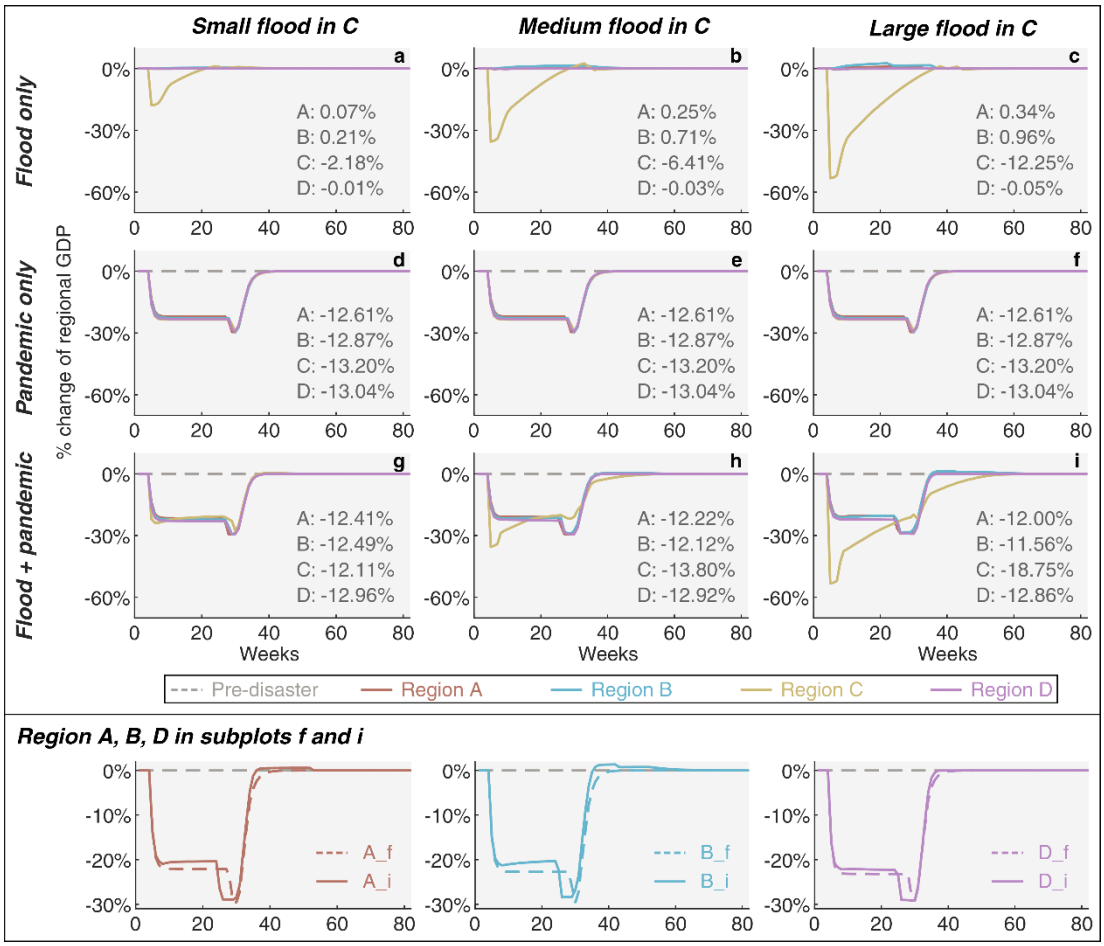

Figure 6-1: Weekly changes of regional GDPs, relative to the pre-disaster levels, in the four regions, under 'flood-only', 'pandemic-only', and 'flood+pandemic' scenarios without trade restrictions.

The numbers in each plot indicate the cumulative losses or gains of regional GDPs over time, relative to the pre-disaster levels of the annual regional GDPs. From left to right, each column represents the small-, medium-, and large-scale flooding in region C. From top to bottom, each row stands for one of the three disaster scenarios: a) flood-only; b) pandemic-only; c) flood+pandemic. The attached row below zooms in on the GDP dynamics of regions A, B, and D in subplots f and i.

6.2.2.2. Pandemic Control in Different Flood Periods with Different Strictness and Duration

In this section, to investigate how the timing, duration, or strictness of pandemic control impacts the economic footprint of the perfect storm, three scenario sets are built: 1) a 30%-24 global pandemic control occurs 7 weeks before flooding; 2) a 30%-24 global pandemic control occurs 7 weeks after flooding; 3) a 60%-8 global pandemic control occurs 7 weeks after flooding. Here the flood hits region C in week 10 and

lasts for 2 weeks on the small, medium, or large scale (Table 6-2). The pandemic control is implemented in all regions.

Table 6-4 and Figure 6-2 summarize the global and regional indirect impacts under these perfect storm scenarios, respectively. Note that this analysis focuses on the indirect or GDP losses rather than the direct damage brought by the perfect storm, as the latter is simply correlated with the scale of flooding. First, it is evident from Table 6-4 that slightly more economic losses are expected when the pandemic control occurs after than before flooding, regardless of the flood scales. The relative losses of global GDP increase by 0.53% (small flood), 0.51% (medium flood) and 0.31% (large flood) when a 30%-24 global pandemic control occurs after than before flooding. On the regional scale, region C suffers the greatest increase in relative GDP losses from the postponement of the pandemic control. For example, the cumulative indirect losses of region C are 19.60% of its annual GDP at the pre-disaster level when a 30%-24 pandemic control takes place 7 weeks before a large flood striking region C (Figure 6-2c). This number rises to 20.22% when the control occurs after flooding (Figure 6-2f). The loss increase of region C is therefore calculated at 0.62%, which is significantly larger than that of region A (0.25%), region B (0.16%), and region D (0.16%). As in Figure 6-2f, the post-flood economic recovery in region C (the yellow line) is curbed by the pandemic control from week 17, suggesting that a subsequent pandemic control has long-lasting impacts on flood-related reconstruction and recovery activities.

Second, it is found that a combination of shorter duration and higher strictness of pandemic control would result in lower economic losses for all regions, regardless of the flood scales. As shown in Table 6-4, the relative losses of global GDP are 14.37% when a 30%-24 pandemic control interfaces with the recovery from a large flood. This number falls to 12.55% when the strictness-duration combination of the control

becomes 60%-8. Similar results are found for the small and medium flood scenarios. The reduction in indirect losses happens across all regions (Figure 6-2g-i). This is consistent with the results of Guan et al. (2020) who studied the global economic costs of COVID-19 control measures in a single-hazard setting. Therefore, an important insight here is that a stricter pandemic control policy for a shorter duration could reduce economic costs when battling both flooding and a pandemic.

Table 6-4: Global indirect impacts, relative to the global annual GDP at the pre-disaster level, of the pandemic control intersecting in different flood periods with different strictness and duration.

Scenarios		Flood scales in region C		
		Small	**Medium**	**Large**
Global pandemic control	**30%-24 control 7 weeks before flooding**	12.43%	12.79%	14.06%
	30%-24 control 7 weeks after flooding	12.96%	13.30%	14.37%
	60%-8 control 7 weeks after flooding	10.50%	11.26%	12.55%

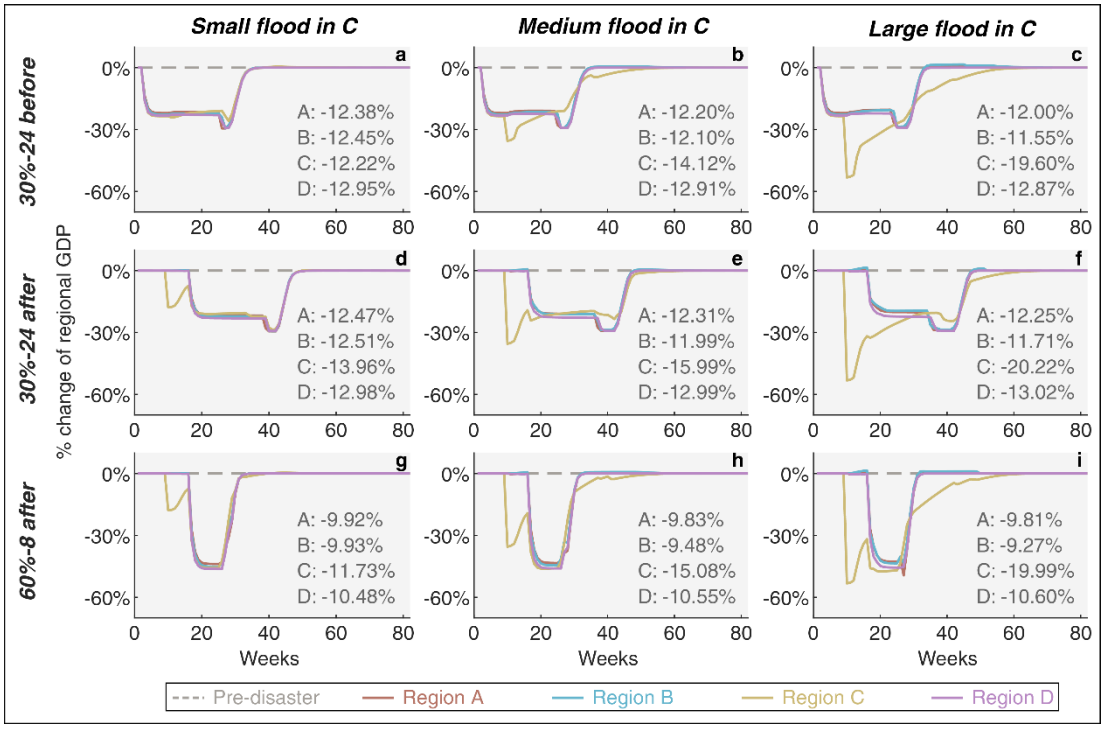

Figure 6-2: Weekly changes of regional GDPs, relative to the pre-disaster levels, in the four regions, when the pandemic control coincides with different flood periods with different

strictness and duration.
The numbers in each plot indicate the cumulative losses or gains of regional GDPs over time, relative to the pre-disaster levels of the annual regional GDPs. From left to right, each column represents the small-, medium-, and large-scale flooding in region C. From top to bottom, each row stands for one of the three perfect storm scenarios: a) a 30%-24 global pandemic control takes effect 7 weeks before flooding; b) a 30%-24 global pandemic control takes effect 7 weeks after flooding; c) a 60%-8 global pandemic control takes effect 7 weeks after flooding.

6.2.3. Influence of Deglobalization on the Magnitude of Economic Losses from the Perfect Storm

This section explores scenarios of triple shocks from flooding, pandemic control, and deglobalization. Global shocks such as the pandemic increase pressures towards deglobalization including the imposition of export restrictions on critical goods, such as medical products and food (Eaton, 2021; Espitia et al., 2020). Export restrictions in one region may push other regions to introduce retaliatory restrictions and trigger a domino effect (World Trade Organization, 2020). The importing regions will suffer if they cannot quickly find alternative trading partners, which relates to the substitutability of the restricted products.

Two groups of scenarios with different cross-regional substitutability of economic production are compared here. First in Section 6.2.3.1, an ideal situation without production specialization is assumed, that is, all products can be replaced by products of the same sector from other regions. It is also assumed that region C, which suffers from the flood, restricts the export of capital manufacturing products (MANK-C) to 'protect' its domestic recovery. The export restriction is applied in parallel with the 30%-24 global pandemic control, which coincides with multi-scales of flooding defined in Table 6-2. The degree of the export restriction, which limits the maximum export volume of the products concerned, is set at 50%. This section also explores the economic effects of different degrees of export restrictions, with results presented in Appendix C.3. Economic Effects of Different Degrees of Export Restrictions in a

Perfect Storm. Next, it is assumed that two weeks later other regions, such as region B, take retaliatory restrictions of the same degree on capital manufacturing products (MANK-B). The indirect economic impacts under the restrictive trade scenarios are compared with the free trade scenario to analyse the role of trade restrictions in disaster recovery under this ideal situation without production specialization. It is worth mentioning that special attention is given to these two 'MANK' sectors as they produce tradable capital products and face increasing demand during the post-flood reconstruction.

Then in Section 6.2.3.2, the study investigates how production specialization, which creates non-substitutable products, influences the economic footprint of the perfect storm together with trade restrictions. It is assumed that the 'MANK-C' and 'MANK-B' sectors make specialized capital products which cannot be substituted elsewhere. The economic consequences under the same restrictive trade scenarios as in Section 6.2.3.1 are compared with the free trade scenario to study how production specialization interacts with trade restrictions during the compound crises. The settings of trade scenarios with or without production specialization are summarized in Table 6-5.

Table 6-5: Settings of trade scenarios.

Trade Scenarios	**Definitions**	**Duration**	**Production Specialization**
Free trade	No export restrictions	-	MANK-C and MANK-B if production specialization exists
Restrictive trade without retaliation	50% reduction of the maximum export volume on MANK-C	24 weeks	
Restrictive trade with retaliation	Same degree of retaliatory restrictions from MANK-B two weeks after the MANK-C restriction	24 weeks for MANK-C; 22 weeks for MANK-B	

Notes: Degree of export restriction refers to the percentage reduction of the maximum export volume relative to the pre-disaster level.

6.2.3.1. Export Restrictions without Production Specialization

As shown in Table 6-6 and the first two rows of Figure 6-3, a 50% export restriction on 'MANK-C' raises the global indirect losses by 0.16%-0.23% during different flood and pandemic intersections. The indirect losses in regions A and D increase by an average of 0.43% and 0.45% respectively, faster than other regions from C's restrictive trade policy. By comparison, region B experiences less loss increase by around 0.17%. It appears that the export restriction on a specific product has moderate impacts on the importing regions when they can easily find a replacement from other exporters.

As for region C itself, it benefits from the export restriction on 'MANK-C' only when the flood is at least the medium scale. On the plus side, the export restriction on 'MANK-C' could prevent outflows of capital products and accelerate domestic reconstruction during the flood aftermath. On the minus side, it may reduce foreign demand for C's products as other regions import and produce less than before. During the small flood, the demand for capital reconstruction is not enough to compensate the reduction in foreign demand and hence higher indirect loss in region C from the export restriction (Figure 6-3a and d). By contrast, a larger flood evokes higher demand for capital reconstruction, which makes the positive impact of the export restriction outweighs the negative one, that is, the backfire effect of restricting the production of other regions. For example, the indirect loss in region C decreases from 18.75% to 18.62% when region C adopts the export restriction during the confluence of the large flood and pandemic control (Figure 6-3c and f).

The study then considers the impacts of a 50% retaliatory export restriction from region B on its 'MANK' sector. As shown in Table 6-6 and the bottom two rows of Figure 6-3, such retaliation adds another 1.30%-1.69% to the global indirect losses comparing to the single 'MANK-C' restriction. At the regional level, regions A and D

are still the most vulnerable to the escalating trade friction, whose cumulative GDP losses increase by an average of 3.22% and 2.57%, respectively, during different flood and pandemic intersections. They also encounter inventory shortages earlier than other regions and themselves as compared to the previous two trade scenarios. By comparison, region B is the least affected by its trade policy, but still goes through an increase by around 0.32% in its indirect losses. This may be partly related to the different levels of trade dependence of the regional economies. Specifically, for regions A and D, their trades with other regions account for around 30% and 31% of their total output, respectively, which are higher than the other two regions. Higher dependence on inter-regional trade increases economic vulnerability when countries impose trade restrictions.

It is worth noting that region C also suffers increasing indirect losses (by around 1.37%) under all flood scales with retaliation from 'MANK-B'. This suggests that it is unwise for region C to initiate trade restrictions in response to the perfect storm if retaliation is expected.

Whether at the global or regional level, the indirect losses increase faster with the 'MANK-B' restriction than the 'MANK-C' restriction, as the former sector is a key node sector in terms of having large trade volumes with other sectors in the economic network. The trade volume with the 'MANK-B' sector reaches 8.2% of the global GDP, ranking the third among all sectors, while that with the 'MANK-C' sector is only 2.7%. The study also investigates how the economic impacts change with the degree of export restriction on 'MANK-C' in Appendix C.3. Economic Effects of Different Degrees of Export Restrictions in a Perfect Storm. The results show that both global and regional indirect losses, except for losses of region C, increase with the degree of export restriction. The indirect losses in region C increase with the degree of export restriction when the flood is at the small scale and decrease with the degree of export

restriction when the flood is at the medium or large scale. The results found in this section is robust with the changing degrees of the export restriction.

Table 6-6: Global indirect impacts, relative to the pre-disaster level of the annual global GDP, of the perfect storm under different trade scenarios without production specialization.

Scenarios		30%-24 pandemic control		
		Small flood	Medium flood	Large flood
Free trade		12.42%	12.71%	13.83%
50% export restriction	**on MANK-C**	12.65%	12.91%	13.99%
	on MANK-C with retaliation from MANK-B	14.34%	14.21%	15.50%

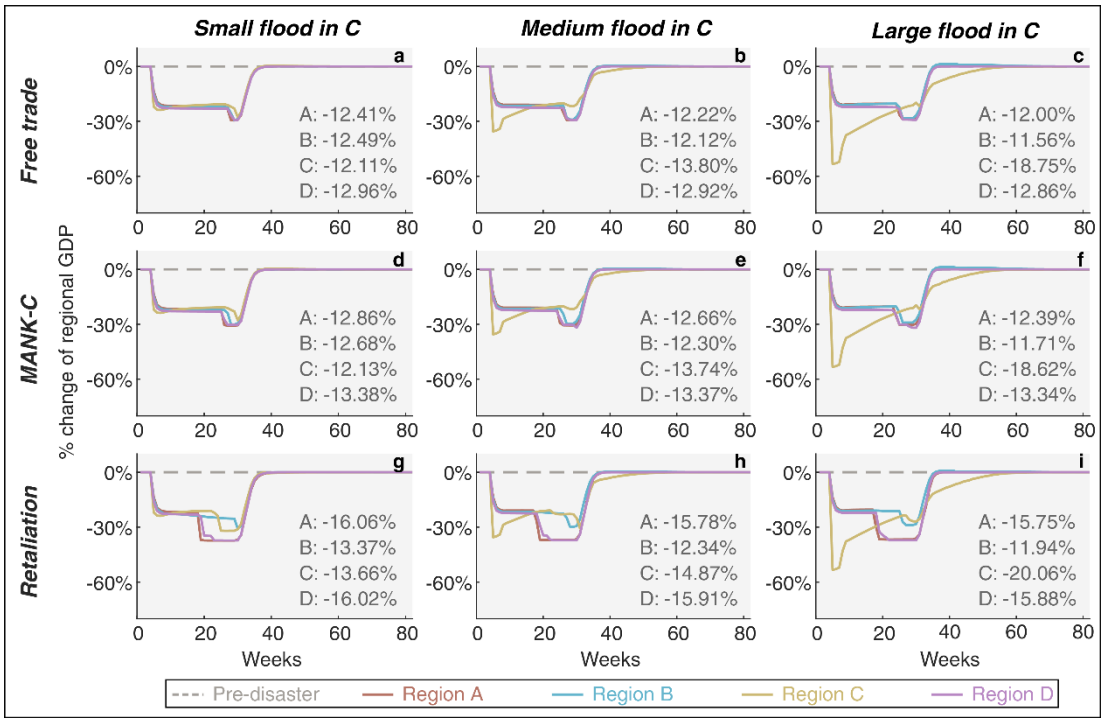

Figure 6-3: Weekly changes of regional GDPs, relative to the pre-disaster levels, in the four regions, when multi-scale floods collide with pandemic control and export restriction without production specialization.

The numbers in each plot indicate the cumulative losses or gains of regional GDPs over time, relative to the pre-disaster levels of the annual regional GDPs. From left to right, each column represents the small-, medium-, and large-scale flooding in region C. From top to bottom, each row stands for one of the three export restriction scenarios: a) free trade scenario without any export restrictions; b) 50% export restriction on product MANK-C; c) 50% export restriction on product MANK-C and 2 weeks later 50% retaliatory export restriction on product MANK-B.

6.2.3.2. Export Restrictions with Production Specialization

Assuming the 'MANK-C' and 'MANK-B' sectors make specialized capital products which cannot be substituted elsewhere, Table 6-7 shows that the 50% restriction on the export of 'MANK-C' increases global indirect losses by 12.10%-12.73% during the confluence of different scales of floods and the 30%-24 pandemic control, and the accompanying retaliatory restriction on the export of 'MANK-B' increases global indirect losses by another 3.44%-4.09%.

When looking into the regional details, Figure 6-4 shows that the indirect losses in regions A, B, and D more than double under the compound scenarios with the export restriction on the non-substitutable 'MANK-C' as these regions cannot find an alternative to refill the inventory shortage. Specifically, their losses are significantly increased by an average of 16.72%, 16.65%, and 15.97%, respectively, of their annual GDPs. This also in turn damages the post-disaster economic performance of region C, by additional ~1.72% of its annual GDP, through the propagation effect of the global supply chain. Secondly, the subsequent retaliation from 'MANK-B' has little extra impact on regions A, B, and D, as their production has been already greatly constrained by the inadequate input of 'MANK-C'. Instead, region C, which encounters ~13.12% increase in the indirect losses, is severely afflicted by the 'MANK-B' retaliation.

Comparing the results in Sections 6.2.3.1 and 6.2.3.2, it is found that production specialization severely aggravates the economic impacts of export restriction when they collide with each other. In general, the export restriction of a region in response to the compound shock always comes at the cost of global economic resilience, while not necessarily promoting its own recovery, notably with insufficient domestic demand, retaliatory actions, and production specialization. Only when the increase in domestic demand suffices to offset the negative impact of the deterioration of the external

economic environment could the region benefit from its restrictive trade policy.

In addition, comparing the two free trade scenarios with or without production specialization in Table 6-6 and Table 6-7, the study finds that the production specialization of 'MANK-C' and 'MANK-B' slightly increases the global losses by 0.01% and 0.46%, respectively, during the medium and large floods colliding with the pandemic control. This indicates that the production specialization, which reduces the cross-regional substitutability of the products concerned, may lead to higher vulnerability of the global economy towards the perfect storm.

Similar with Section 6.2.3.1, the study also examines the sensitivity of economic impacts to the degree of the export restriction on 'MANK-C' with production specialization, and finds robust results that both global and regional indirect losses (including losses in region C) increase with the degree of the export restriction at faster rates than without production specialization (see Appendix C.3. Economic Effects of Different Degrees of Export Restrictions in a Perfect Storm).

Table 6-7: Global indirect impacts, relative to the pre-disaster level of the annual global GDP, of the perfect storm under different trade scenarios with production specialization.

Scenarios		**30%-24 pandemic control**		
		Small flood	**Medium flood**	**Large flood**
Free trade		12.42%	12.72%	14.29%
50% export restriction	**on MANK-C**	24.52%	25.06%	27.02%
	on MANK-C with retaliation from MANK-B	28.61%	29.03%	30.46%

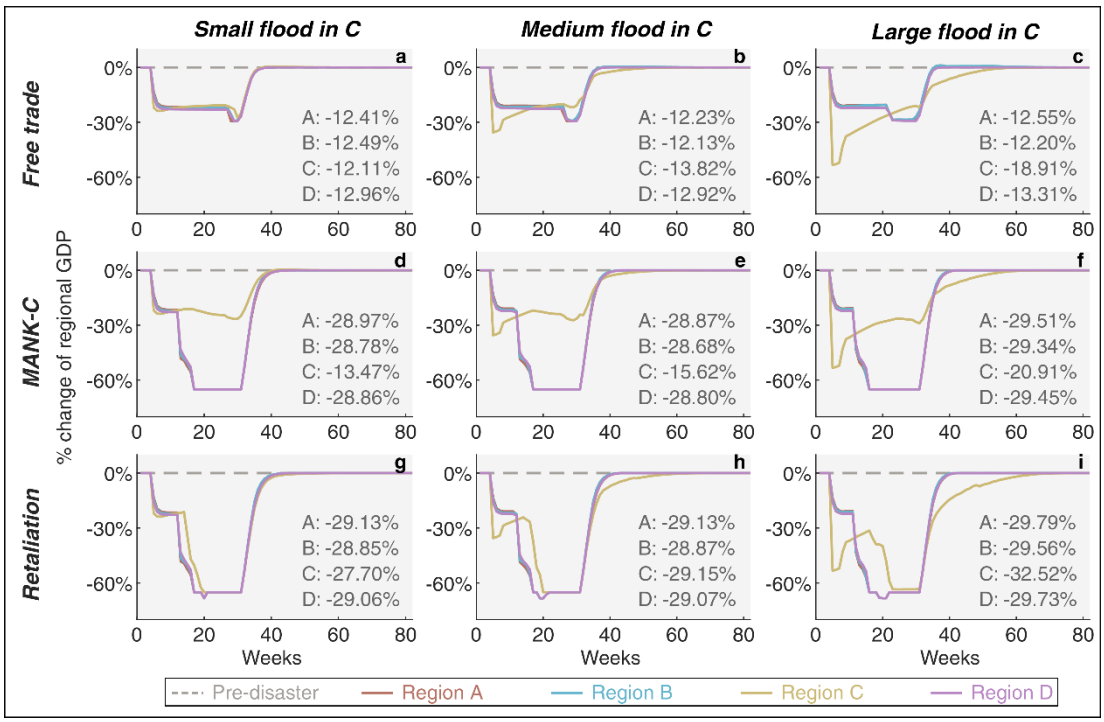

Figure 6-4: Weekly changes of regional GDPs, relative to the pre-disaster levels, in the four regions, when multi-scale floods collide with pandemic control and export restriction with production specialization.

The numbers in each plot indicate the cumulative losses or gains of regional GDPs over time, relative to the pre-disaster levels of the annual regional GDPs. From left to right, each column represents the small-, medium-, and large-scale flooding in region C. From top to bottom, each row stands for one of the three export restriction scenarios: a) free trade scenario without any export restrictions; b) 50% export restriction on product MANK-C; c) 50% export restriction on product MANK-C and 2 weeks later 50% retaliatory export restriction on product MANK-B.

6.3. Sensitivity Analysis

In this section, a sensitivity analysis on key parameters, mainly on inventory and overproduction adjustment, is carried out to check the robustness of modelling results. The study examines how the regional and global indirect impacts (i.e., losses of GDP relative to the pre-disaster levels), caused by a perfect storm, change with these parameters. For simplicity, it only demonstrates a typical compound scenario covering triple shocks, that is, region C, which is hit by a large flood, restricts the export of its 'MANK' sector by 50% and region B imposes retaliatory restriction on the same sector

by the same degree during a 30%-24 pandemic control. The reference results are illustrated in Table 6-6 and Figure 6-3i in Section 6.2.3.1. Here the possibility of production specialization is not considered to avoid extreme simulations which may obscure the variability of results.

Finally, the study examines how economic losses, as well as some main findings, change if a different MRIO table is used to construct the hypothetical global economy. The new MRIO table is obtained from an aggregated 2014 version of GTAP 10 Data Base (Aguiar et al., 2019), still consisting of four regions and the same five sectors. The new table is scaled to keep the global annual GDP the same as in the old table (9613 units), but the proportion that each region accounts for is changed, that is, 24% for region A, 29% for region B, 25% for region C, and 22% for region D (see Appendix Table A7).

6.3.1. Inventory Size

As explained in the methodology part of the CHEFA model (see Section 3.2.4.1), the targeted inventory size of each sector before and after the compound shock is defined by the parameter n_{js}^{i}. Figure 6-5 shows that model results are quite sensitive to this parameter, notably with regions A and D. Increasing inventory size can help improve economic resilience by lowering the risk of inventory shortage amid negative shocks. For instance, the production constraint resulting from an inventory shortage in region A is delayed from week 10 to 31 as the inventory size increases from 2 to 8 weeks, and there is no more such reduction in production when the inventory size is larger than or equal to 10 weeks. Globally, the cumulative GDP losses resulting from the perfect storm decrease from 18.1% to 12.5% as the inventory size increases from 2 to 12 weeks.

Although high inventory levels are beneficial to improving supply chain resilience

towards complex shocks, they have different impacts on inventory costs. Increasing inventory may increase the costs associated with storing inventory but decrease the costs related to ordering and delivering inventory (Mack, 2019). A more thorough cost-benefit analysis of inventory management is needed to find the perfect balance between maximizing resilience and minimizing expenses. Technical progress sometimes can help to address this issue, such as the use of smart information sharing systems based on artificial intelligence, machine learning, and blockchain techniques (Lotfi et al., 2022). The equipment and training of new techniques and systems may be costly in the short term but will eventually increase the resilience and robustness of supply chains at low inventory levels and management costs in the long term.

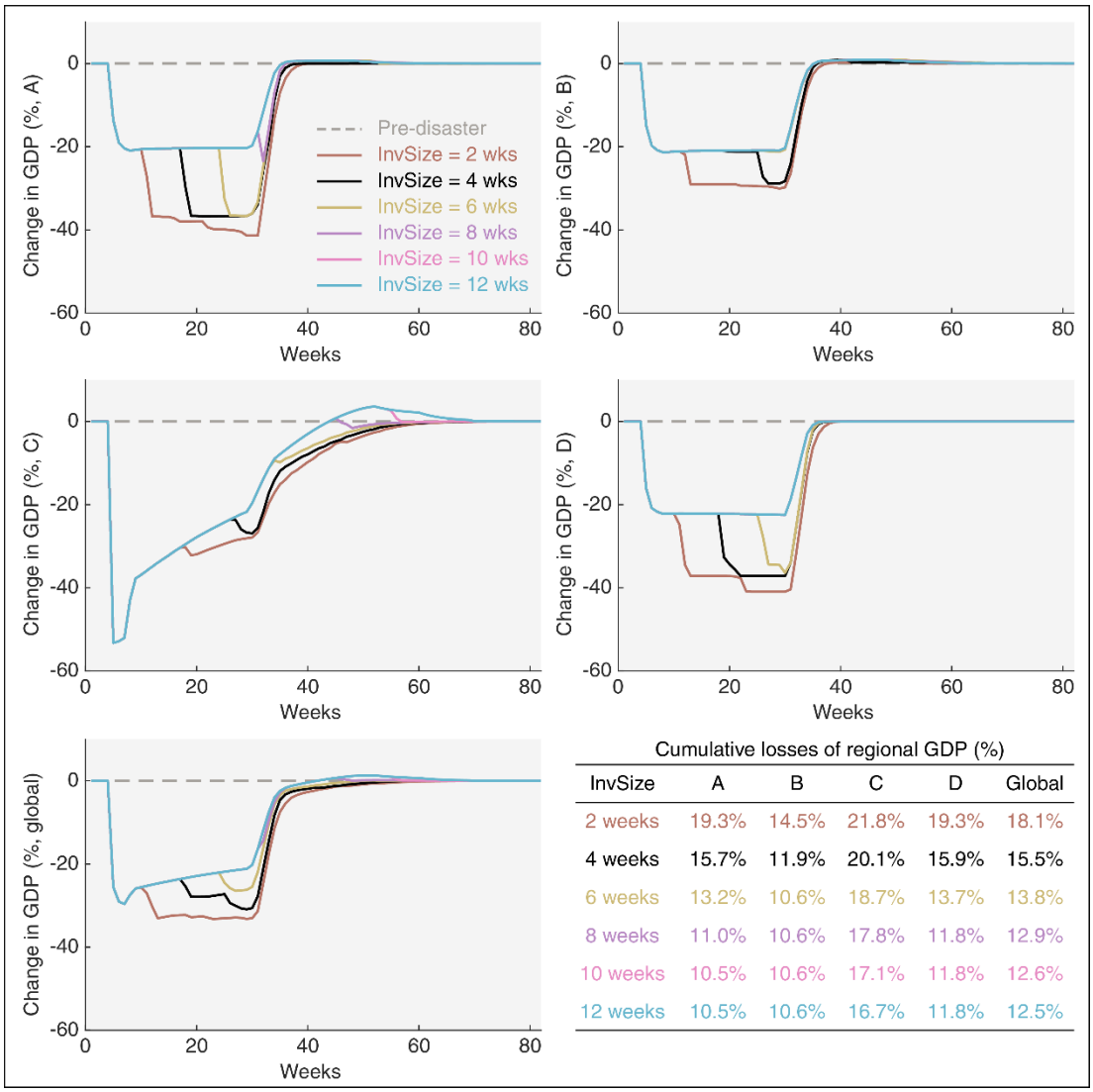

Cumulative losses of regional GDP (%)

InvSize	A	B	C	D	Global
2 weeks	19.3%	14.5%	21.8%	19.3%	18.1%
4 weeks	15.7%	11.9%	20.1%	15.9%	15.5%
6 weeks	13.2%	10.6%	18.7%	13.7%	13.8%
8 weeks	11.0%	10.6%	17.8%	11.8%	12.9%
10 weeks	10.5%	10.6%	17.1%	11.8%	12.6%
12 weeks	10.5%	10.6%	16.7%	11.8%	12.5%

Figure 6-5: Weekly changes in regional and global GDPs, relative to their pre-disaster levels, for the six values of inventory size, during the perfect storm of flooding, pandemic control, and deglobalization.
The first four plots illustrate the robustness of results in regions A, B, C, and D, respectively, and the last plot stands for the global economy. The table at the bottom right presents the cumulative losses of regional and global GDPs, relative to the pre-disaster annual levels, for the six values of inventory size.

6.3.2. Inventory Restoration Rate

In the CHEFA model, a new parameter τ_s is introduced to address the issue of dynamic instability that may occur when sectors attempt to restore their inventory too fast (see Section 3.2.4.1). This parameter describes the proportion of inventory losses that economic sectors try to restore in the next time step, which is a metric indicating the inventory restoration rate. Figure 6-6 illustrates how the regional and global economic losses change with five different values of inventory restoration rate. In general, these losses are less sensitive to the inventory restoration rate than the inventory size. Although lowering the inventory restoration rate may spare more goods for reconstruction and other final demands, it accelerates the occurrence of inventory shortages and finally slows down the whole recovery process. The economic losses in regions A, B, and D grow by roughly 1% when the inventory restoration rate is cut from 1 to 0.2. By contrast, the loss in region C, which is hit by the flood, Is the least sensitive to this parameter, reaching its lowest when the inventory restoration rate is between 0.4 and 0.6.

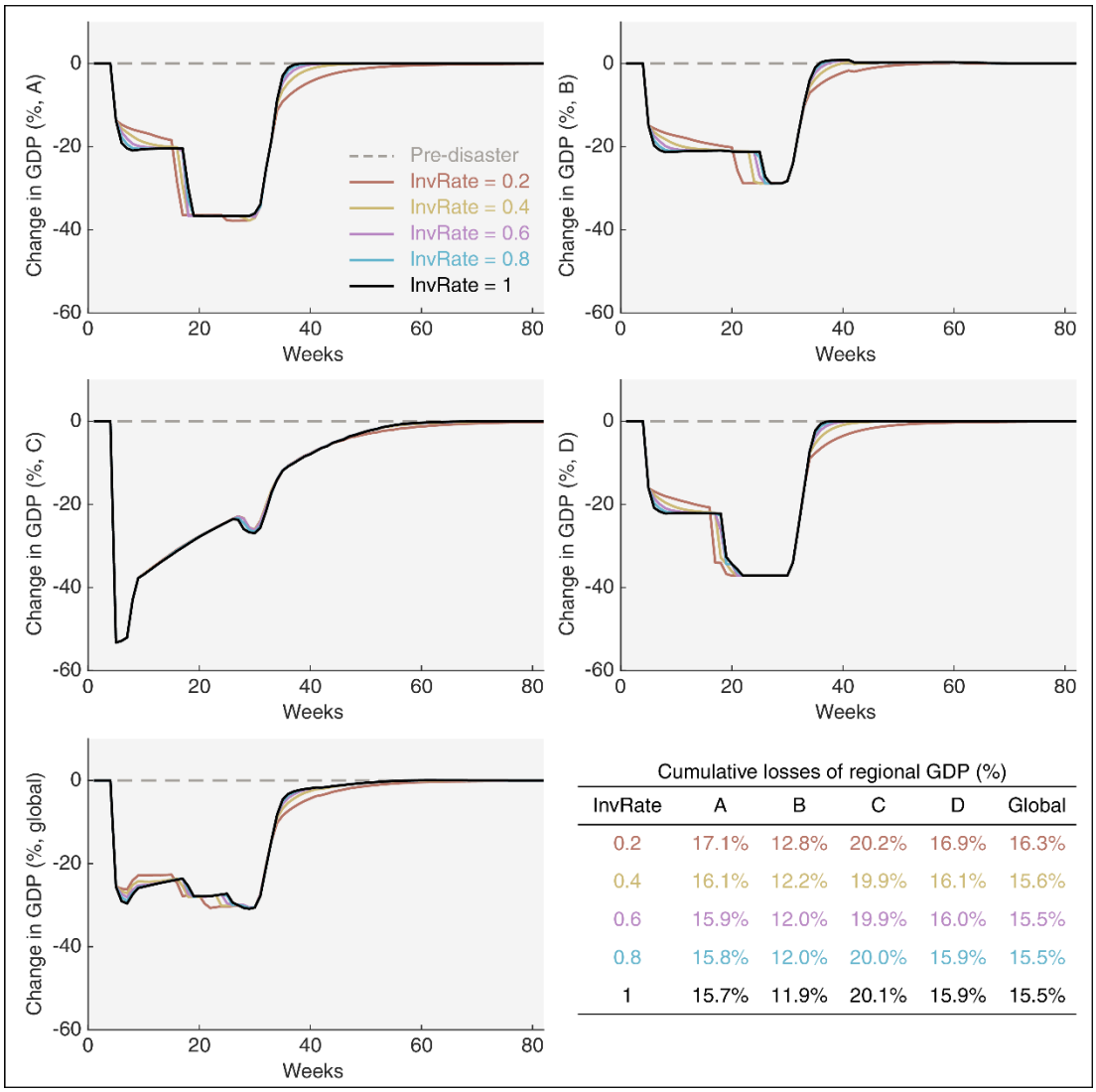

Cumulative losses of regional GDP (%)

InvRate	A	B	C	D	Global
0.2	17.1%	12.8%	20.2%	16.9%	16.3%
0.4	16.1%	12.2%	19.9%	16.1%	15.6%
0.6	15.9%	12.0%	19.9%	16.0%	15.5%
0.8	15.8%	12.0%	20.0%	15.9%	15.5%
1	15.7%	11.9%	20.1%	15.9%	15.5%

Figure 6-6: Weekly changes in regional and global GDPs, relative to their pre-disaster levels, for the five values of inventory restoration rate, during the perfect storm of flooding, pandemic control, and deglobalization.

The first four plots illustrate the robustness of results in regions A, B, C, and D, respectively, and the last plot stands for the global economy. The table at the bottom right presents the cumulative losses of regional and global GDPs, relative to the pre-disaster annual levels, for the five values of inventory restoration rate.

6.3.3. Maximum Overproduction Capacity

As explained in Section 3.2.4.4, the overproduction module describes how economic sectors, particularly those involved in reconstruction, adapt their production capacity to an increasing demand for post-disaster recovery. It introduces two important

parameters: the maximum overproduction capacity $\alpha_{ir}^{\max}$ and the overproduction adjustment time τ_{α}.

This section first examines the result robustness to the first parameter $\alpha_{ir}^{\max}$, which defines the upper limit of overproduction capacity. As shown in Figure 6-7, the economic recovery of region C is much more sensitive to this parameter than that of other regions. This is not surprising as region C is the only region hit by the flood. When the maximum overproduction capacity is large, the production in sectors involved in reconstruction (i.e., the 'MANK' and 'CON' sectors) soars to address the increasing need for reconstruction, which offsets some of the output loss in other sectors. The economic losses in regions A and B also decrease slightly with the increase in maximum overproduction capacity, as some of their products are needed by region C for reconstruction. Globally, the cumulative GDP loss declines from 17.0% to 15.3% when the maximum overproduction capacity increases from 100% (no overproduction) to 150%.

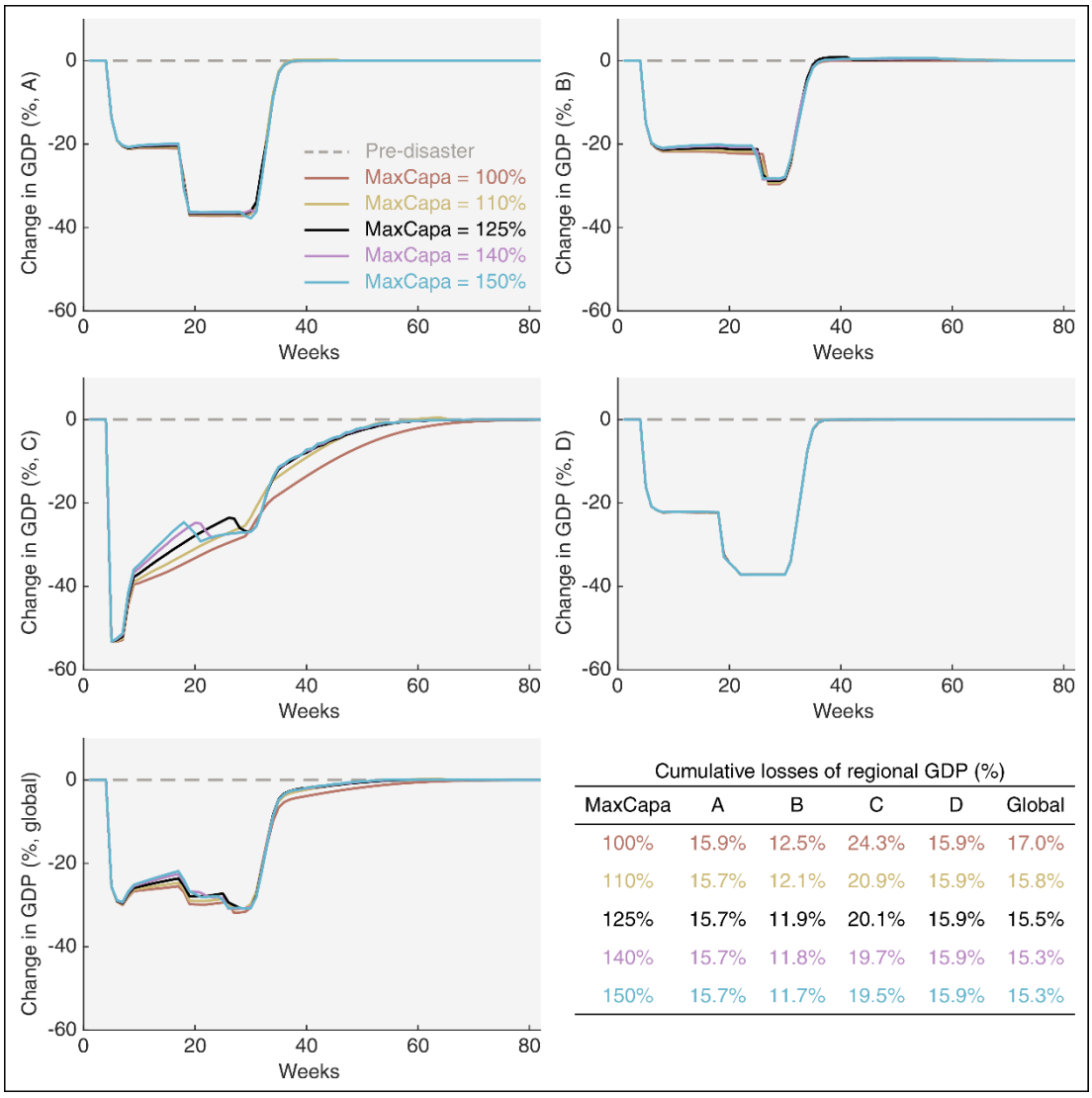

Cumulative losses of regional GDP (%)

MaxCapa	A	B	C	D	Global
100%	15.9%	12.5%	24.3%	15.9%	17.0%
110%	15.7%	12.1%	20.9%	15.9%	15.8%
125%	15.7%	11.9%	20.1%	15.9%	15.5%
140%	15.7%	11.8%	19.7%	15.9%	15.3%
150%	15.7%	11.7%	19.5%	15.9%	15.3%

Figure 6-7: Weekly changes in regional and global GDPs, relative to their pre-disaster levels, for the five values of maximum overproduction capacity, during the perfect storm of flooding, pandemic control, and deglobalization.

The first four plots illustrate the robustness of results in regions A, B, C, and D, respectively, and the last plot stands for the global economy. The table at the bottom right presents the cumulative losses of regional and global GDPs, relative to the pre-disaster annual levels, for the five values of maximum overproduction capacity.

6.3.4. Overproduction Adjustment Time

Here the influence of the second parameter, overproduction adjustment time τ_α, in the overproduction module on disaster-induced economic losses is assessed. This parameter describes the time (in weeks) needed for economic sectors to achieve their

maximum overproduction capacity. The results are presented in Figure 6-8. Compared with the previous section, the economic losses are less sensitive to overproduction adjustment time than maximum overproduction capacity. This is consistent with the results of the sensitivity analysis in Hallegatte (2008), which concludes that the overproduction adjustment time does not matter much in post-disaster economic recovery. Nevertheless, the economic loss in region C is still more sensitive than other regions and shows an upward trend as the adjustment time increases. This is because the adjustment time is essentially an inverse of the adjustment speed. When sectors need more time to reach their maximum overproduction capacity, their production climbs at smaller steps each time after the shock, leading to a slower recovery and more economic losses.

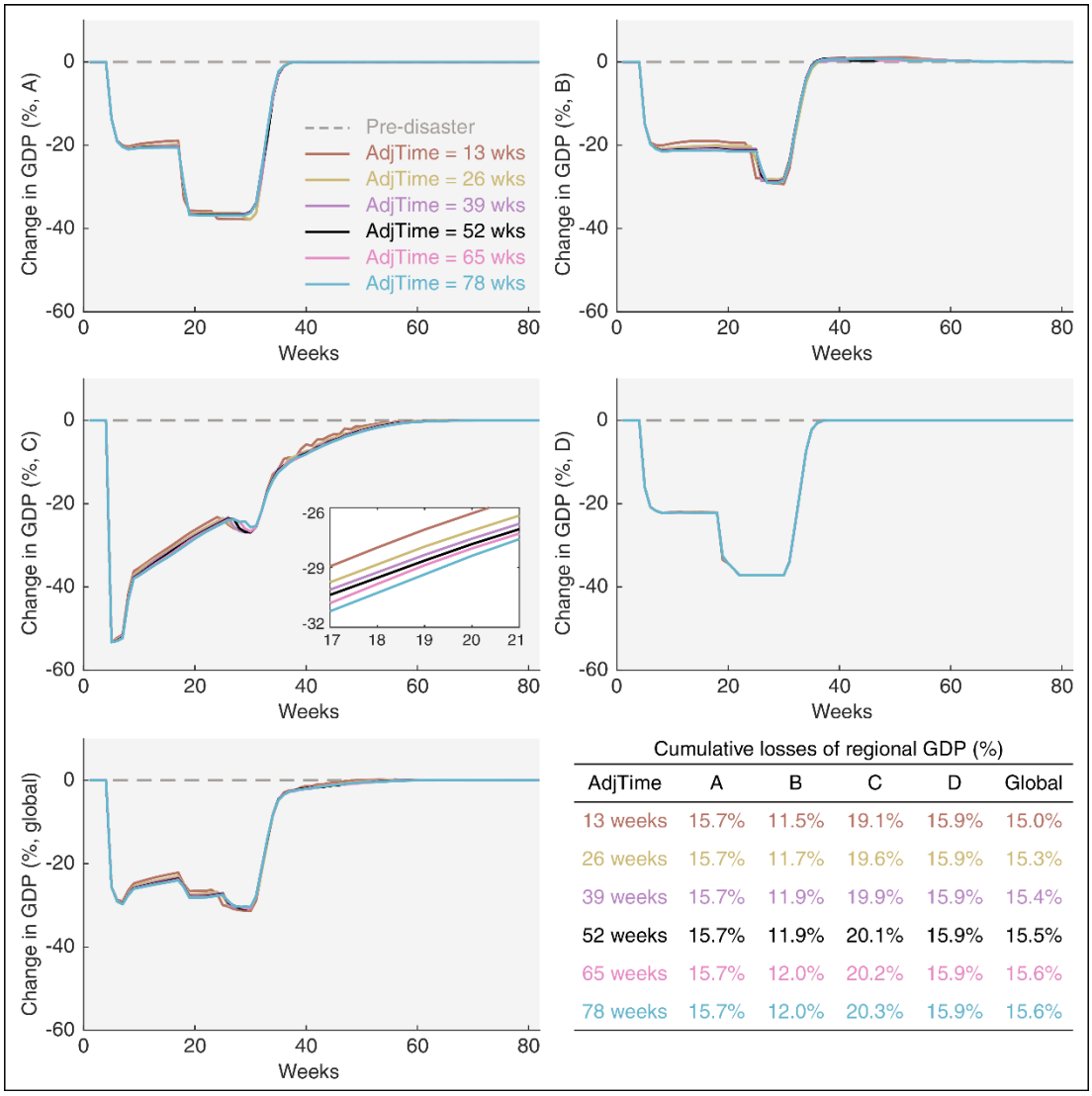

Cumulative losses of regional GDP (%)

AdjTime	A	B	C	D	Global
13 weeks	15.7%	11.5%	19.1%	15.9%	15.0%
26 weeks	15.7%	11.7%	19.6%	15.9%	15.3%
39 weeks	15.7%	11.9%	19.9%	15.9%	15.4%
52 weeks	15.7%	11.9%	20.1%	15.9%	15.5%
65 weeks	15.7%	12.0%	20.2%	15.9%	15.6%
78 weeks	15.7%	12.0%	20.3%	15.9%	15.6%

Figure 6-8: Weekly changes in regional and global GDPs, relative to their pre-disaster levels, for the six values of overproduction adjustment time, during the perfect storm of flooding, pandemic control, and deglobalization.

The first four plots illustrate the robustness of results in regions A, B, C, and D, respectively, and the last plot stands for the global economy. The table at the bottom right presents the cumulative losses of regional and global GDPs, relative to the pre-disaster annual levels, for the six values of overproduction adjustment time.

6.3.5. A Different MRIO Table

This section uses a different MRIO table (Appendix Table A7), which is an aggregation of the 2014 version of GTAP 10 Data Base (Aguiar et al., 2019), to construct the hypothetical global economy of four regions and five sectors and explore how the main findings of this study will change.

First, Table 6-8 summarizes the global economic losses resulting from flooding, pandemic control, and their compounds, respectively, without trade restrictions for the GTAP MRIO table. Comparing with the reference MRIO table used in Section 6.2, the GTAP MRIO table results in lower economic losses under the 'pandemic-only' scenario, but more than doubles the direct damage of floods at various scales (see Table 6-8 and Table 6-3). This is because the GTAP MRIO table implies a higher capital intensity in the same amount of GDP than the reference table used in Section 6.2. This also incurs higher indirect losses and correspondingly longer recovery time. However, the ratios of indirect to direct impacts of flooding, ranging from 0.12 to 0.38 in Table 6-8, stay close to the results in Table 6-3.

Table 6-8: Global economic footprint under the 'flood-only', 'pandemic-only', and 'flood+pandemic' scenarios without trade restrictions for GTAP MRIO table.

Scenarios		**Direct damage**	**Indirect losses**	**Total impacts**	**% of global annual GDP**	**Capital recovery weeks**	**GDP recovery weeks**
Pandemic-only		0.0	1,150.2	1,150.2	12.0%	-	40
Small	flood-only	748.0	91.7	839.8	8.7%	81	60
	flood+pandemic	748.0	1,138.5	1,886.5	19.6%	90	68
Medium	flood-only	1,496.0	386.1	1,882.1	19.6%	122	92
	flood+pandemic	1,496.0	1,385.9	2,881.9	30.0%	132	100
Large	flood-only	2,244.0	852.6	3,096.6	32.2%	160	125
	flood+pandemic	2,244.0	1,843.5	4,087.5	42.5%	168	131

Besides, it is obvious from Table 6-8 that similar findings on the interaction between flooding and pandemic control (see Section 6.2.2.1) can be elicited with the GTAP MRIO table. On the one hand, a global pandemic control will extend the recovery time of capital damaged by flooding, and therefore exacerbate its economic consequences. On the other hand, flood responses can sometimes alleviate the negative impacts of pandemic control due to the stimulus effect of post-flood reconstruction, but this only

happens when the flood damage is small. If the flood damage is large enough to exceed the reconstruction stimulus, then the pandemic impacts will be aggravated.

Second, the study then examines the results related to pandemic control in different flood periods with different strictness and duration. As shown in Table 6-9, a pandemic control occurring after flooding leads to slightly more economic losses than it before flooding, and a stricter but shorter pandemic control is conducive to mitigate the negative impacts of the compound crises. These findings are consistent with those using the reference MRIO table in Section 6.2.2.2.

Table 6-9: Global indirect impacts, relative to the global annual GDP at the pre-disaster level, of the pandemic control intersecting in different flood periods with different strictness and duration for GTAP MRIO table.

Scenarios		**Flood scales in region C**		
		Small	**Medium**	**Large**
Global pandemic control	**30%-24 control 7 weeks before flooding**	11.97%	14.47%	19.22%
	30%-24 control 7 weeks after flooding	12.14%	14.62%	19.36%
	60%-8 control 7 weeks after flooding	10.09%	12.73%	17.61%

Third, the study explores the role of export restriction in the economic footprint of a perfect storm for the GTAP MRIO table. Table 6-10 presents the changes in cumulative GDP losses, both on the regional and global scales, by different export restriction scenarios without production specialization. The first row sets the free trade scenario when there are no export restrictions and thus no changes in the losses resulting from the compound crises. The second row assumes that region C imposes a 50% restriction on the exports of its MANK sector to 'protect' its post-flood reconstruction. The results show that all regions except C suffer loss increases to various extents due to the restriction. Region C, in particular, is the only region that benefits from the restriction under all flood scales. This is because that the flood-induced capital damage is large

with the GTAP MRIO table at all flood scales, making the economic stimulus from the reconstruction demand outpace the negative impact of export declines. The third row presents the loss changes from the 'MANK-C' restriction scenario to an escalating scenario including B's retaliation. This time, region C also suffers increased losses of an average of 1.37%, which exceeds the economic gains of its own restriction and leads to a net increase in its GDP losses by 1.29%. In addition, the loss of region B falls by 0.7%, back to the loss level of the free trade scenario. This may in turn enhance the motivation of region B to take retaliatory measures, which supplements the results using the reference MRIO table in Section 6.2.3.1.

Table 6-10: Changes in cumulative GDP losses, on regional and global scales, by escalating export restrictions without production specialization for GTAP MRIO table.

Scenarios		**Region A**	**Region B**	**Region C**	**Region D**	**Global change**
Free trade		0.00%	0.00%	0.00%	0.00%	0.00%
Export restriction	MANK-C	0.33%	0.70%	-0.08%	1.18%	0.53%
	MANK-C, MANK-B	0.24%	-0.70%	1.37%	0.57%	0.32%

Notes: The cumulative GDP losses are in relative terms of the annual GDPs at the pre-disaster levels. Results in each row are the loss changes compared to the scenario of the previous row. The results are given as the ensemble mean of scenarios where different scales of floods collide with a 30%-24 pandemic control.

Finally, the study considers the effect of production specialization in the context of deglobalization. Table 6-11 is similar with Table 6-10, except that all scenarios are simulated under the assumption that the 'MANK-B' and 'MANK-C' sectors make specialized goods which cannot be substituted elsewhere. The loss changes in the first row, which reflects the role of production specialization under the free trade scenario, are obtained by comparing with the free trade scenario without production specialization (i.e., the first row in Table 6-10). It is obvious that the specialization itself raises the vulnerabilities of both regional and global economies to the compound crises. From the second row, it is found that the export restriction of region C on a specialized product triggers much severer economic losses to other regions, which in

turn makes region C also suffer more losses through the propagation effect of the supply chains. The third row tells that the retaliation from another region and sector would trap region C, which initiates the trade war, into further losses, and ultimately slow down the global recovery. These results are consistent with those using the reference MRIO table in Section 6.2.3.2.

Table 6-11: Changes in cumulative GDP losses, on regional and global scales, by escalating export restrictions with production specialization for GTAP MRIO table.

Scenarios		**Region A**	**Region B**	**Region C**	**Region D**	**Global change**
Free trade		0.24%	0.37%	0.36%	0.26%	0.31%
Export restriction	MANK-C	14.46%	17.13%	2.27%	15.77%	12.52%
	MANK-C, MANK-B	0.17%	0.17%	6.76%	0.20%	1.80%

Notes: The cumulative GDP losses are in relative terms of the annual GDPs at the pre-disaster levels. Results in each row are the loss changes compared to the scenario of the previous row, while those in the first row are compared to the free trade scenario without production specialization. The results are given as the ensemble mean of scenarios where different scales of floods collide with a 30%-24 pandemic control.

Overall, despite higher flood-induced direct damages and stronger retaliatory motivation towards trade restrictions, switching to the GTAP MRIO table has not changed the main findings of this study about the economic interplay between flooding and pandemic control, or about the roles of trade restriction and production specialization in the economic footprint of a perfect storm.

6.4. Discussion and Conclusions

This chapter applies the CHEFA model to simulate the economic footprint of a pandemic-induced perfect storm, taking the collision of flooding, pandemic control, and export restrictions as an example. The CHEFA model improves the standard ARIO model, which is commonly used in single-hazard impact analysis, by considering the interplay between different types of hazardous events for the first time. It also

incorporates the possibilities of cross-regional substitution and production specialization, which have opposite impacts on the substitutability of suppliers of the same sector from different regions and thus the economic resilience towards a perfect storm and estimates of the economic consequences. In this chapter, various scenario sets are built to test the robustness of the CHEFA model on a hypothetical global economy of four regions and five sectors. These scenarios are designed to investigate how the economic impacts of the perfect storm react to 1) the timing, strictness, and duration of the pandemic control; 2) the export restrictions imposed on specific sectors and regions; and 3) the presence of specialized production. The latter two special scenarios sets are included here as a reflection on the ongoing deglobalization.

Two major conclusions can be drawn from the simulation results. The first conclusion is about the economic interplay between pandemic control and flood responses in a free trade global economy. On the one hand, a global pandemic control aggravates the flood impacts by hampering the post-flood capital reconstruction. This confirms the idea from an economic perspective that restrictions targeted at virus containment result in inadequate flood responses, aggravating the flood impacts (Ishiwatari et al., 2020; Selby and Kagawa, 2020; Swaisgood, 2020). On the other hand, a flood disaster exacerbates the pandemic impacts only when the flood damage is large enough to exceed the stimulus effect from the flood-related reconstruction activities. The flood disaster would accelerate and extend the shortage of inventories brought by the pandemic control and increase the negative impact on GDP. Its related reconstruction demand, however, could stimulate regional recoveries, which is also confirmed by Koks and Thissen (2016), and alleviate to some extent the negative impact of the pandemic control.

Here two suggestions are made regarding pandemic intervention with flood disasters under the free trade scenarios. First, an early pandemic intervention is advocated to

reduce the economic footprint when the pandemic outbreak is colliding with flood disasters. The results of this chapter show that the pandemic control taking place after flooding leads to severer economic impacts than the control implemented before flooding, mainly due to a longer-lasting disruption of the post-flood recovery. Second, a stricter but shorter pandemic control strategy is also suggested. By comparing the impacts of a 30%-24 pandemic control with a 60%-8 pandemic control applied intermittently in the recovery period of multiple scales of flooding, the study discovers that the latter one results in less economic losses in all regions. This is in line with one of the major insights provided by Guan et al. (2020).

The second conclusion refers to the role of trade or deglobalization in the economic footprint of compound risks. When the increasing trade barriers intertwines with the collision between flooding and pandemic control, it creates a triple perfect storm. In general, a region implementing export restriction is always at the cost of global economic recovery, whether itself benefits from this policy or not. Although the export restriction prioritizes domestic needs for post-disaster recovery, it does not necessarily mitigate the economic losses of the region if the stimulus of the surge in domestic demand cannot overtake the negative impact of the decline in exports. For other regions, those with high trade dependence would be more vulnerable to the export restriction and suffer faster increases in indirect losses.

For another, specialization, which leads to the concentration of key sectors in particular regions and limits the possibilities for substitution, may sometimes delay economic recovery and raise the vulnerability of the economic network to such compound risks. The export restriction imposed on the non-substitutable specialized sector in a region, would put other regions at higher risks with significant surges in economic losses. This may also backfire at the economic resilience of the region itself through the propagation effect of the global supply chain.

The introduction of trade restrictions may also push other regions to make retaliatory movements, which further deteriorate the global recovery and make everyone lose. Among all the regions, the region which initiates the trade war loses much more when the retaliatory restriction is also imposed on a non-substitutable product. The collision of export restriction and production specialization, particularly with the expectation of retaliation, can trigger devastating impacts on the global economy at a time when it is already heavily burdened by tackling the compound hazards of extreme weather events and pandemic control.

Therefore, regional or global cooperation is advocated to ease the negative impacts of deglobalization, at least rigorous trade policies that avoid highly specialized sectors are required confronting a perfect storm. Policies that lead to higher trade barriers undermine the efforts of other countries battling extreme weather events and a pandemic. The use of trade restrictions has a particularly deleterious impact in a world with production specialization in key sectors, raising the need for effective discipline at the global level of the use of such measures.

Beyond these policy implications, the CHEFA model has demonstrated its flexibility in this chapter addressing various compound-hazard scenarios and can help governments refine their emergency policies by identifying the potential positive or negative externalities on wider economic systems. This could be used to guide regional or global cooperation in mitigating such spillover effects of the compound shocks, particularly in the context of deglobalization. The research also highlights the importance of an integrated approach in managing the compound risks. By utilizing the CHEFA model, decision makers can grasp a better view of the economic interlinkages between multiple hazards which ultimately develop into a perfect storm. Knowing the constraints from one hazard while responding to another assists the

formation of a balanced strategy which can minimize the economic losses from the trade-offs between emergency response and pandemic control.

Finally, the CHEFA model provides consistent and comparable loss metrics with that of single-hazard analysis, as it is based on the popular ARIO model in this field. One of the commonly used metrics should be the ratio of indirect to direct economic impacts resulting from a disaster, the so-called cascading effect indicating the resilience of the supply chain towards the disruption (Mendoza-Tinoco et al., 2020). In this analysis, the indirect/direct ratio is 0.16-0.30 for the flood of multiple scales. This is close to the estimate (0.17) of Hallegatte (2014) for the Hurricane Katrina, but lower than that (0.39) of Hallegatte (2008) for the same event. This is because this analysis and that of Hallegatte (2014) both consider a certain level of substitutability and inventory dynamics that improves the economic resilience. Under the compound scenarios, this ratio soars up to 1.27-3.93 with the intervention of pandemic control, further to 1.41-4.35 with export restrictions on substitutable products, and ultimately to 2.73-8.67 when the restrictions are imposed on specialized non-substitutable products. The CHEFA model will facilitate future comparisons between various compound or single hazards under a similar methodological framework.

Nevertheless, the CHEFA model used here is limited by not considering technical progress and is relevant for a short-term time scale, where the production patterns of economic sectors do not shift significantly. This outlook explains why the study only considers the substitution between intermediate inputs of the same kind from different regions, rather than the substitution between different types of inputs. Moreover, the CHEFA model used in this chapter follows the assumption in Hallegatte (2008) that capital damage will all be repaired and that the insurance companies will pay the whole repair cost. The crowding-out effects of the reconstruction costs on household consumption will be researched in the following chapter (i.e., Chapter 7). In addition,

the event settings for flooding, pandemic control, and export restriction in each scenario are simple abstractions of reality, which only characterizes their economic features. The study does not distinguish their differences in other aspects in the warning, impact, and response phases, but focuses on their interconnections in economic risk transmission. Admittedly, there are other kinds of interactions between natural and biological hazards, but it is beyond the research scope of this chapter to model all these factors. For one thing, some response measures towards flooding, such as evacuation and displacement, could increase the number of people exposed to the pandemic and the burden on the healthcare system. For another, some pandemic mitigation measures like testing, therapeutics, and vaccines may benefit the economic recovery in complex situations. The health-related interactions and the accompanying economic consequences will be incorporated into future studies.

Chapter 7 Economic Impacts of the 2021 Zhengzhou 'Flood-COVID' Compound Event in China

The outcomes of this chapter have been published in a Chinese paper co-authored by Lili Yang and Dabo Guan. Yixin Hu is responsible for data collection, impact modelling, result interpretation, and drafting. The sections in this chapter have been reproduced under the permission of co-authors.

Hu, Y., Yang, L., & Guan, D*. (2022). Assessing the economic impact of "natural disaster-public health" major compound extreme events: a case study of the compound event of floods and COVID epidemic in Zhengzhou China (in Chinese). *China Journal of Econometrics, 2*(2), 257-290. https://doi.org/10.12012/CJoE2021-0090

The purpose of this chapter is to fulfil Research Objectives 5 and 6, which are the empirical application of the CHEFA model for the compound-hazard impact analysis (see Section 3.2) and the exploration of factors influencing the compound resilience of the economic system. This contributes to Research Questions 3 and 4 raised in Section 1.4.1. In this chapter, the CHEFA model is applied to assess the overall economic impacts of a real case, namely the compound event of extreme floods and a COVID-19 wave in the Zhengzhou city of China in the summer of 2021. From July 17 to 23, 2021, Central China's Henan Province was hit by unprecedented heavy rainfalls and massive floods, and its capital city Zhengzhou suffered heavy casualties and property damage. The event has been listed as the deadliest natural disaster in 2021 in China. The situation was worsened in Zhengzhou by a local COVID-19 wave a week later, which affected the progress of post-flood recovery and compounded climate risks. This chapter investigates how such compound shocks propagate through the cross-regional

supply chains, as well as the factors that influence economic resilience in the aftermath. The results indicate that: (1) most of the economic impacts are found within Zhengzhou with non-metallic mineral products and food and tobacco sectors suffering the largest indirect economic losses. These two sectors also have the strongest propagation effects through the supply chain; (2) the pandemic risks during the post-flood recovery period in Zhengzhou have exacerbated the total indirect economic losses by 77% and reshaped the spatial and sectoral distribution of the economic footprint; (3) the post-disaster economic resilience is most sensitive to factors such as road recovery rate, reconstruction efficiency and consumption subsidies, and COVID-19 control tends to reduce the marginal economic benefits of flood emergency efforts. In combination these results suggest that the government should consider the balance between disaster relief, COVID-19 control and economic recovery in response to compound hazards: for one thing, the emergency response and reconstruction activities should progress in accordance to the dynamic requirements of COVID-19 control; for another, taking into account the regional economic characteristics such as industrial structure and saving preference, the recovery of key-node sectors in basic industries should be given the priority in terms of reconstruction funds and technical support, subsidies for production and consumption should be allocated accordingly and flexibly, so as to boost the regional economy in the disaster aftermath.

Note that the health impacts are not modelled in this study. The wave of COVID-19 is simply proxied by the corresponding control measures taken to stop virus transmission, and its severity is linked to the strictness and duration of the control required. All monetary values in this chapter are given in 2021 CNY values.

7.1. Introduction

The year 2021 was a year of frequent meteorological disasters for China. Events

included sandstorms in Beijing, tornadoes in Wuhan, torrential rains in Zhengzhou, high temperatures in the south, extreme precipitation in Shanxi. Climate change is driving the occurrence and magnitude of extreme weather events, globally and in China (Wang, 2021). In parallel, due to the ongoing mutations and global spread of COVID-19, China is constantly faced with the risk of case surges in many places. The confluence of pandemic risks and natural disasters poses great challenges to the emergency management system in China (Zhao, Hu, et al., 2021). For example, after the extreme rainstorm and flooding on July 20, 2021, in Zhengzhou, a wave of COVID-19 struck the city immediately, leading to the suspension of post-flood recovery[16] (Figure 7-1). In such a complex situation of flooding and a COVID-19 wave, lockdown measures to contain the spread of the virus have made the flood control and disaster relief more difficult, which delayed the processes of post-flood reconstruction and production restoration and might result in additional economic losses. With climate change and continued COVID-19 pandemic, the co-occurrence of natural disasters and public health emergencies will appear more frequently (Phillips et al., 2020).

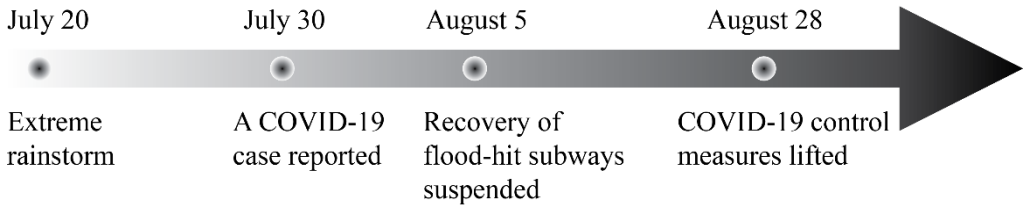

Figure 7-1: Timeline of the compound event of Zhengzhou's extreme floods and a COVID-19 wave in 2021.

As noted in the literature review (Chapter 2), the economic impacts of disaster events include direct and indirect ones: the former refers to the monetary values of human

[16] For example, after the flood, the no-load operation of Zhengzhou Metro was suspended due to COVID-19 control. Please see the webpage: http://sina.com.cn/news/2021-08-05/detail-ikqcfncc1154105.shtml.

and physical assets directly damaged by the disaster[17], while the latter refers to the changes of output or added value in wider regions and sectors due to the business interruptions caused by direct impacts and the imbalances between supply and demand in the supply chain (Koks and Thissen, 2016; Mendoza-Tinoco et al., 2017). Although direct impacts of disasters usually draw more attention because of their explicitness, indirect economic impacts can better depict the spread or footprint of disaster shocks along the production supply chain on both the temporal and spatial scales, and thus should not be ignored (Avelino and Dall'Erba, 2019; Carrera et al., 2015). Especially, when natural disasters (e.g., floods) and public health emergencies (e.g., pandemics) collide, the formation mechanism of indirect economic impacts becomes more complicated. In this situation, economic production is not only faced with capital constraints caused by natural disasters, but also limited by insufficient labour supply due to pandemic control (Brinca et al., 2021; Guan et al., 2020). The transportation bans due to pandemic control may further disrupt the production supply chain and cause shortages of industrial inventories (Ivanov, 2020; Nikolopoulos et al., 2021). Customers may also change their consumption behaviours in response to the compound-hazard events, which is another reason for the fluctuation of economic output (Cox et al., 2020; Hallegatte, 2008). In fact, in some countries, COVID-19 control measures are aggravating the socio-economic consequences associated with natural disasters (Walton et al., 2021).

In addition to the complexity of the impact mechanism, the combination of natural disasters and public health emergencies also poses great challenges to the rebuilding of post-disaster economic resilience. Economic resilience refers to the ability of the economic system to recover from disasters, which can be quantified by indirect economic losses accumulated during the post-disaster economic recovery (Zhang, Li,

[17] For instance, the life and health costs of casualties, the market values of impacted crops, the reconstruction costs of collapsed houses, and the maintenance or replacement costs of damaged equipment.

Feng, et al., 2018). Economic resilience is found to be closely related to the regional capacity of emergency management and investment of emergency funds (Shi, 2005). During the risk of compound disasters, large-scale natural disaster emergency and response activities, such as road repairing, house reconstruction, injury treatment, etc., may accelerate the spread of the virus; however, if the efficiency of emergency relief is reduced by pandemic control, the recovery time after the disaster may be prolonged, resulting in more economic losses (Ishiwatari et al., 2020; Salas et al., 2020). In addition, at the financial level, Mahul and Signer (2020) pointed out that simultaneously confronting two types of hazards may deplete the financial budgets or contingent financing arrangements. Therefore, it is necessary to formulate an efficient emergency fund allocation and utilization scheme to boost financial preparedness for compound hazards (ibid.). The mutual constraints between disaster emergency and pandemic control will reshape the post-disaster economic resilience in unexpected ways. A key concern in the risk management of compound disasters and in governance is how to balance disaster relief, pandemic control and economic goals.

Current studies on compound hazards mostly focus on the management or governance level, while the quantitative evaluation of their economic impacts or resilience is still scarce (see Section 2.3 for a literature review on compound hazards). Faced with the increasing possibility of compound hazards and a series of complex problems thereby, it is necessary to develop an interdisciplinary and multi-sectoral model to systematically assess the overall economic impacts of compound events and provide quantitative basis for post-disaster reconstruction and recovery policies (Phillips et al., 2020).

Against this backdrop, this chapter uses the CHEFA model developed in this thesis to assess the economic impacts of the 2021 compound event of extreme flooding and a COVID-19 wave in Zhengzhou, China. Both the direct and indirect disaster footprints

are traced, through the backward and forward propagation effects along the production supply chain, from the affected city of Zhengzhou, to the province of Henan, in which the city is located, and finally to the national level. A series of sensitivity analyses is carried out to examine how factors such as COVID-19 control, flood recovery, and financial aid, would influence the post-disaster economic resilience. This study represents the first multi-city-level assessment of direct and indirect economic impacts of compound-hazard events in China, using field measurement flood data and the first Chinese city-level MRIO table. The objective is to enhance public understanding of compound hazard impacts and inform public policies to boost preparedness for future risks.

7.2. Data and Model Parameters

The flood-induced direct damages are estimated at the 300 metre spatial resolution for four land use types (i.e., residential, agricultural, industrial, and commercial land) in Zhengzhou, using the China-specific depth-damage functions developed by Huizinga et al. (2017) (see methods described in Section 3.1.1.1). Damage to agricultural, industrial, and commercial land sectors are then disaggregated into the corresponding sub-divided economic sectors in proportion to the sectoral capital stock. The CHEFA model developed in Section 3.2 can evaluate the indirect economic footprint of the Zhengzhou compound-hazard event using inputted damage data from the residential and industrial productive capital, as well as information on local COVID-19 controls or lockdowns.

Note that this study does not consider the health impacts of COVID-19, which is similar with Chapter 6. The wave of COVID-19 in the 2021 Zhengzhou compound event affected the economy mainly through a reduction in labour supply due to strict traffic restrictions/lockdowns. The spread of COVID-19 was under control shortly in

a month with no deaths and few illnesses (i.e., 28 confirmed cases out of 12.7 million residents) in the city[18]. Therefore, ignoring the health outcomes would have little influence on the economic impact modelling of such a compound event.

7.2.1. Source of Data

Two types of data, i.e., disaster data and socio-economic data, are used in the disaster footprint modelling of the 2021 compound event in the Zhengzhou city of China. Disaster data includes information on flood characteristics and COVID-19 control measures. The flood data, including inundation depths and area, is collected from the data project carried out by the 'Water Hazard Action Group' of Zhengzhou University[19]. In this project, the maximum inundation depths at 808 selected locations in the city were measured on site, together with other data from questionnaire surveys and the Internet. On the other hand, combined with the information online, news and other channels, the wave of COVID-19 in Zhengzhou was reported to have lasted about 4 weeks (July 30 to August 28) with 28 confirmed cases (all cured) in total. During this period, a series of control measures such as closed-loop management of residential areas in the city, suspension of passenger lines, and closure of dining places were adopted, resulting in a great impact on transportation and labour commuting[20].

For socio-economic data used in the calculation of direct impacts, the land use data of Zhengzhou is sourced from the ESA CCI land use database (ESA, 2017), and is calibrated based on the data of Zhengzhou in the China Urban Construction Statistical Yearbook in 2019 (Ministry of Housing and Urban-Rural Development of China, 2019). In the assessment of indirect impacts, China's economy is divided into 48

[18] The number of confirmed COVID-19 cases is obtained from https://www.sohu.com/a/496513872_121237775.

[19] For specific data information, please refer to the article "Sino-British Universities Cooperate to Complete the Simulation of July 20 Rainstorm" published by WeChat official account 'Water Hazard Action Group of Zhengzhou University' on August 31, 2021, https://mp. weixin.qq. com/s/5VY04fbD3VCynSantxtABg.

[20] Source of data: http://henan. people. com. cn/n2/2021/0806/c351638-34856245. html.

regions, i.e., 18 prefecture-level cities (including Zhengzhou) in Henan Province and 30 other provinces in China[21], and 26 economic production sectors (Table 7-1), based on the 2015 Chinese city-level MRIO table released by the CEADs database of Tsinghua University (Zheng et al., 2021). In the economic equilibrium, the amount of productive capital in each economic sector is assumed to be 4 times of its annual value added, which is similar to other macroeconomic models (Hallegatte, 2008; Koks and Thissen, 2016; Wang et al., 2021). The amount of residential capital is then extrapolated according to the ratio of residential to non-residential land areas in Zhengzhou. Relevant GDP and population data is collected from the WDI database (World Bank, 2021) and the Bulletin of the Seventh National Census of Zhengzhou (Zhengzhou Municipal Bureau of Statistics, 2021), respectively. In this study, the post-disaster economic dynamics are simulated in weeks and assumed to recover to the pre-disaster state in 2020, while the Chinese MRIO table used reflects the annual economic flows between regions and sectors in 2015. To bridge these time gaps, the 2015 MRIO table is first scaled up to the year of 2020 according to the ratio of national GDPs between 2015 and 2020, and then divided by the number of weeks per year (i.e., 52 weeks) to obtain the weekly flows of economic transactions between regions and sectors.

[21] Here the Hong Kong, Macao and Taiwan regions of China are excluded in the analysis.

Table 7-1: List of 26 economic production sectors.

Land use classes	Economic production sectors
Agricultural land	Agriculture
Industrial land	Mining
	Food and tobacco
	Textiles
	Timbers and furniture
	Paper and printing
	Petroleum, coking, and nuclear fuel
	Chemicals
	Non-metallic mineral products
	Metal products
	Ordinary machinery
	Transport equipment
	Electrical equipment
	Electronic equipment
	Other manufactured products
	Electricity, gas, and water
	Construction
Commercial land	Transport
	Wholesale and retail
	Accommodation and catering
	Information services
	Finance
	Real estate
	Rental and business services
	Scientific research and technical services
	Other services

7.2.2. Parameter Setting

The descriptions and values of model parameters are shown in Table 7-2. The maximum overproduction capacity $\alpha_{ir}^{\max}$ and the characteristic time of overproduction τ_{α} are set according to the study of Zhang, Li, et al. (2019). Based on information obtained from the news and investigations, the public has donated 3 billion yuan and the government has allocated 3.3 billion yuan from the financial budget reserve funds, respectively, to the city of Zhengzhou for battling the flood.

About 52% of these funds were used for industrial capital reconstruction and production recovery, while the rest were used for residential housing repair and living allowance. Reconstruction funds are assumed to be distributed among the production sectors of Zhengzhou in proportion to their gross value added at the pre-disaster level. This would increase the maximum overproduction capacity of these sectors by a percentage subjected to the reconstruction efficiency (i.e., the adjustment time required to reach the maximum overproduction capacity $\tau_\alpha = 16$). More specifically, the study assumes that the maximum overproduction capacity of sectors outside Zhengzhou is benchmarked at 101%, while that of sectors within Zhengzhou rises to 102% as the invested reconstruction funds reach about 1% of Zhengzhou's 16-week GDP. Subsidies to households in Zhengzhou can alleviate their income losses after paying for the reconstruction costs in the flood aftermath. This would cause further changes in their current and future consumption behaviours, considering a regionalized intertemporal consumption or saving preference (see Equations (137)-(138) in Section 3.2.1.5). Moreover, the values of inventory size n_{ir}^{j} and adjustment time τ_s are referred to the study of Hallegatte (2014). Other parameter values such as flood-related transport recovery rate, labour recovery rate, strictness and duration of COVID-19 control, and intertemporal consumption preference come from news and investigations.

Table 7-2: Parameter values of the CHEFA model applied in the compound event of Zhengzhou.

Parameters	Definitions	Values
$\overline{\alpha}_{ir}$	Production capacity of sector i in region r at the initial level	100%
$\alpha_{ir}^{\max}$	Maximum overproduction capacity of sector i in region r relative to the pre-disaster level	102% for Zhengzhou, 101% for other regions
τ_{α}	Weeks needed by a sector to achieve its maximum overproduction capacity	16
n_{ir}^{j}	Weeks of intermediate use of inventory product j that sector i in region r wants to hold	4
τ_{s}	Proportion of inventory loss that a production sector tries to restore in the next time step	100%
β_{L}	Labour recovery rate – proportion by which the affected labours are reduced per next period	0.5
β_{Z}	Flood-related transport recovery rate – proportion by which the flood-related transport disruptions are alleviated per next period	0.7
$\gamma_{r}^{Z,C}$	Strictness of COVID-19 control – percentage by which the transport capacity from region r to other regions is reduced due to the COVID-19 lockdown	30%
β_{C}	Intertemporal consumption preference – the impacts of an income change on consumption are reduced by $1-\beta_{C}$ per next period	0.5

It should be noted that there were other regions in China impacted by either extreme floods (e.g., other cities in Henan Province) or COVID-19 waves (e.g., cities of Nanjing and Zhangjiajie in other provinces) during the study period, but Zhengzhou was the only region affected by both hazards in close succession. Therefore, this chapter uses the 2021 Zhengzhou 'flood-COVID' compound event as a typical case to study the economic footprint of a compound hazard from the directly affected region to wider economic systems along the production supply chain. In the meantime, the direct damage resulting from floods or COVID-19 waves in other regions is ignored.

7.3. Direct and Indirect Economic Impacts of the 2021 Zhengzhou 'Flood-COVID' Compound Event

This section presents the results of the disaster footprint assessment of the 2021 Zhengzhou 'flood-COVID' compound event using the CHEFA model developed in this thesis. In particular, the differences in the results of compound-hazard and single-flood events (i.e., the increased losses resulting from COVID-19 control) are emphasized.

7.3.1. Overall Economic Impacts and Spatial Spillover Effects

The total economic losses of this compound event were estimated at 131,714 million yuan, equivalent to 0.13% of China's GDP of the previous year 2020, excluding health costs (Table 7-3). Among them, the flood-induced direct damage reached 66,603 million yuan, equivalent to 6.17% of Zhengzhou's GDP in 2020. This was slightly higher than the official announcement (53,200 million yuan)[22] at the tenth press conference on August 2, 2021, with a reasonable error of about 25%. Although the flood-induced direct damage only occurred in Zhengzhou, it further caused widespread supply chain disruptions with a total indirect economic loss of 36,795 million yuan. 65.63% of the indirect economic loss took place within Zhengzhou, while 19.40% and 14.97% spilled over to other cities in Henan Province and other provinces in China, respectively. The wave of COVID-19, which hit the city around a week later when it had not fully recovered from the previous flood, continued to worsen the situation with additional recovery time and economic costs. The traffic lockdowns to control virus transmission have restricted the efficiency in flood emergency and responses, which extended the recovery period of the national economy from 18 weeks to 19 weeks (see Figure 7-2A). In addition to this time delay, the COVID-19 control also aggravated the

[22] Source of data: http://news.cnr.cn/native/city/20210802/t20210802_525550674.shtml (2021-08-02).

national indirect economic loss by 28,316 million yuan, which was close to the counterpart impact of the flood. Nearly 30% of the pandemic-related indirect loss overflowed to other regions outside Zhengzhou due to the economic interrelations between regions. It was assumed that the COVID-19 control mainly affected labour supply and transportation capacity and did not cause direct damage to physical assets. Finally, the ratio of indirect to direct loss increased from 0.55 to 0.98 due to the COVID-19 intervention, indicating a greater cascading effect of a direct shock in the economic network. In other words, the concomitant COVID-19 control during the flood recovery in Zhengzhou increased the indirect economic loss by 77%. In China's current stage of regular COVID-19 prevention and control, the disaster footprint assessment of an extreme event should not only consider the indirect footprint of the event itself, but also the additional footprint brought by COVID-19 control.

Table 7-3: Economic losses due to the 2021 Zhengzhou 'flood-COVID' compound event in the directly affected city of Zhengzhou, Henan Province (outside Zhengzhou), and the whole country (outside Henan).

Regions	Direct losses	Indirect losses		Total losses	% of local GDP
		Flood-related	Pandemic-related		
Zhengzhou	66,603	24,149	20,191	110,943	10.28%
Henan (outside Zhengzhou)	-	7,137	5,040	12,177	0.29%
China (outside Henan)	-	5,509	3,085	8,595	0.01%
Sum	66,603	36,795	28,316	131,714	0.13%

Notes: The absolute loss is given in millions of 2021 CNY and the relative loss is expressed as a percentage of the local GDP in the previous year 2020.

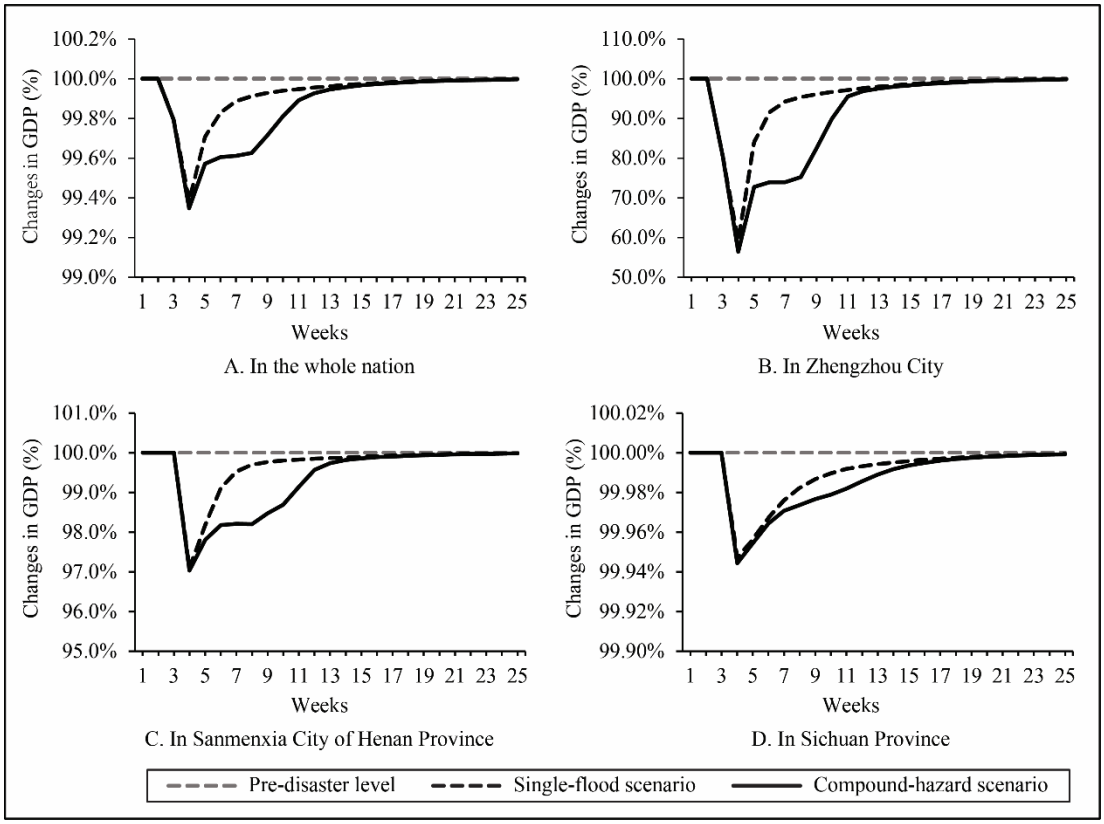

Figure 7-2: Recovery dynamics of weekly GDPs in the whole country and representative regions relative to the pre-disaster levels in the compound-hazard and single-flood scenarios.

A more detailed spatial distribution of the indirect economic footprint caused by the 2021 Zhengzhou 'flood-COVID' compound event is shown in Appendix Table A9. Overall, there were about 32% of the total indirect losses spreading to regions outside Zhengzhou, of which 59% were within Henan Province. Cities of Nanyang, Zhumadian, and Pingdingshan in Henan Province ranked high in both absolute and relative indirect losses, indicating strong influence of Zhengzhou's business activities on the economic performance of these three cities. Outside Henan Province, provinces of Jiangsu and Shandong suffered the greatest absolute losses but small relative losses, implying that these two provinces, though closely economically connected with Zhengzhou, were well resistant to the business disruptions from Zhengzhou due to their high economic resilience or stability. In contrast, provinces of Hainan and Gansu suffered small absolute losses but large relative losses, suggesting that these two provinces, though having fewer economic ties with Zhengzhou, were heavily

subjected to the business disruptions from Zhengzhou due to the low resilience or high vulnerability of their economies.

Figure 7-2B-D and Appendix Table A9 also present the marginal or additional impacts of Zhengzhou's COVID-19 control on the economic outcomes of other regions. It was found that cities of Sanmenxia and Jiyuan in Henan Province and the whole Qinghai Province had the largest proportion (over 45%) of indirect economic losses accounted by Zhengzhou's COVID-19 control. This means that these three regions are more vulnerable to the impact of COVID-19 control in Zhengzhou than other regions, and their indirect economic losses have greatly increased thereby. Comparatively, most regions outside Henan Province were less impacted by Zhengzhou's COVID-19 control, among which provinces of Hubei and Sichuan had the smallest proportion of pandemic-related losses, both of which were less than 25%.

7.3.2. Sectoral Cascading Effect along Production Supply Chain

7.3.2.1. Sectoral Distribution of Economic Losses in Zhengzhou City

The direct economic losses resulting from the studied compound event in Zhengzhou were relatively concentrated among sectors (see Table 7-4). The real estate sector suffered the largest direct loss of 19,146 million yuan, accounting for 29% of the total direct losses in Zhengzhou, equivalent to 23% of the value added of this sector in the previous year 2020. This is followed by the transport sector (3,928 million yuan) and the other services sector (3,904 million yuan), accounting for about 6% of the total direct losses respectively. By comparison, the indirect economic losses were more distributed in the non-metallic mineral products sector (5,603 million yuan), the food and tobacco sector (4,496 million yuan) and the transport sector (4,476 million yuan), accounting for 13%, 10% and 10% of the total indirect losses in Zhengzhou respectively. This has proved that the direct impact of the compound event has strong cascading effect among economic sectors in Zhengzhou. Considering the sectoral

losses in both absolute and relative terms, the sectors most impacted by the compound event were concentrated in the tertiary industry of Zhengzhou, especially the real estate and the transport sectors, followed by the non-metallic mineral products sector in the secondary industry. Therefore, more attention should be paid to the recovery of these sectors in the disaster aftermath.

It is worth noting that during the flood disaster in Zhengzhou, the communication interruption caused by the damage of communication infrastructure has drawn much attention. Many base stations, optical cables and other facilities were seriously damaged due to the flood inundation, road collapse and other reasons[23]. As presented in Table 7-4, the direct loss of the information services sector reached 3,197 million yuan, even exceeding that of the electricity, gas, and water sector. These two sectors are both capital-intensive sectors, which are vulnerable to floods caused by extreme rainfall. In the future, attention should be paid to strengthen the resilience of the infrastructure in these sectors to cope with extreme weather events.

[23] Source of data: http://henan.china.com.cn/finance/2021-07/24/content_41626309.htm.

Table 7-4: Sectoral distribution of direct and indirect economic losses in Zhengzhou City due to the 2021 Zhengzhou 'flood-COVID' compound event.

Sectors	Direct losses	Indirect losses		Total losses	% of sectoral value added
		Flood-related	Pandemic-related		
Agriculture	5	943	581	1,529	6.20%
Mining	407	994	678	2,079	8.56%
Food and tobacco	1,305	2,363	2,133	5,800	9.03%
Textiles	163	221	177	560	7.32%
Timbers and furniture	57	26	81	164	5.11%
Paper and printing	504	301	400	1,206	9.75%
Petroleum, coking, and nuclear fuel	10	21	20	51	9.22%
Chemicals	765	658	795	2,217	9.80%
Non-metallic mineral products	2,563	2,514	3,089	8,166	8.33%
Metal products	1,309	822	1,197	3,328	9.20%
Ordinary machinery	856	330	1,070	2,256	5.32%
Transport equipment	813	254	800	1,867	5.89%
Electrical equipment	72	51	149	271	4.59%
Electronic equipment	1,234	618	1,144	2,996	6.45%
Other manufactured products	35	12	45	92	5.16%
Electricity, gas, and water	2,553	879	524	3,956	17.66%
Construction	941	480	82	1,503	2.23%
Transport	3,928	2,605	1,871	8,404	13.00%
Wholesale and retail	1,583	1,730	930	4,244	4.86%
Accommodation and catering	523	769	773	2,065	7.94%
Information services	3,197	458	63	3,719	18.61%
Finance	1,882	2,724	1,124	5,730	4.28%
Real estate	19,146	932	670	20,748	25.04%
Rental and business services	998	381	249	1,628	8.29%
Scientific research and technical services	902	205	23	1,129	6.25%
Other services	3,904	2,858	1,523	8,285	7.23%
Residential houses	16,949	-	-	16,949	-

Notes: The absolute loss is given by millions of 2021 CNY and the relative loss is expressed as a percentage of the sectoral value added in the previous year 2020. Damage to residential capital is counted as the direct loss of the residential sector, which does not participate in production and thus has no indirect losses.

7.3.2.2. Sectoral Distribution of Economic Losses outside Zhengzhou City in Henan Province

Impacted by the 2021 Zhengzhou 'flood-COVID' compound event, the agriculture, other services, and finance sectors in Henan Province (outside Zhengzhou) suffered the largest economic losses, which were 2,760 million yuan, 1,908 million yuan, and 1,108 million yuan respectively (see Table 7-5). However, as a percentage of the sectoral added value in the previous year, the top three sectors with the greatest relative losses were the petroleum, coking, and nuclear fuel sector (1.03%), the accommodation and catering sector (0.82%), and the mining sector (0.60%). It is worth noting that, with the presence of reconstruction demand, overproduction capacity and cross-regional substitutability, some production in capital goods sectors (such as the construction, ordinary machinery, and transport equipment sectors) have been transferred from Zhengzhou City to other cities in Henan Province, resulting in the increased (rather than decreased) value added of these sectors in Henan Province (outside Zhengzhou), that is, positive economic benefits (or negative economic losses) have been made.

Table 7-5: Sectoral distribution of indirect economic losses in Henan Province (outside Zhengzhou) due to the 2021 Zhengzhou 'flood-COVID' compound event.

Sectors	Indirect losses		Total losses	% of sectoral value added
	Flood-related	Pandemic-related		
Agriculture	1,814	946	2,760	0.44%
Mining	501	544	1,045	0.60%
Food and tobacco	612	193	805	0.34%
Textiles	259	198	457	0.28%
Timbers and furniture	-3	0	-3	-0.01%
Paper and printing	127	118	244	0.42%
Petroleum, coking, and nuclear fuel	206	184	390	1.03%
Chemicals	437	322	759	0.40%
Non-metallic mineral products	208	254	462	0.26%
Metal products	119	188	307	0.15%
Ordinary machinery	-32	1	-31	-0.02%
Transport equipment	-23	1	-22	-0.03%
Electrical equipment	-8	1	-7	-0.01%
Electronic equipment	17	3	21	0.08%
Other manufactured products	18	20	38	0.21%
Electricity, gas, and water	92	93	185	0.40%
Construction	-68	6	-62	-0.02%
Transport	164	264	428	0.23%
Wholesale and retail	11	38	50	0.02%
Accommodation and catering	413	344	757	0.82%
Information services	-1	60	58	0.09%
Finance	649	459	1,108	0.55%
Real estate	162	111	273	0.12%
Rental and business services	139	114	253	0.48%
Scientific research and technical services	-6	0	-6	-0.02%
Other services	1,331	577	1,908	0.38%

Notes: The absolute loss is given by millions of 2021 CNY and the relative loss is expressed as a percentage of the sectoral value added in the previous year 2020. The study did not consider floods or COVID-19 occurring outside Zhengzhou, so other regions only suffered indirect economic losses from the Zhengzhou compound event. Negative values indicate the positive economic gains or value-added increases due to the stimulus effects of cross-regional substitution and post-disaster reconstruction.

7.3.2.3. Sectoral Distribution of Economic Losses outside Henan Province in China

There are 30 other provinces (including cities directly under central government jurisdiction) outside Henan Province in mainland China, consisting of a total of 780 region-sector pairs in the economy. Among all these region-sectors outside Henan Province, the agriculture sectors in 13 regions ranked among the top 30 with the largest absolute economic losses due to the 2021 Zhengzhou 'flood-COVID' compound event. More specifically, the agricultural losses in provinces of Heilongjiang, Hebei, Hunan, and Guangxi exceeded 100 million yuan, which were equivalent to 0.04%, 0.03%, 0.03%, and 0.03% of their agricultural value added in the previous year 2020 respectively. Among the top 30 region-sectors with the greatest absolute losses, the relative losses of 7 region-sectors also ranked among the top 30, which were over 0.05% as a percentage of the sectoral value added in 2020. These 7 region-sectors were Fujian-other services, Shaanxi-mining, Inner Mongolia-mining, Shaanxi-petroleum, coking, and nuclear fuel, Zhejiang-accommodation and catering, Hainan-agriculture, and Tianjin-mining, which have been asterisked in Table 7-6.

As for the compound impact of COVID-19 control, the agriculture sectors in most regions were found to be less affected by Zhengzhou's COVID-19 control, and their rankings in economic losses decreased slightly in the compound-hazard scenario compared to the single-flood scenario. On the contrary, the mining sector, the chemical sector, the petroleum, coking, and nuclear fuel sector in the secondary industry and the accommodation and catering sector in the tertiary industry were more vulnerable to Zhengzhou's COVID-19 control, and the loss rankings of these sectors increased greatly in the compound-hazard scenario compared to the single-flood scenario. Similar sectoral characteristics of the pandemic impacts were also found in Zhengzhou City and Henan Province (outside Zhengzhou City) (see Table 7-4 and Table 7-5). The agriculture, construction, and some services sectors (e.g., scientific research and technical services, other services) were less impacted by Zhengzhou's COVID-19

intervention (i.e., the COVID-19 accountability was smaller than 40%), while the mining, most manufacturing, and some other services sectors (e.g., accommodation and catering, transport) were more impacted by Zhengzhou's COVID-19 intervention (i.e., the COVID-19 accountability was greater than 40%).

Table 7-6: Top 30 region-sectors in China (outside Henan) with the largest indirect economic losses due to the 2021 Zhengzhou 'flood-COVID' compound event.

Rankings	Region-sectors	Indirect losses	% of sectoral value added	Changes in ranking	COVID-19 accountability
1	Jiangsu-chemicals	188	0.02%	↑ 2	37.82%
2	Fujian-other services*	175	0.05%	↓ 1	30.58%
3	Heilongjiang-agriculture	168	0.04%	↓ 1	29.04%
4	Shaanxi-mining*	163	0.05%	↑ 4	49.94%
5	Hebei-agriculture	157	0.03%	↓ 1	26.87%
6	Hunan-agriculture	134	0.03%	-	24.95%
7	Jiangsu-other services	129	0.01%	↓ 2	19.79%
8	Inner Mongolia-mining*	128	0.05%	↑ 7	52.36%
9	Fujian-textiles	123	0.04%	↓ 2	32.87%
10	Shandong-chemicals	121	0.02%	↑ 2	42.85%
11	Guangxi-agriculture	108	0.03%	↓ 2	27.22%
12	Liaoning-agriculture	99	0.03%	↓ 1	25.64%
13	Shaanxi-agriculture	96	0.04%	-	28.55%
14	Jiangsu-agriculture	93	0.02%	↓ 4	20.71%
15	Xinjiang-agriculture	85	0.04%	↑ 1	30.23%
16	Zhejiang-other services	82	0.01%	↓ 2	22.83%
17	Shaanxi-petroleum, coking, and nuclear fuel*	82	0.08%	↑ 17	47.49%
18	Jiangsu-textiles	81	0.02%	-	32.57%
19	Inner Mongolia-agriculture	81	0.03%	-	32.23%
20	Jiangsu-finance	76	0.01%	↓ 3	25.65%
21	Shandong-other services	74	0.01%	-	29.92%
22	Jilin-agriculture	74	0.03%	↓ 2	27.65%
23	Shanghai-finance	71	0.01%	↑ 8	38.64%
24	Guizhou-agriculture	71	0.03%	-	27.95%
25	Hunan-other services	67	0.01%	↓ 2	23.05%
26	Liaoning-other services	64	0.01%	-	24.28%
27	Zhejiang-accommodation and catering*	64	0.06%	↑ 10	41.82%
28	Hainan-agriculture*	63	0.05%	↑ 5	31.60%
29	Anhui-agriculture	61	0.02%	↓ 4	19.46%
30	Tianjin-mining*	61	0.05%	↑ 29	55.03%

Notes: The absolute loss is given by millions of 2021 CNY and the relative loss is expressed as a percentage of the sectoral value added in the previous year 2020. The asterisk '*' indicates that the relative loss of this region-sector is also in the top 30 among all region-sectors in China (outside Henan). Changes in ranking are compared to the single-flood scenario. COVID-19 accountability refers to the additional indirect economic loss caused by the COVID-19 control as a percentage of the total sectoral indirect economic loss during the compound event.

7.3.2.4. Loss of Economic Transactional Flows Between Sectors and Regions

In this section, a supply chain relationship is defined as the economic transactional relation directed from an upstream supplying region-sector to a downstream buying region-sector in the economic network. In the affected Chinese economy consisting of 48 regions and 26 sectors, there are a total of 1.3 million pieces of valid supply chain relationships[24] between the 1,248 pairs of region-sectors based on the MRIO table used in this study (see Section 7.2.1). The supply chain relationships largely affected by the 2021 Zhengzhou 'flood-COVID' compound event were mainly concentrated in Henan Province, especially in the secondary industry of Zhengzhou City. The upstream supplying sectors of these greatly affected supply chain relationships were mostly concentrated in Zhengzhou, while the downstream buying sectors were more distributed over regions in the country (see Appendix Table A10). More specifically, the business trade from Zhengzhou's mining sector to Zhengzhou's electricity, gas, and water sector experienced the largest reduction by 2,368 million yuan, reaching 7.02% of the pre-disaster level, due to the compound event.

Two supply networks could be extracted from the top 30 supply chain relationships suffering the greatest losses: 1) the first network originated from Zhengzhou's mining sector with a total economic transactional loss of 16,196 million yuan. 65.06% of these losses were linked to Zhengzhou's non-metallic mineral products sector, which was therefore identified as the most important node sector in this network (Figure 7-3); 2) the second network started from Zhengzhou's agriculture sector with a total economic transactional loss of 2,930 million yuan. 81.21% of these losses were connected to Zhengzhou's food and tobacco sector, which was thus identified as the most important node sector in this network (Figure 7-4). It is worth noting that the loss of business transactions from Zhengzhou's mining sector to Zhengzhou's non-metallic mineral

[24] Valid supply chain relationships are those having real (i.e., non-zero) transactions between the two related region-sectors.

products sector has triggered an amplification of the loss by 16 times more than itself, indicating a strategic role of this supply chain pathway in resource transmission during the economic recovery. Besides, Zhengzhou's non-metallic mineral sector is also a critical sector with strong propagation effects. The reduction in its production has caused a supply chain loss of 10,537 million yuan in terms of trades with other sectors and regions, which nearly doubled its value-added loss. Therefore, it is necessary to give priority to the restoration of the supply chain relationship from Zhengzhou's mining sector to Zhengzhou's non-metallic mineral products sector, as well as the production of the latter sector itself, so as to boost the economic recovery in Henan Province and the whole country back to the normal times after the compound event.

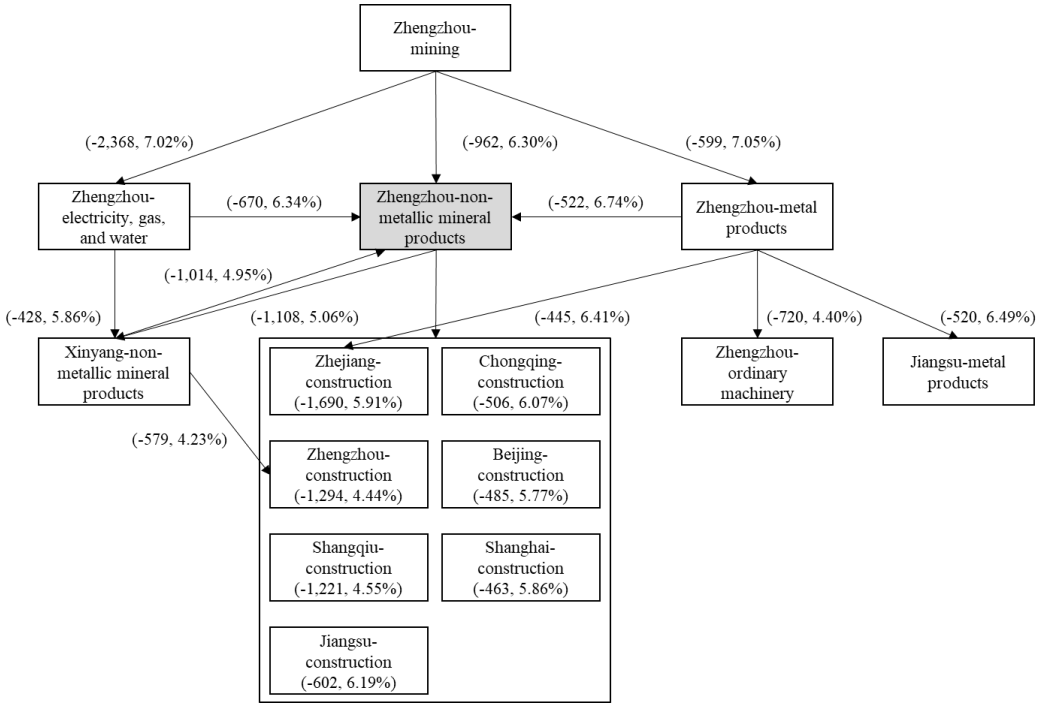

Figure 7-3: The supply network starting from Zhengzhou's mining sector largely affected by the 2021 Zhengzhou 'flood-COVID' compound event.

Numbers in the figure represent the absolute losses (in millions of 2021 CNY) and relative losses (as a percentage of the economic transactions flowing through the supply chain relationships in the previous year 2020) of the economic transactions from the upstream supplying region-sectors to the downstream buying region-sectors, respectively, due to the 2021 Zhengzhou 'flood-COVID' compound event.

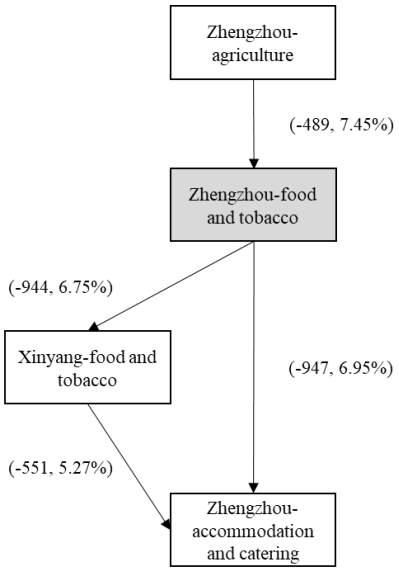

Figure 7-4: The supply network starting from Zhengzhou's agriculture sector largely affected by the 2021 Zhengzhou 'flood-COVID' compound event.
Numbers in the figure represent the absolute losses (in millions of 2021 CNY) and relative losses (as a percentage of the economic transactions flowing through the supply chain relationships in the previous year 2020) of the economic transactions from the upstream supplying region-sectors to the downstream buying region-sectors, respectively, due to the 2021 Zhengzhou 'flood-COVID' compound event.

7.4. Factors Influencing the Compound Resilience of the Affected Economy

According to Zhang, Li, Feng, et al. (2018), the economic resilience can be quantified by the indirect economic losses accumulated during the post-disaster recovery[25], and the recovery period is the time required for the economic system to recover to its initial state. The greater the cumulative losses and the longer the recovery period, the lower the economic resilience. This section examines the main factors which may influence the compound resilience of the affected economy through a series of sensitivity analyses of parameters including COVID-19 control characteristics, road repair rate,

[25] The direct economic losses are fixed given a specific flood and do not change with the parameters examined in this section.

labour recovery rate, consumption subsidies and intertemporal preference, reconstruction funds and efficiency.

7.4.1. COVID-19 Control Measures

As the health impacts of COVID-19 are not considered in this analysis, the wave of COVID-19 mainly affected the economy through the corresponding control/lockdown measures, which can be characterized by different combinations of strictness and duration. Like the case study of Chapter 6, the strictness is measured by the percentage reduction of the transportation capacity due to lockdown measures relative to the pre-disaster level. Different combinations of strictness and duration of COVID-19 control may cause different levels of disturbance to the post-flood recovery and reconstruction and further influence the overall recovery period and economic losses. From the perspective of time costs, the required recovery time of China's economy extended with both increases in strictness and duration of Zhengzhou's COVID-19 control. Comparatively, it increased faster with the duration than the strictness. For every 10% increase in the strictness of COVID-19 control, the recovery period will be extended by an average of 2.53%; while for every additional 2 weeks in the duration of COVID-19 control (about one incubation period of COVID-19), the recovery period will be prolonged by 3.73% on average. Similar results are found from the perspective of economic costs. For every 10% increase in the strictness of COVID-19 control, the total indirect economic losses will increase by an average of 20.94%; while for every additional 2 weeks in the duration of COVID-19 control period, the total indirect economic losses will increase by 21.95% on average. These results indicate that the compound resilience of China's economy is more sensitive to the duration than the strictness of Zhengzhou's COVID-19 control (see Table 7-7). This is consistent with the findings when studying the COVID-19 pandemic impacts without floods (Guan et al., 2020). Therefore, whenever the pandemic occurs, a shorter but stricter containment that can quickly eradicate the disease imposes a smaller economic loss than a longer

but milder one that can also eliminate the disease gradually and eventually, and therefore is more conducive to enhancing the compound resilience of the affected economy.

Table 7-7: Changes in compound resilience of China's economy under different strictness or duration of Zhengzhou's COVID-19 control.

Strictness of COVID-19 control	% changes in indirect loss	% changes in recovery period	Weeks of COVID-19 control	% changes in indirect loss	% changes in recovery period
-10%	-20.69%	0.00%	-2	-21.16%	0.00%
+10%	22.36%	5.26%	+2	22.76%	5.26%
+20%	45.98%	5.26%	+4	47.98%	10.53%
+30%	69.66%	10.53%	+6	74.36%	15.79%

Note: Strictness is expressed as the percentage by which the transportation capacity is reduced due to the implementation of COVID-19 control measures. The changes of indirect loss and recovery time are relative to the baseline results of indirect loss (65,111 million yuan) and recovery time (19 weeks) of the compound event under the current/benchmark COVID-19 control level (i.e., 30% - 4 weeks).

7.4.2. Road Repair Rate

Post-disaster reconstruction and supply chain recovery depend on the capacity of urban transportation system. In the aftermath of the 2021 Zhengzhou 'flood-COVID' compound event, the transportation capacity between economic sectors not only relies on the repair rate of roads damaged by the flood, but also is limited by the COVID-19 control measures. This section examines the influence of road repair rate β_Z on economic resilience under various COVID-19 control levels (including the no control, i.e., single-flood scenario). In general, the total indirect economic loss of the compound event decreases as the road repair rate increases. In other words, the faster the roads are repaired, the more beneficial it is to enhance the compound resilience of the affected economy. However, the marginal reduction in the indirect loss shows a diminishing trend with the increase of the road repair rate (see Figure 7-5).

When there is no COVID-19 control (i.e., no pandemic risks), the indirect economic loss declines the fastest with the increase of the road repair rate; however, with the strengthening of COVID-19 control (when faced with severer pandemic risks), the effect of increasing road repair rate on mitigating economic loss (i.e., boosting economic resilience) gradually weakens (see Table 7-8). Specifically, without the implementation of COVID-19 control, the indirect economic loss is reduced by 12.82% and the recovery time is shortened by 4.68% on average for every 0.1 increase in the road repair rate; while under the current/benchmark COVID-19 control level (i.e., 30% - 4 weeks), the indirect economic loss is reduced by 4.64% and the recovery time is shortened by 3.13% on average for every 0.1 increase in the road repair rate.

In addition, the minimum road repair rate required to achieve the optimal recovery is different under different COVID-19 control levels. Under the current COVID-19 control level (i.e., 30% - 4 weeks), when the road repair rate exceeds 0.6, continuing to accelerate road repair nearly has no positive effect on improving economic resilience. When faced with a severer wave of COVID-19 and a stricter or longer containment is taken (e.g., 40% - 4 weeks or 30% - 6 weeks), the continuous increase of road repair rate above 0.5-0.6 could no longer significantly mitigate the indirect economic loss caused by the compound event. Instead, accelerating the road repair might increase the risk of virus transmission and impair public health with extra costs (Ishiwatari et al., 2020; Pei et al., 2020; Salas et al., 2020). In comparison, under a moderate COVID-19 control (30% - 2 weeks or 20% - 4 weeks), the indirect economic loss appears to be more sensitive to the road repair rate, and the minimum road repair rate required to achieve the optimal economic recovery is also higher (about 0.6-0.7). Therefore, the optimal road repair rate is related to the severity of the pandemic shock during the compound event: with the presence of a severe wave of COVID-19, moderately slowing down the progress of road repair due to flood damage not only is attuned to the requirement of disease control to ensure public health, but also can avoid

the waste of economic resources; while in a small-scale COVID-19 wave, more emergency resources should be directed to road repair and traffic recovery, so that connections between economic sectors can be restored faster, which eventually reduces the disaster-induced economic loss and improves the compound resilience.

It should be noted that the health impacts of COVID-19 are not modelled in this analysis and the severity of a COVID-19 wave is simply linked to the strictness and duration of the control measures required to cut off virus transmission. In other words, a 30% - 6 weeks of control (longer) or 40% - 4 weeks of control (stricter) implies a severer wave of COVID-19 than the 30% - 4 weeks of the baseline control in the 2021 Zhengzhou case, while a 20% - 4 weeks of control (weaker) or 30% - 2 weeks of control (shorter) indicates a milder wave. Besides, the no control scenario refers to an extreme situation in which there are no pandemic risks (i.e., the single-flood scenario) and thus always has lower indirect economic losses than other control scenarios, as in Figure 7-5 and figures in following sections. This may seem counterfactual in countries like the UK which lifted all COVID-19 restrictions when there are still pandemic risks and suffered high health costs and serious labour shortages (Reuschke and Houston, 2022). However, this could be possible in China at least before December 2022[26], as the country always took active actions (i.e., the dynamic 'zero-COVID' policy) to fight COVID-19 and there is no control only when there are no detectable risks of virus transmission.

[26] China ended the 'zero-COVID' policies and lifted nearly all restrictions in December 2022 after three years' hard efforts to keep COVID-19 in control: https://www.usnews.com/news/world/articles/2022-12-07/factbox-china-covid-policy-major-changes-in-further-easing.

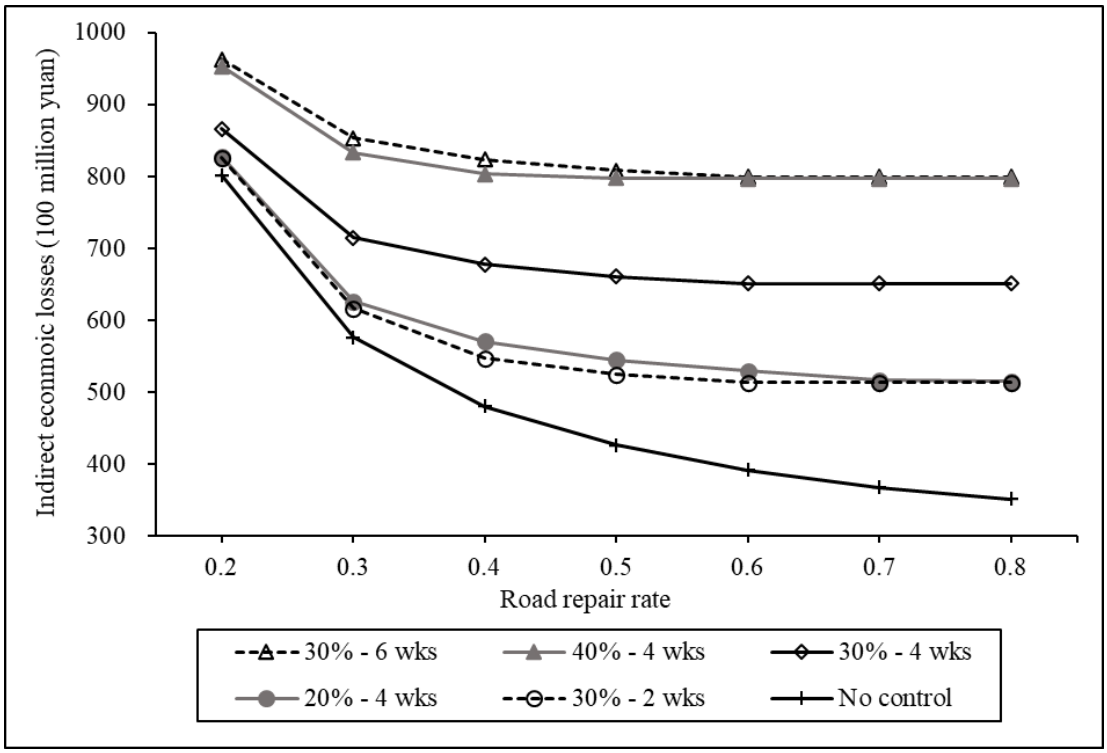

Figure 7-5: Influence of road repair rate on indirect economic losses under different COVID-19 control levels.

Table 7-8: Average sensitivity of compound resilience to increases in the road repair rate under different COVID-19 control levels.

Strictness and duration of COVID-19 control	Average change of indirect economic loss (%)	Average change of recovery period (%)
30% - 6 weeks	-3.05%	-2.99%
40% - 4 weeks	-2.94%	-2.99%
30% - 4 weeks	-4.64%	-3.13%
20% - 4 weeks	-7.58%	-3.82%
30% - 2 weeks	-7.62%	-3.13%
No control	-12.82%	-4.68%

Notes: The second and third column presents the percentage of mean change in the indirect economic loss and recovery period, respectively, for every 0.1 increase in the road repair rate. The negative sign indicates a deterioration of compound resilience (i.e., reduced indirect loss and shortened recovery period).

7.4.3. Labour Recovery Rate

Floods not only cause damage to capital assets, but also cause casualties and impact

labour commuting. Unlike the endogenous recovery of capital in post-disaster reconstruction, the supply of labour is recovered at an exogenous rate in the CHEFA model. This section analyses the influence of labour recovery rate β_L on indirect economic loss or economic resilience under various COVID-19 control levels (including the no control or single-flood scenario). In general, increasing the labour recovery rate contributes to alleviating the total indirect economic loss of the compound event, though this mitigation impact is relatively small (0.07%-0.90%). In other words, increasing the labour recovery rate can only slightly increase the compound resilience of the affected economy (see Figure 7-6 and Table 7-9). This could be due to the facts that economic sectors often find it hard to replace labour shortages with other types of production inputs shortly after the disruption and the sectoral production is limited by the minimum of input productivity and final demand. Therefore, simply restoring labour supply has little effect on the full economic resumption when capital reconstruction is inadequate, transportation is still restricted, and final consumption is still sluggish after the compound event. It may even accelerate the spread of COVID-19 and increase public health risks.

Although accelerating labour recovery can slightly boost the economic resilience, this positive effect diminishes as COVID-19 containment turns stricter or longer, which is similar to the road repair rate; when there is no COVID-19 control, the influence of labour recovery rate on economic resilience is the greatest, i.e., the indirect loss is reduced by an average of 0.90% for every 0.1 increase in the labour recovery rate (see Table 7-9).

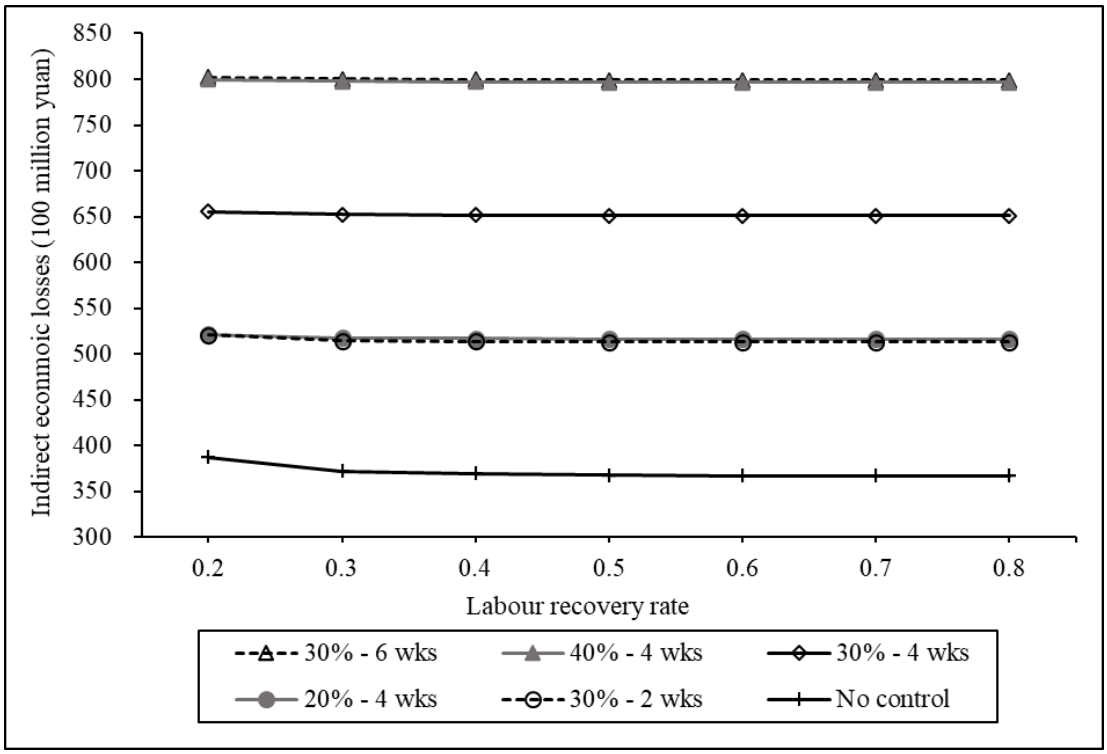

Figure 7-6: Influence of labour recovery rate on indirect economic losses under different COVID-19 control levels.

Table 7-9: Average sensitivity of compound resilience to increases in the labour recovery rate under different COVID-19 control levels.

Strictness and duration of COVID-19 control	Average change of indirect economic loss (%)	Average change of recovery period (%)
30% - 6 weeks	-0.07%	0.00%
40% - 4 weeks	-0.07%	0.00%
30% - 4 weeks	-0.11%	0.00%
20% - 4 weeks	-0.18%	0.00%
30% - 2 weeks	-0.24%	0.00%
No control	-0.90%	0.00%

Notes: The second and third column presents the percentage of mean change in the indirect economic loss and recovery period, respectively, for every 0.1 increase in the labour recovery rate. The negative sign indicates a deterioration of compound resilience (i.e., reduced indirect loss and shortened recovery period).

7.4.4. Consumption Subsidies and Preference

During the disaster response, the emergency funds from social donations and financial

allocations can be used as: 1) consumption subsidies for residents in the disaster area to repair their houses and maintain basic living; and 2) reconstruction funds for economic sectors to repair damaged capital assets and restore production. The following sections will investigate the influence of consumption subsidies and reconstruction funds, respectively, on economic resilience towards the 2021 Zhengzhou 'flood-COVID' compound event.

7.4.4.1. Consumption Subsidies for Residents in Zhengzhou

In response to the 2021 Zhengzhou 'flood-COVID' compound event, the government allocated nearly 3 billion yuan from the emergency fund budget to Zhengzhou's residents as consumption subsidies[27], which was close to 5% of the flood-induced direct damage. This section then examines how changes in this financial aid (at an interval of 5% relative to the direct damage) would influence the indirect economic losses and recovery time. As shown in Figure 7-7 and Table 7-10, a 5% increase in the consumption subsidies can reduce indirect economic losses by 0.48%-1.34% on average but cannot significantly shorten the recovery time in the compound-hazard scenarios. In comparison, expanding the consumption subsidies has a more significant effect in mitigating the negative disaster impacts in the single-flood scenario (i.e., without COVID-19 control), where the cumulative indirect economic losses are reduced by an average of 2.17%.

[27] The total amount of consumption subsidies is sorted from official information on use of funds related to flood control and disaster relief released by local governments, Red Cross Society, Charity Federation, and other public institutions.

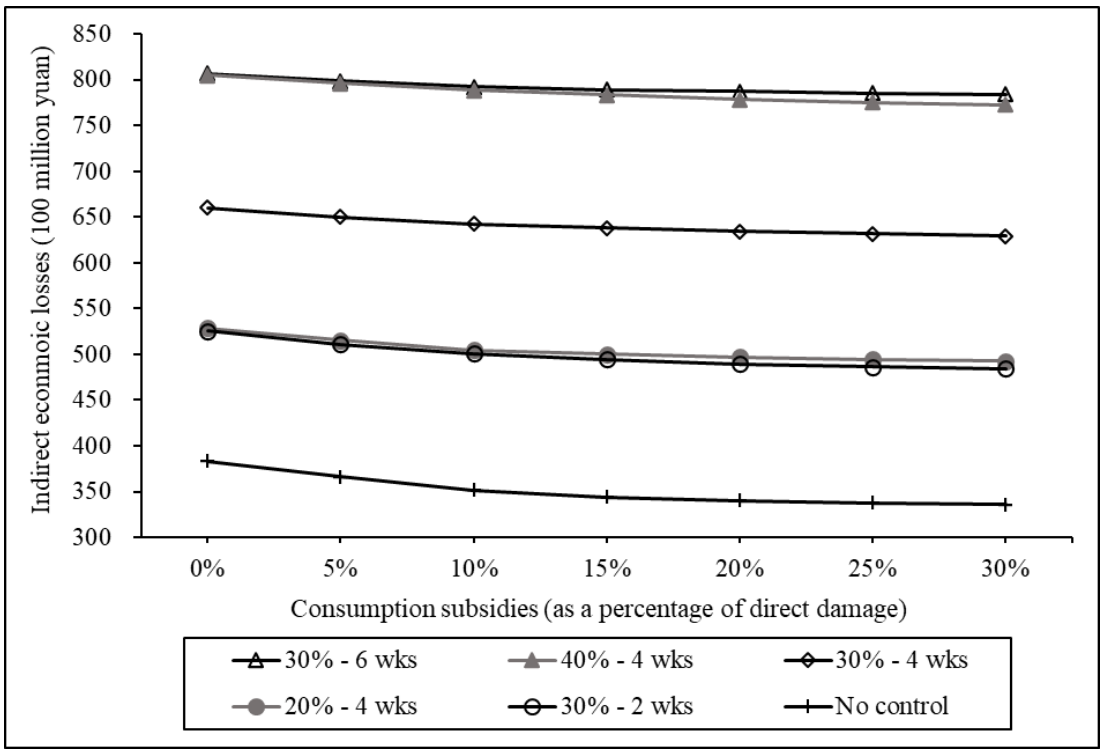

Figure 7-7: Influence of consumption subsidies on indirect economic losses under different COVID-19 control levels.

Table 7-10: Average sensitivity of compound resilience to increases in consumption subsidies under different COVID-19 control levels.

Strictness and duration of COVID-19 control	Average change of indirect economic loss (%)	Average change of recovery period (%)
30% - 6 weeks	-0.48%	0.00%
40% - 4 weeks	-0.68%	-0.85%
30% - 4 weeks	-0.80%	0.00%
20% - 4 weeks	-1.16%	-0.90%
30% - 2 weeks	-1.34%	-0.90%
No control	-2.17%	0.00%

Notes: The second and third column presents the percentage of mean change in the indirect economic loss and recovery period, respectively, for every 5% increase in consumption subsidies. The negative sign indicates a deterioration of compound resilience (i.e., reduced indirect loss and shortened recovery period).

7.4.4.2. Intertemporal Consumption Preference in Zhengzhou

Intertemporal consumption preference β_C reflects the distribution of personal

income between current and future consumption. The lower the coefficient, the more households tend to consume at present, and the lower the savings rate, thus the greater the stimulating/inhibiting effect of income increase/decrease on current consumption. On the one hand, the extra expenditure for repairing damaged houses after the flood has taken up a portion of the household spending budget and crowded out other types of consumption; on the other hand, the consumption subsidies for residents affected by the disaster can make up for some of their income losses and stimulate their willingness to consume. The change of household income may have different impacts on current and future consumption according to the intertemporal consumption preference, and then influence the post-disaster recovery and economic resilience. This section compares the influences of household intertemporal consumption preference on the economic resilience under different COVID-19 control levels in Zhengzhou, and the results are shown in Figure 7-8 and Table 7-11. In the single-flood scenario without COVID-19 control, the impact of intertemporal consumption preference on economic resilience is uncertain. The indirect economic loss is reduced by an average of 0.03% with each 0.1 increase in intertemporal consumption preference coefficient, but the recovery time is extended by an average of 1.77%. In contrast, in the compound-hazard scenarios with different levels of COVID-19 control, the indirect economic loss and recovery time are more sensitive to the change of intertemporal consumption preference. Every 0.1 increase in this coefficient would lead to an increase by 0.13%-0.16% in the indirect economic loss and 1.68%-2.60% in the recovery period under different levels of COVID-19 control. This indicates that regions with the kind of households who are more inclined to current consumption or with lower savings rate tend to be more economically resilient to the compound event with consumption subsidies at the current level.

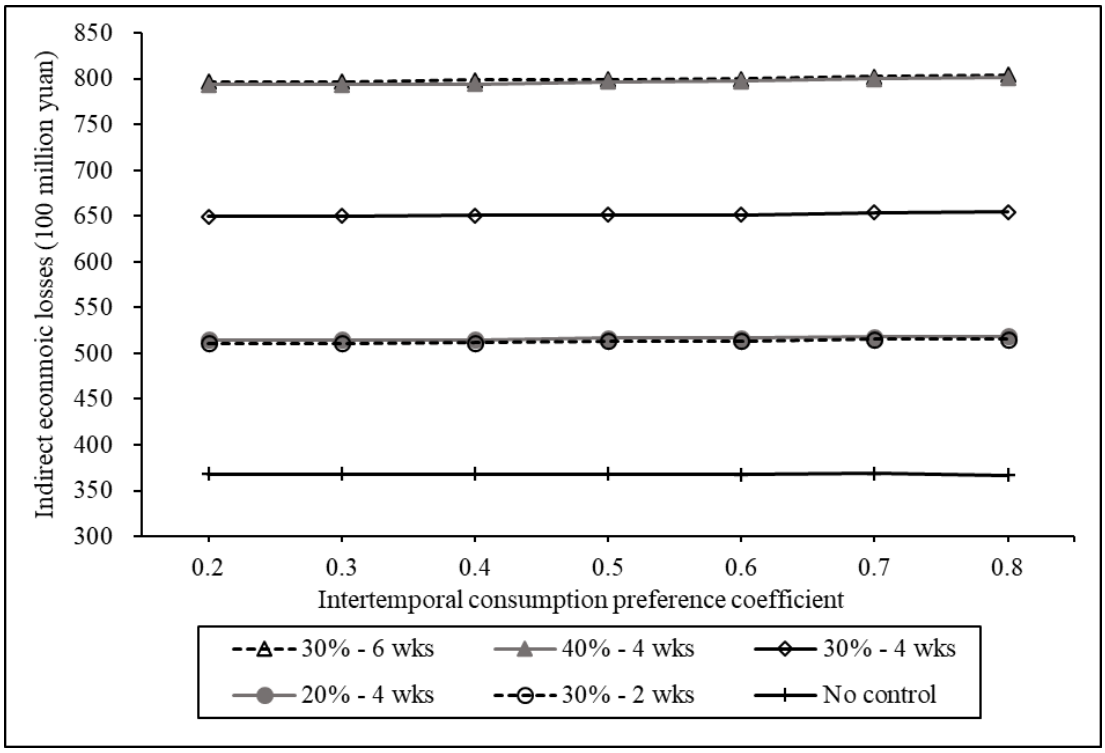

Figure 7-8: Influence of intertemporal consumption preference on indirect economic losses under different COVID-19 control levels.

Table 7-11: Average sensitivity of compound resilience to changes in the intertemporal consumption preference under different COVID-19 control levels.

Strictness and duration of COVID-19 control	Average change of indirect economic loss (%)	Average change of recovery period (%)
30% - 6 weeks	0.16%	2.47%
40% - 4 weeks	0.16%	2.47%
30% - 4 weeks	0.13%	1.68%
20% - 4 weeks	0.14%	2.60%
30% - 2 weeks	0.15%	2.60%
No control	-0.03%	1.77%

Notes: The second and third column presents the percentage of mean change in the indirect economic loss and recovery period, respectively, for every 0.1 increase in the intertemporal consumption preference coefficient. The negative sign indicates a deterioration of compound resilience (i.e., reduced indirect loss and shortened recovery period).

7.4.4.3. Compound Effect of Consumption Subsidies and Intertemporal Consumption Preference

This section further investigates the compound effect of consumption subsidies and

intertemporal consumption preference on the disaster-induced indirect economic losses under the current COVID-19 control level (i.e., 30% - 4 weeks). The results are illustrated in Figure 7-9 and Table 7-12. On the one hand, increasing the consumption subsidies for residents in Zhengzhou can mitigate the indirect economic loss more significantly when consumers there tend to save more for future consumption. In other words, the economic resilience is more sensitive to consumption subsidies in regions with higher values of the intertemporal consumption preference coefficient. On the other hand, the indirect economic loss changes in opposite directions with the increase of the preference coefficient at different scales of consumption subsidies. When the amount of consumption subsidies is small (i.e., less than 10%-15% of the direct damage), the indirect economic loss increases as the preference coefficient increases, indicating a higher economic resilience when residents in Zhengzhou are more inclined to consume at present. However, when the amount of consumption subsidies is large (i.e., greater than 10%-15% of the direct damage), the indirect economic loss decreases as the preference coefficient increases, displaying a higher economic resilience when residents in Zhengzhou are more inclined to save for future consumption. Therefore, it can be inferred that a small-scale consumption subsidy values the short-term economic benefits whereas a large-scale one stresses the long-term economic benefits.

While issuing consumption subsidies in regions hit by the disaster, other policy tools which can adjust the household intertemporal consumption preference or savings rate should be supplemented accordingly to stimulate the post-disaster economy as much as possible. Although more subsidies are better for mitigating the disaster-induced economic loss, the amount is usually bounded by the emergency fund budget and only a small proportion of the disaster damage. For instance, in the case of the 2021 Zhengzhou ‘flood-COVID’ compound event, the amount of consumption subsidies is around 5% of the direct damage caused by the flood. The optimal combinations of

consumption subsidies and the preference coefficient with the least economic loss is 25% - 0.8 as shown in Table 7-12. However, it is unrealistic to expand the consumption subsidies to 25% of the direct damage given the limited financial budget. Thus, at the current scale of consumption subsidies, supplementary measures, such as lowering deposit rates, increasing preferential consumption loans, issuing shopping vouchers, and other innovative financial instruments, could be introduced to encourage current consumption (i.e., to reduce the intertemporal consumption preference coefficient), so that a smaller economic loss resulting from the compound event could be achieved.

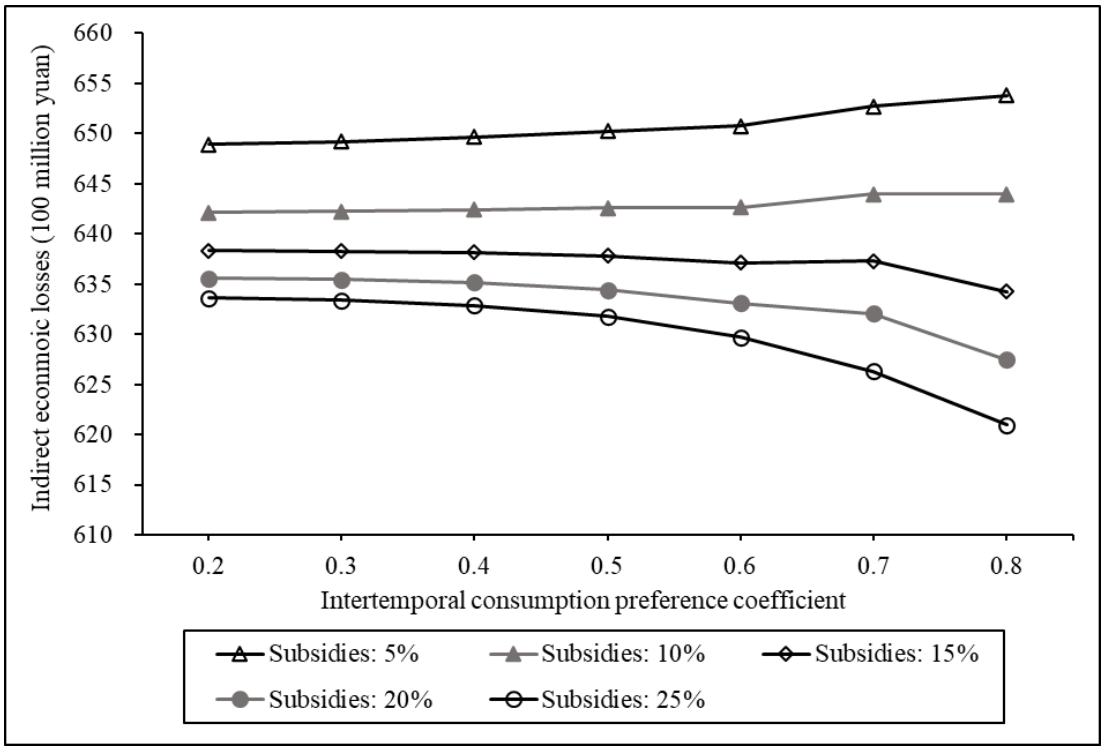

Figure 7-9: Compound influence of consumption subsidies and intertemporal consumption preference on indirect economic losses under the current COVID-19 control level.

Table 7-12: Relative changes of indirect economic losses due to varying combinations of consumption subsidies and intertemporal consumption preference under the current COVID-19 control level.

		Consumption subsidies					Sensitivity (a)
		5%	10%	15%	20%	25%	
Intertemporal consumption preference coefficient	**0.2**	-0.20%	-1.24%	-1.83%	-2.25%	-2.55%	-0.59%
	0.3	-0.16%	-1.23%	-1.83%	-2.27%	-2.59%	-0.62%
	0.4	-0.08%	-1.20%	-1.86%	-2.32%	-2.67%	-0.65%
	0.5	0.00%	-1.18%	-1.91%	-2.43%	-2.83%	-0.72%
	0.6	0.08%	-1.17%	-2.02%	-2.64%	-3.15%	-0.82%
	0.7	0.39%	-0.96%	-1.99%	-2.79%	-3.67%	-1.03%
	0.8	0.55%	-0.96%	-2.46%	-3.50%	-4.50%	-1.28%
Sensitivity (b)		0.12%	0.05%	-0.11%	-0.21%	-0.34%	

Notes: The matrix in the middle presents the percentage changes of indirect economic losses under different combinations of consumption subsidies and intertemporal consumption preference, relative to the baseline scenario (i.e., 5% - 0.5). The rightmost column of sensitivity (a) shows the percentage of mean change in the indirect economic loss per 5% increase in consumption subsidies under each specific intertemporal consumption preference. The bottom row of sensitivity (b) shows the percentage of mean change in the indirect economic loss for every 0.1 increase in the intertemporal consumption preference coefficient under each specific level of consumption subsidies. The negative sign indicates a reduction in indirect economic losses.

7.4.5. Reconstruction Funds and Efficiency

During the disaster response, a portion of the emergency funds can also be used as reconstruction funds to support economic sectors to repair damaged productive capital and restore production. The investment of reconstruction funds is conducive to expanding the overproduction capacity of economic sectors when faced with supply shortages or demand surges, and the reconstruction efficiency can affect the time required for economic sectors to reach their maximum production capacity (Zhang, Li, Feng, et al., 2018).

7.4.5.1. Reconstruction Funds

During the 2021 Zhengzhou 'flood-COVID' compound event, the reconstruction funds invested in post-disaster reconstruction and production recovery were worth 3.3 billion

yuan, which was also around 5% of the flood-induced direct damage. As shown in Figure 7-10 and Table 7-13, both indirect economic loss and recovery time are reduced as more reconstruction funds are devoted, and the greater the reduction with the ease of COVID-19 control. Particularly when there is no COVID-19 control, the marginal benefit of expanding the reconstruction funds is the largest. In this scenario, the indirect loss and recovery time decreased by an average of 1.17% and 2.82%, respectively, with every 5% increase in the reconstruction funds. This, again, indicates that the disease control in the 'flood-COVID' compound event would inhibit the marginal economic benefit of reconstruction funds invested to repair the flood damage and this inhibitory effect becomes more serious with the strengthening of the control measures (i.e., a stricter or longer containment).

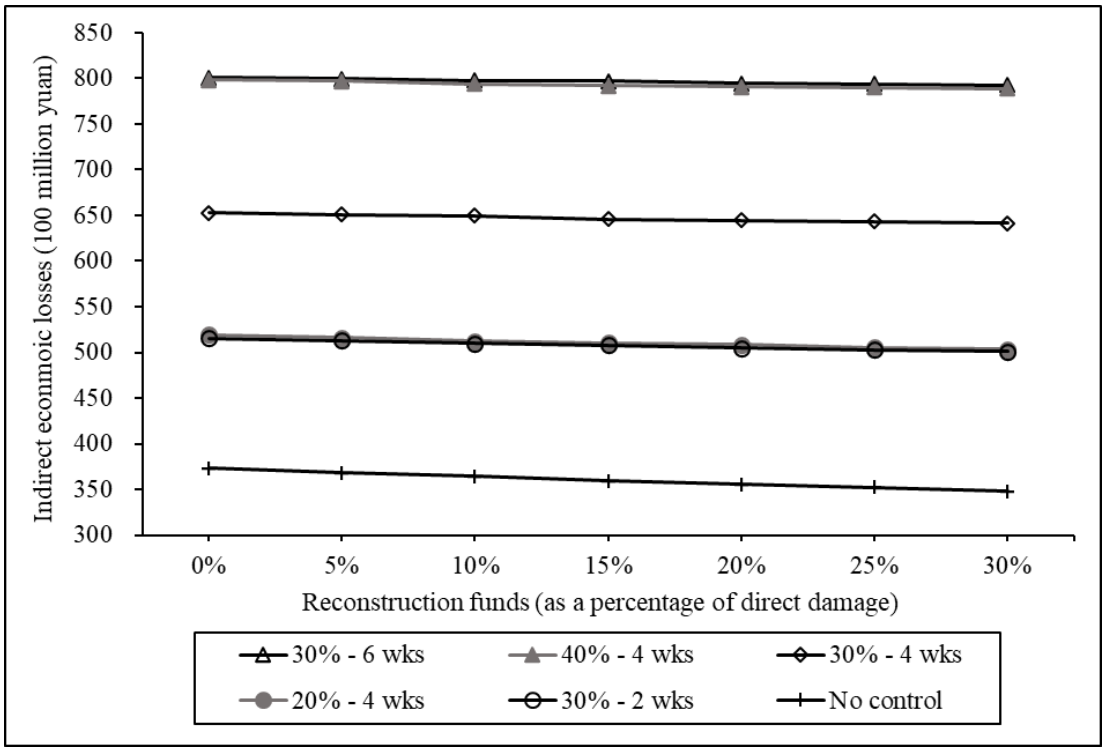

Figure 7-10: Influence of reconstruction funds on indirect economic losses under different COVID-19 control levels.

Table 7-13: Average sensitivity of compound resilience to increases in reconstruction funds under different COVID-19 control levels.

Strictness and duration of COVID-19 control	Average change of indirect economic loss (%)	Average change of recovery period (%)
30% - 6 weeks	-0.17%	-0.85%
40% - 4 weeks	-0.20%	-0.85%
30% - 4 weeks	-0.29%	-0.90%
20% - 4 weeks	-0.51%	-1.84%
30% - 2 weeks	-0.47%	-1.84%
No control	-1.17%	-2.82%

Notes: The second and third column presents the percentage of mean change in the indirect economic loss and recovery period, respectively, for every 5% increase in reconstruction funds. The negative sign indicates a deterioration of compound resilience (i.e., reduced indirect loss and shortened recovery period).

7.4.5.2. Reconstruction Efficiency

Reconstruction efficiency is defined as the reciprocal of the time required for an economic sector to achieve its maximum overproduction capacity. If it takes τ_α weeks for the sector to reach the maximum overproduction capacity, then the reconstruction efficiency is $1/\tau_\alpha$. Figure 7-11 and Table 7-14 show how the indirect economic loss caused by or the economic resilience towards the compound event changes with the reconstruction efficiency. It is found that, for every 4-week increase in the time required to reach the maximum overproduction capacity (i.e., reduction in the reconstruction efficiency), the disaster-induced indirect economic loss and the economic recovery time would increase by an average between 0.62%-2.34% and 2.75%-5.22%, respectively, at various COVID-19 control levels (including the no control scenario). With the ease of COVID-19 control until it is completely removed, the indirect economic loss becomes more sensitive to the change of reconstruction efficiency. This finding is consistent with that for other factors examined in previous sections. In addition, compared with investing more reconstruction funds, increasing the reconstruction efficiency is more effective in boosting the economic resilience

towards the compound event.

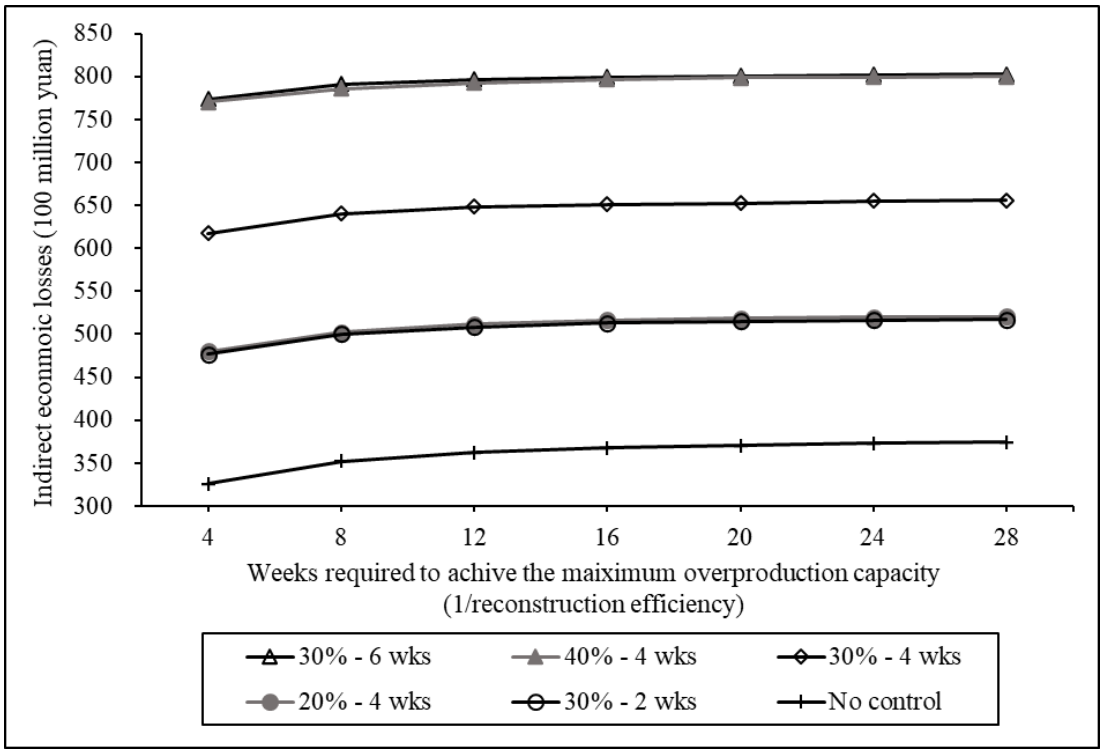

Figure 7-11: Influence of reconstruction efficiency on indirect economic losses under different COVID-19 control levels.

Table 7-14: Average sensitivity of compound resilience to decreases in the reconstruction efficiency under different COVID-19 control levels.

Strictness and duration of COVID-19 control	Average change of indirect economic loss (%)	Average change of recovery period (%)
30% - 6 weeks	0.62%	2.75%
40% - 4 weeks	0.63%	2.75%
30% - 4 weeks	1.02%	4.91%
20% - 4 weeks	1.36%	4.02%
30% - 2 weeks	1.37%	5.22%
No control	2.34%	5.22%

Notes: The second and third column presents the percentage of mean change in the indirect economic loss and recovery period, respectively, for every 4-week increase in the time required for an economic sector to reach its maximum overproduction capacity (i.e., reduction in the reconstruction efficiency).

7.4.5.3. Compound Effect of Reconstruction Funds and Efficiency

This section further investigates the compound effect of reconstruction funds and efficiency on the indirect economic losses induced by the compound event under the current COVID-19 control level (i.e., 30% - 4 weeks in Zhengzhou). As shown in Figure 7-12 and Table 7-15, the indirect economic loss is more sensitive to the change of the amount of reconstruction funds at a higher reconstruction efficiency (i.e., less weeks needed to achieve the maximum overproduction capacity), and similarly, to the change of reconstruction efficiency with a greater amount of the reconstruction funds invested in production recovery. More generally, the indirect economic loss decreases most rapidly along the direction of increasing reconstruction funds and efficiency at the same time. When the amount of reconstruction funds reaches 25% of the flood-induced direct damage and the maximum overproduction capacity can be achieved in only 4 weeks, the total indirect economic loss would fall by 10.12% compared to the baseline scenario (i.e., 5% - 16). On average, the increased economic loss due to a 4-week increase in the overproduction adjustment time (i.e., reduction in the reconstruction efficiency) could be offset through raising the reconstruction funds by around 10% relative to the direct damage. Therefore, the investment of reconstruction funds should be in accordance with the overproduction adjustment time (i.e., reconstruction efficiency). Technical support for production expansion should be provided for sectors in difficulties, so that their reconstruction efficiency could be increased to make the best use of the reconstruction funds during the post-disaster recovery.

Comparing Table 7-10 and Table 7-13, it can be found that, in the baseline scenario (i.e., the COVID-19 control is 30% - 4 weeks, the intertemporal consumption preference coefficient is 0.5, and the reconstruction efficiency is 1/16), increasing the reconstruction funds is not as good as increasing the consumption subsidies in reducing the indirect economic loss, but it can shorten the economic recovery time more rapidly.

In this situation, trade-offs should be made between reconstruction funds and consumption subsidies within the financial budget of emergency funds according to the governance objective adopted (i.e., to mitigate the disaster loss or to recover production fast). Nonetheless, if the reconstruction efficiency is raised to 1/8 and above, increasing the reconstruction funds will reduce the indirect economic loss by more than 0.81% on average (see Table 7-15), which is greater than the mitigation effect of expanding consumption subsidies, and therefore, more emergency funds within the financial budget should be directed to addressing the need for capital reconstruction and production restoration, so as to achieve the maximum possible economic resilience towards the compound event.

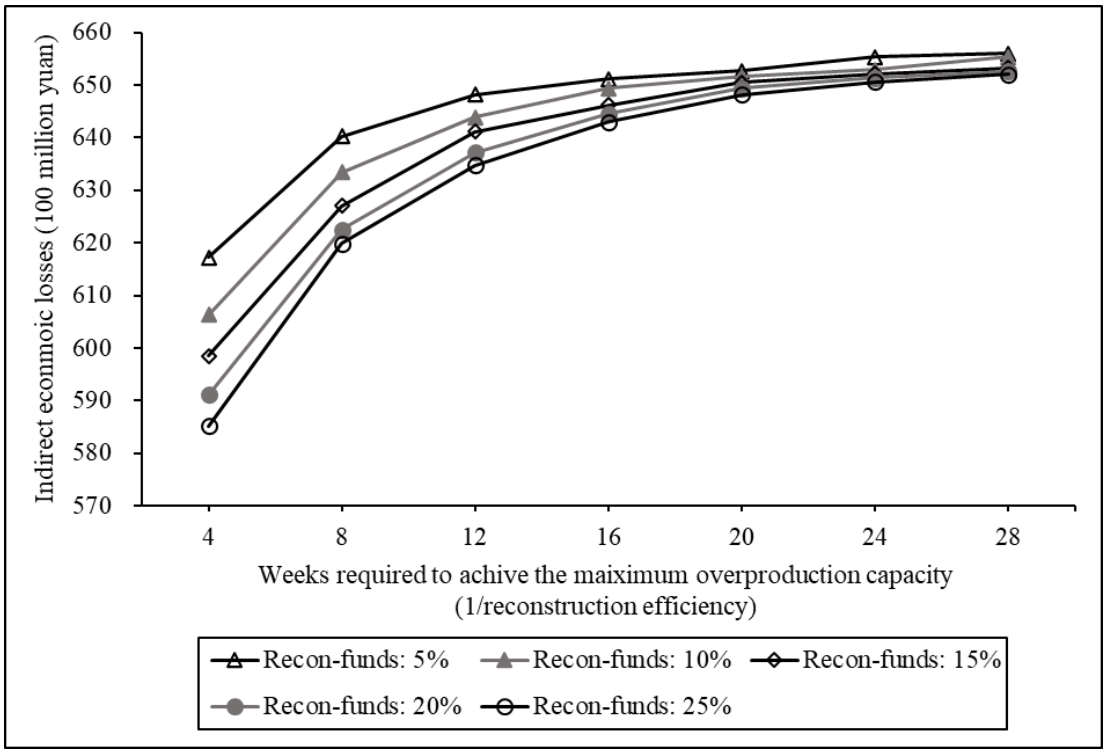

Figure 7-12: Compound influence of reconstruction funds and efficiency on indirect economic losses under the current COVID-19 control level.

Table 7-15: Relative changes of indirect economic losses due to varying combinations of reconstruction funds and efficiency under the current COVID-19 control level.

		Reconstruction funds					Sensitivity (a)
		5%	10%	15%	20%	25%	
1/reconstruction efficiency (weeks to reach the maximum overproduction capacity)	4	-5.20%	-6.89%	-8.08%	-9.21%	-10.12%	-1.32%
	8	-1.66%	-2.72%	-3.69%	-4.39%	-4.79%	-0.81%
	12	-0.45%	-1.11%	-1.54%	-2.14%	-2.52%	-0.52%
	16	0.00%	-0.27%	-0.76%	-1.00%	-1.24%	-0.31%
	20	0.25%	0.07%	-0.10%	-0.27%	-0.44%	-0.17%
	24	0.64%	0.28%	0.16%	0.04%	-0.08%	-0.18%
	28	0.76%	0.66%	0.32%	0.23%	0.15%	-0.15%
Sensitivity (b)		1.02%	1.31%	1.47%	1.66%	1.82%	

Notes: The matrix in the middle presents the percentage changes of indirect economic losses under different combinations of reconstruction funds and efficiency, relative to the baseline scenario (i.e., 5% - 16). The rightmost column of sensitivity (a) shows the percentage of mean change in the indirect economic loss per 5% increase in reconstruction funds under each specific level of reconstruction efficiency. The bottom row of sensitivity (b) shows the percentage of mean change in the indirect economic loss for every 4-week increase in the time required to reach the maximum overproduction capacity under each specific level of reconstruction funds. The negative sign indicates a reduction in indirect economic losses.

7.5. Discussion and Conclusions

This chapter uses the CHEFA model developed in this thesis to simulation how the direct shocks resulting from the 2021 Zhengzhou 'flood-COVID' compound event are transmitted to wider economic systems along China's production supply chain. Both the direct and indirect disaster footprint are quantified, at the sectoral level, first in the directly affected city of Zhengzhou, then in the province of Henan which is the city located in, and finally in the whole nation of China. A series of sensitivity analyses is also carried out to examine how the economic resilience towards the compound event changes with factors including the characteristics of COVID-19 control, road repair rate, labour recovery rate, financial aid, intertemporal consumption preference, and reconstruction efficiency.

As for the spatial distribution of the disaster footprint, the 2021 Zhengzhou 'flood-COVID' compound event has caused not only direct damage worth 66,603 million yuan in the city of Zhengzhou (equivalent to 6.17% of Zhengzhou's GDP in 2020), but also indirect economic loss worthy of 65,111 million yuan in China (equivalent to 0.06% of China's GDP in 2020), which was approximate to the direct damage. Although most of the indirect economic losses occurred in Zhengzhou, more than 30% overflowed to other regions. Regions outside Zhengzhou in Henan Province suffered a total indirect economic loss worthy of 12,177 million yuan, mainly concentrated in cities of Nanyang, Luoyang, and Zhoukou. Then, regions outside Henan in China suffered a total indirect economic loss worthy of 8,595 million yuan, mainly concentrated in provinces of Jiangsu, Shandong, and Inner Mongolia.

In terms of the sectoral distribution of the disaster footprint, the biggest part of the direct damage induced by the Zhengzhou flood was concentrated in the real estate sector in Zhengzhou. The flood-induced direct damage was then compounded by Zhengzhou's COVID-19 control, which caused further disruptions in business between economic sectors, resulting in a trail of indirect economic footprint in the affected economy. The top three sectors with the largest indirect economic losses in Zhengzhou were the non-metallic mineral products, food and tobacco, and transport sectors. In regions outside Zhengzhou in Henan Province, the agriculture sector and petroleum, coking, and nuclear fuel sector suffered the greatest indirect losses in the absolute and relative terms respectively. Then in regions outside Henan in China, there were 7 sectors in 6 provinces ranking top 30 in terms of both absolute and relative indirect losses, i.e., the other services sector in Fujian, the mining sector and Petroleum, coking, and nuclear fuel sector in Shaanxi, the mining sector in Inner Mongolia, the accommodation and catering sector in Zhejiang, the agriculture sector in Hainan, and the mining sector in Tianjin. In the national economic network, the business transactions from the mining sector to the non-metallic mineral products sector in

Zhengzhou were reduced by 962 million yuan due to the compound event, and this absolute loss ranked 8th among all valid supply chain relationships in China. It triggered further losses in the business trade flows with other sectors and regions (especially the downstream construction sectors in multiple regions), which was worth 16,196 million yuan and 16 times more than its own loss. It was therefore identified as the most vital supply chain relationship with a far-reaching impact on the economic recovery after this compound event.

In terms of the compounded impact of Zhengzhou's COVID-19 control, firstly and explicitly, it has caused extra economic costs and prolonged recovery time for battling the compound event, as well as changing the spatial and sectoral distribution of the disaster footprint. Specifically, the COVID-19 control in Zhengzhou has extended the economic recovery time by one week and increased the indirect economic loss by 28,316 million yuan, which was close to that caused by the flood and raised the ratio of indirect to direct losses from 0.55 to 0.98 (equivalent to an increase by 77%). On the geographical scale, cities of Sanmenxia, Jiyuan, and Zhengzhou itself in Henan Province, as well as Qinghai province, were most negatively affected by Zhengzhou's COVID-19 control. On the sectoral scale, the mining sector, most manufacturing sectors, and some services sectors (e.g., accommodation and catering, transport) experienced relatively more significant increases in the indirect loss due to the COVID-19 control. Secondly, the economic resilience tends to be more sensitive to the change of the duration of the containment than its strictness. The indirect economic loss and recovery time increased more on average for each 2-week increase in the containment's duration than for each 10% increase in its strictness. This suggests a stricter but shorter containment that can quickly eradicate the disease to mitigate the overall economic impacts and improve the economic resilience towards the compound event. Thirdly, the COVID-19 control could inhibit the marginal resilience benefits of most flood emergency measures. In general, the economic resilience increases with

the increase of road repair rate, labour recovery rate, financial aid in consumption and production, and reconstruction efficiency. Among these factors, the economic resilience is most sensitive to the change of road repair rate, followed by reconstruction efficiency and consumption subsidies. However, the implementation of COVID-19 control during the compound event would lower the sensitivity of economic resilience to these factors. In other words, the marginal effects of these emergency measures in boosting the economic recovery and resilience are reduced by the COVID-19 control, and such restriction becomes severer in a stricter or longer containment.

The 2021 Zhengzhou 'flood-COVID' compound event studied in this chapter represents a type of extreme events compounded by natural disasters and public health crises. In response to such a compound event, trade-offs have to be made between the needs for disaster relief, pandemic control, and economic stability according to the recovery objective and actual situation. By simulating the post-disaster recovery dynamics and policy effects using the CHEFA model, several policy recommendations are made based on the results in this study.

Although most of the economic impacts resulting from the compound event were concentrated in Zhengzhou's services sectors (i.e., the tertiary industry), sectors in the primary and secondary industries, such as the agriculture, food and tobacco, mining, and non-metallic mineral products sectors, have demonstrated a more profound influence on the production supply chain in wider economic systems (from Henan Province to the whole country), therefore these sectors should be given the priority in the post-disaster reconstruction support and financial aid. This is conducive to achieving a faster restoration of the economic stability from business interruptions, while avoiding a hasty and reckless re-opening of the services sectors which may increase the risk of virus transmission.

Recovery activities in response to the natural disaster should be carried out prudently according to the requirements of COVID-19 control during the compound event. In the serious pandemic risk requiring a strict control, the large-scale responses to the natural disaster to accelerate the economic recovery may not significantly reduce the overall economic loss due to the strong inhibitory effect of COVID-19 control. Besides, although not modelled in this study, literature has shown that the flood-related responses can increase the risk of virus transmission and put further burden on disease control (Ishiwatari et al., 2020; Pei et al., 2020; Salas et al., 2020). Therefore, hasty flood emergency and responses inconsistent with the COVID-19 control requirements will result in a double waste of economic and public health resources. Only when the pandemic risk is alleviated and the containment is relaxed, accelerating the disaster response and recovery can yield better effects in economic loss mitigation and resilience building.

The distribution of financial aid in the fields of production and consumption should take into account the reconstruction efficiency and intertemporal consumption preference in the disaster areas based on the specific recovery target (i.e., to minimize the economic loss or to recover fast) within the budget for emergency funds. Economic sectors can make better use of the reconstruction funds at a higher reconstruction efficiency during the production restoration, leading to less indirect losses. Special support is thus needed for sectors with difficulties in post-disaster reconstruction, including offering professional technical guidance, improving production-facilitated infrastructure services, accelerating the maintenance and renewal of production machinery and equipment, etc. Consumption subsidies can also significantly stimulate the post-disaster economy and abate the economic loss, notably with an appropriate intertemporal consumption preference of the households in the region. The allocation of consumption subsidies could be supplemented by other policy tools which adjust the household consumption propensity or savings rate to the most suitable level, such

as the adjustment of interest rates, issuance of consumer vouchers, and introduction of some innovative financial instruments. In this way, the minimal economic loss of the compound event can be approached given the specific amount of consumption subsidies, which enhances the compound resilience of the affected economy.

The compound events of natural disasters and public health crises generate not only complex impacts on the economic system, but also serious burdens on the public health system. Due to the different scales of measurement, the health and medical costs resulting from the compound event are not considered in this chapter. In the 2021 Zhengzhou 'flood-COVID' compound event, this might not be a big issue as the spread of COVID-19 is under control shortly in a month with little health influence. In this case, most of the economic impacts comes from a reduction in labour supply due to strict traffic restrictions/lockdowns. However, the health impacts can be increasingly significant as cases accumulate quickly during recurring waves of COVID-19 with inadequate responses and restrictions. Rampant infections may put an overwhelming strain on local medical resources and lead to substantial deaths, illnesses, and long-COVID sufferers of working age. In this case, most of the labour shortage arises from no longer the COVID-19 restrictions but the direct health outcomes of the disease itself, which then cannot be ignored in the economic impact modelling. An increasing number of studies have discovered profound impacts of (long-term) COVID on workers in countries such as the US, the UK, and Germany (Do Prado et al., 2022; Goda and Soltas, 2022; Peters et al., 2022; Reuschke and Houston, 2022). With more and more countries (including China after December 2022) lifting all COVID-19 restrictions, it raises the necessity of integrating the health and economic modelling for such compound hazards in future research.

Overall, when battling compound events of natural disasters and public health crises, the specific strategy to be adopted requires a full consideration of not only economic

but also public health implications. The quantitative analysis in this chapter provides estimations on the potential economic costs of different response and recovery strategies, which can be used in combination with other epidemiological or health models by policy makers to find a balance between the economic and health needs during the compound risk governance. Estimation of labour productivity or working time loss due to COVID-19 infections (e.g., deaths, illnesses, and long-COVID sufferers of working age) may provide a possible way to integrate the health impacts into economic modelling, which is similar to that of heat stress (Section 3.1.1.2). However, information about COVID-19 in labours has only been investigated for very limited countries (mainly developed countries, e.g., the US, the UK, and Germany) so far (Goda and Soltas, 2022; Peters et al., 2022; Reuschke and Houston, 2022). A well-established database covering numerous (developed and developing) countries on the empirical relationship between labour productivity loss and COVID-19 infection rate is still needed to benefit future studies in this regard.

Finally, the modelling framework used in this chapter can be generalized to a wide range of compound events comprising of various natural disasters (e.g., floods, heatwaves, droughts, and wildfires), air pollution, public health emergencies, trade wars, or even military attacks, etc., facilitating the investment decisions on improving the preparedness for future crises.

Chapter 8 Conclusions

This PhD thesis has explored an integrated and holistic way of accounting for the total economic impacts of compound hazards against the complex backdrop of climate change, COVID-19 pandemic, and deglobalisation. The notion of 'disaster footprint' is introduced to capture the cascading effects of adverse shocks through interdependencies between sectors and regions over the entire period of economic recovery. Interactions between compound shocks and their risk transmission channels are embedded within a macroeconomic risk assessment framework with the development of the CHEFA model in this thesis (Chapter 3). The model has provided a consistent metric and framework for impact estimation that bridges single-hazard and compound-hazard analysis, with wide applicability to various natural and manmade hazards with or without climate change and socio-economic development (Chapter 4 to Chapter 7). This research has filled in part of the research gaps in hazard analysis and offered policy implications on disaster risk mitigation and adaptation. Key findings, contributions, and limitations of this work are discussed in this chapter.

8.1. Summary of Work and Key Findings

This thesis has successfully addressed the six research objectives (ROs) raised in Section 1.4.2. Specifically, Chapter 1 contributes to RO1 by introducing the increasing likelihood of concurrent extreme events to create a compound hazard and how different hazards interact in the economic system to challenge disaster response and recovery. Chapter 2 contributes to RO2 by offering a systematic review of the existing literature on assessing the direct and indirect economic impacts of various types of natural and manmade hazards, as well as the emerging concerns for compound hazards. Chapter 3 first contributes to RO3 by developing the Disaster Footprint model (DF-

growth and DF-substitution versions) which improves on traditional models for hazard-induced indirect economic impact assessment from the perspectives of supply chain cascading effects. It then contributes to RO4 by constructing the CHEFA model for compound hazard economic impact assessment based on the DF-substitution model proposed previously. Chapters 4-7 contribute to RO5 together by providing a series of applications of the models developed in this thesis from different angles. Chapter 4 applies the DF-substitution model to analyse the historical trends of hazard impacts (including heat stress, air pollution, and extreme weather events) in China under a single-hazard analytical framework. Chapter 5 uses the DF-growth model to project the economic impacts of future fluvial flooding in six vulnerable countries under climate change and socio-economic development. Chapter 6 offers a numerical illustration of the CHEFA model to test its robustness under a wide range of hypothetical compound hazard scenarios. Chapter 7 applies the CHEFA model to examine the multi-regional supply chain impacts of a real compound hazard case comprising of extreme floods and a COVID-19 wave in 2021 in the Zhengzhou city of China. Chapter 6 and Chapter 7 also contribute to RO6 through a series of sensitivity analyses to explore factors that may have significant influence on the compound resilience or recovery of the economy. This helps to draw useful suggestions for policy makers to improve disaster management in complex situations, which will be discussed in Section 8.3 of Chapter 8.

Based on the work of this thesis, the four research questions (RQs) can be briefly answered as below:

RQ1) What are the unique characteristics of a compound hazard in terms of disrupting the production supply chains?

A compound hazard driven by multiple individual hazards can cause greater economic impacts than individual hazards in isolation, as the concurrent hazards can

interconnectedly propagate through the production supply chain and exceed the coping capacity of a system more quickly (Chapter 1). Therefore, it requires a different way of accounting for the compound hazard-induced economic impacts from the traditional single-hazard analytical framework.

RQ2) What is the most suitable framework applied to assess the economic impacts of a traditionally single hazard considering supply chain effects?

It has been confirmed that the hybrid approach has an advantage in assessing the hazard-induced economic impacts by combining the simplicity of IO modelling with the greater plausibility of the CGE approach (Chapter 2). Following this vein, the Disaster Footprint framework is proposed to capture the cascading effects of a hazardous shock along the production supply chain (Chapter 3) and proves applicable under a wide range of single-hazard scenarios (Chapters 4-5). It outperforms other methods by the greater flexibility to include important hazard-induced economic constraints and adaptive factors (e.g., capital recovery, inventory adjustment, and demand redistribution in the DF-substitution version for the short-term analysis and capital recovery and economic development in the DF-growth version for the long-term analysis), leading to more reliable simulation of post-hazard economic dynamics.

RQ3) How to incorporate the characteristics of a compound hazard into this framework, which is previously intended for a single hazard, in order to properly assess the compound impacts?

The CHEFA model, which is built under the Disaster Footprint framework (DF-substitution in particular), has proved an effective tool for assessing the economic impacts of a compound hazard along the production supply chain (Chapter 3). Using the confluence of flooding, pandemic waves, and/or export restrictions as examples (Chapters 6-7), the model first interprets each individual hazard as a direct labour or capital shock to production, an external constraint to output delivery and allocation, or

an abrupt disruption to final demand, and then integrates the impacts on these different parts of the economy into the backward and forward supply-chain risk transmission channels to simulate how the overlapping hazards are interweaved in the economic network. The effects of production specialization, external subsidies, and reconstruction expenditures are also considered in the modelling of relevant compound-hazard scenarios.

RQ4) How to evaluate the relevant factors that may influence the economic resilience towards such a compound hazard?

Economic resilience to a compound hazard (including hazard-induced economic losses and/or recovery time) is confirmed to be sensitive to model parameters (e.g., inventory size, inventory restoration rate, maximum overproduction capacity, overproduction adjustment time, duration and strictness of pandemic control, road repair rate, labour recovery rate, intertemporal consumption preference, and reconstruction efficiency) or external factors (e.g., consumption subsidies and reconstruction funds) through a series of sensitivity analyses (Chapters 6-7). Comparatively, changes in inventory size, road repair rate, and pandemic control characteristics have the most significant impacts on the compound resilience among all parameters and factors. Some useful policy implications can be drawn from the results of these sensitivity analyses (Chapter 8).

Table 8-1 summarizes the results for the case studies in this thesis. Though using a rather consistent accounting framework, the cumulative economic impacts of different single-hazard or compound-hazard events vary substantially due to the distinctive hazard characteristics and socio-economic contexts presented in these case studies. Here all impacts are expressed in relative terms as a share of regional GDP to eliminate the influence caused by discrepancies in the size of the economy and currency unit used in these case studies.

Table 8-1: Summary of results of case studies in this thesis.

Hazard scenarios			**Direct DF**	**Indirect DF**	**I/D ratio**
Historical patterns in China (2015-2020)	Heat extremes		0.54%-0.72%	0.69%-0.92%	1.28-1.27
	Air pollution		0.064%-0.055%	0.011%-0.008%	0.17-0.14
	Weather extremes		0.3632%-0.3633%	0.12%-0.09%	0.32-0.24
Future river flood risks under climate change (CC+SE, global warming level increases from below 1.5°C to 4°C in 2100)	China	Baseline period (1961-1990)	0.24%	2.43%	10.30
		Future period (2086-2115, <1.5°C-4°C)	0.12%-0.37%	0.14%-0.73%	1.20-1.98
	Ghana	Baseline	0.03%	0.21%	6.77
		Future	0.01%-0.06%	0.09%-0.62%	12.68-10.85
	Egypt	Baseline	0.01%	0.46%	66.85
		Future	0.08%-0.29%	1.13%-2.99%	13.54-10.25
	Brazil	Baseline	0.04%	0.36%	9.16
		Future	0.02%-0.17%	0.17%-1.80%	9.23-10.81
	Ethiopia	Baseline	0.09%	1.09%	12.26
		Future	0.01%-0.02%	0.09%-0.28%	10.79-11.77
	India	Baseline	0.05%	0.53%	11.81
		Future	0.02%-0.22%	0.13%-1.31%	5.919-5.916
Hypothetical perfect storm in a multiregional economy	Single flood (from small to large scales)		3.30%-9.90%	0.52%-3.01%	0.16-0.30
	+ Pandemic (30% - 24 weeks)		3.30%-9.90%	12.42%-13.83%	3.76-1.40
	+ Trade restrictions (50% with retaliation)		3.30%-9.90%	14.34%-15.50%	4.35-1.57
	+ Production specialization		3.30%-9.90%	28.61%-30.46%	8.67-3.08
The 2021 Zhengzhou 'flood-COVID' compound event in China			0.07%	0.06%	0.98

Notes: Direct and indirect Disaster Footprint (DF) are the disaster-induced economic impacts expressed in relative terms as a percentage of the regional GDP. I/D ratio is the ratio of indirect DF to direct DF. For the case study of future river flood risks, the direct and indirect DF are given by the average annual estimates under CC+SE experiments, i.e., considering the combined effects of climate change and socio-economic development.

First, China has witnessed an alarming upward trend in heat-related economic costs between 2015 and 2020, while suffering slightly decreased losses resulting from air pollution and other extreme weather events like floods and storms. Changes in air pollution-related economic costs have reflected the progress towards air pollution control seen in previous years in China. The relative impacts of extreme weather events have fluctuated downward over a longer time frame (2009-2021), but with notable surges in specific years (i.e., 2010, 2013, and 2016) (see Figure 4-7). Still, the economic impacts of these three hazards have been increasing on the whole, in relative terms of the national GDP, as heat extremes have dominated the climate risk in these years. Regionally, southern provinces in China appeared to be more vulnerable to heat stress while northern provinces more susceptible to air pollution. Other weather-related extreme events were more distributed in Chinese provinces, with Jiangxi (a province in southern China) and Heilongjiang (a province in northern China) suffering the greatest economic losses.

Second, while considering the joint effects of climate change and socio-economic development, Egypt faces the greatest increase in flood-induced average annual economic losses as the global temperature climbs from below 1.5°C to 4°C at the end of the 21st century, compared to the baseline period (1961-1990). Whilst flood risk was low in the baseline period in Egypt, it increases in the future, driven by increased precipitation in upstream areas and increased exposure of population and economic activities in the Nile Valley within the country. By contrast, the economic losses in Ethiopia and China decrease from the baseline levels in future warming scenarios from <1.5°C to 4°C, mainly due to a rapid socio-economic development that makes the two countries more resilient towards the intensified river flood risks under climate change. Such positive effects of socio-economic development are also seen in Brazil, India, and Ghana, but only when the global warming is controlled well beneath a certain level (2.5°C for Brazil and Ghana and 3°C for India). In other words, for these three

countries, while the economic losses as a proportion of GDP initially decline from the baseline at lower levels of warming, increases are observed from 2.5°C or 3°C warming onwards, suggesting a tipping point where increasing flood risk outweighs any relative benefits of socio-economic development (see Figure 5-2). This is consistent with the finding of Dottori et al. (2018) where the relative flood damage decrease with warming particularly for fast growing economies. Therefore, it is important to consider changing socio-economic characteristics such as population change, land-use change and economic growth trajectories, alongside climate change.

Third, as the world enters the third year of COVID-19 pandemic, there has been an increasing likelihood of perfect storms created by the confluence of climate extremes (exemplified by floods), pandemic lockdowns, and geoeconomic tensions (proxied by trade restrictions). By simulating the disaster footprint of such a perfect storm in a hypothetical global economy, this thesis distils the potential interplays between these three different types of hazards in the economic system (see Chapter 6). It has been found that a pandemic control can seriously aggravate the flood impacts mainly by disrupting the reconstruction process of damaged capital, supporting the prevalent claims on the negative effects of virus containment on flood responses in the literature (Ishiwatari et al., 2020; Selby and Kagawa, 2020; Swaisgood, 2020). Conversely, a flood can only exacerbate the pandemic impacts when the negative effects of capital damage exceed the stimulus effects of capital reconstruction (usually for large-scale floods). A flood can also accelerate and extend the shortage of inventories connected to the pandemic control, which is another way of aggravating the pandemic impacts. Moreover, the combination of trade restriction and production specialization can further greatly worsen the compound economic losses during the perfect storm. The trade restriction of a region on a substitutable product, which hampers the global recovery, may alleviate its own losses only if the increasing domestic demand exceeds the negative impacts of the falling exports. However, the trade restriction of a region

on a non-substitutable product would always exacerbate its own losses as the restriction impairs the recovery of the global supply chain so severely that it backfires at the economic resilience of the region itself. Finally, the subsequent retaliation from another region and sector would further deteriorate the global recovery and make everyone lose, with the region which initiates the trade war losing much more when the retaliatory restriction is also imposed on a non-substitutable product.

Fourth, using the CHEFA model developed in this thesis, the case study of the disaster footprint of the 2021 Zhengzhou 'flood-COVID' compound event in China has provided further evidence on the interactions between flood hazards and pandemic control, as well as factors that may affect the compound resilience of China's economy. This compound event has caused substantial economic consequences not only to the city directly hit, but also the whole nation due to the propagation effects along the production supply chain (see Chapter 7). The COVID-19 control in Zhengzhou has increased the indirect economic loss by 77% from 36.8 billion yuan to 65.1 billion yuan nationwide and delayed the full recovery of the economy by one week (from 18 weeks to 19 weeks). It has also weakened the marginal effects of flood emergency efforts in mitigating the indirect economic losses or boosting the compound economic resilience. Resilience can be enhanced through the acceleration of post-disaster road repairs, followed by improvements to reconstruction efficiency, consumption subsidies, and reconstruction funds, and least by the speeding up of labour recovery. The impact of intertemporal consumption preference, which reflects the marginal propensity to consume for each unit of income change at present, on the compound resilience is uncertain and depends on the size of consumption subsidies. The compound resilience increases with increasing willingness to consume for a smaller-scale consumption subsidy (less than 10%-15% of the direct damage), while decreases for a larger-scale consumption subsidy.

Apart from the above-mentioned case-specific findings, some general insights on the features of disaster footprint can also be drawn from the results of these case studies.

The indirect disaster footprint, which arises from the propagation effects along the production supply chain, can account for a considerable part of the total economic impacts and sometimes even exceed the scale of direct damage of extreme events. In estimating the short-term disaster footprint of single-hazard events, the ratio of indirect to direct economic costs (I/D ratio) ranges from 1.27 to 1.28 for heat stress, from 0.14 to 0.17 for air pollution, and from 0.24 to 0.32 for extreme weather events in China over the period of 2015-2020. This indicates that heat stress tends to trigger higher cascading effects to wider economic systems and thus more attention should be paid to heat adaptation. The I/D ratios of extreme weather events (mainly floods and storms) calculated in this study is close to the estimates of Hallegatte (2008, 2014) for the Hurricane Katrina (0.17-0.39), demonstrating a certain degree of consistency between the Disaster Footprint model and the ARIO model. Surprisingly, for the long-run estimation in combination of climate change and socio-economic development, the I/D ratio of a fluvial flood hazard rises substantially to a wider range between 1.20-66.85 in countries of China, Ghana, Egypt, Brazil, Ethiopia, and India under various global warming levels (<1.5°C-4°C). This has been explained by the lost opportunities for economic growth due to flood damage, which pushes the economy further and further away from its potential growth trajectory if the floods had not occurred (see Figure 5-6). Consequently, the indirect economic losses can continuously accumulate over the long run when allowing for economic growth. Moreover, the compounding of multiple hazards may also greatly amplify the indirect economic losses and the corresponding I/D ratio due to the potential interactions between these hazards. In hypothetical scenarios of perfect storms, the I/D ratio soars up from 0.16-0.30 (in the single-flood scenarios) to 1.27-3.93 with the intervention of pandemic control, further to 1.41-4.35 with export restrictions on substitutable products, and ultimately to 2.73-8.67 when the

restrictions are imposed on specialized non-substitutable products. In the real case of the 2021 Zhengzhou 'flood-COVID' compound event, the non-pharmaceutical interventions of COVID-19, such as lockdown restrictions, has increased the indirect economic losses from 55% to 98% of the direct damage caused by the flood.

Second, despite the generally negative impacts on the total output of the directly and indirectly affected economies, some sectors and regions may experience a temporary boom in the disaster aftermath due to their roles in reconstruction or by taking over the lost production of other more severely damaged suppliers. In China, such economic gains have been seen in Qinghai Province in the aftermath of heatwaves in 2021 and air pollution in 2020 (Figure 4-4 and Figure 4-6), as well as in provinces or cities of Tianjin, Shanghai, Jiangsu, and Hainan following extreme weather events in 2019 (Figure 4-7). Production in these regions has been less directly affected by the hazards, but instead more stimulated by the combined effects of post-disaster reconstruction, overproduction expansion, and inter-regional substitution. The stimulus effects of a natural hazard can also help alleviate the negative impacts of a pandemic control, as has been found in the perfect storm scenarios (Chapter 6). Likewise, after the 2021 Zhengzhou 'flood-COVID' compound event, the construction, ordinary machinery, and transport equipment sectors in Henan Province (outside Zhengzhou) have witnessed an increase in their value added for similar reasons (Table 7-5).

Third, regarding the effect of pandemic control in aggravating the compound disaster footprint, it has been found that a stricter but shorter containment that can quickly eradicate the virus would impose a smaller economic loss than a milder but longer one in collision with natural hazards like floods (Chapter 6 and Chapter 7). The compound disaster footprint appears to be more sensitive to the duration of a lockdown than its strictness. This is consistent with the results of Guan et al. (2020) who examined the global supply-chain effects of COVID-19 control measures in a single-hazard setting.

Moreover, if a pandemic intervention is implemented when the economy has not been fully recovered from the previous flood, it would result in more economic losses than an earlier pandemic control prior to the flood. This is because the subsequent containment tends to cause longer-lasting interference with the flood-related reconstruction and recovery than the preceding one (Figure 6-2). Therefore, a timely pandemic intervention is advocated to mitigate the disaster footprint or enhance the economic resilience in compound crises.

8.2. Contributions and Innovations

This PhD thesis has advanced the current understanding of the economic impacts of compound hazards from a holistic perspective. It improves the methodologies in integrated disaster footprint accounting, provides quantitative evidence on the economic interplay between individual and interrelated hazards, and explores the potential factors conducive to the building of compound resilience to future risks.

Regarding the methodological innovations, this thesis has comprehensively addressed the primary research aim of 'how to measure the economic impacts of a compound hazard cascading through the production supply chains?' through the original development of the CHEFA model with the notion of disaster footprint along the production supply chain. As noted in Section 2.4, studies that have tried to model compound hazards are still very limited. The CHEFA model has managed to combine the risk transmission channels for climate, pandemic, and geoeconomic shocks and embed their interactions into economic impact assessment, filling some of the research gaps in compound hazard analysis. Particularly, it analyses the interactions between climate and pandemic responses, that is, the negative externality of pandemic control on the recovery of capital destructed by natural disasters and the stimulus effects of capital reconstruction to offset the negative impacts of pandemic control. It also

considers the roles of export restriction and production specialization in exacerbating the economic consequences of compound events. Export restriction is a common trade policy signalling deglobalization, while production specialization reduces the substitutability of regional products and may increase the economic vulnerability for negative shocks.

By linking the CHEFA model with catastrophe models, this thesis presents the first integrated framework for capturing both the direct and indirect disaster footprint of compound hazards on the sectoral and regional scales. This provides consistent and comparable impact metrics between single-hazard and compound-hazard analysis and can be easily generalized to a broad variety of compound hazard scenarios, pushing the boundaries of applications and knowledge in relevant fields.

Also, this thesis has improved the methods of indirect disaster footprint accounting, on which the CHEFA model is based. This includes: 1) the expansion to a multiregional approach allowing for substitution between or demand redistribution among suppliers from different regions, 2) the endogenization of capital recovery through the introduction of reconstruction demand, 3) the modelling of inventory dynamics to buffer an immediate input shortage with a specific adjustment time, and 4) the incorporation of the effects of external subsidies, reconstruction expenditures, and intertemporal consumption preferences on post-disaster production and consumption adaptations. Although some of these factors have been considered in the literature, this thesis establishes the first framework that brings all these factors together to provide a more complete assessment of the indirect disaster footprint of an extreme event. It also considers the crowding-out effect of reconstruction costs on household consumption, which has been previously ignored in existing models.

In terms of contributions to applications, this thesis has applied the proposed methods

to several representative case scenarios, demonstrating the flexibility and feasibility of the approach and offering valuable insights on the risk management of various single- or compound-hazards.

First, this thesis has conducted the first retrospective investigation on the economic costs of major hazards (i.e., heat stress, air pollution, and extreme weather events) at the provincial level in China. A further comparative analysis of these hazards has shed some light on where the past hazard control efforts have made encouraging progress and where to strengthen the risk governance in China. The results have been synthesized into a policy report to support the formation of the national climate change adaptation strategy for future risks.

Second, this thesis has complemented the current knowledge of future fluvial flood risks for several developing and most vulnerable countries. While previous studies have projected future fluvial flood risks on spatial scales from national to global, most of them were only focused on direct flood damage or carried out with fixed socio-economic conditions under a limited range of global warming. This study is novel in that it presents an integrated flood risk analysis on both direct and indirect economic impacts of future fluvial floods due to the combined effects of climate change and socio-economic development covering the full plausible range of warming levels from <1.5°C to 4°C. The socio-economic drivers have included land cover change, capital accruement, population growth, technical progress, and economic structural shift. The post-flood economy is also allowed to recover to a higher level than the initial state to reflect a long-term impact of flood shocks, of which previous studies have fallen short. The results of this study have demonstrated that socio-economic drivers can be just as or more important than climate drivers and therefore should be included when estimating the future dynamics of fluvial flood risks.

Finally, this thesis has provided timely information on the comprehensive economic consequences if a pandemic control collides with other types of hazards. Despite an extensive concern in academia about the rising likelihood of compound hazards, quantitative studies of their potential economic impacts are still rare. For the first time, the direct and indirect disaster footprint of a triple event comprising of natural, pandemic, and trade shocks has been tracked down along the global supply chain, though using hypothetical case scenarios. The analysis has revealed how these hazards are interrelated and transmitted within the economic system, which is important for advancing understanding and governance of compound risks. In a similar vein, this thesis has also offered the first piece of evidence on how the collision of pandemic control and extreme floods can affect the local economy and spilled over to wider regions focusing on a real compound event in the capital city Zhengzhou of Central China's Henan Province in 2021. Sectors and regions that are crucial for pushing the economic recovery have been identified, as well as mitigating factors for compound hazard impacts through a series of sensitivity analyses on modelling parameters and other external factors. These factors include pandemic control policies, inventory adjustment and overproduction expansion strategies, financial aid for consumption and reconstruction, road and labour recovery rates, and intertemporal consumption preferences. Results in these studies have real-world significances in a more balanced response to the colliding hazards. They have shown how the confluence of different hazards can aggravate the socio-economic consequences and where to prioritize the recovery efforts and funds to boost the compound resilience. The potential for huge economic costs of compound hazards has demonstrated the value of ex ante risk assessment, planning and the implementation of early and adequate adaptation and mitigation actions towards climate change.

8.3. Policy Implications

Knowledge of economic impacts after a compound event is required to responsibly invest in the building of economic resilience towards an increasing likelihood of compound hazards in a post-pandemic world under climate change. After all, the potential benefit of taking active risk reduction and adaptation measures is equal to the decline in economic loss due to these measures. Moreover, recognizing the constraints from one hazard while responding to another can facilitate the formation of a balanced strategy which minimizes the economic losses from the trade-offs between the conflicting emergency needs. The CHEFA model developed in this thesis can serve as a tool to assist in evaluating different strategies for battling compound hazards, with multi-sectoral and -regional results contributing to the formation of an integrated risk governance system. This is important to achieving the objectives of the Sendai Framework for Disaster Risk Reduction, which explicitly calls for a multi-hazard and multi-sectoral approach to increase the efficiency and effectiveness of disaster risk reduction practices (UNISDR, 2015). In light of this, the main findings of this thesis have elicited several policy implications, which are discussed below.

First, after analysing the economic costs of multiple hazards (including heat stress, air pollution, and extreme weather events) in China over the past years, it has been concluded that heat stress has accounted for a dominant part of the total economic costs, mainly driven by the reduction in labour productivity, and thus should be given the priority in the integrated disaster risk management. Considering the sectoral distribution of direct and indirect costs of heat stress, efforts should be made to increase the heat adaptability of outdoor sectors (such as agriculture and construction), as well as to improve the supply chain resilience to mitigate the spillover effects of heat-related health impacts. Different provinces in China tend to suffer diverse impacts from different hazards. These location-specific economic impacts of climate change require

location-specific response measures, including enhancing inter-departmental cooperation, strengthening climate emergency preparedness, supporting scientific research, raising public awareness, and promoting climate change mitigation and adaptation.

Second, national mitigation and adaptation strategies for future flood risks should consider the effects of not only climate change but also socio-economic development, as indirect economic losses could rise significantly if the lost potential for economic growth is also included. Another reason is that the increasing flood risks due to climate change can result in different economic consequences according to the level of development in different countries. Some fast-growing economies (e.g., China) may experience decreases of relative economic losses from the baseline in all, or some lower levels of, future warming scenarios, while other economies become increasingly exposed and vulnerable. The tipping point from a decreasing to increasing economic loss differs between countries, which may eventually affect their climate ambitions. Therefore, global cooperation in climate change mitigation and adaptation should not only consider the differentiated responsibilities of countries, but also take full advantage of their diversified incentives.

Third, in response to the collision of pandemic and natural hazards, trade-offs have to be made between the needs for disaster relief, pandemic control, and economic stability. Fast and reckless recovery of labour supply or transportation capacity following an extreme weather event has proved to be uneconomical and increase the burden of disease control during a serious pandemic. Instead, post-disaster reconstruction should be carried out prudently according to the progress of pandemic control to help the economy through the compound crisis as smoothly as possible.

Fourth, a timely, stricter but shorter pandemic control is generally suggested to reduce

the total economic losses resulting from the compound event comprising of pandemic and other hazards. Also, more policy and financial support should be directed to the recovery of sectors and regions that are more closely connected to other sectors and regions within the economic network.

Fifth, financial policies on reconstruction funds and consumption subsidies need to take into account the roles of reconstruction efficiency and intertemporal consumption preference, respectively, of sectors or regions hit by the compound event. For one thing, an increased reconstruction efficiency can help sectors make better use of the reconstruction funds in accelerating the restoration of production. Support to boost the reconstruction efficiency for sectors in difficulties includes offering professional technical guidance, improving production-facilitated infrastructure services, accelerating the maintenance and renewal of production machinery and equipment, etc. For another, an appropriate intertemporal consumption preference of the households in the region can help promote the stimulating effects of consumption subsidies on the post-event economic performance. Therefore, financial tools which can adjust this household characteristic should be leveraged accordingly, such as interest rates, consumer vouchers, and other innovative instruments. In addition, the distribution of financial aid in these two fields within the emergency budget depends on the comparison of economic benefits from investment in each side, as well as the specific recovery target (i.e., to minimize the economic loss or to recover fast).

Sixth, regional or global cooperation is also advocated to ease the negative impacts of deglobalization, at least rigorous trade policies that avoid highly specialized sectors are required confronting the perfect storm. After all, policies that lead to higher trade barriers undermine the efforts of other countries battling extreme weather events and a pandemic, particularly when these barriers are imposed on specialized products that cannot be substituted elsewhere. This raises the need for effective discipline at the

global level of the use of such measures.

Finally, the results of case studies on compound hazards have confirmed that the intersection of interrelated hazards will amplify the economic consequences to various degrees compared to individual hazards. However, most insurance/reinsurance companies, institutions, and governments in the world are still recording and acting on individual hazards without fully considering their combined effects. The underestimation of economic impacts and ignoring the interplay between hazards may lead to insufficient and improper responses of communities during compound hazards. Therefore, a holistic strategy that can address multiple co-existing hazards within a system is advocated in preparing for future crises. Interdisciplinary, cross-sectoral, and multi-hazard risk assessments could provide relevant stakeholders (e.g., residents, insurers, industries, and governments) with a more complete picture of risks to their business or lives. A platform integrating multiple types of data and information should be established to encourage multi-stakeholder collaboration at different scales and inform the deployment of emergency resources across sectors and hazards. This should eventually facilitate the formation of integrated and robust solutions and the planning of anticipatory actions, considering the interactions between hazards and trade-offs or co-benefits across emergency needs under a range of complex scenarios.

8.4. Limitations and Future Work

Despite the efforts to fill the existing research gaps, this thesis is subject to some limitations and inherent uncertainties in terms of data and methodologies. Such shortcomings are critically reviewed in this section and suggestions for further research are provided.

First, regarding the methodology of assessing the disaster-induced direct economic

impact, this thesis has adopted a very limited set of heat-related or air pollution-related ERFs and loss functions, as well as flood-related depth-damage functions, for subnational-level analysis. This is because region-specific information on these functions for a developing country like China is usually not available so far. It should be also noted that these functions are assumed to remain constant during the study period due to little investigation and limited data on how the population has adapted or will adapt to the related hazards. Uncertainties in these functions might create estimation biases, which necessitates further research on more localized provincial- or city-level ERFs and hazard-loss functions, as well as research that incorporates the factor of population adaptation into the direct impact modelling.

Second, regarding the methodology of assessing the disaster-induced indirect economic impact, although this thesis has allowed for inventory adjustment, interregional substitution, and other factors to increase the flexibility of the economic system in response to external shocks, the market-based price mechanism has not been included. After an extreme event, prices of some products may increase due to supply shortages or demand surges, which may have higher-order impacts on the production of other connected sectors in the economy. However, in most short-term post-disaster situations, price fluctuations have been observed to be very limited due to socioeconomic inertia, transaction costs, and antigouging legislation (Hallegatte, 2014). Moreover, another limitation is that the production expansion, rationing scheme, and demand adaptation (i.e., through redistribution) following an extreme event are modelled based on ad-hoc behavioural rules in this thesis. While these rules are usually assumed to approximate the average decision-making of a representative agent confronting the disaster hazard according to real-world observations, they may not equally well represent the decision of everyone in the affected group due to the heterogeneity of micro-agents. Therefore, the author suggests that more solid microeconomic foundations should be included in future modelling of indirect hazard

impact, for instance, by drawing on some agent-based methods, to enable a more reliable analysis at micro levels.

Third, in terms of validating results, estimates for flood-induced direct damage have been compared with data from the global dataset or official reports for case studies in this thesis. However, it is difficult to verify the estimates for disaster-induced indirect impacts due to the lack of empirical data on dynamics of business recovery in the disaster aftermath. Even if there exists some aggregate data on post-disaster economic changes, it is still difficult to distinguish the disaster impact from other socio-economic factors that simultaneously influence the economy. Instead, this thesis has compared the results with other related studies in literature and explained the consistencies and discrepancies in findings about indirect disaster impact.

Fourth, with respect to case studies, Chapter 4 has not considered morbidities caused by heat stress and air pollution due to data limitations. It is argued that morbidity rates of these hazards could entail larger economic costs than mortality rates (Xia et al., 2016; Xia, Li, et al., 2018). To provide a more complete estimation on economic costs, it is urged that the effects of both mortality and morbidity rates of heat stress and air pollution should be taken into consideration in future studies. Besides, the impact assessment for historical extreme weather events in China has not considered the potential labour constraints caused by these events, also due to data limitations. However, evidence from other studies, in Chapter 5 for example, has shown that labour supply is often much less affected by an extreme weather event than capital assets and therefore tends to have little effect on the estimated economic impacts. In addition, it is recognized that the multi-provincial analysis is only carried out for the year with access to the latest data, which differs among the studied hazards. The provincial-level results could be much enriched if data on the same spatial scale becomes available for consecutive years over a longer time span.

Fifth, while Chapter 5 has included changes in land cover and economic structure to examine how socio-economic development will affect flood-induced economic impacts under climate change, this is done by updating the land cover map and national IO table to the latest available year for each of the studied countries. Projecting future land use and economic structure, particularly for multiple countries over a period as far as 2100, is always difficult. Even if such projections do exist, they are often at a coarser resolution and subject to complex assumptions, which may increase the uncertainty of economic calculations. Therefore, this chapter simply assumes that the land cover and economic structure of each country are constant within each of the baseline and future periods, though different sets of land cover maps and IO tables (earliest version vs. latest version) are used to reflect, to some extent, changes in land use and economic structure from the baseline to future period. In other words, all sectors are assumed to grow at the rate with the recorded or projected national GDP during the baseline or future periods. Yet, it would be interesting if the impacts of economic structural change and land use change could be further separated. This could be done in future work by adding a third group of experiments which only updates the land cover map to the latest available year and uses the same baseline IO table for future projections.

Sixth, when applying the CHEFA model to the collision of pandemic and other hazards, Chapter 6 and Chapter 7 have mainly focused on the economic-wise hazard characteristics and their interconnections in economic risk transmission and do not distinguish the differences in hazard warning, physical impact, and response phases. Particularly for the pandemic hazard, these case studies are limited to the economic impacts of non-pharmaceutical interventions, such as transportation restrictions, rather than other mitigation measures like testing, therapeutics, and vaccines. Admittedly, these pandemic interventions could bring in new economic costs and/or benefits which

may interact with the effects of responses to other hazards, but it is beyond the research scope of this thesis to model all these factors. Also, the health costs (i.e., monetary values of health impairment) caused by the pandemic itself are not considered in this thesis. However, the health-related interactions and impacts could be incorporated in future research through the combination of macroeconomic and epidemiological models. This could provide more comprehensive perspectives guiding policy makers to find a balance between socioeconomic stability and public health needs during the compound risk governance, which could be of vital importance for boosting the preparedness for future crises.

Appendices

Appendix A. Tables

Appendix Table A1: Main characteristics of the Leontief IO, Ghosh, ARIO, ARIO-inventory, DF-growth, DF-substitution and CHEFA models.

Models	Spatial scales	External shocks	Propagation effects	Production functions	Production bottlenecks
Leontief IO	Single-regional	Demand-side	Backward	Leontief type	×
Ghosh	Single-regional	Supply-side	Forward	Leontief type	×
ARIO	Single-regional	Supply-side	Backward and forward	Leontief type	Addressed by iteratively reducing production to satisfy the intermediate orders
ARIO-inventory	Single-regional	Supply-side	Backward and forward	Leontief type	Addressed by inventory dynamics
DF-growth	Single-regional	Supply-side	Backward and forward	Modified Leontief type with labour-side technical progress	Addressed by a linear programming technique to optimize the production and imports
DF-substitution	Multi-regional	Supply-side	Backward and forward	Modified Leontief type allowing for substitution of inputs from the same sector in different regions	Addressed by inventory dynamics
CHEFA	Multi-regional	Supply- and demand-side (i.e., compound)	Backward and forward	Modified Leontief type distinguishing between specialized and non-specialized intermediate inputs	Addressed by inventory dynamics

Notes: × means that the model does not take this into consideration.

Appendix Table A2: Main characteristics of the Leontief IO, Ghosh, ARIO, ARIO-inventory, DF-growth, DF-substitution and CHEFA models (continued).

Models	**Rationing scheme**	**Substitution effects**	**Adaptive behaviours**	**Recovery**	**Relevant literature**
Leontief IO	×	×	×	× (Depend on the disappearance of external shocks)	Miller and Blair (2009)
Ghosh	×	×	×	× (Depend on the disappearance of external shocks)	Ghosh (1958); Xia et al. (2016)
ARIO	Mixed scheme: prioritize intermediate orders, then ration final orders proportionally	Substitution by imports from outside the region	Price responses, intermediate and final demand adaptation, and overproduction capacity	Recover to the pre-disaster level through capital reconstruction	Hallegatte (2008)
ARIO-inventory	Proportional rationing scheme among all orders	×	Overproduction capacity	Recover to the pre-disaster level through capital reconstruction	Hallegatte (2014)
DF-growth	Mixed scheme: prioritize intermediate orders and basic consumption orders, then ration other final orders proportionally	×	Satisfaction of a basic demand	Recover to a higher level considering economic growth (for the long-term analysis)	Developed by this thesis
DF-substitution	Mixed scheme: prioritize intermediate orders, then ration final orders	Substitution between regions within the economy	Overproduction capacity and demand redistribution	Recover to the pre-disaster level through capital reconstruction	Developed by this thesis
CHEFA	Mixed scheme: prioritize intermediate orders, then ration final orders	Substitution between regions within the economy, but with export restrictions	Overproduction capacity, demand redistribution, crowding-out effect of reconstruction costs on final consumption, and external subsidies	Recover to the pre-disaster level through capital reconstruction	Developed by this thesis

Notes: × means that the model does not take this into consideration.

Appendix Table A3: List of key variables in the CHEFA model.

Variables	Definitions
N	Number of production sectors making unique products in the economy
M	Number of specialized products
R	Number of regions in the economy
R^i	Set of regions supplying product i
$a_{j,ir}$	Intermediate input j required to produce one unit of product i in region r
$b_{q,ir}$	Primary input q required to produce one unit of product i in region r
n_{ir}^j	Weeks of intermediate use of inventory product j that sector i in region r wants to hold
$S_{ir}^{j,G}$	Targeted inventory level of intermediate input j held by sector i in region r
η_r^{js}	Product j in region s invested in one unit of capital formation of sectors in region r
$\alpha_{ir}^{\max}$	Maximum overproduction capacity of sector i in region r relative to the pre-disaster level
τ_α	Weeks needed by a sector to achieve its maximum overproduction capacity
τ_s	Proportion of inventory losses that a sector attempts to restore in the next time step
ρ_i	Impact multiplier of transport disruption on the operation of sector i
β_L	Labour recovery rate - proportion by which the affected labours are reduced per next period
β_Z	Flood-related transport recovery rate - proportion by which the flood-related transport disruptions are alleviated per next period
β_C	Intertemporal consumption preference - the impacts of an income change on consumption are reduced by $1-\beta_C$ per next period
$\alpha_{ir}^q(t)$	Overproduction capacity of primary input q in sector i of region r at time t
$x_{ir}^a(t)$	Actual output of sector i in region r at time t
$x_{ir}^L(t)$	The remaining production capacity of labour in sector i of region r at time t
$x_{ir}^K(t)$	The remaining production capacity of productive capital in sector i of region r at time t
$x_{ir}^j(t)$	The potential production level of sector i in region r that the inventory of intermediate product j can support at time t
$x_{ir}^{\max}(t)$	Maximum production capacity of sector i in region r at time t
$x_{ir}^{loc}(t)$	Remaining output of sector i in region r available for local clients after export adjustments at time t

$exq_{ir}^{rem}(t)$	Remaining export quota of product i in region r after distributed to business clients in other regions at time t
$K_{ir}(t)$	Amount of productive capital of sector i in region r at the beginning of time t
$K_{res,r}(t)$	Amount of residential capital in region r at the beginning of time t
$K_{ir}^{dam}(t)$	Productive capital damaged by flooding of sector i in region r at time t
$K_{res,r}^{dam}(t)$	Residential capital damaged by flooding in region r at time t
$K_{ir}^{rec}(t)$	Productive capital recovered in sector i of region r from reconstruction during time t
$K_{res,r}^{rec}(t)$	Residential capital recovered in region r from reconstruction during time t
$\gamma_{ir}^{K}(t)$	Percentage reduction in available productive capital of sector i in region r at the beginning of time t relative to the pre-disaster level
$\gamma_{ir}^{L}(t)$	Percentage reduction in available working time in sector i in region r at the beginning of time t relative to the pre-disaster level
$\gamma_{r}^{Z}(t)$	Percentage reduction in transport capacity from region r to other regions at time t relative to the pre-disaster level
$\gamma_{ir}^{Z}(t)$	Connectivity loss of the supplying sector i in region r to its business and household clients in other regions at time t relative to the pre-disaster level
$\gamma_{ir}^{E}(t)$	Percentage reduction in the maximum export volume of product i in region r at time t relative to the pre-disaster level
$S_{ir}^{j}(t)$	Inventory of intermediate input j held by sector i in region r at the beginning of time t
$S_{ir}^{j,used}(t)$	Intermediate input j used in the production of sector i in region r at time t
$S_{ir}^{j,restored}(t)$	Inventory of intermediate input j restored by sector i in region r during time t
$ic_{js}^{ir,*}(t)$	Output of sector i in region r allocated to sector j in region s as intermediate use at time t under export restrictions
$fc_{h}^{ir,*}(t)$	Output of sector i in region r allocated to households in region h as consumption use at time t under export restrictions
$rc_{js}^{ir,*}(t)$	Output of sector i in region r allocated to sector j in region s as reconstruction use at time t under export restrictions
$rc_{res,h}^{ir,*}(t)$	Output of sector i in region r allocated to households in region h as reconstruction use at time t under export restrictions
$id_{js}^{ir}(t)$	Orders issued by sector j in region s to the supplying sector i in region r at time t
$fd_{h}^{ir}(t)$	Orders issued by households in region h to the supplying sector i in region r at time t

$rd_{js}^{ir}(t)$	Orders issued to rebuild damaged productive capital of sector j in region s to the supplying sector i in region r at time t
$rd_{res,h}^{ir}(t)$	Orders issued to rebuild damaged residential capital in region h to the supplying sector i in region r at time t
$TD_{ir}(t)$	Total demand of product i in region r at time t
$sub_r(t)$	External subsidies from public finance or social donations to households in region r at time t
$va_{ir}(t)$	Value added of sector i in region r at time t

Appendix Table A4: Weights of the three major industries against each of the eight emission sectors in disaggregating air pollution-related labour deaths.

Sectors / Industries	Power plants	Industry	Transport	Households	Waste	Agriculture	Other	Natural
Primary	0.2	0.2	0.2	0.5	0.2	1	1	1
Secondary	1	1	1	1	1	0.2	1	0.2
Tertiary	0.8	0.2	0.8	1	0.2	0.2	1	0.2

Notes: The labour deaths attributable to air pollution sourced from each emission sector are disaggregated into the three major industries in weighted proportion to the regional employment of the three industries. These weights are given by expert judgement due to data limitations.

Appendix Table A5: Years of IO tables used for each country under the baseline and future runs and coverage of sectoral data in Chapter 5.

Countries	Periods	Years of IO tables	Economic Sectors									
			AGR	MIN	FDM	OTM	UTL	CON	TRD	TRA	PUB	OTS
Ghana	Baseline	2005	✓	✓	✓	✓	✓	✓	✓	✓	✓	✓
	Future	2015	✓	✓	✓	✓	✓	✓	✓	✓	✓	✓
Ethiopia	Baseline	2005	✓	✓	✓	✓	✓	✓	✓	✓	✓	✓
	Future	2010	✓	✓	✓	✓	✓	✓	✓	✓	✓	✓
Egypt	Baseline	1996	✓	✓(oils)	✓	✓	✓(electricity)	✓	×	✓	✓	✓
	Future	2010	✓	✓	✓	✓	✓	✓	✓	✓	✓	✓
India	Baseline	1993	✓	✓	✓	✓	✓	✓	✓	✓	✓	✓
	Future	2015	✓	✓	✓	✓	✓	✓	✓	✓	✓	✓
China	Baseline	1997	✓	✓	✓	✓	✓	✓	✓	✓	✓	×
	Future	2017	✓	✓	✓	✓	✓	✓	✓	✓	✓	✓
Brazil	Baseline	2000	✓	✓	✓	✓	✓	✓	✓	✓	✓	✓
	Future	2015	✓	✓	✓	✓	✓	✓	✓	✓	✓	✓

Notes: Economic sectors include agriculture (AGR), mining (MIN), food manufacturing (FDM), other manufacturing (OTM), utilities (UTL), construction (CON), trade (TRA), transport (TRA), public services (PUB) and other services (OTS).

Appendix Table A6: A sample IO table of a hypothetical global economy adopted in Chapter 6.

		Intermediate Use																				Final Use				Output
		A					B					C					D								
		AGR	MANG	MANK	CON	OTH	AGR	MANG	MANK	CON	OTH	AGR	MANG	MANK	CON	OTH	AGR	MANG	MANK	CON	OTH	A	B	C	D	
A	AGR	42	135	0	3	17	3	14	0	1	4	5	20	0	0	1	1	2	0	0	0	60	15	6	2	331
	MANG	61	732	128	159	177	6	148	38	34	19	3	70	9	7	9	2	27	6	11	6	125	24	11	10	1,820
	MANK	4	63	189	33	57	0	2	22	2	3	0	3	17	2	4	0	1	4	2	2	170	14	40	11	645
	CON	0	2	1	8	10	0	0	0	0	0	0	0	0	1	0	0	0	0	0	0	443	7	12	10	495
	OTH	18	264	83	84	541	2	47	27	23	71	1	28	10	12	20	1	11	4	6	16	716	65	30	35	2,115
B	AGR	1	4	0	0	1	32	176	1	17	34	2	10	0	0	0	0	1	0	0	0	2	103	3	1	388
	MANG	6	50	9	18	35	65	1,839	461	340	294	5	64	11	13	19	3	37	8	14	17	49	505	39	35	3,936
	MANK	1	15	42	12	33	5	113	902	98	117	1	16	50	11	14	0	7	23	7	11	106	592	158	57	2,390
	CON	0	0	0	2	2	1	6	2	68	13	0	0	0	3	1	0	0	0	1	1	134	769	60	49	1,113
	OTH	0	17	7	6	38	20	496	293	203	1,118	1	32	11	11	29	1	13	4	8	23	41	1,274	44	34	3,726
C	AGR	1	5	0	0	1	2	10	0	1	3	75	281	0	6	14	1	1	0	0	0	2	11	128	1	544
	MANG	6	45	10	26	28	7	154	58	66	25	99	1,736	273	284	197	3	32	10	22	11	21	32	326	15	3,486
	MANK	0	5	10	4	7	1	5	27	5	5	2	109	416	46	58	0	3	6	3	3	25	16	449	14	1,216
	CON	0	0	0	0	1	0	0	0	0	0	0	8	2	28	10	0	0	0	0	0	36	9	651	13	761
	OTH	0	5	3	2	12	1	21	12	9	34	17	361	118	136	450	0	5	2	3	9	23	36	775	21	2,055
D	AGR	1	5	0	0	1	2	8	0	1	2	3	11	0	0	0	36	75	0	1	10	2	9	3	62	231
	MANG	2	21	3	6	7	2	76	20	15	9	2	38	4	5	5	32	390	61	125	81	6	10	5	119	1,047
	MANK	0	2	5	1	3	0	1	13	1	2	0	2	10	1	3	1	21	130	22	24	12	9	28	105	393
	CON	0	0	0	0	0	0	0	0	0	0	0	0	0	1	0	0	1	0	8	5	26	7	12	342	403
	OTH	0	3	1	1	8	1	12	7	5	22	0	7	3	3	6	12	130	49	56	204	12	20	10	354	926
Value-added	Capital	13	151	43	15	250	7	252	115	16	476	10	228	65	21	299	7	104	20	7	108					
	Labour	174	294	111	113	888	232	556	391	207	1,476	316	459	217	172	918	130	184	65	107	397					
Input		331	1,820	645	495	2,115	388	3,936	2,390	1,113	3,726	544	3,486	1,216	761	2,055	231	1,047	393	403	926					

Notes: AGR, MANG, MANK, CON and OTH refer to the five sectors of agriculture, general manufacturing, capital manufacturing, construction, and other services, respectively.

Appendix Table A7: An aggregated GTAP IO table of a hypothetical global economy adopted for sensitivity analysis in Chapter 6.

		Intermediate Use																				Final Use				Output
		A					B					C					D								
		AGR	MANG	MANK	CON	OTH	AGR	MANG	MANK	CON	OTH	AGR	MANG	MANK	CON	OTH	AGR	MANG	MANK	CON	OTH	A	B	C	D	
	AGR	78	97	0	3	25	0	0	0	0	0	0	0	0	0	0	0	1	0	0	0	96	0	0	1	302
	MANG	43	878	233	173	211	0	10	4	2	6	0	24	3	1	7	2	30	9	6	10	245	19	13	24	1,955
A	MANK	2	55	361	46	73	0	3	21	4	11	0	3	19	3	6	1	7	24	6	7	277	43	18	45	1,034
	CON	0	8	3	10	21	0	0	0	0	0	0	0	0	0	0	0	0	0	0	0	433	0	1	1	478
	OTH	23	230	132	75	525	0	1	0	0	5	0	3	2	1	12	0	2	1	1	6	1,126	4	4	5	2,158
	AGR	1	5	0	0	1	33	26	0	0	10	0	1	0	0	0	1	3	0	0	0	2	38	1	2	125
	MANG	0	27	3	1	3	18	318	70	57	195	0	13	3	1	6	1	15	2	2	6	4	265	6	9	1,026
B	MANK	0	1	8	0	2	1	22	118	32	51	0	1	6	1	2	0	2	5	1	2	9	211	7	15	496
	CON	0	0	0	0	0	2	20	4	14	59	0	0	0	0	0	0	0	0	0	0	1	280	0	0	379
	OTH	0	2	1	1	6	23	166	94	76	737	0	5	2	1	19	0	2	1	1	8	7	1,916	8	9	3,085
	AGR	0	1	0	0	0	0	0	0	0	0	23	31	0	0	9	0	1	0	0	0	1	0	44	1	112
	MANG	1	12	4	1	6	1	9	3	1	9	20	305	77	44	195	2	20	6	5	9	8	12	230	19	998
C	MANK	0	2	14	2	4	0	1	8	2	3	2	35	159	28	46	0	5	9	4	4	20	19	162	29	557
	CON	0	0	0	0	0	0	0	0	0	0	1	8	3	63	49	0	0	0	0	0	2	0	217	1	345
	OTH	0	5	3	1	12	0	3	1	1	16	17	178	96	63	815	1	5	2	2	19	11	12	1,602	15	2,881
	AGR	2	5	0	0	1	0	1	0	0	0	1	3	0	0	1	73	77	0	3	17	2	1	3	191	381
	MANG	1	94	7	3	6	0	29	4	1	6	1	48	5	2	8	37	430	52	72	156	10	17	18	344	1,352
D	MANK	0	1	13	1	2	0	1	4	1	2	0	1	7	1	2	2	25	57	24	24	8	8	8	123	316
	CON	0	0	0	0	0	0	0	0	0	0	0	0	0	0	0	1	5	1	27	18	1	0	0	289	344
	OTH	0	3	2	1	8	0	2	1	0	9	0	6	3	1	23	33	158	49	42	331	8	7	9	1,014	1,709
Value-added	Capital	36	311	117	56	677	19	204	45	32	663	20	202	83	77	953	78	396	56	70	564					
	Labour	114	221	133	105	573	26	210	120	154	1,303	26	129	91	58	729	147	168	44	78	526					
Input		302	1,955	1,034	478	2,158	125	1,026	496	379	3,085	112	998	557	345	2,881	381	1,352	316	344	1,709					

Notes: AGR, MANG, MANK, CON and OTH refer to the five sectors of agriculture, general manufacturing, capital manufacturing, construction, and other services, respectively.

Appendix Table A8: A sample of capital matrix adopted in Chapter 6.

Region-Sector		A	B	C	D
	AGR	0	0	0	0
	MANG	0	0	0	0
A	**MANK**	0.15	0	0.02	0
	CON	0.61	0	0	0
	OTH	0	0	0	0
	AGR	0	0	0	0
	MANG	0	0	0	0
B	**MANK**	0.06	0.25	0.06	0
	CON	0.12	0.7	0.04	0
	OTH	0	0	0	0
	AGR	0	0	0	0
	MANG	0	0	0	0
C	**MANK**	0.02	0.05	0.2	0
	CON	0.04	0	0.68	0
	OTH	0	0	0	0
	AGR	0	0	0	0
	MANG	0	0	0	0
D	**MANK**	0	0	0	0.3
	CON	0	0	0	0.7
	OTH	0	0	0	0

Notes: The matrix presents the quantities of products required to rebuild one unit of capital in each region. The study assumes that different sectors in the same region have the same capital matrix coefficients.

Appendix Table A9: Indirect economic losses due to the 2021 Zhengzhou 'flood-COVID' compound event in all regions of China.

Regions	Indirect losses	% of local GDP	COVID-19 accountability	Regions	Indirect losses	% of local GDP	COVID-19 accountability
Zhengzhou	44340	4.11%	45.54%	Liaoning	369	0.01%	35.21%
Nanyang	1305	0.33%	41.74%	Zhejiang	357	0.01%	37.50%
Luoyang	1098	0.22%	44.57%	Guangdong	311	0.00%	29.93%
Zhoukou	928	0.30%	37.73%	Jilin	292	0.01%	32.65%
Xinxiang	855	0.30%	42.05%	Anhui	280	0.01%	34.10%
Xinyang	854	0.31%	37.04%	Shanghai	258	0.01%	44.76%
Zhumadian	848	0.35%	38.72%	Sichuan	255	0.01%	24.39%
Pingdingshan	835	0.44%	44.46%	Jiangxi	245	0.01%	36.35%
Xuchang	833	0.27%	44.65%	Shanxi	243	0.01%	42.78%
Jiangsu	745	0.01%	29.32%	Guangxi	234	0.01%	34.83%
Kaifeng	711	0.30%	37.18%	Xinjiang	228	0.02%	39.03%
Shangqiu	689	0.26%	38.15%	Yunnan	212	0.01%	32.50%
Puyang	660	0.33%	41.44%	Hebi	207	0.21%	39.41%
Jiaozuo	636	0.23%	42.73%	Guizhou	207	0.01%	34.61%
Anyang	632	0.27%	42.94%	Beijing	203	0.01%	42.19%
Shandong	604	0.01%	38.81%	Tianjin	187	0.01%	44.18%
Sanmenxia	529	0.30%	50.56%	Jiyuan	180	0.27%	47.70%
Inner Mongolia	498	0.02%	44.59%	Gansu	165	0.02%	42.03%
Shaanxi	497	0.02%	43.60%	Hubei	148	0.00%	22.66%
Hebei	475	0.01%	36.47%	Hainan	115	0.02%	37.85%
Fujian	473	0.01%	33.04%	Chongqing	86	0.00%	39.11%
Heilongjiang	418	0.02%	33.19%	Ningxia	57	0.01%	41.85%
Luohe	377	0.27%	34.30%	Qinghai	48	0.01%	45.69%
Hunan	377	0.01%	26.17%	Tibet	10	0.01%	43.11%

Notes: The absolute loss is given in millions of 2021 CNY and the relative loss is expressed as a percentage of the local GDP in the previous year 2020. COVID-19 accountability indicates the additional indirect economic loss caused by the COVID-19 control as a percentage of the total regional indirect economic loss during the compound event.

Appendix Table A10: Top 30 supply chain relationships in the national economic network most affected by the 2021 Zhengzhou 'flood-COVID' compound event.

Rankings	Supply chain relationships between region-sectors	Absolute losses of economic flows	Relative losses of economic flows	Changes in ranking	COVID-19 accountability
1	'Zhengzhou-mining', 'Zhengzhou-electricity, gas, and water'	2368	7.02%	-	34.22%
2	'Zhengzhou-non-metallic mineral products', 'Zhejiang-construction'	1690	5.91%	-	62.37%
3	'Zhengzhou-non-metallic mineral products', 'Zhengzhou-construction'	1294	4.44%	-	52.41%
4	'Zhengzhou-non-metallic mineral products', 'Shangqiu-construction'	1221	4.55%	-	53.56%
5	'Zhengzhou-non-metallic mineral products', 'Xinyang-non-metallic mineral products'	1108	5.06%	↑2	58.17%
6	'Xinyang-non-metallic mineral products', 'Zhengzhou-non-metallic mineral products'	1014	4.95%	↑3	56.17%
7	'Xinyang-information services', 'Zhengzhou-information services'	989	4.23%	↑1	55.02%
8	'Zhengzhou-mining', 'Zhengzhou-non-metallic mineral products'	962	6.30%	↓2	48.53%
9	'Zhengzhou-food and tobacco', 'Zhengzhou-accommodation and catering'	947	6.95%	↑1	53.28%
10	'Zhengzhou-food and tobacco', 'Xinyang-food and tobacco'	944	6.75%	↑1	57.83%
11	'Zhengzhou-finance', 'Zhengzhou-transport'	888	7.31%	↓6	39.30%
12	'Zhengzhou-metal products', 'Zhengzhou-ordinary machinery'	720	4.40%	↑2	52.91%
13	'Zhengzhou-electricity, gas, and water', 'Zhengzhou-non-metallic mineral products'	670	6.34%	-	49.35%
14	'Zhengzhou-non-metallic mineral products', 'Jiangsu-construction'	602	6.19%	↑8	62.48%
15	'Zhengzhou-mining', 'Zhengzhou-metal products'	599	7.05%	↑1	54.05%
16	'Xinyang-non-metallic mineral products', 'Zhengzhou-construction'	579	4.23%	↑3	55.02%
17	'Zhengzhou-finance', 'Zhengzhou-electricity, gas, and water'	568	6.66%	↓5	35.06%
18	'Xinyang-food and tobacco', 'Zhengzhou-accommodation and catering'	551	5.27%	↓3	47.80%
19	'Zhengzhou-metal products', 'Zhengzhou-non-metallic mineral products'	522	6.74%	↑2	55.71%

20	‘Zhengzhou-metal products’, ‘Jiangsu-metal products’	520	6.49%	↑5	60.26%
21	‘Pingdingshan-mining’, ‘Zhengzhou-electricity, gas, and water’	520	4.66%	↓4	47.38%
22	‘Zhengzhou-non-metallic mineral products’, ‘Chongqing-construction’	506	6.07%	↑6	62.55%
23	‘Zhengzhou-agriculture’, ‘Zhengzhou-food and tobacco’	489	7.45%	↓5	45.29%
24	‘Zhengzhou-non-metallic mineral products’, ‘Beijing-construction’	485	5.77%	↑8	61.86%
25	‘Zhengzhou-information services’, ‘Xinyang-information services’	484	4.53%	↑1	57.99%
26	‘Sanmenxia-mining’, ‘Zhengzhou-metal products’	479	4.91%	↑5	61.28%
27	‘Zhengzhou-non-metallic mineral products’, ‘Shanghai-construction’	463	5.86%	↑7	62.18%
28	‘Zhengzhou-metal products’, ‘Zhejiang-construction’	445	6.41%	↑8	61.15%
29	‘Zhengzhou-electricity, gas, and water’, ‘Xinyang-non-metallic mineral products’	428	5.86%	↓9	39.74%
30	‘Zhengzhou-wholesale and retail’, ‘Zhengzhou-metal products’	415	6.07%	↓3	52.90%

Notes: The supply chain relationship is defined as the economic transactional relation directed from the former region-sector (supplier) to the latter region-sector (buyer). The absolute loss is given by millions of 2021 current CNY and the relative loss is expressed as a percentage of the economic transactions flowing through the supply chain relationship in the previous year 2020. Changes in ranking are compared to the single-flood scenario. COVID-19 accountability refers to the additional transactional loss caused by the COVID-19 control as a percentage of the total transactional loss in the supply chain relationship during the compound event.

Appendix B. Figures

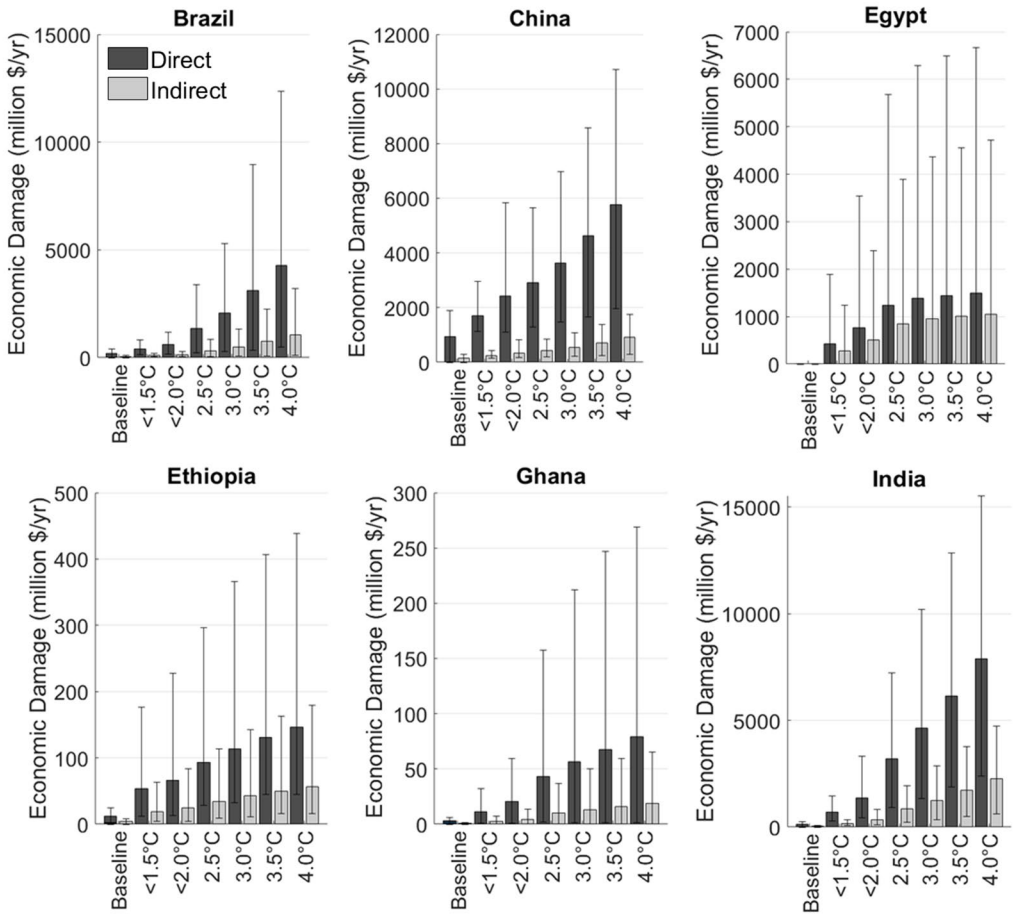

Appendix Figure B1: Direct and indirect fluvial flood damages for the baseline and six warming scenarios in the six countries expressed in million US$/yr for the CC experiment. *Bars represent the ensemble average of the five GCMs, with whiskers indicating the ensemble maximum and minimum. Note the different scale of the y-axis.*

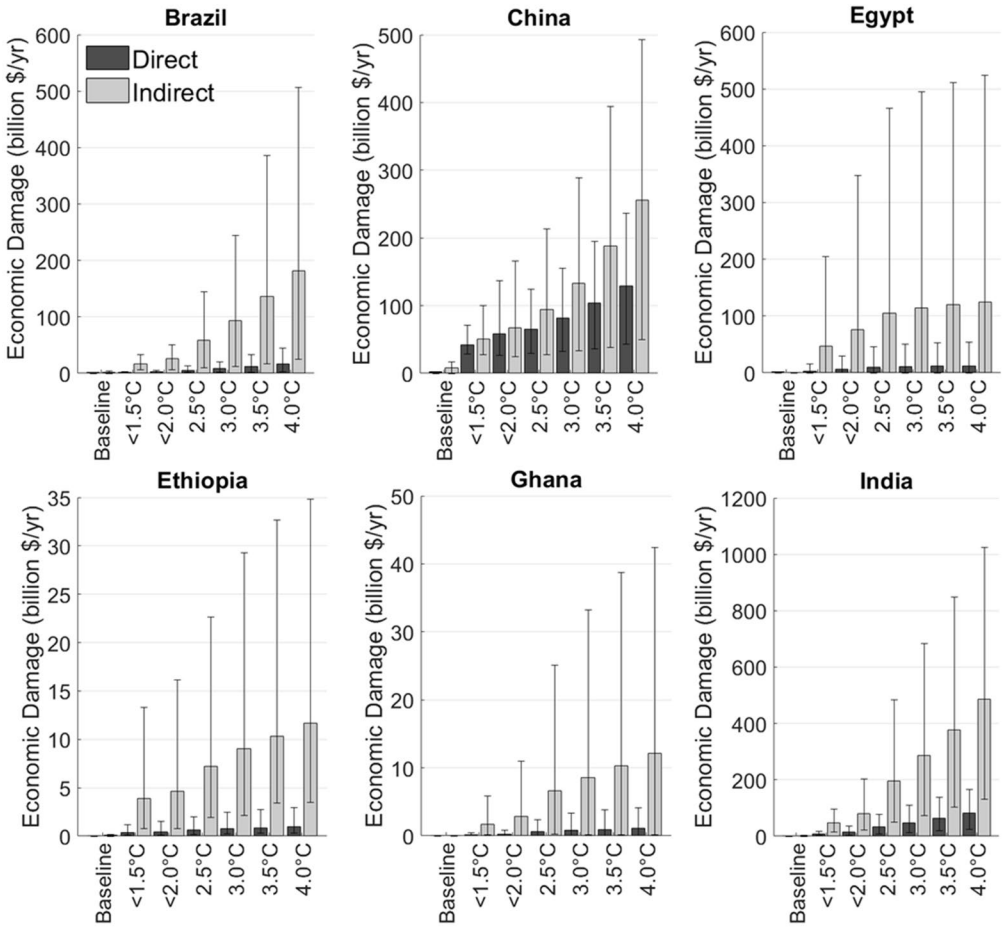

Appendix Figure B2: Direct and indirect fluvial flood damages for the baseline and six warming scenarios in the six countries expressed in billion US$/yr for the CC+SE experiment.

Bars represent the ensemble average of the five GCMs, with whiskers indicating the ensemble maximum and minimum. Note the different scale of the y-axis.

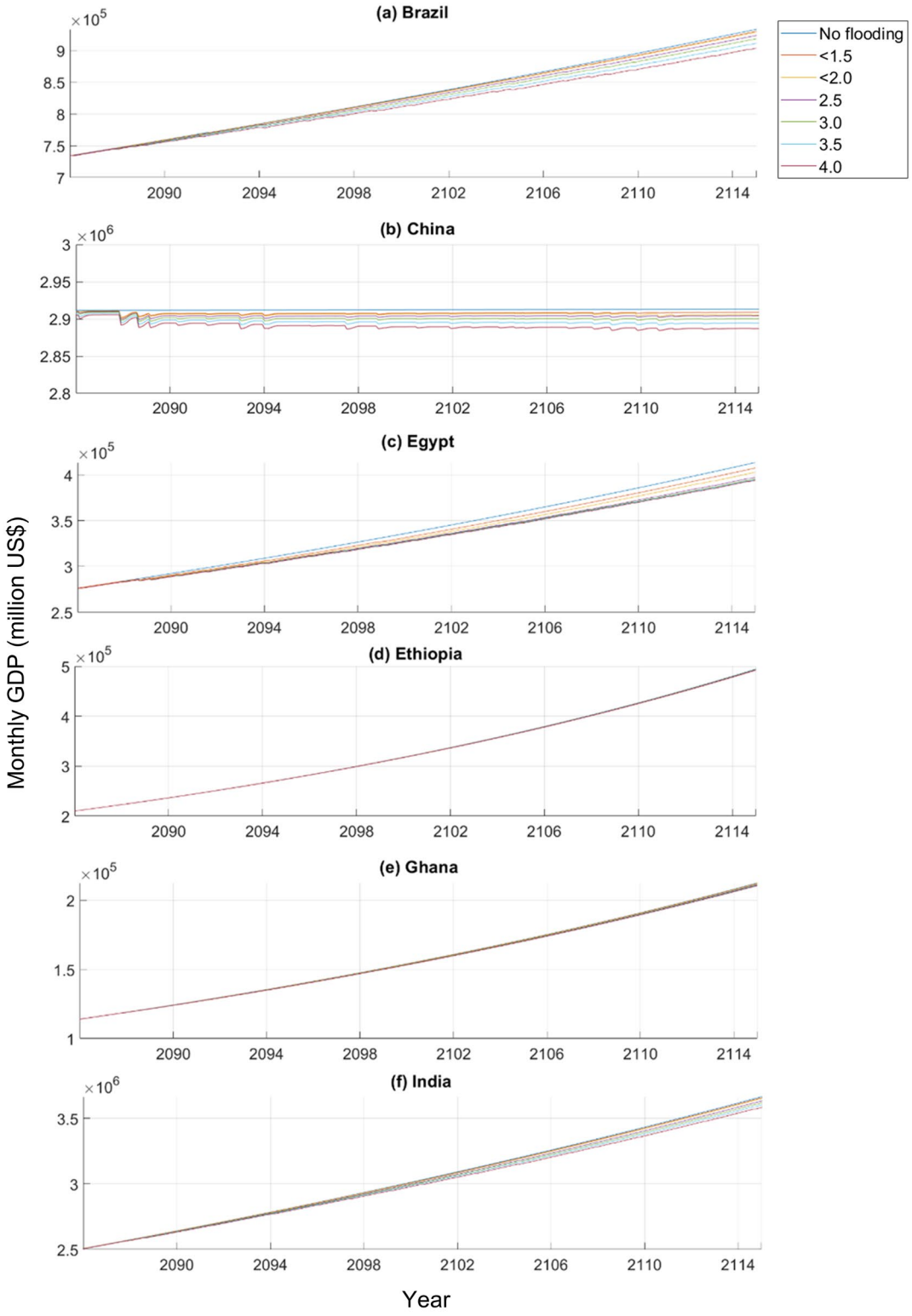

Appendix Figure B3: Monthly GDP (million US$) growth projections for each of the six countries under the climate scenarios.

Results are shown for the CC+SE model experiments (based on exogenous growth data between 2086-2115). Please note the different scale of y-axis for each panel.

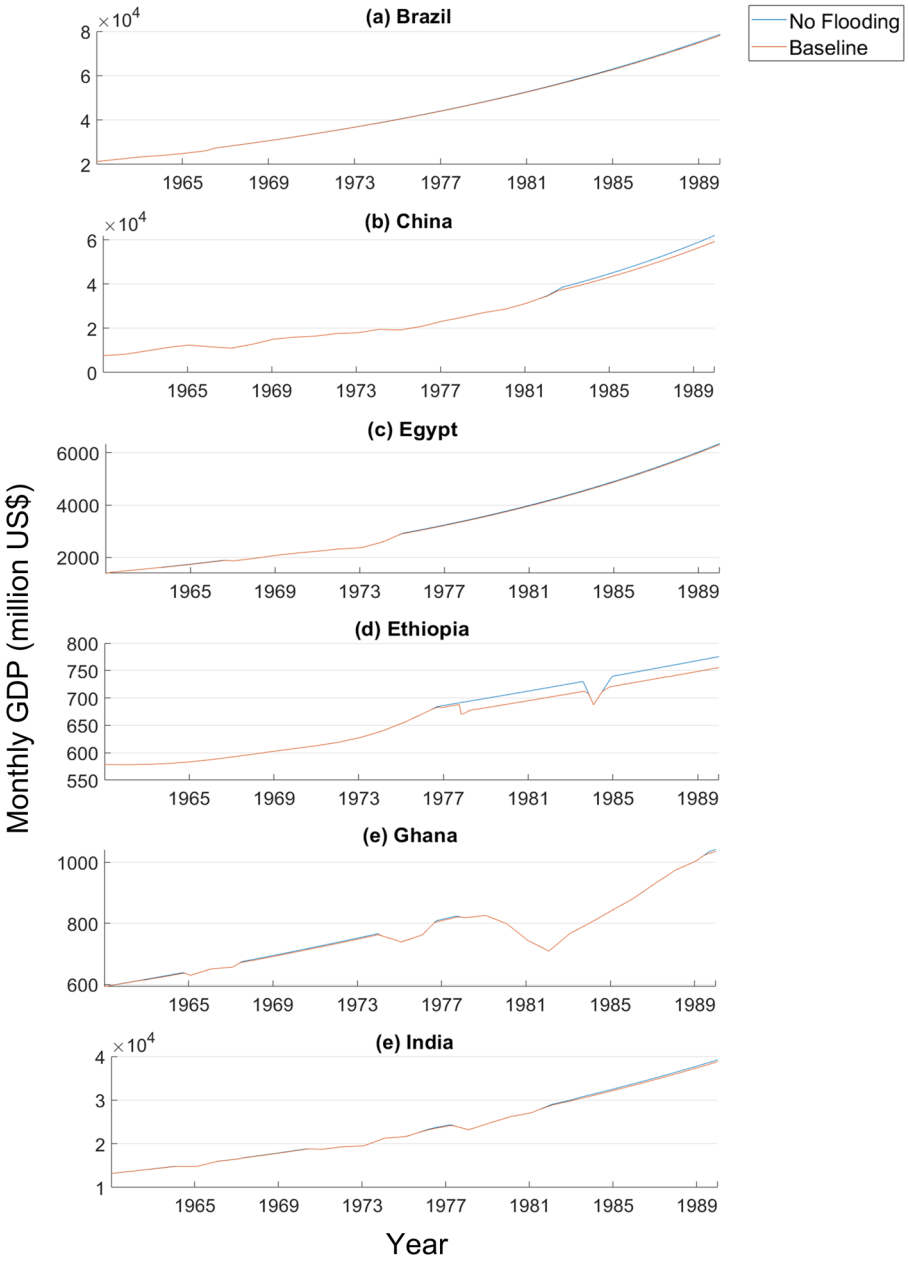

Appendix Figure B4: Monthly GDP (million US$) growth projections for each of the six countries under the baseline scenario.

Results are shown for the CC+SE model experiments (based on exogenous growth data between 1961-1990). Please note the different scale of y-axis for each panel.

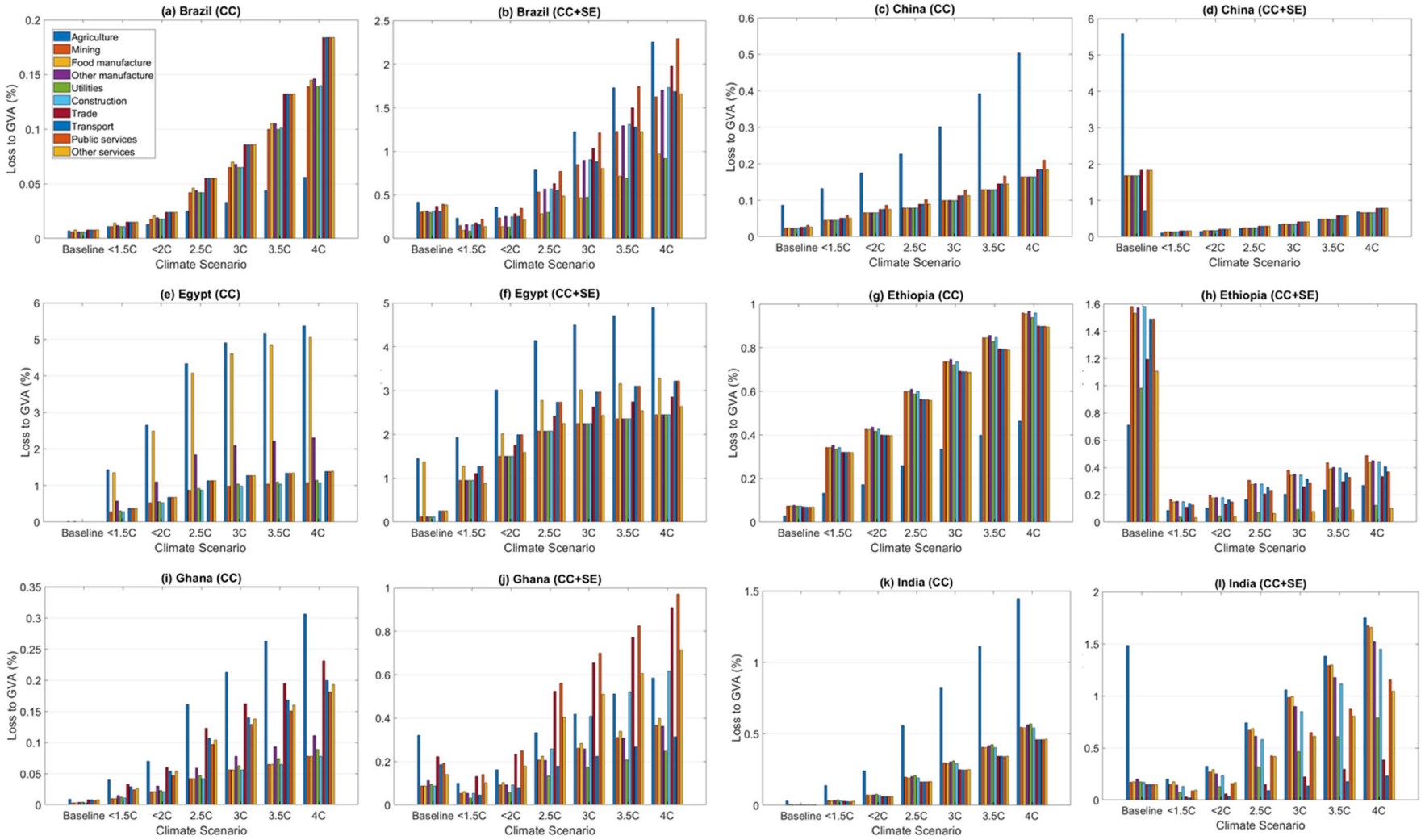

Appendix Figure B5: Average annual indirect economic loss of gross value added (GVA) in each economic sector for the baseline (1961-1990) and future warming scenarios (using SSP2 from 2086-2115) in the six countries.

Results are shown for both the CC and CC+SE experiments.

Appendix C. Supplementary Material

C.1. Literature on Risks of Fluvial Flooding in the Study Countries of Chapter 5

Since the beginning of 2010, the total damage of fluvial flooding has been 2.8 billion US$ for Brazil, 74.4 billion US$ for China, 2.2 million US$ for Ethiopia, and 22.5 billion US$ for India, corresponding to 23, 58, 4, and 36 flood events respectively, in the EM-DAT database[28]. The total damage from fluvial flooding is not available for Egypt and Ghana, but there were 2 and 5 flooding events in Egypt and Ghana respectively during this period.

A global analysis showed that large direct economic losses of fluvial floods will be observed in China and India, among other countries (Willner et al., 2018). In China production losses were estimated to be 214 billion US$ in 1996-2015 increasing to 389 billion US$ in 2016-2035 (ibid.). You and Ringler (2010) modelled the impacts of climate change on three major factors which affect the Ethiopian economy, including flooding, under the SRES emissions scenarios. Results showed the occurrence of flooding events will increase and cause substantial economic losses in both the agricultural and non-agricultural sectors.

Although few country-level studies exist, there are some city or river basin level studies that project future impacts within the six countries. Ranger et al. (2011) estimated the direct total economic losses for floods of different return periods in Mumbai. A 1 in 50-year flood in the future is estimated to cause 210-550 million US$ of damage, excluding infrastructure. A 1 in 100-year flood is projected to cause

[28] This is sourced from EM-DAT: the Emergency Events Database - Université catholique de Louvain (UCL) - CRED, D. Guha-Sapir - www.emdat.be, Brussels, Belgium (accessed 7 Feb 2020).

damage of 490-1,350 million US$ and a 1 in 200-year flood damage of 510-1,420 million US$. When the damage to infrastructure is included, these costs increase. Sarkodie et al. (2015) modelled the damage of flooding for each river basin within the Greater Accra City, Ghana, under the SRES emissions scenarios using the Aqueduct model. This research only considered 2011-2020 and did not project flood economic damages further into the future. A 1 in 10-year flood is projected to cause 98.5 million US$ in urban damage without flood protection. A 1 in 100-year flood is projected to cause 162.9 million US$ in urban damage without flood protection.

Hu et al. (2019) used an IO model to estimate the potential macroeconomic impact of fluvial flooding on the manufacturing sector in China, based on historical floods exceeding 1 in 100-year return periods between 2003 and 2010. The study reported a 12.3% direct loss in annual total output, with further indirect losses of 2.3% of the annual total output at the macro-level.

References:

Sarkodie, S. A., Owusu, P. A., & Rufangura, P. (2015). Impact analysis of flood in Accra, Ghana. *Advances in Applied Science Research 6*(9), 53-78. https://doi.org/10.6084/m9.figshare.3381460

Hu, X., Pant, R., Hall, J. W., Surminski, S., & Huang, J. (2019). Multi-scale assessment of the economic impacts of flooding: evidence from firm to macro-level analysis in the Chinese manufacturing sector. *Sustainability, 11*(7), 1933. https://doi.org/10.3390/su11071933

Ranger, N., Hallegatte, S., Bhattacharya, S., Bachu, M., Priya, S., Dhore, K., Rafique, F., Mathur, P., Naville, N., Henriet, F., Herweijer, C., Pohit, S., & Corfee-Morlot, J. (2011). An assessment of the potential impact of climate change on flood risk in Mumbai. *Climatic Change, 104*(1), 139-167. https://doi.org/10.1007/s10584-010-9979-2

Willner, S. N., Otto, C., & Levermann, A. (2018). Global economic response to river floods. *Nature Climate Change 8*(7), 594-598. https://doi.org/10.1038/s41558-018-0173-2

You, G. J.-Y., & Ringler, C. (2010). *Hydro-economic modeling of climate change impacts in Ethiopia* (00960) [IFPRI Discussion Paper]. International Food Policy Research Institute. https://www.ifpri.org/publication/hydro-economic-

modeling-climate-change-impacts-ethiopia

C.2. Direct and Indirect Impacts of a Perfect Storm under Free Trade Scenarios

This section discusses the direct and indirect economic impacts of flooding, pandemic control, and their collisions under the free trade scenarios. The direct damage refers to the monetary value of damage due to inundation of physical assets and occurs only in the flooded region C. The indirect losses are the GDP losses along the global supply chain caused by the compound event. They start from the directly affected regions and spill over to other regions through inter-sectoral and inter-regional dependencies.

C.2.1. On the Global Scale

As shown in Table 6-3, when there is only flooding in region C, the direct damage increases from 317.2 to 951.5 units as the flood scale grows from small to large. Apart from direct damage, the flood disaster brings about additional supply chain losses of 50.0-288.9 units according to flood scales. The ratios between indirect and direct losses range from 0.16 to 0.30 as flood scale increases and are lower than the ratio 0.39 estimated by Hallegatte (2008). This is because the incorporation of cross-regional substitutability increases the resilience of the economy against disaster events and reduces estimates of indirect losses.

In the scenario where there is only pandemic control, there is no direct damage as the pandemic has no impacts on physical assets. The indirect losses due to a 30%-24 global pandemic control is assessed at 1,242.6 units, equivalent to 12.9% of the annual global GDP.

Then the study examines the economic footprint of the compound event of flooding and pandemic control. The direct damage under such circumstances is always equal to

that caused by flooding alone, as the pandemic does not create any direct damage. The indirect losses resulting from the compound events show diverging patterns according to flood scales. First, when the flood in region C is on the small or medium scale, the indirect losses of the compound event are between the separate losses brought by flooding and pandemic control. For example, the concurrence of a small flood in region C and a 30%-24 global pandemic control incurs 1194.1 units of indirect losses to the global economy, which is larger than the indirect losses caused by the flood (50.0 units) and slightly smaller than the indirect losses of the pandemic control (1,242.6 units). Second, when the flood in region C is on the large scale, the indirect losses of the compound event, which is measured at 1,329.5 units, exceed the separate losses of both flooding and pandemic control.

C.2.2. On the Regional Scale

As shown in Figure 6-1, under the 'flood-only' scenarios (Figure 6-1a-c), the cumulative indirect or GDP losses in region C (yellow lines), relative to its pre-disaster level of its annual GDP, increase from 2.18% (small flood), to 6.41% (medium flood) and finally to 12.25% (large flood). Region D also experiences increasing losses in its GDP, although very tiny (0.01%-0.05%), attributable to the spill-over effects along the supply chain. By contrast, the other two non-flooded regions A and B, witness slight growth in their GDPs (0.07%-0.34% for A and 0.21%-0.98% for B). This comes from the stimulus effect of reconstruction activities to recover capital damaged by flooding, which has been discussed in the main text of Chapter 6.

Figure 6-1d-f show the regional economic footprint of the pandemic control, which is irrelevant to the flood scales. The four regions experience similar weekly relative changes in their GDPs during a 30%-24 global pandemic control. Their GDPs drop gradually by around 22% during the first three weeks (week 5-8) of the pandemic control, then remain almost constant for the remaining weeks of the pandemic control,

and finally recover back to the pre-disaster levels when the control measures are lifted. The recovery takes another around 10 weeks in all regions. Before that, there are sudden slumps of regional GDPs around week 30, due to the shortage of intermediate inputs arising from delivery failures under persistent transport constraints during the pandemic control. The cumulative GDP losses in region A, B, C, and D caused by a 30%-24 pandemic control account for 12.61%, 12.87%, 13.20%, and 13.04% of their annual GDP at the pre-pandemic levels.

Figure 6-1g-i illustrate the regional losses resulting from the perfect storm of flooding and pandemic control. It takes longer weeks in region C to recover its economy compared to the above two groups of scenarios, particularly with the large flood scale. The cumulative GDP losses in region C increase significantly with the flood scale from 12.11% to 18.75%. By comparison, other regions experience different levels of declines in their GDP losses as the flood scale increases (12.41%-12.00% for A, 12.49%-11.56% for B, and 12.96%-12.86% for D), owing to an expanding stimulus effect of post-flood reconstruction.

C.3. Economic Effects of Different Degrees of Export Restrictions in a Perfect Storm

This section investigates how the economic impacts of the perfect storm change with the degree of the trade restriction limiting the export of sector ‘MANK’ in region C. It is assumed that the degree of the export restriction increases from 0% to 75% with an interval of 25%.

First, Table C1 illustrates the changes in cumulative GDP losses, both on the regional and global scales, by the export restriction without production specialization, that is, products in one region can be freely replaced by products of the same sector from other regions. It is found that not only the global loss but also its increment expands with the

degree of the export restriction. In other words, a stronger export restriction results in a larger increase in the GDP loss than a weaker one. For every 25% increase in the degree of the export restriction, the global loss rises by an average of 0.02%, 0.18% and 0.22%, respectively, during different flood and pandemic intersections. The GDP loss in each region, except region C, follows the same pattern as the global one with increases in the degree of the export restriction. In comparison, region A and D appear to be more vulnerable to the escalating trade restriction than other regions. In region C, its loss increases by 0.01% with each 25% increase in the degree of the export restriction under the small flood colliding with pandemic control, but decreases by 0.03% and 0.07%, respectively, under the medium and large floods (Figure C1).

Second, the study examines the role of production specialization in compound scenarios with varying degrees of the export restriction on 'MANK-C'. As shown in Table C2 and Figure C2, the regional and global GDP losses both grow rapidly with the degree of the export restriction when the restricted sector 'MANK-C' happens to make specialized products which cannot be substituted elsewhere. Such restrictive policy of region C puts other regional economies, as well as the global economy, at considerably higher risks than the former one, which in turn damages its own recovery through the propagation effect of the global supply chain.

These results are consistent with those of Section 6.2.3 in the main text of Chapter 6.

Table C1: Changes in cumulative GDP losses, on regional and global scales, by each 25% increase in the degree of the export restriction on 'MANK-C' without production specialization.

Export Restriction	Region A	Region B	Region C	Region D	Global Change
0%-25%	0.08%	0.00%	-0.03%	0.06%	0.02%
25%-50%	0.35%	0.17%	-0.03%	0.39%	0.18%
50%-75%	0.38%	0.21%	-0.03%	0.52%	0.22%

Notes: The cumulative GDP losses are in relative terms of the annual GDPs at the pre-disaster levels. The results are given as the ensemble mean of scenarios where different scales of floods

collide with a 30%-24 pandemic control.

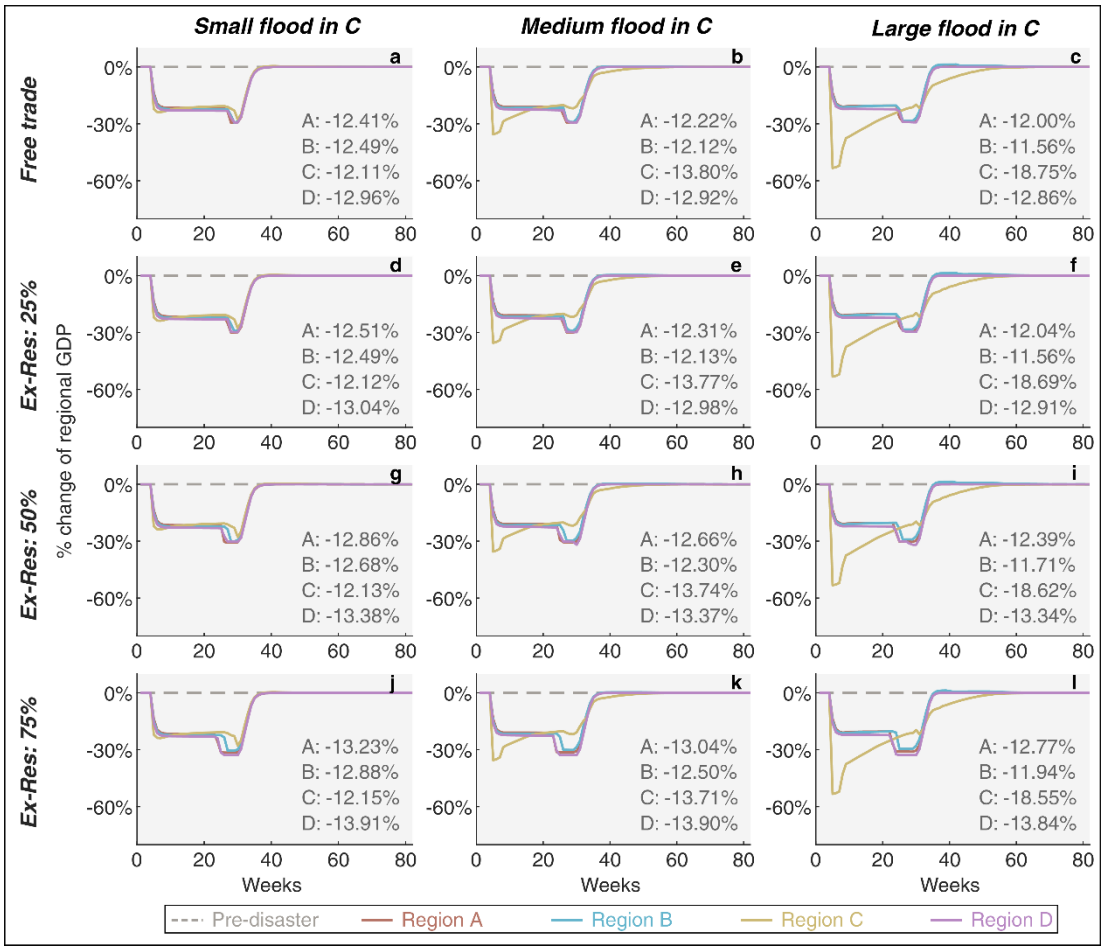

Figure C1: Weekly changes of regional GDPs, relative to the pre-disaster level, in the four regions, when the export restriction is imposed on 'MANK-C' at different degrees without production specialization during the compound flood and pandemic crises.

The numbers in each plot indicate the cumulative losses or gains of regional GDPs over time, relative to the pre-disaster levels of the annual regional GDPs. From left to right, each column represents the small-, medium-, and large-scale flooding in region C. From top to bottom, each row stands for the 0%, 25%, 50% or 75% export restriction on the 'MANK' sector in region C.

Table C2: Changes in cumulative GDP losses, on regional and global scales, by each 25% increase in the degree of the export restriction on 'MANK-C' with production specialization.

Export Restriction	Region A	Region B	Region C	Region D	Global Change
0%-25%	7.26%	7.27%	0.56%	6.56%	5.30%
25%-50%	9.46%	9.38%	1.17%	9.41%	7.09%
50%-75%	9.87%	9.85%	1.05%	9.86%	7.38%

Notes: The cumulative GDP losses are in relative terms of the annual GDPs at the pre-disaster levels. The results are given as the ensemble mean of scenarios where different scales of floods

collide with a 30%-24 pandemic control.

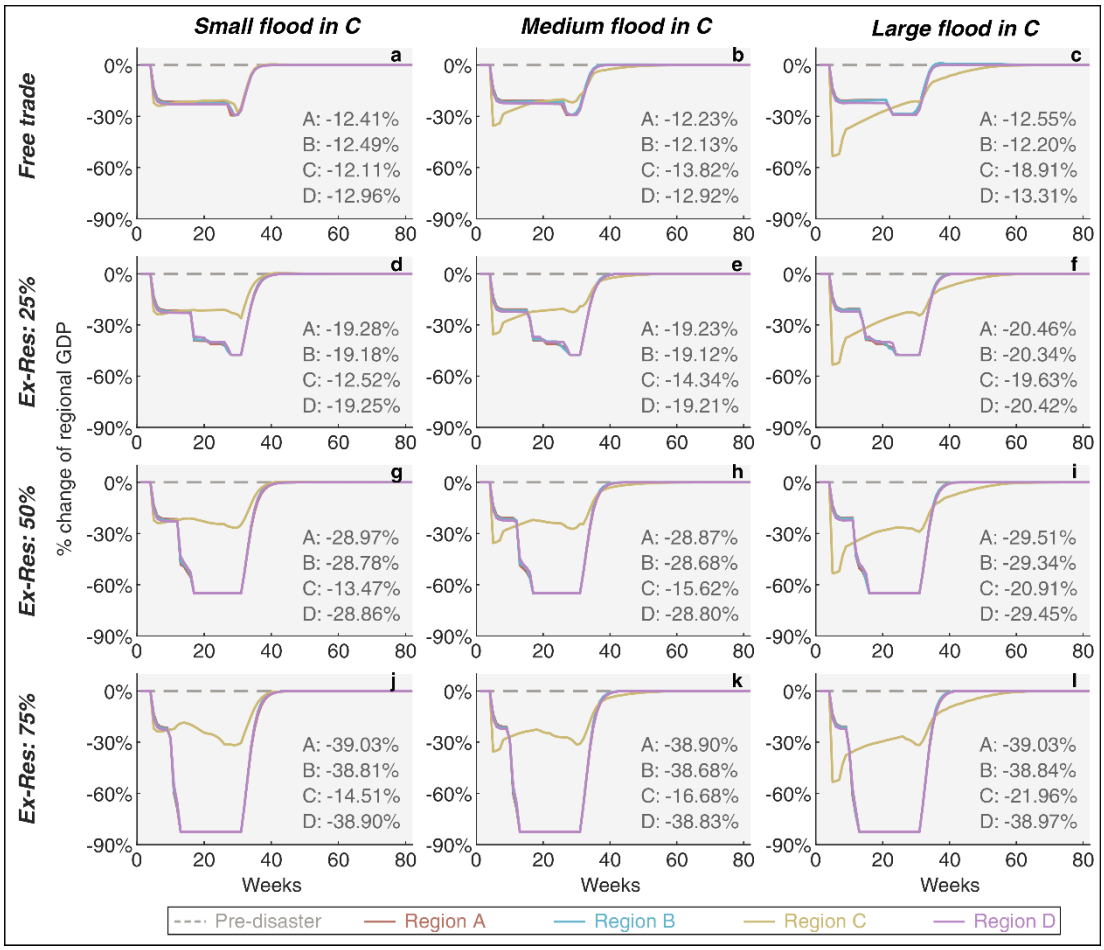

Figure C2: Weekly changes of regional GDPs, relative to the pre-disaster level, in the four regions, when the export restriction is imposed on 'MANK-C' at different degrees with production specialization during the compound flood and pandemic crises.

The numbers in each plot indicate the cumulative losses or gains of regional GDPs over time, relative to the pre-disaster levels of the annual regional GDPs. From left to right, each column represents the small-, medium-, and large-scale flooding in region C. From top to bottom, each row stands for the 0%, 25%, 50% or 75% export restriction on the 'MANK' sector in region C.

References

Abdal, A., and Ferreira, D. M. (2021). Deglobalization, globalization, and the pandemic: current impasses of the capitalist world-economy. *Journal of World-Systems Research*, *27*(1), 202-230. https://doi.org/10.5195/jwsr.2021.1028

Acemoglu, D. (2003). Labor- and capital-augmenting technical change. *Journal of the European Economic Association*, *1*(1), 1-37. https://doi.org/10.1162/154247603322256756

AghaKouchak, A., Chiang, F., Huning, L. S., Love, C. A., Mallakpour, I., Mazdiyasni, O., . . . Sadegh, M. (2020). Climate extremes and compound hazards in a warming world. *Annual Review of Earth and Planetary Sciences*, *48*(1), 519-548. https://doi.org/10.1146/annurev-earth-071719-055228

Aghion, P., and Howitt, P. (1990). *A model of growth through creative destruction* [Working Paper](No. 3223). National Bureau of Economic Research. http://www.nber.org/papers/w3223

Aguiar, A., Chepeliev, M., Corong, E. L., McDougall, R., and van der Mensbrugghe, D. (2019). The GTAP data base: version 10. *Journal of Global Economic Analysis*, *4*(1), 1-27. https://doi.org/10.21642/JGEA.040101AF

AIFDR. (2022). *InaSafe-Eartquake tool*. Australia-Indonesia Facility for Disaster Reduction. Retrieved May 31, 2022 from http://inasafe.org/

Alfieri, L., Bisselink, B., Dottori, F., Naumann, G., de Roo, A., Salamon, P., . . . Feyen, L. (2017). Global projections of river flood risk in a warmer world. *Earth's Future*, *5*(2), 171-182. https://doi.org/10.1002/2016EF000485

Alfieri, L., Feyen, L., Dottori, F., and Bianchi, A. (2015). Ensemble flood risk assessment in Europe under high end climate scenarios. *Global Environmental Change*, *35*, 199-212. https://doi.org/10.1016/j.gloenvcha.2015.09.004

Aliboni, R. (2012). *Egypt's Economic Potential (RLE Egypt)* (R. Aliboni, A. H. Dessouki, S. E. Ibrahim, G. Luciano, and P. Padoan, Eds. 1st ed., Vol. 7). Routledge.

Amann, M., Kiesewetter, G., Schöpp, W., Klimont, Z., Winiwarter, W., Cofala, J., . . . Pavarini, C. (2020). Reducing global air pollution: the scope for further policy interventions. *Philosophical Transactions of the Royal Society A: Mathematical, Physical and Engineering Sciences*, *378*(2183), 20190331. https://doi.org/10.1098/rsta.2019.0331

Anttila-Hughes, J., and Hsiang, S. M. (2013). *Destruction, disinvestment, and death: economic and human losses following environmental disaster*. https://ssrn.com/abstract=2220501

Apel, H., Aronica, G. T., Kreibich, H., and Thieken, A. H. (2009). Flood risk analyses - how detailed do we need to be? *Natural Hazards*, *49*(1), 79-98. https://doi.org/10.1007/s11069-008-9277-8

Arnell, N. W., and Gosling, S. N. (2016). The impacts of climate change on river flood risk at the global scale. *Climatic Change*, *134*(3), 387-401. https://doi.org/10.1007/s10584-014-1084-5

Arnell, N. W., and Lloyd-Hughes, B. (2014). The global-scale impacts of climate change on water resources and flooding under new climate and socio-economic scenarios. *Climatic Change*, *122*(1), 127-140. https://doi.org/10.1007/s10584-013-0948-4

Atkinson, R. W., Kang, S., Anderson, H. R., Mills, I. C., and Walton, H. A. (2014). Epidemiological time series studies of PM2.5 and daily mortality and hospital admissions: a systematic review and meta-analysis. *Thorax*, *69*(7), 660. https://doi.org/10.1136/thoraxjnl-2013-204492

Avelino, A. F. T., and Dall'Erba, S. (2019). Comparing the economic impact of natural disasters generated by different input-output models: an application to the 2007 Chehalis River Flood. *Risk Analysis*, *39*(1), 85-104. https://doi.org/10.1111/risa.13006

Bal, I. E., Bommer, J. J., Stafford, P. J., Crowley, H., and Pinho, R. (2010). The influence of geographical resolution of urban exposure data in an earthquake loss model for Istanbul. *Earthquake Spectra*, *26*(3), 619-634. https://doi.org/10.1193/1.3459127

Barker, K., and Santos, J. R. (2010). Measuring the efficacy of inventory with a dynamic input-output model. *International Journal of Production Economics*, *126*(1), 130-143. https://doi.org/10.1016/j.ijpe.2009.08.011

Basu, R., and Samet, J. M. (2002). Relation between elevated ambient temperature and mortality: a review of the epidemiologic evidence. *Epidemiologic Reviews*, *24*(2), 190-202. https://doi.org/10.1093/epirev/mxf007

Bayentin, L., El Adlouni, S., Ouarda, T. B. M. J., Gosselin, P., Doyon, B., and Chebana, F. (2010). Spatial variability of climate effects on ischemic heart disease hospitalization rates for the period 1989-2006 in Quebec, Canada. *International Journal of Health Geographics*, *9*(1), 5. https://doi.org/10.1186/1476-072X-9-5

BBC News. (2021). *Saharan dust: orange skies and sandy snow in southern Europe*. Retrieved May 29, 2021 from https://www.bbc.com/news/av/world-europe-55966867

Bergström, S. (1992). *The HBV model - its structure and applications* [SMHI Report](RH No. 4). Swedish Meteorological and Hydrological Institute. https://www.smhi.se/polopoly_fs/1.83592!/Menu/general/extGroup/attachmentColHold/mainCol1/file/RH_4.pdf

Bevacqua, E., Vousdoukas, M. I., Zappa, G., Hodges, K., Shepherd, T. G., Maraun, D., . . . Feyen, L. (2020). More meteorological events that drive compound coastal flooding are projected under climate change. *Communications Earth & Environment*, *1*(1), 47. https://doi.org/10.1038/s43247-020-00044-z

Bezner Kerr, R., Hasegawa, T., Lasco, R., Bhatt, I., Deryng, D., Farrell, A., . . .

Thornton, P. (2022). Food, fibre, and other ecosystem products. In H.-O. Pörtner, D. C. Roberts, M. Tignor, E. S. Poloczanska, K. Mintenbeck, A. Alegría, . . . B. Rama (Eds.), *Climate Change 2022: Impacts, Adaptation, and Vulnerability. Contribution of Working Group II to the Sixth Assessment Report of the Intergovernmental Panel on Climate Change*. Cambridge University Press.

Bierkandt, R., Wenz, L., Willner, S. N., and Levermann, A. (2014). Acclimate - a model for economic damage propagation. Part 1: basic formulation of damage transfer within a global supply network and damage conserving dynamics. *Environment Systems and Decisions*, *34*(4), 507-524. https://doi.org/10.1007/s10669-014-9523-4

Boehm, C. E., Flaaen, A., and Pandalai-Nayar, N. (2019). Input linkages and the transmission of shocks: firm-Level evidence from the 2011 Tōhoku earthquake. *The Review of Economics and Statistics*, *101*(1), 60-75. https://doi.org/10.1162/rest_a_00750

Bonaccorsi, G., Pierri, F., Cinelli, M., Flori, A., Galeazzi, A., Porcelli, F., . . . Pammolli, F. (2020). Economic and social consequences of human mobility restrictions under COVID-19. *Proceedings of the National Academy of Sciences*, *117*(27), 15530-15535. https://doi.org/10.1073/pnas.2007658117

Bose-O'Reilly, S., Daanen, H., Deering, K., Gerrett, N., Huynen, M. M. T. E., Lee, J., . . . Nowak, D. (2021). COVID-19 and heat waves: new challenges for healthcare systems. *Environmental Research*, *198*, 111153. https://doi.org/10.1016/j.envres.2021.111153

Bosello, F., Nicholls, R. J., Richards, J., Roson, R., and Tol, R. S. J. (2012). Economic impacts of climate change in Europe: sea-level rise. *Climatic Change*, *112*(1), 63-81. https://doi.org/10.1007/s10584-011-0340-1

Botzen, W. J. W., Deschenes, O., and Sanders, M. (2019). The economic impacts of natural disasters: a review of models and empirical studies. *Review of Environmental Economics and Policy*, *13*(2), 167-188. https://doi.org/10.1093/reep/rez004

Bouwer, L. M., Bubeck, P., Wagtendonk, A. J., and Aerts, J. C. J. H. (2009). Inundation scenarios for flood damage evaluation in polder areas. *Natural Hazards and Earth System Sciences*, *9*(6), 1995-2007. https://doi.org/10.5194/nhess-9-1995-2009

Bouwmeester, M. C., and Oosterhaven, J. (2017). Economic impacts of natural gas flow disruptions between Russia and the EU. *Energy Policy*, *106*, 288-297. https://doi.org/10.1016/j.enpol.2017.03.030

Boyle, L. (2020). *2020 has been a bleak year in the climate crisis. So here's the good news*. Retrieved January 21, 2021 from https://www.independent.co.uk/environment/climate-change/climate-change-2020-record-good-news-b1780393.html

Brando, P. M., Balch, J. K., Nepstad, D. C., Morton, D. C., Putz, F. E., Coe, M. T., . . .

Soares-Filho, B. S. (2014). Abrupt increases in Amazonian tree mortality due to drought-fire interactions. *Proceedings of the National Academy of Sciences*, *111*(17), 6347-6352. https://doi.org/10.1073/pnas.1305499111

Brenton, P., and Chemutai, V. (2021). *The Trade and Climate Change Nexus: The Urgency and Opportunities for Developing Countries*. The World Bank. https://openknowledge.worldbank.org/handle/10986/36294

Brinca, P., Duarte, J. B., and Faria-E-Castro, M. (2021). Measuring labor supply and demand shocks during COVID-19. *European Economic Review*, *139*, 103901. https://doi.org/10.1016/j.euroecorev.2021.103901

Bröde, P., Fiala, D., Lemke, B., and Kjellstrom, T. (2018). Estimated work ability in warm outdoor environments depends on the chosen heat stress assessment metric. *International Journal of Biometeorology*, *62*(3), 331-345. https://doi.org/10.1007/s00484-017-1346-9

Bubeck, P., Otto, A., and Weichselgartner, J. (2017). *Societal impacts of flood hazards*. Oxford University Press. Retrieved May 31, 2022 from https://oxfordre.com/naturalhazardscience/view/10.1093/acrefore/9780199389407.001.0001/acrefore-9780199389407-e-281

Burnett, R. T., Pope, C. A., Ezzati, M., Olives, C., Lim, S. S., Mehta, S., . . . Cohen, A. (2014). An integrated risk function for estimating the global burden of disease attributable to ambient fine particulate matter exposure. *Environmental Health Perspectives*, *122*(4), 397-403. https://doi.org/10.1289/ehp.1307049

Cai, W., Zhang, C., Zhang, S., Ai, S., Bai, Y., Bao, J., . . . Gong, P. (2021). The 2021 China report of the Lancet Countdown on health and climate change: seizing the window of opportunity. *The Lancet Public Health*, *6*(12), e932-e947. https://doi.org/10.1016/S2468-2667(21)00209-7

Cai, X., Lu, Y., and Wang, J. (2018). The impact of temperature on manufacturing worker productivity: evidence from personnel data. *Journal of Comparative Economics*, *46*(4), 889-905. https://doi.org/10.1016/j.jce.2018.06.003

Caretta, M. A., Mukherji, A., Arfanuzzaman, M., Betts, R. A., Gelfan, A., Hirabayashi, Y., . . . Supratid, S. (2022). Water. In H.-O. Pörtner, D. C. Roberts, M. Tignor, E. S. Poloczanska, K. Mintenbeck, A. Alegría, . . . B. Rama (Eds.), *Climate Change 2022: Impacts, Adaptation, and Vulnerability. Contribution of Working Group II to the Sixth Assessment Report of the Intergovernmental Panel on Climate Change* (pp. 551-712). Cambridge University Press. https://doi.org/10.1017/9781009325844.006

Carrera, L., Standardi, G., Bosello, F., and Mysiak, J. (2015). Assessing direct and indirect economic impacts of a flood event through the integration of spatial and computable general equilibrium modelling. *Environmental Modelling & Software*, *63*, 109-122. https://doi.org/10.1016/j.envsoft.2014.09.016

Chambers, J. (2020). *Hybrid gridded demographic data for the world, 1950-2020* (Version 1.0) [Dataset]. https://doi.org/10.5281/zenodo.3768003

Charvet, I., Macabuag, J., and Rossetto, T. (2017). Estimating tsunami-induced

building damage through fragility functions: critical review and research needs. *Frontiers in Built Environment*, *3*(36). https://doi.org/10.3389/fbuil.2017.00036

Chen, R., Yin, P., Wang, L., Liu, C., Niu, Y., Wang, W., . . . Zhou, M. (2018). Association between ambient temperature and mortality risk and burden: time series study in 272 main Chinese cities. *BMJ*, *363*, k4306. https://doi.org/10.1136/bmj.k4306

Chen, X., and Yang, L. (2019). Temperature and industrial output: firm-level evidence from China. *Journal of Environmental Economics and Management*, *95*, 257-274. https://doi.org/10.1016/j.jeem.2017.07.009

Cho, S., Gordon, P., Moore Ii, J. E., Richardson, H. W., Shinozuka, M., and Chang, S. (2001). Integrating transportation network and regional economic models to estimate the costs of a large urban earthquake. *Journal of Regional Science*, *41*(1), 39-65. https://doi.org/10.1111/0022-4146.00206

Chondol, T., Bhardwaj, S., Panda, A. K., and Gupta, A. K. (2020). Multi-hazard risk management during pandemic. In *Integrated Risk of Pandemic: Covid-19 Impacts, Resilience and Recommendations* (pp. 445-461). Springer Singapore. https://doi.org/10.1007/978-981-15-7679-9_22

Cochrane, H. (2004). Economic loss: myth and measurement. *Disaster Prevention and Management: An International Journal*, *13*(4), 290-296. https://doi.org/10.1108/09653560410556500

Collins, J., Polen, A., Dunn, E., Cortes, L. M., Ackerson, E., Valmond, J., . . . Colón-Burgos, D. (2021). Compound hazards, evacuations, and shelter choices: implications for public health practices in the Puerto Rico and the U.S. Virgin Islands. In *Natural Hazards Center Public Health Report Series, 6*. Natural Hazards Center, University of Colorado Boulder. https://hazards.colorado.edu/public-health-disaster-research/compound-hazards-evacuations-and-shelter-choices

Cox, N., Ganong, P., Noel, P., Vavra, J., Wong, A., Farrell, D., . . . Deadman, E. (2020). Initial impacts of the pandemic on consumer behavior: evidence from linked income, spending, and savings data. *Brookings Papers on Economic Activity*, *2020*(2), 35-82. https://doi.org/10.1353/eca.2020.0006

CRED. (1988). *The Emergency Events Database* [Database]. EM-DAT. https://emdat.be/

Crowley, H., Bommer, J. J., Pinho, R., and Bird, J. (2005). The impact of epistemic uncertainty on an earthquake loss model. *Earthquake Engineering & Structural Dynamics*, *34*(14), 1653-1685. https://doi.org/10.1002/eqe.498

Crowther, K. G., and Haimes, Y. Y. (2005). Application of the inoperability input-output model (IIM) for systemic risk assessment and management of interdependent infrastructures. *Systems Engineering*, *8*(4), 323-341. https://doi.org/10.1002/sys.20037

Curriero, F. C. (2002). Temperature and mortality in 11 cities of the eastern United

States. *American Journal of Epidemiology*, *155*(1), 80-87. https://doi.org/10.1093/aje/155.1.80

Cuschieri, S., Calleja, N., Devleesschauwer, B., and Wyper, G. M. A. (2021). Estimating the direct Covid-19 disability-adjusted life years impact on the Malta population for the first full year. *BMC Public Health*, *21*(1), 1827. https://doi.org/10.1186/s12889-021-11893-4

Cutler, D. M., and Summers, L. H. (2020). The COVID-19 pandemic and the $16 trillion virus. *JAMA*, *324*(15), 1495-1496. https://doi.org/10.1001/jama.2020.19759

Dabbeek, J., and Silva, V. (2020). Modeling the residential building stock in the Middle East for multi-hazard risk assessment. *Natural Hazards*, *100*(2), 781-810. https://doi.org/10.1007/s11069-019-03842-7

Darwin, R. F., and Tol, R. S. J. (2001). Estimates of the economic effects of sea level rise. *Environmental and Resource Economics*, *19*(2), 113-129. https://doi.org/10.1023/a:1011136417375

de Moel, H., and Aerts, J. C. J. H. (2011). Effect of uncertainty in land use, damage models and inundation depth on flood damage estimates. *Natural Hazards*, *58*(1), 407-425. https://doi.org/10.1007/s11069-010-9675-6

de Moel, H., Jongman, B., Kreibich, H., Merz, B., Penning-Rowsell, E., and Ward, P. J. (2015). Flood risk assessments at different spatial scales. *Mitigation and Adaptation Strategies for Global Change*, *20*(6), 865-890. https://doi.org/10.1007/s11027-015-9654-z

de Ruiter, M. C., Ward, P. J., Daniell, J. E., and Aerts, J. C. J. H. (2017). Review article: a comparison of flood and earthquake vulnerability assessment indicators. *Natural Hazards and Earth System Sciences*, *17*(7), 1231-1251. https://doi.org/10.5194/nhess-17-1231-2017

Dear, K., Ranmuthugala, G., Kjellström, T., Skinner, C., and Hanigan, I. (2005). Effects of temperature and ozone on daily mortality during the August 2003 heat wave in France. *Archives of Environmental & Occupational Health*, *60*(4), 205-212. https://doi.org/10.3200/AEOH.60.4.205-212

Dell, M., Jones, B. F., and Olken, B. A. (2012). Temperature shocks and economic growth: evidence from the last half century. *American Economic Journal: Macroeconomics*, *4*(3), 66-95. https://doi.org/10.1257/mac.4.3.66

Dickinson, R., and Zemaityte, G. (2021). *How has the COVID-19 pandemic affected global trade?* Retrieved August 29, 2022 from https://www.weforum.org/agenda/2021/08/covid19-pandemic-trade-services-goods/

Dietzenbacher, E., and Miller, R. E. (2015). Reflections on the inoperability input-output model. *Economic Systems Research*, *27*(4), 478-486. https://doi.org/10.1080/09535314.2015.1052375

Do Prado, C. B., Emerick, G. S., Cevolani Pires, L. B., and Salaroli, L. B. (2022). Impact of long-term COVID on workers: a systematic review protocol. *PLOS*

ONE, *17*(9), e0265705. https://doi.org/10.1371/journal.pone.0265705

Dottori, F., Szewczyk, W., Ciscar, J.-C., Zhao, F., Alfieri, L., Hirabayashi, Y., . . . Feyen, L. (2018). Increased human and economic losses from river flooding with anthropogenic warming. *Nature Climate Change*, *8*(9), 781-786. https://doi.org/10.1038/s41558-018-0257-z

Douglas, J. (2007). Physical vulnerability modelling in natural hazard risk assessment. *Natural Hazards and Earth System Sciences*, *7*(2), 283-288. https://doi.org/10.5194/nhess-7-283-2007

Dunz, N., Mazzocchetti, A., Monasterolo, I., Hrast Essenfelder, A., and Raberto, M. (2021). Compounding COVID-19 and climate risks: the interplay of banks' lending and government's policy in the shock recovery. *Journal of Banking & Finance*, 106306. https://doi.org/10.1016/j.jbankfin.2021.106306

Eaton, L. (2021). Covid-19: WHO warns against "vaccine nationalism" or face further virus mutations. *BMJ*, *372*, n292. https://doi.org/10.1136/bmj.n292

Eckhardt, D., Leiras, A., and Thomé, A. M. T. (2019). Systematic literature review of methodologies for assessing the costs of disasters. *International Journal of Disaster Risk Reduction*, *33*, 398-416. https://doi.org/10.1016/j.ijdrr.2018.10.010

Efimov, D., and Ushirobira, R. (2021). On an interval prediction of COVID-19 development based on a SEIR epidemic model. *Annual Reviews in Control*, *51*, 477-487. https://doi.org/10.1016/j.arcontrol.2021.01.006

EMA. (2002). *Disaster loss assessment guidelines*. Lllycroft Pty Ltd and Brisbane and PenUltimate. https://doms.csu.edu.au/csu/file/78a6c5d7-fd8b-ff7e-fff3-2ffb78764ebe/1/resources/manuals/Manual-27.pdf

ESA. (2017). *Land cover CCI product user guide version 2* (Technical Report). https://climate.esa.int/media/documents/CCI_Land_Cover_PUG_v2.0.pdf

ESCAP. (2019). *Asia-pacific disaster report 2019*. Economic and Social Commission for Asia and the Pacific of the United Nations. https://www.unescap.org/publications/asia-pacific-disaster-report-2019

Espitia, A., Rocha, N., and Ruta, M. (2020). *Covid-19 and Food Protectionism: The Impact of the Pandemic and Export Restrictions on World Food Markets*. The World Bank. https://doi.org/10.1596/1813-9450-9253

Falloon, P., and Betts, R. (2010). Climate impacts on European agriculture and water management in the context of adaptation and mitigation - the importance of an integrated approach. *Science of the Total Environment*, *408*(23), 5667-5687. https://doi.org/10.1016/j.scitotenv.2009.05.002

Faturay, F., Sun, Y.-Y., Dietzenbacher, E., Malik, A., Geschke, A., and Lenzen, M. (2019). Using virtual laboratories for disaster analysis - a case study of Taiwan. *Economic Systems Research*, *32*(1), 1-26. https://doi.org/10.1080/09535314.2019.1617677

Felbermayr, G., and Gröschl, J. (2014). Naturally negative: the growth effects of natural disasters. *Journal of Development Economics*, *111*, 92-106.

https://doi.org/10.1016/j.jdeveco.2014.07.004

FEMA. (2009). *HAZUS-MH MR4 flood model technical manual*. Federal Emergency Management Agency.

Ferrantino, M. J., Arvis, J. F., Brotsis, C. J., Constantinescu, I. C., Dairabayeva, K. S., Gillson, I. J. D., . . . Souza Muramatsu, K. (2020). *COVID-19 Trade Watch (May 29, 2020) (English)*. http://documents.worldbank.org/curated/en/976521591020893415/COVID-19-Trade-Watch-May-29-2020

FEWS NET. (2020). *Zimbabwe famine early warning systems network*. Retrieved August 29, 2022 from https://fews.net/southern-africa/zimbabwe

Field, C. B., Barros, V., Stocker, T. F., and Dahe, Q. (2012). *Managing the Risks of Extreme Events and Disasters to Advance Climate Change Adaptation: Special Report of the Intergovernmental Panel on Climate Change*. Cambridge University Press.

Fiore, A. M., Naik, V., and Leibensperger, E. M. (2015). Air quality and climate connections. *Journal of the Air & Waste Management Association*, *65*(6), 645-685. https://doi.org/10.1080/10962247.2015.1040526

Fu, T.-M., and Tian, H. (2019). Climate change penalty to ozone air quality: review of current understandings and knowledge gaps. *Current Pollution Reports*, *5*(3), 159-171. https://doi.org/10.1007/s40726-019-00115-6

Garschagen, M., and Romero-Lankao, P. (2015). Exploring the relationships between urbanization trends and climate change vulnerability. *Climatic Change*, *133*(1), 37-52. https://doi.org/10.1007/s10584-013-0812-6

Ghosh, A. (1958). Input-output approach in an allocation system. *Economica*, *25*(97), 58-64.

Giani, P., Castruccio, S., Anav, A., Howard, D., Hu, W., and Crippa, P. (2020). Short-term and long-term health impacts of air pollution reductions from COVID-19 lockdowns in China and Europe: a modelling study. *The Lancet Planetary Health*, *4*(10), e474-e482. https://doi.org/10.1016/S2542-5196(20)30224-2

Giarratani, F. (1981). A supply-constrained interindustry model: forecasting performance and an evaluation. In W. Buhr and P. Friedrich (Eds.), *Regional Development under Stagnation* (pp. 281–291). Nomos.

Global Burden of Disease Collaborative Network. (2021). *Global burden of disease study 2019 (GBD 2019): particulate matter risk curves* [Dataset]. Institute for Health Metrics and Evaluation (IHME). https://doi.org/10.6069/KHWH-2703

Goda, G. S., and Soltas, E. J. (2022). *The impacts of Covid-19 illnesses on workers* [Working Paper](No. 30435). National Bureau of Economic Research. http://www.nber.org/papers/w30435

Gohd, C. (2021). *2020 ties record for the hottest year ever, NASA analysis shows*. Retrieved January 21, 2021 from https://www.space.com/nasa-confirms-2020-hottest-year-on-record

Greenberg, M. R., Lahr, M., and Mantell, N. (2007). Understanding the economic costs

and benefits of catastrophes and their aftermath: a review and suggestions for the U.S. federal government. *Risk Analysis*, *27*(1), 83-96. https://doi.org/10.1111/j.1539-6924.2006.00861.x

Gruver, G. W. (1989). On the plausibility of the supply-driven input-output model: a theoretical basis for input-coefficient change. *Journal of Regional Science*, *29*(3), 441-450. https://doi.org/10.1111/j.1467-9787.1989.tb01389.x

Gu, L., Chen, J., Yin, J., Slater, L. J., Wang, H.-M., Guo, Q., . . . Zhao, T. (2022). Global increases in compound flood-hot extreme hazards under climate warming. *Geophysical Research Letters*, *49*(8), e2022GL097726. https://doi.org/10.1029/2022GL097726

Guan, D., Wang, D., Hallegatte, S., Davis, S. J., Huo, J., Li, S., . . . Gong, P. (2020). Global supply-chain effects of COVID-19 control measures. *Nature Human Behaviour*, *4*(6), 577-587. https://doi.org/10.1038/s41562-020-0896-8

Guimaraes, P., Hefner, F. L., and Woodward, D. P. (1993). Wealth and income effects of natural disasters: an econometric analysis of Hurricane Hugo. *Review of Regional Studies*, *23*(2), 97-114.

Gütschow, J., Jeffery, M. L., Schaeffer, M., and Hare, B. (2018). Extending near-term emissions scenarios to assess warming implications of Paris Agreement NDCs. *Earth's Future*, *6*(9), 1242-1259. https://doi.org/10.1002/2017EF000781

Hallegatte, S. (2008). An adaptive regional input-output model and its application to the assessment of the economic cost of Katrina. *Risk Analysis*, *28*(3), 779-799. https://doi.org/10.1111/j.1539-6924.2008.01046.x

Hallegatte, S. (2014). Modeling the role of inventories and heterogeneity in the assessment of the economic costs of natural disasters. *Risk Analysis*, *34*(1), 152-167. https://doi.org/10.1111/risa.12090

Hallegatte, S., Green, C., Nicholls, R. J., and Corfee-Morlot, J. (2013). Future flood losses in major coastal cities. *Nature Climate Change*, *3*(9), 802-806. https://doi.org/10.1038/nclimate1979

Hallegatte, S., Hourcade, J.-C., and Dumas, P. (2007). Why economic dynamics matter in assessing climate change damages: illustration on extreme events. *Ecological Economics*, *62*(2), 330-340. https://doi.org/10.1016/j.ecolecon.2006.06.006

Hallegatte, S., Ranger, N., Mestre, O., Dumas, P., Corfee-Morlot, J., Herweijer, C., and Wood, R. M. (2011). Assessing climate change impacts, sea level rise and storm surge risk in port cities: a case study on Copenhagen. *Climatic Change*, *104*(1), 113-137. https://doi.org/10.1007/s10584-010-9978-3

Hammond, M. J., Chen, A. S., Djordjevic, S., Butler, D., and Mark, O. (2015). Urban flood impact assessment: a state-of-the-art review. *Urban Water Journal*, *12*(1), 14-29. https://doi.org/10.1080/1573062X.2013.857421

Hao, Z., AghaKouchak, A., and Phillips, T. J. (2013). Changes in concurrent monthly precipitation and temperature extremes. *Environmental Research Letters*, *8*(3), 034014. https://doi.org/10.1088/1748-9326/8/3/034014

Hao, Z., and Singh, V. P. (2020). Compound events under global warming: a dependence perspective. *Journal of Hydrologic Engineering*, *25*(9), 03120001. https://doi.org/10.1061/(ASCE)HE.1943-5584.0001991

Hariri-Ardebili, M. A. (2020). Living in a multi-risk chaotic condition: pandemic, natural hazards and complex emergencies. *International Journal of Environmental Research and Public Health*, *17*(16), 5635. https://doi.org/10.3390/ijerph17165635

Hatzigeorgiou, A., and Lodefalk, M. (2021). A literature review of the nexus between migration and internationalization. *The Journal of International Trade & Economic Development*, *30*(3), 319-340. https://doi.org/10.1080/09638199.2021.1878257

He, S., Peng, Y., and Sun, K. (2020). SEIR modeling of the COVID-19 and its dynamics. *Nonlinear Dynamics*, *101*(3), 1667-1680. https://doi.org/10.1007/s11071-020-05743-y

He, Y., Manful, D., Warren, R., Forstenhäusler, N., Osborn, T. J., Price, J., . . . Yamazaki, D. (2022). Quantification of impacts between 1.5 and 4 °C of global warming on flooding risks in six countries. *Climatic Change*, *170*(1), 15. https://doi.org/10.1007/s10584-021-03289-5

Hekmatpour, P., and Leslie, C. M. (2022). Ecologically unequal exchange and disparate death rates attributable to air pollution: a comparative study of 169 countries from 1991 to 2017. *Environmental Research*, *212*, 113161. https://doi.org/10.1016/j.envres.2022.113161

Hirabayashi, Y., and Kanae, S. (2009). First estimate of the future global population at risk of flooding. *Hydrological Research Letters*, *3*, 6-9. https://doi.org/10.3178/hrl.3.6

Hirabayashi, Y., Mahendran, R., Koirala, S., Konoshima, L., Yamazaki, D., Watanabe, S., . . . Kanae, S. (2013). Global flood risk under climate change. *Nature Climate Change*, *3*(9), 816-821. https://doi.org/10.1038/nclimate1911

Hirabayashi, Y., Tanoue, M., Sasaki, O., Zhou, X., and Yamazaki, D. (2021). Global exposure to flooding from the new CMIP6 climate model projections. *Scientific Reports*, *11*(1), 3740. https://doi.org/10.1038/s41598-021-83279-w

Hoekstra, A. Y., Chapagain, A. K., Mekonnen, M. M., and Aldaya, M. M. (2011). *The Water Footprint Assessment Manual: Setting the Global Standard*. Earthscan.

Hoekstra, A. Y., and Hung, P. Q. (2002). Virtual water trade: a quantification of virtual water flows between nations in relation to international crop trade. In *Value of Water Research Report Series No. 11*. UNESCO-IHE.

Honda, Y., Kondo, M., McGregor, G., Kim, H., Guo, Y.-L., Hijioka, Y., . . . Kovats, R. S. (2014). Heat-related mortality risk model for climate change impact projection. *Environmental health and preventive medicine*, *19*(1), 56-63. https://doi.org/10.1007/s12199-013-0354-6

Horton, D. E., Skinner, C. B., Singh, D., and Diffenbaugh, N. S. (2014). Occurrence and persistence of future atmospheric stagnation events. *Nature Climate*

Change, *4*(8), 698-703. https://doi.org/10.1038/nclimate2272

Hosseinpour, V., Saeidi, A., Nollet, M.-J., and Nastev, M. (2021). Seismic loss estimation software: a comprehensive review of risk assessment steps, software development and limitations. *Engineering Structures*, *232*, 111866. https://doi.org/10.1016/j.engstruct.2021.111866

Hsiang, S. M. (2010). Temperatures and cyclones strongly associated with economic production in the Caribbean and Central America. *Proceedings of the National Academy of Sciences*, *107*(35), 15367-15372. https://doi.org/10.1073/pnas.1009510107

Hsiang, S. M., and Jina, A. S. (2014). *The causal effect of environmental catastrophe on long-run economic growth: evidence from 6,700 cyclones* [Working Paper](No. 20352). National Bureau of Economic Research. https://www.nber.org/papers/w20352

Hu, Y., Wang, D., Huo, J., Yang, L., Guan, D., Brenton, P., and Chemutai, V. (2021). *Assessing the economic impacts of a 'perfect storm' of extreme weather, pandemic control and deglobalization: a methodological construct* [Working Paper](No. 160571). The World Bank. https://documents.worldbank.org/en/publication/documents-reports/documentdetail/744851623848784106/assessing-the-economic-impacts-of-a-perfect-storm-of-extreme-weather-pandemic-control-and-deglobalization-a-methodological-construct

Huang, B., Wang, J., Cai, J., Yao, S., Chan, P. K. S., Tam, T. H.-w., . . . Lai, S. (2021). Integrated vaccination and physical distancing interventions to prevent future COVID-19 waves in Chinese cities. *Nature Human Behaviour*, *5*(6), 695-705. https://doi.org/10.1038/s41562-021-01063-2

Huang, C., and Barnett, A. (2014). Winter weather and health. *Nature Climate Change*, *4*(3), 173-174. https://doi.org/10.1038/nclimate2146

Huizinga, J., Moel, H. d., and Szewczyk, W. (2017). *Global flood depth-damage functions: methodology and the database with guidelines* [JRC Working Papers](JRC105688). Joint Research Centre (Seville site). https://ideas.repec.org/p/ipt/iptwpa/jrc105688.html

IEA. (2021). *World energy outlook 2021* [Report]. International Energy Agency. https://www.iea.org/reports/world-energy-outlook-2021

IHME. (2021). *Global burden of disease collaborative network. Particulate matter risk curves* [Dataset]. Institute for Health Metrics and Evaluation (IHME). http://ghdx.healthdata.org/gbd-2019

Imada, Y., Watanabe, M., Kawase, H., Shiogama, H., and Arai, M. (2019). The July 2018 high temperature event in Japan could not have happened without human-induced global warming. *SOLA*, *15A*, 8-12. https://doi.org/10.2151/sola.15A-002

IMF. (2015). *Investment and capital stock (ICSD)* [Dataset]. International Monetary Fund. https://data.imf.org/?sk=1CE8A55F-CFA7-4BC0-BCE2-

256EE65AC0E4

IPCC. (2012). Summary for policymakers. In C. B. Field, V. Barros, T. F. Stocker, D. Qin, D. J. Dokken, K. L. Ebi, . . . P. M. Midgley (Eds.), *Managing the Risks of Extreme Events and Disasters to Advance Climate Change Adaptation* (pp. 1-19). Cambridge University Press.

IPCC. (2021). Summary for policymakers. In V. Masson-Delmotte, P. Zhai, A. Pirani, S. L. Connors, C. Péan, S. Berger, . . . B. Zhou (Eds.), *Climate Change 2021: The Physical Science Basis. Contribution of Working Group I to the Sixth Assessment Report of the Intergovernmental Panel on Climate Change* (pp. 3-32). Cambridge University Press. https://doi.org/10.1017/9781009157896.001

IPCC. (2022). Summary for policymakers. In H.-O. Pörtner, D.C. Roberts, M. Tignor, E.S. Poloczanska, K. Mintenbeck, A. Alegría, . . . B. Rama (Eds.), *Climate Change 2022: Impacts, Adaptation, and Vulnerability. Contribution of Working Group II to the Sixth Assessment Report of the Intergovernmental Panel on Climate Change* (pp. 3-33). Cambridge University Press. https://doi.org/10.1017/9781009325844.001

Irwin, D. (2020). *The pandemic adds momentum to the deglobalisation trend*. Retrieved May 3, 2022 from https://voxeu.org/article/pandemic-adds-momentum-deglobalisation-trend

Ishiwatari, M., Koike, T., Hiroki, K., Toda, T., and Katsube, T. (2020). Managing disasters amid COVID-19 pandemic: approaches of response to flood disasters. *Progress in Disaster Science*, *6*, 100096. https://doi.org/10.1016/j.pdisas.2020.100096

Itakura, K. (2020). Evaluating the impact of the US-China trade war. *Asian Economic Policy Review*, *15*(1), 77-93. https://doi.org/10.1111/aepr.12286

Ivanov, D. (2020). Predicting the impacts of epidemic outbreaks on global supply chains: a simulation-based analysis on the coronavirus outbreak (COVID-19/SARS-CoV-2) case. *Transportation Research Part E: Logistics and Transportation Review*, *136*, 101922. https://doi.org/10.1016/j.tre.2020.101922

Jacob, D. J., and Winner, D. A. (2009). Effect of climate change on air quality. *Atmospheric Environment*, *43*(1), 51-63. https://doi.org/10.1016/j.atmosenv.2008.09.051

Jiménez Cisneros, B. E., Oki, T., Arnell, N. W., Benito, G., Cogley, J. G., Döll, P., . . . Mwakalila, S. S. (2014). Freshwater resources. In C. B. Field, V. R. Barros, D. J. Dokken, K. J. Mach, M. D. Mastrandrea, T. E. Bilir, . . . L. L. White (Eds.), *Climate Change 2014: Impacts, Adaptation, and Vulnerability. Part A: Global and Sectoral Aspects. Contribution of Working Group II to the Fifth Assessment Report of the Intergovernmental Panel on Climate Change* (pp. 229-269). Cambridge University Press.

Johnstone, W. M., and Lence, B. J. (2009). Assessing the value of mitigation strategies in reducing the impacts of rapid-onset, catastrophic floods. *Journal of Flood*

Risk Management, *2*(3), 209-221. https://doi.org/10.1111/j.1753-318X.2009.01035.x

Jongman, B., Kreibich, H., Apel, H., Barredo, J. I., Bates, P. D., Feyen, L., . . . Ward, P. J. (2012). Comparative flood damage model assessment: towards a European approach. *Natural Hazards and Earth System Sciences*, *12*(12), 3733-3752. https://doi.org/10.5194/nhess-12-3733-2012

Jongman, B., Ward, P. J., and Aerts, J. C. J. H. (2012). Global exposure to river and coastal flooding: long term trends and changes. *Global Environmental Change*, *22*(4), 823-835. https://doi.org/10.1016/j.gloenvcha.2012.07.004

Jongman, B., Winsemius, H. C., Aerts, J. C. J. H., Coughlan de Perez, E., van Aalst, M. K., Kron, W., and Ward, P. J. (2015). Declining vulnerability to river floods and the global benefits of adaptation. *Proceedings of the National Academy of Sciences*, *112*(18), E2271-E2280. https://doi.org/10.1073/pnas.1414439112

Jonkeren, O., and Giannopoulos, G. (2014). Analysing critical infrastructure failure with a resilience inoperability input-output model. *Economic Systems Research*, *26*(1), 39-59. https://doi.org/10.1080/09535314.2013.872604

Jonkman, S. N., Bockarjova, M., Kok, M., and Bernardini, P. (2008). Integrated hydrodynamic and economic modelling of flood damage in the Netherlands. *Ecological Economics*, *66*(1), 77-90. https://doi.org/10.1016/j.ecolecon.2007.12.022

Jovel, R. J., and Mudahar, M. (2010). *Damage, loss and needs assessment guidance notes*. The World Bank. https://openknowledge.worldbank.org/handle/10986/19047

Kahn, M. E. (2005). The death toll from natural disasters: the role of income, geography, and institutions. *The Review of Economics and Statistics*, *87*(2), 271-284. http://www.jstor.org.uea.idm.oclc.org/stable/40042902

Kajitani, Y., and Tatano, H. (2018). Applicability of a spatial computable general equilibrium model to assess the short-term economic impact of natural disasters. *Economic Systems Research*, *30*(3), 289-312. https://doi.org/10.1080/09535314.2017.1369010

Kalakonas, P., Silva, V., Mouyiannou, A., and Rao, A. (2020). Exploring the impact of epistemic uncertainty on a regional probabilistic seismic risk assessment model. *Natural Hazards*, *104*(1), 997-1020. https://doi.org/10.1007/s11069-020-04201-7

Keeling, M. J., Hollingsworth, T. D., and Read, J. M. (2020). Efficacy of contact tracing for the containment of the 2019 novel coronavirus (COVID-19). *Journal of Epidemiology and Community Health*, *74*(10), 861. https://doi.org/10.1136/jech-2020-214051

Kellenberg, D. K., and Mobarak, A. M. (2008). Does rising income increase or decrease damage risk from natural disasters? *Journal of Urban Economics*, *63*(3), 788-802. https://doi.org/10.1016/j.jue.2007.05.003

Kinoshita, Y., Tanoue, M., Watanabe, S., and Hirabayashi, Y. (2018). Quantifying the

effect of autonomous adaptation to global river flood projections: application to future flood risk assessments. *Environmental Research Letters*, *13*(1), 014006. https://doi.org/10.1088/1748-9326/aa9401

Kircher, C. A., Whitman, R. V., and Holmes, W. T. (2006). HAZUS earthquake loss estimation methods. *Natural Hazards Review*, *7*(2), 45-59. https://doi.org/10.1061/(ASCE)1527-6988(2006)7:2(45)

Kjellstrom, T., Freyberg, C., Lemke, B., Otto, M., and Briggs, D. (2018). Estimating population heat exposure and impacts on working people in conjunction with climate change. *International Journal of Biometeorology*, *62*(3), 291-306. https://doi.org/10.1007/s00484-017-1407-0

Kjellstrom, T., Holmer, I., and Lemke, B. (2009). Workplace heat stress, health and productivity - an increasing challenge for low and middle-income countries during climate change. *Global Health Action*, *2*(1), 2047. https://doi.org/10.3402/gha.v2i0.2047

Klijn, F., Baan, P. J. A., De Bruijn, K. M., and Kwadijk, J. (2007). *Overstromingsrisico's in Nederland in een veranderend klimaat* (Q4290). http://resolver.tudelft.nl/uuid:015c62a1-558d-422c-8706-efc0e4db2fc3

Koks, E. E., Bočkarjova, M., de Moel, H., and Aerts, J. C. J. H. (2015). Integrated direct and indirect flood risk modeling: development and densitivity analysis. *Risk Analysis*, *35*(5), 882-900. https://doi.org/10.1111/risa.12300

Koks, E. E., Carrera, L., Jonkeren, O., Aerts, J. C. J. H., Husby, T. G., Thissen, M., . . . Mysiak, J. (2016). Regional disaster impact analysis: comparing input-output and computable general equilibrium models. *Natural Hazards and Earth System Sciences*, *16*(8), 1911-1924. https://doi.org/10.5194/nhess-16-1911-2016

Koks, E. E., and Thissen, M. (2016). A multiregional impact assessment model for disaster analysis. *Economic Systems Research*, *28*(4), 429-449. https://doi.org/10.1080/09535314.2016.1232701

Koks, E. E., Thissen, M., Alfieri, L., de Moel, H., Feyen, L., Jongman, B., and Aerts, J. C. J. H. (2019). The macroeconomic impacts of future river flooding in Europe. *Environmental Research Letters*, *14*(8), 084042. https://doi.org/10.1088/1748-9326/ab3306

Kousky, C. (2014). Informing climate adaptation: a review of the economic costs of natural disasters. *Energy Economics*, *46*, 576-592. https://doi.org/10.1016/j.eneco.2013.09.029

Kreibich, H., Seifert, I., Merz, B., and Thieken, A. H. (2010). Development of FLEMOcs - a new model for the estimation of flood losses in the commercial sector. *Hydrological Sciences Journal*, *55*(8), 1302-1314. https://doi.org/10.1080/02626667.2010.529815

Krichene, H., Geiger, T., Frieler, K., Willner, S. N., Sauer, I., and Otto, C. (2021). Long-term impacts of tropical cyclones and fluvial floods on economic growth - empirical evidence on transmission channels at different levels of

development. *World Development*, *144*, 105475. https://doi.org/10.1016/j.worlddev.2021.105475

Kruczkiewicz, A., Klopp, J., Fisher, J., Mason, S., McClain, S., Sheekh, N. M., . . . Braneon, C. (2021). Opinion: compound risks and complex emergencies require new approaches to preparedness. *Proceedings of the National Academy of Sciences*, *118*(19), e2106795118. https://doi.org/10.1073/pnas.2106795118

Kundzewicz, Z. W., Kanae, S., Seneviratne, S. I., Handmer, J., Nicholls, N., Peduzzi, P., . . . Sherstyukov, B. (2014). Flood risk and climate change: global and regional perspectives. *Hydrological Sciences Journal*, *59*(1), 1-28. https://doi.org/10.1080/02626667.2013.857411

Kuo, M. A. (2021). *TSMC and Samsung: semiconductor chip shortage*. Retrieved November 12, 2021 from https://thediplomat.com/2021/07/tsmc-and-samsung-semiconductor-chip-shortage/

Laframboise, N., and Loko, B. (2012). *Natural disasters: mitigating impact, managing risks* [IMF Working Paper](No. 12/245). International Monetary Fund. https://papers.ssrn.com/sol3/papers.cfm?abstract_id=2169784

Leiter, A. M., Oberhofer, H., and Raschky, P. A. (2009). Creative disasters? Flooding effects on capital, labour and productivity within European firms. *Environmental and Resource Economics*, *43*(3), 333-350. https://doi.org/10.1007/s10640-009-9273-9

Lenzen, M. (2011). Aggregation versus disaggregation in input-output analysis of the environment. *Economic Systems Research*, *23*(1), 73-89. https://doi.org/10.1080/09535314.2010.548793

Lenzen, M. (2019). Aggregating input-output systems with minimum error. *Economic Systems Research*, *31*(4), 594-616. https://doi.org/10.1080/09535314.2019.1609911

Lenzen, M., Malik, A., Kenway, S., Daniels, P., Lam, K. L., and Geschke, A. (2019). Economic damage and spillovers from a tropical cyclone. *Natural Hazards and Earth System Sciences*, *19*(1), 137-151. https://doi.org/10.5194/nhess-19-137-2019

Leonard, M., Westra, S., Phatak, A., Lambert, M., van den Hurk, B., McInnes, K., . . . Stafford-Smith, M. (2014). A compound event framework for understanding extreme impacts. *WIREs Climate Change*, *5*(1), 113-128. https://doi.org/10.1002/wcc.252

Li, J., Crawford-Brown, D., Syddall, M., and Guan, D. (2013). Modeling imbalanced economic recovery following a natural disaster using input-output analysis. *Risk Analysis*, *33*(10), 1908-1923. https://doi.org/10.1111/risa.12040

Lian, C., and Haimes, Y. Y. (2006). Managing the risk of terrorism to interdependent infrastructure systems through the dynamic inoperability input-output model. *Systems Engineering*, *9*(3), 241-258. https://doi.org/10.1002/sys.20051

Liang, W.-M., Liu, W.-P., Chou, S.-Y., and Kuo, H.-W. (2008). Ambient temperature and emergency room admissions for acute coronary syndrome in Taiwan.

International Journal of Biometeorology, *52*(3), 223-229. https://doi.org/10.1007/s00484-007-0116-5

Liao, Z., Chen, Y., Li, W., and Zhai, P. (2021). Growing threats from unprecedented sequential flood-hot extremes across China. *Geophysical Research Letters*, *48*(18), e2021GL094505. https://doi.org/10.1029/2021GL094505

Linka, K., Peirlinck, M., Sahli Costabal, F., and Kuhl, E. (2020). Outbreak dynamics of COVID-19 in Europe and the effect of travel restrictions. *Computer Methods in Biomechanics and Biomedical Engineering*, *23*(11), 710-717. https://doi.org/10.1080/10255842.2020.1759560

Liu, Y., Zhang, Z., Chen, X., Huang, C., Han, F., and Li, N. (2021). Assessment of the regional and sectoral economic impacts of heat-related changes in labor productivity under climate change in China. *Earth's Future*, *9*(8), e2021EF002028. https://doi.org/10.1029/2021EF002028

Loayza, N. V., Olaberría, E., Rigolini, J., and Christiaensen, L. (2012). Natural disasters and growth: going beyond the averages. *World Development*, *40*(7), 1317-1336. https://doi.org/10.1016/j.worlddev.2012.03.002

Lotfi, R., Kargar, B., Rajabzadeh, M., Hesabi, F., and Özceylan, E. (2022). Hybrid fuzzy and data-driven robust optimization for resilience and sustainable health care supply chain with vendor-managed inventory approach. *International Journal of Fuzzy Systems*, *24*(2), 1216-1231. https://doi.org/10.1007/s40815-021-01209-4

Ma, W., Chen, R., and Kan, H. (2014). Temperature-related mortality in 17 large Chinese cities: how heat and cold affect mortality in China. *Environmental Research*, *134*, 127-133. https://doi.org/10.1016/j.envres.2014.07.007

Mack, S. (2019). *What effect will inventory increase have on a company?* Retrieved January 16, 2023 from https://yourbusiness.azcentral.com/effect-inventory-increase-company-25510.html

MacKenzie, C. A., and Barker, K. (2011). *Conceptualizing the broader impacts of industry preparedness strategies with a risk-based input-output model* [Conference Paper]. The 19th International Input-Output Conference, Alexandria, Virginia, USA. https://www.iioa.org/conferences/19th/papers/files/445_20110501111_MacKenzieandBarkerConceptualizingtheBroaderImpactsofIndustryPreparednessStrategieswithaRisk-BasedInput-OutputModel.pdf

MacKenzie, C. A., Santos, J. R., and Barker, K. (2012). Measuring changes in international production from a disruption: case study of the Japanese earthquake and tsunami. *International Journal of Production Economics*, *138*(2), 293-302. https://doi.org/10.1016/j.ijpe.2012.03.032

Mahul, O., and Signer, B. (2020). The perfect storm: how to prepare against climate risk and disaster shocks in the time of COVID-19. *One Earth*, *2*(6), 500-502. https://doi.org/10.1016/j.oneear.2020.05.023

Martiello, M. A., and Giacchi, M. V. (2010). High temperatures and health outcomes:

a review of the literature. *Scandinavian Journal of Public Health*, *38*(8), 826-837. https://doi.org/10.1177/1403494810377685

Martin, A., Markhvida, M., Hallegatte, S., and Walsh, B. (2020). Socio-economic impacts of COVID-19 on household consumption and poverty. *Economics of Disasters and Climate Change*, *4*(3), 453-479. https://doi.org/10.1007/s41885-020-00070-3

Mazhin, S. A., Farrokhi, M., Noroozi, M., Roudini, J., Hosseini, S. A., Motlagh, M. E., . . . Khankeh, H. (2021). Worldwide disaster loss and damage databases: a systematic review. *Journal of education and health promotion*, *10*, 329-329. https://doi.org/10.4103/jehp.jehp_1525_20

McCarthy, N. (2021). *The U.S. car models most impacted by the microchip shortage*. Retrieved November 12, 2021 from https://www.forbes.com/sites/niallmccarthy/2021/06/01/the-us-car-models-most-impacted-by-the-microchip-shortage-infographic/?sh=2cd3f50580d2

McKibbin, W. J., and Fernando, R. (2020). *The global macroeconomic impacts of COVID-19: seven scenarios* [CAMA Working Paper](No. 19/2020). Centre for Applied Macroeconomic Analysis of Australian National University. https://papers.ssrn.com/sol3/papers.cfm?abstract_id=3547729

Mendoza-Tinoco, D., Guan, D., Zeng, Z., Xia, Y., and Serrano, A. (2017). Flood footprint of the 2007 floods in the UK: the case of the Yorkshire and The Humber region. *Journal of Cleaner Production*, *168*, 655-667. https://doi.org/10.1016/j.jclepro.2017.09.016

Mendoza-Tinoco, D., Hu, Y., Zeng, Z., Chalvatzis, K. J., Zhang, N., Steenge, A. E., and Guan, D. (2020). Flood footprint assessment: a multiregional case of 2009 Central European floods. *Risk Analysis*, *40*(8), 1612-1631. https://doi.org/10.1111/risa.13497

Merz, B., Blöschl, G., Vorogushyn, S., Dottori, F., Aerts, J. C. J. H., Bates, P., . . . Macdonald, E. (2021). Causes, impacts and patterns of disastrous river floods. *Nature Reviews Earth & Environment*, *2*(9), 592-609. https://doi.org/10.1038/s43017-021-00195-3

Merz, B., Kreibich, H., Schwarze, R., and Thieken, A. (2010). Review article: assessment of economic flood damage. *Natural Hazards and Earth System Sciences*, *10*(8), 1697-1724. https://doi.org/10.5194/nhess-10-1697-2010

Merz, B., and Thieken, A. H. (2009). Flood risk curves and uncertainty bounds. *Natural Hazards*, *51*(3), 437-458. https://doi.org/10.1007/s11069-009-9452-6

Meyer, V., Becker, N., Markantonis, V., Schwarze, R., Van Den Bergh, J. C. J. M., Bouwer, L. M., . . . Viavattene, C. (2013). Review article: assessing the costs of natural hazards - state of the art and knowledge gaps. *Natural Hazards and Earth System Sciences*, *13*(5), 1351-1373. https://doi.org/10.5194/nhess-13-1351-2013

Miller, R. E., and Blair, P. D. (2009). *Input-Output Analysis: Foundations and Extensions*. Cambridge University Press.

https://doi.org/10.1017/CBO9780511626982

Ministry of Housing and Urban-Rural Development of China. (2019). National urban population and construction land in 2019 (by cities) (in Chinese). In Z. Hu (Ed.), *China Urban Construction Statistical Yearbook* (pp. 48-83). China Statistics Press.

MOA. (2017). *The action plan for zero growth of chemical fertilizer use by 2020 and the action plan for zero growth of pesticide use by 2020*. Ministry of Agriculture and Rural Affairs of China. Retrieved June 10, 2022 from http://www.moa.gov.cn/nybgb/2015/san/201711/t20171129_5923401.htm

Moftakhari, H. R., Salvadori, G., AghaKouchak, A., Sanders, B. F., and Matthew, R. A. (2017). Compounding effects of sea level rise and fluvial flooding. *Proceedings of the National Academy of Sciences*, *114*(37), 9785. https://doi.org/10.1073/pnas.1620325114

Mokrech, M., Kebede, A. S., Nicholls, R. J., Wimmer, F., and Feyen, L. (2015). An integrated approach for assessing flood impacts due to future climate and socio-economic conditions and the scope of adaptation in Europe. *Climatic Change*, *128*(3), 245-260. https://doi.org/10.1007/s10584-014-1298-6

Molina, S., and Lindholm, C. (2005). A logic tree extension of the capacity spectrum method developed to estimate seismic risk in Oslo, Norway. *Journal of Earthquake Engineering*, *9*(6), 877-897. https://doi.org/10.1142/S1363246905002201

Molinari, D., De Bruijn, K. M., Castillo-Rodríguez, J. T., Aronica, G. T., and Bouwer, L. M. (2019). Validation of flood risk models: current practice and possible improvements. *International Journal of Disaster Risk Reduction*, *33*, 441-448. https://doi.org/10.1016/j.ijdrr.2018.10.022

Muis, S., Güneralp, B., Jongman, B., Aerts, J. C. J. H., and Ward, P. J. (2015). Flood risk and adaptation strategies under climate change and urban expansion: a probabilistic analysis using global data. *Science of the Total Environment*, *538*, 445-457. https://doi.org/10.1016/j.scitotenv.2015.08.068

Murray, C. J. L., Aravkin, A. Y., Zheng, P., Abbafati, C., Abbas, K. M., Abbasi-Kangevari, M., . . . Lim, S. S. (2020). Global burden of 87 risk factors in 204 countries and territories, 1990-2019: a systematic analysis for the Global Burden of Disease Study 2019. *The Lancet*, *396*(10258), 1223-1249. https://doi.org/10.1016/s0140-6736(20)30752-2

National Bureau of Statistics of China. (2010). *Tabulation on the 2010 Population Census of the People's Republic of China*. China Statistics Press.

Nelson, S. A. (2018). *Natural disasters & assessing hazards and risk*. Tulane University. Retrieved May 21, 2022 from https://www2.tulane.edu/~sanelson/Natural_Disasters/introduction.htm

Nikolopoulos, K., Punia, S., Schäfers, A., Tsinopoulos, C., and Vasilakis, C. (2021). Forecasting and planning during a pandemic: COVID-19 growth rates, supply chain disruptions, and governmental decisions. *European Journal of*

Operational Research, *290*(1), 99-115. https://doi.org/10.1016/j.ejor.2020.08.001

Noy, I. (2009). The macroeconomic consequences of disasters. *Journal of Development Economics*, *88*(2), 221-231. https://doi.org/10.1016/j.jdeveco.2008.02.005

OECD. (2012). *Mortality Risk Valuation in Environment, Health and Transport Policies*. OECD Publishing. https://doi.org/10.1787/9789264130807-en

Okuyama, Y. (2007). Economic modeling for disaster impact analysis: past, present, and future. *Economic Systems Research*, *19*(2), 115-124. https://doi.org/10.1080/09535310701328435

Okuyama, Y. (2008). *Critical review of methodologies on disaster impact estimation* [Background paper for the joint World Bank - UN report on the Economics of Disaster Risk Reduction]. https://onlineasdma.assam.gov.in/kmp/pdf/1491474441Okuyama_Critical_Review.pdf

Okuyama, Y., and Santos, J. R. (2014). Disaster impact and input-output analysis. *Economic Systems Research*, *26*(1), 1-12. https://doi.org/10.1080/09535314.2013.871505

Oosterhaven, J. (1988). On the plausibility of the supply-driven input-output model. *Journal of Regional Science*, *28*(2), 203-217. https://doi.org/10.1111/j.1467-9787.1988.tb01208.x

Oosterhaven, J. (2017). On the limited usability of the inoperability IO model. *Economic Systems Research*, *29*(3), 452-461. https://doi.org/10.1080/09535314.2017.1301395

Oosterhaven, J., and Bouwmeester, M. C. (2016). A new approach to modeling the impact of disruptive events. *Journal of Regional Science*, *56*(4), 583-595. https://doi.org/10.1111/jors.12262

Oosterhaven, J., and Többen, J. (2017). Wider economic impacts of heavy flooding in Germany: a non-linear programming approach. *Spatial Economic Analysis*, *12*(4), 404-428. https://doi.org/10.1080/17421772.2017.1300680

Orlov, A., Sillmann, J., Aunan, K., Kjellstrom, T., and Aaheim, A. (2020). Economic costs of heat-induced reductions in worker productivity due to global warming. *Global Environmental Change*, *63*, 102087. https://doi.org/10.1016/j.gloenvcha.2020.102087

Orsi, M. J., and Santos, J. R. (2010). Estimating workforce-related economic impact of a pandemic on the Commonwealth of Virginia. *IEEE Transactions on Systems, Man, and Cybernetics - Part A: Systems and Humans*, *40*(2), 301-305. https://doi.org/10.1109/tsmca.2009.2033032

Otto, C., Willner, S. N., Wenz, L., Frieler, K., and Levermann, A. (2017). Modeling loss-propagation in the global supply network: the dynamic agent-based model acclimate. *Journal of Economic Dynamics and Control*, *83*, 232-269. https://doi.org/10.1016/j.jedc.2017.08.001

Oxford Analytica. (2020). Pandemic-induced trade protectionism will persist. *Expert Briefings*. https://doi.org/10.1108/OXAN-ES257613

Pandey, A., Brauer, M., Cropper, M. L., Balakrishnan, K., Mathur, P., Dey, S., . . . Dandona, L. (2021). Health and economic impact of air pollution in the states of India: the Global Burden of Disease Study 2019. *The Lancet Planetary Health*, *5*(1), e25-e38. https://doi.org/10.1016/S2542-5196(20)30298-9

Pant, M. (2022). *The economic impact of the Russia-Ukraine conflict*. Retrieved May 16, 2022 from https://www.businesstoday.in/magazine/current/story/the-economic-impact-of-the-russia-ukraine-conflict-324788-2022-03-04

Park, C.-E., Jeong, S., Harrington, L. J., Lee, M.-I., and Zheng, C. (2020). Population ageing determines changes in heat vulnerability to future warming. *Environmental Research Letters*, *15*(11), 114043. https://doi.org/10.1088/1748-9326/abbd60

Parsons, L. A., Shindell, D., Tigchelaar, M., Zhang, Y., and Spector, J. T. (2021). Increased labor losses and decreased adaptation potential in a warmer world. *Nature Communications*, *12*(1), 7286. https://doi.org/10.1038/s41467-021-27328-y

Pascal, M., Wagner, V., Alari, A., Corso, M., and Le Tertre, A. (2021). Extreme heat and acute air pollution episodes: a need for joint public health warnings? *Atmospheric Environment*, *249*, 118249. https://doi.org/10.1016/j.atmosenv.2021.118249

Patri, P., Sharma, P., and Patra, S. K. (2022). Does economic development reduce disaster damage risk from floods in India? Empirical evidence using the ZINB model. *International Journal of Disaster Risk Reduction*, *79*, 103163. https://doi.org/10.1016/j.ijdrr.2022.103163

Pauw, K., Thurlow, J. p., Bachu, M., and Seventer, D. E. v. (2011). The economic costs of extreme weather events: a hydrometeorological CGE analysis for Malawi. *Environment and Development Economics*, *16*(2), 177-198. https://doi.org/10.1017/s1355770x10000471

Pei, S., Dahl, K. A., Yamana, T. K., Licker, R., and Shaman, J. (2020). Compound risks of hurricane evacuation amid the COVID-19 pandemic in the United States. *GeoHealth*, *4*(12), e2020GH000319. https://doi.org/10.1029/2020GH000319

Penning-Rowsell, E., Priest, S., Parker, D., Morris, J., Tunstall, S., Viavattene, C., . . . Owen, D. (2013). *Flood and Coastal Erosion Risk Management: A Manual for Economic Appraisal* (1st ed.). Routledge. https://doi.org/10.4324/9780203066393

Peters, C., Dulon, M., Westermann, C., Kozak, A., and Nienhaus, A. (2022). Long-term effects of COVID-19 on workers in health and social services in Germany. *International Journal of Environmental Research and Public Health*, *19*(12), 6983. https://doi.org/10.3390/ijerph19126983

Phillips, C. A., Caldas, A., Cleetus, R., Dahl, K. A., Declet-Barreto, J., Licker, R., . . . Carlson, C. J. (2020). Compound climate risks in the COVID-19 pandemic.

Nature Climate Change, *10*(7), 586-588. https://doi.org/10.1038/s41558-020-0804-2

Porsse, A. A., Souza, K. B., Carvalho, T. S., and Vale, V. A. (2020). The economic impacts of COVID‐19 in Brazil based on an interregional CGE approach. *Regional Science Policy Practice*, *12*(6), 1105-1121. https://doi.org/10.1111/rsp3.12354

Ramanathan, V., Chung, C., Kim, D., Bettge, T., Buja, L., Kiehl, J. T., . . . Wild, M. (2005). Atmospheric brown clouds: impacts on South Asian climate and hydrological cycle. *Proceedings of the National Academy of Sciences*, *102*(15), 5326-5333. https://doi.org/10.1073/pnas.0500656102

Raschky, P. A. (2008). Institutions and the losses from natural disasters. *Natural Hazards and Earth System Sciences*, *8*(4), 627-634. https://doi.org/10.5194/nhess-8-627-2008

Rees, W. E. (1992). Ecological footprints and appropriated carrying capacity: what urban economics leaves out. *Environment and Urbanization*, *4*(2), 121-130. https://doi.org/10.1177/095624789200400212

Reuschke, D., and Houston, D. (2022). The impact of Long COVID on the UK workforce. *Applied Economics Letters*, 1-5. https://doi.org/10.1080/13504851.2022.2098239

Reuters. (2020). *Hyundai Motor suspends output as coronavirus disrupts supply chain*. Retrieved December 16, 2021 from https://www.reuters.com/article/hyundai-motor-virus-china-idUSS6N29P03H

Riahi, K., van Vuuren, D. P., Kriegler, E., Edmonds, J., O'Neill, B. C., Fujimori, S., . . . Tavoni, M. (2017). The Shared Socioeconomic Pathways and their energy, land use, and greenhouse gas emissions implications: an overview. *Global Environmental Change*, *42*, 153-168. https://doi.org/10.1016/j.gloenvcha.2016.05.009

Ridder, N. N., Pitman, A. J., Westra, S., Ukkola, A., Do, H. X., Bador, M., . . . Zscheischler, J. (2020). Global hotspots for the occurrence of compound events. *Nature Communications*, *11*(1), 5956. https://doi.org/10.1038/s41467-020-19639-3

Robinson, D. J., Dhu, T., and Row, P. (2007). *EQRM: an open-source event-based earthquake risk modeling program* [Conference Paper]. American Geophysical Union Fall Meeting, San Francisco, US. https://ui.adsabs.harvard.edu/abs/2007AGUFMPA33A1027R

Rojas, R., Feyen, L., and Watkiss, P. (2013). Climate change and river floods in the European Union: socio-economic consequences and the costs and benefits of adaptation. *Global Environmental Change*, *23*(6), 1737-1751. https://doi.org/10.1016/j.gloenvcha.2013.08.006

Romanello, M., McGushin, A., Di Napoli, C., Drummond, P., Hughes, N., Jamart, L., . . . Hamilton, I. (2021). The 2021 report of the Lancet Countdown on health and climate change: code red for a healthy future. *The Lancet*, *398*(10311),

1619-1662. https://doi.org/10.1016/S0140-6736(21)01787-6

Rose, A., and Allison, T. (1989). On the plausibility of the supply-driven input-output model: empirical evidence on joint stability. *Journal of Regional Science*, *29*(3), 451-458. https://doi.org/10.1111/j.1467-9787.1989.tb01390.x

Rose, A., and Liao, S.-Y. (2005). Modeling regional economic resilience to disasters: a computable general equilibrium analysis of water service disruptions. *Journal of Regional Science*, *45*(1), 75-112. https://doi.org/10.1111/j.0022-4146.2005.00365.x

Rose, A., Oladosu, G., and Liao, S.-Y. (2005). *Regional economic impacts of terrorist attacks on the electric power system of Los Angeles: a computable general disequilibrium analysis* [Paper presented at the Second Annual Symposium of the DHS Center for Risk and Economic Analysis of Terrorism Events]. University of Southern California.

Rose, A., and Wei, D. (2013). Estimating the economic consequences of a port shutdown: the special role of resilience. *Economic Systems Research*, *25*(2), 212-232. https://doi.org/10.1080/09535314.2012.731379

Rose, A., Wing, I. S., Wei, D., and Wein, A. (2016). Economic impacts of a California tsunami. *Natural Hazards Review*, *17*(2), 04016002. https://doi.org/10.1061/(ASCE)NH.1527-6996.0000212

Rossetto, T., D'Ayala, D., Ioannou, I., and Meslem, A. (2014). Evaluation of existing fragility curves. In K. Pitilakis, H. Crowley, and A. M. Kaynia (Eds.), *SYNER-G: Typology Definition and Fragility Functions for Physical Elements at Seismic Risk: Buildings, Lifelines, Transportation Networks and Critical Facilities* (pp. 47-93). Springer Netherlands. https://doi.org/10.1007/978-94-007-7872-6_3

Salas, R. N., Shultz, J. M., and Solomon, C. G. (2020). The climate crisis and Covid-19 - a major threat to the pandemic response. *New England Journal of Medicine*, *383*(11), 70. https://doi.org/10.1056/NEJMp2022011

Santos, J. R., and Haimes, Y. Y. (2004). Modeling the demand reduction input‐output (I‐O) inoperability due to terrorism of interconnected infrastructures. *Risk Analysis*, *24*(6), 1437-1451. https://doi.org/10.1111/j.0272-4332.2004.00540.x

Schnell, J. L., and Prather, M. J. (2017). Co-occurrence of extremes in surface ozone, particulate matter, and temperature over eastern North America. *Proceedings of the National Academy of Sciences*, *114*(11), 2854-2859. https://doi.org/10.1073/pnas.1614453114

Schultz, A. B., Chen, C.-Y., and Edington, D. W. (2009). The cost and impact of health conditions on presenteeism to employers. *PharmacoEconomics*, *27*(5), 365-378. https://doi.org/10.2165/00019053-200927050-00002

Schumacher, I., and Strobl, E. (2011). Economic development and losses due to natural disasters: the role of hazard exposure. *Ecological Economics*, *72*, 97-105. https://doi.org/10.1016/j.ecolecon.2011.09.002

Scortichini, M., De Sario, M., De'Donato, F. K., Davoli, M., Michelozzi, P., and

Stafoggia, M. (2018). Short-term effects of heat on mortality and effect modification by air pollution in 25 Italian cities. *International Journal of Environmental Research and Public Health*, *15*(8), 1771. https://doi.org/10.3390/ijerph15081771

Scussolini, P., Aerts, J. C. J. H., Jongman, B., Bouwer, L. M., Winsemius, H. C., de Moel, H., and Ward, P. J. (2016). FLOPROS: an evolving global database of flood protection standards. *Natural Hazards and Earth System Sciences*, *16*(5), 1049-1061. https://doi.org/10.5194/nhess-16-1049-2016

Selby, D., and Kagawa, F. (2020). Climate change and coronavirus: a confluence of crises as learning moment. In Pádraig Carmody, Gerard McCann, C. Colleran, and C. O'Halloran (Eds.), *COVID-19 in the Global South: Impacts and Responses*. Bristol University Press.

Seneviratne, S. I., Nicholls, N., Easterling, D., Goodess, C. M., Kanae, S., Kossin, J., . . . Zhang, X. (2012). Changes in climate extremes and their impacts on the natural physical environment. In C. B. Field, V. Barros, T. F. Stocker, D. Qin, D. J. Dokken, K. L. Ebi, . . . P. M. Midgley (Eds.), *Managing the Risks of Extreme Events and Disasters to Advance Climate Change Adaptation* (pp. 109-230). A Special Report of Working Groups I and II of the Intergovernmental Panel on Climate Change. Cambridge University Press, Cambridge, United Kingdom and New York, NY, USA.

Seneviratne, S. I., Zhang, X., Adnan, M., Badi, W., Dereczynski, C., Luca, A. D., . . . Zhou, B. (2021). Weather and climate extreme events in a changing climate. In V. Masson-Delmotte, P. Zhai, A. Pirani, S. L. Connors, C. Péan, S. Berger, . . . B. Zhou (Eds.), *Climate Change 2021: The Physical Science Basis. Contribution of Working Group I to the Sixth Assessment Report of the Intergovernmental Panel on Climate Change*. Cambridge University Press.

Service(C3S) CCC. (2022). *ERA5: Fifth generation of ECMWF atmospheric reanalyses of the global climate* [Dataset]. Copernicus Climate Change Service Climate Data Store (CDS). https://doi.org/https://doi.org/10.5065/BH6N-5N20

Shahid, S. (2020). *Deglobalization and its discontents: the pandemic effect*. Retrieved January 30, 2021 from https://economics.td.com/domains/economics.td.com/documents/reports/ss/deglobalization.pdf

Shen, X., Cai, C., Yang, Q., Anagnostou, E. N., and Li, H. (2021). The US COVID-19 pandemic in the flood season. *Science of the Total Environment*, *755*, 142634. https://doi.org/10.1016/j.scitotenv.2020.142634

Shi, H., Jiang, Z., Zhao, B., Li, Z., Chen, Y., Gu, Y., . . . Worden, J. (2019). Modeling study of the air quality impact of record-breaking Southern California wildfires in December 2017. *Journal of Geophysical Research: Atmospheres*, *124*(12), 6554-6570. https://doi.org/10.1029/2019JD030472

Shi, P. (2005). Theory and practice on disaster system research in a fourth time (in

Chinese). *Journal of Natural Disasters*, *14*(6), 1-7.

Shoven, J. B., and Whalley, J. (1992). *Applying General Equilibrium*. Cambridge University Press.

Shughrue, C., Werner, B., and Seto, K. C. (2020). Global spread of local cyclone damages through urban trade networks. *Nature Sustainability*, *3*(8), 606-613. https://doi.org/10.1038/s41893-020-0523-8

Sieg, T., Schinko, T., Vogel, K., Mechler, R., Merz, B., and Kreibich, H. (2019). Integrated assessment of short-term direct and indirect economic flood impacts including uncertainty quantification. *PLOS ONE*, *14*(4), e0212932. https://doi.org/10.1371/journal.pone.0212932

Sillmann, J., Aunan, K., Emberson, L., Büker, P., Van Oort, B., O'Neill, C., . . . Brisebois, A. (2021). Combined impacts of climate and air pollution on human health and agricultural productivity. *Environmental Research Letters*, *16*(9), 093004. https://doi.org/10.1088/1748-9326/ac1df8

Sillmann, J., Stjern, C. W., Myhre, G., and Forster, P. M. (2017). Slow and fast responses of mean and extreme precipitation to different forcing in CMIP5 simulations. *Geophysical Research Letters*, *44*(12), 6383-6390. https://doi.org/10.1002/2017GL073229

Silva, V., Crowley, H., Pagani, M., Monelli, D., and Pinho, R. (2014). Development of the OpenQuake engine, the Global Earthquake Model's open-source software for seismic risk assessment. *Natural Hazards*, *72*(3), 1409-1427. https://doi.org/10.1007/s11069-013-0618-x

Simpson, D., Benedictow, A., Berge, H., Bergström, R., Emberson, L. D., Fagerli, H., . . . Wind, P. (2012). The EMEP MSC-W chemical transport model - technical description. *Atmospheric Chemistry and Physics*, *12*(16), 7825-7865. https://doi.org/10.5194/acp-12-7825-2012

Skidmore, M., and Toya, H. (2002). Do natural disasters promote long-run growth? *Economic Inquiry*, *40*(4), 664-687. https://doi.org/10.1093/ei/40.4.664

Sneader, K., and Lund, S. (2020). *COVID-19 and climate change expose dangers of unstable supply chains*. Retrieved May 3, 2022 from https://www.mckinsey.com/business-functions/operations/our-insights/covid-19-and-climate-change-expose-dangers-of-unstable-supply-chains

Solow, R. M. (1957). Technical change and the aggregate production function. *The Review of Economics and Statistics*, *39*(3), 312-320. https://doi.org/10.2307/1926047

Sperna Weiland, F. C., van Beek, L. P. H., Kwadijk, J. C. J., and Bierkens, M. F. P. (2012). Global patterns of change in discharge regimes for 2100. *Hydrology and Earth System Sciences*, *16*(4), 1047-1062. https://doi.org/10.5194/hess-16-1047-2012

State Council of China. (2018). *Three-year action plan for winning the blue sky defence battle*. Retrieved June 10, 2022 from http://english.mee.gov.cn/News_service/news_release/201807/t20180713_44

6624.shtml

Steen-Olsen, K., Owen, A., Hertwich, E. G., and Lenzen, M. (2014). Effects of sector aggregation on CO2 multipliers in multiregional input-output analyses. *Economic Systems Research*, *26*(3), 284-302. https://doi.org/10.1080/09535314.2014.934325

Swaisgood, M. (2020). *When COVID-19 and natural hazards collide: building resilient infrastructure in South Asia in the face of multiple crises*. Observer Research Foundation (ORF). Retrieved May 31, 2021 from https://www.orfonline.org/expert-speak/when-covid19-and-natural-hazards-collide/?MvBriefArticleId=18469

Sweeney, S., Capeding, T. P. J., Eggo, R., Huda, M., Jit, M., Mudzengi, D., . . . Vassall, A. (2021). Exploring equity in health and poverty impacts of control measures for SARS-CoV-2 in six countries. *BMJ Global Health*, *6*(5), e005521. https://doi.org/10.1136/bmjgh-2021-005521

Taguchi, R., Tanoue, M., Yamazaki, D., and Hirabayashi, Y. (2022). Global-scale assessment of economic losses caused by flood-related business interruption. *Water*, *14*(6), 967. https://doi.org/10.3390/w14060967

Tanoue, M., Hirabayashi, Y., and Ikeuchi, H. (2016). Global-scale river flood vulnerability in the last 50 years. *Scientific Reports*, *6*, 36021. https://doi.org/10.1038/srep36021

Tanoue, M., Taguchi, R., Alifu, H., and Hirabayashi, Y. (2021). Residual flood damage under intensive adaptation. *Nature Climate Change*, *11*(10), 823-826. https://doi.org/10.1038/s41558-021-01158-8

Tanoue, M., Taguchi, R., Nakata, S., Watanabe, S., Fujimori, S., and Hirabayashi, Y. (2020). Estimation of direct and indirect economic losses caused by a flood with long‐lasting inundation: application to the 2011 Thailand flood. *Water Resources Research*, *56*(5), e2019WR026092. https://doi.org/10.1029/2019wr026092

Tatano, H., and Tsuchiya, S. (2008). A framework for economic loss estimation due to seismic transportation network disruption: a spatial computable general equilibrium approach. *Natural Hazards*, *44*(2), 253-265. https://doi.org/10.1007/s11069-007-9151-0

Taylor, K. E., Stouffer, R. J., and Meehl, G. A. (2012). An overview of CMIP5 and the experiment design. *Bulletin of the American Meteorological Society*, *93*(4), 485-498. https://doi.org/10.1175/BAMS-D-11-00094.1

Tellman, B., Sullivan, J. A., Kuhn, C., Kettner, A. J., Doyle, C. S., Brakenridge, G. R., . . . Slayback, D. A. (2021). Satellite imaging reveals increased proportion of population exposed to floods. *Nature*, *596*(7870), 80-86. https://doi.org/10.1038/s41586-021-03695-w

The Lancet Planetary Health. (2020). A tale of two emergencies. *The Lancet Planetary Health*, *4*(3), e86. https://doi.org/10.1016/S2542-5196(20)30062-0

Toya, H., and Skidmore, M. (2007). Economic development and the impacts of natural

disasters. *Economics Letters*, *94*(1), 20-25. https://doi.org/10.1016/j.econlet.2006.06.020

Tripathy, S. S., Bhatia, U., Mohanty, M., Karmakar, S., and Ghosh, S. (2021). Flood evacuation during pandemic: a multi-objective framework to handle compound hazard. *Environmental Research Letters*, *16*(3), 034034. https://doi.org/10.1088/1748-9326/abda70

Tsuchiya, S., Tatano, H., and Okada, N. (2007). Economic loss assessment due to railroad and highway disruptions. *Economic Systems Research*, *19*(2), 147-162. https://doi.org/10.1080/09535310701328567

Turner, L. R., Barnett, A. G., Connell, D., and Tong, S. (2012). Ambient temperature and cardiorespiratory morbidity: a systematic review and meta-analysis. *Epidemiology*, *23*(4), 594-606. https://doi.org/10.1097/EDE.0b013e3182572795

UNEP. (2020). *Locust swarms and climate change*. United Nations Environment Programme. Retrieved May 29, 2021 from https://www.unep.org/news-and-stories/story/locust-swarms-and-climate-change

UNFCCC. (2015). *Adoption of the Paris Agreement* (Report No. FCCC/CP/2015/L.9/Rev.1). http://unfccc.int/resource/docs/2015/cop21/eng/l09r01.pdf

UNISDR. (2015). *Sendai framework for disaster risk reduction 2015-2030*. http://www.wcdrr.org/uploads/Sendai_Framework_for_Disaster_Risk_Reduction_2015-2030.pdf

UNISDR. (2017). *Terminology on disaster risk reduction*. United Nations Office for Disaster Risk Reduction. Retrieved May 16, 2022 from https://www.undrr.org/terminology

Vaidyanathan, A., Malilay, J., Schramm, P., and Saha, S. (2020). Heat-related deaths - United States, 2004-2018. *MMWR. Morbidity and Mortality Weekly Report*, *69*(24), 729-734. https://doi.org/10.15585/mmwr.mm6924a1

van der Veen, A., and Logtmeijer, C. (2005). Economic hotspots: visualizing vulnerability to flooding. *Natural Hazards*, *36*(1-2), 65-80. https://doi.org/10.1007/s11069-004-4542-y

van Donkelaar, A., Martin, R. V., Brauer, M., and Boys, B. L. (2015). Use of satellite observations for long-term exposure assessment of global concentrations of fine particulate matter. *Environmental Health Perspectives*, *123*(2), 135-143. https://doi.org/10.1289/ehp.1408646

van Vuuren, D. P., Stehfest, E., Gernaat, D. E. H. J., Doelman, J. C., van den Berg, M., Harmsen, M., . . . Tabeau, A. (2017). Energy, land-use and greenhouse gas emissions trajectories under a green growth paradigm. *Global Environmental Change*, *42*, 237-250. https://doi.org/10.1016/j.gloenvcha.2016.05.008

Vautard, R., Honoré, C., Beekmann, M., and Rouil, L. (2005). Simulation of ozone during the August 2003 heat wave and emission control scenarios. *Atmospheric Environment*, *39*(16), 2957-2967.

https://doi.org/10.1016/j.atmosenv.2005.01.039

Verschuur, J., Li, S., Wolski, P., and Otto, F. E. L. (2021). Climate change as a driver of food insecurity in the 2007 Lesotho-South Africa drought. *Scientific Reports*, *11*(1), 3852. https://doi.org/10.1038/s41598-021-83375-x

Wagenaar, D. J., de Bruijn, K. M., Bouwer, L. M., and de Moel, H. (2016). Uncertainty in flood damage estimates and its potential effect on investment decisions. *Natural Hazards and Earth System Sciences*, *16*(1), 1-14. https://doi.org/10.5194/nhess-16-1-2016

Wahl, T., Jain, S., Bender, J., Meyers, S. D., and Luther, M. E. (2015). Increasing risk of compound flooding from storm surge and rainfall for major US cities. *Nature Climate Change*, *5*(12), 1093-1097. https://doi.org/10.1038/nclimate2736

Walker Patrick, G. T., Whittaker, C., Watson Oliver, J., Baguelin, M., Winskill, P., Hamlet, A., . . . Ghani Azra, C. (2020). The impact of COVID-19 and strategies for mitigation and suppression in low- and middle-income countries. *Science*, *369*(6502), 413-422. https://doi.org/10.1126/science.abc0035

Walker, P. G. T., Whittaker, C., Watson, O. J., Baguelin, M., Winskill, P., Hamlet, A., . . . Ghani, A. C. (2020). The impact of COVID-19 and strategies for mitigation and suppression in low- and middle-income countries. *Science*, *369*(6502), 413-422. https://doi.org/10.1126/science.abc0035

Walton, D., Arrighi, J., van Aalst, M., and Claudet, M. (2021). *The compound impact of extreme weather events and COVID-19. An update of the number of people affected and a look at the humanitarian implications in selected contexts*. IFRC Climate Center. https://www.ifrc.org/media/49590

Wang, B. (2021). Extreme rainfall sounds the alarm for climate change (in Chinese). *Science News*, *23*(4), 47-49.

Wang, D., Guan, D., Zhu, S., Kinnon, M. M., Geng, G., Zhang, Q., . . . Davis, S. J. (2021). Economic footprint of California wildfires in 2018. *Nature Sustainability*, *4*(3), 252-260. https://doi.org/10.1038/s41893-020-00646-7

Wang, S. S.-Y., Kim, H., Coumou, D., Yoon, J.-H., Zhao, L., and Gillies, R. R. (2019). Consecutive extreme flooding and heat wave in Japan: are they becoming a norm? *Atmospheric Science Letters*, *20*(10), e933. https://doi.org/10.1002/asl.933

Wang, X., Wang, L., Zhang, X., and Fan, F. (2022). The spatiotemporal evolution of COVID-19 in China and its impact on urban economic resilience. *China Economic Review*, *74*, 101806. https://doi.org/10.1016/j.chieco.2022.101806

Wang, X., and Zhou, H. (2018). Progress and prospect of statistics and assessment of large-scale natural disaster damage and losses. *Advances in Earth Science*, *33*(9), 914-921. https://doi.org/10.11867/j.issn.1001-8166.2018.09.0914

Ward, P. J., Jongman, B., Aerts, J. C. J. H., Bates, P. D., Botzen, W. J. W., Diaz Loaiza, A., . . . Winsemius, H. C. (2017). A global framework for future costs and benefits of river-flood protection in urban areas. *Nature Climate Change*, *7*(9),

642-646. https://doi.org/10.1038/nclimate3350

Ward, P. J., Jongman, B., Weiland, F. S., Bouwman, A., van Beek, R., Bierkens, M. F. P., . . . Winsemius, H. C. (2013). Assessing flood risk at the global scale: model setup, results, and sensitivity. *Environmental Research Letters*, *8*(4), 044019. https://doi.org/10.1088/1748-9326/8/4/044019

Warren, R., Hope, C., Gernaat, D. E. H. J., Van Vuuren, D. P., and Jenkins, K. (2021). Global and regional aggregate damages associated with global warming of 1.5 to 4 °C above pre-industrial levels. *Climatic Change*, *168*(3), 24. https://doi.org/10.1007/s10584-021-03198-7

Watts, N., Amann, M., Arnell, N., Ayeb-Karlsson, S., Belesova, K., Boykoff, M., . . . Montgomery, H. (2019). The 2019 report of The Lancet Countdown on health and climate change: ensuring that the health of a child born today is not defined by a changing climate. *The Lancet*, *394*(10211), 1836-1878. https://doi.org/10.1016/S0140-6736(19)32596-6

Weedon, G. P., Balsamo, G., Bellouin, N., Gomes, S., Best, M. J., and Viterbo, P. (2014). The WFDEI meteorological forcing data set: WATCH Forcing Data methodology applied to ERA-Interim reanalysis data. *Water Resources Research*, *50*(9), 7505-7514. https://doi.org/10.1002/2014WR015638

Weinzettel, J. (2022). Aggregation error of the material footprint: the case of the EU. *Economic Systems Research*, *34*(3), 320-342. https://doi.org/10.1080/09535314.2021.1947782

Wenz, L., Willner, S. N., Bierkandt, R., and Levermann, A. (2014). Acclimate - a model for economic damage propagation. Part II: a dynamic formulation of the backward effects of disaster-induced production failures in the global supply network. *Environment Systems and Decisions*, *34*(4), 525-539. https://doi.org/10.1007/s10669-014-9521-6

White, D. A. L. (2020). *2020 Atlantic hurricane season most active on record*. National Oceanic and Atmospheric Administration (NOAA). Retrieved January 21, 2021 from https://www.msn.com/en-us/weather/topstories/2020-atlantic-hurricane-season-most-active-on-record-noaa/ar-BB1aStCW

WHO. (2005). *Air quality guidelines: global update 2005*. WHO Regional Office for Europe.

WHO. (2015). *Climate change and human health*. World Health Organization. Retrieved January 21, 2021 from https://www.who.int/globalchange/global-campaign/cop21/en/

WHO. (2016). *Ambient air pollution: a global assessment of exposure and burden of disease* [Report](No. 9789241511353). World Health Organisation. https://www.who.int/publications/i/item/9789241511353

Wiedmann, T., and Minx, J. (2008). A definition of 'carbon footprint'. In C. C. Pertsova (Ed.), *Ecological Economics Research Trends* (Vol. 1, pp. 1-11). Nova Science Publishers. https://novapublishers.com/catalog/product_info.php?products_id=5999

Willers, S. M., Jonker, M. F., Klok, L., Keuken, M. P., Odink, J., van den Elshout, S., . . . Burdorf, A. (2016). High resolution exposure modelling of heat and air pollution and the impact on mortality. *Environment International*, *89-90*, 102-109. https://doi.org/10.1016/j.envint.2016.01.013

Willner, S. N., Otto, C., and Levermann, A. (2018). Global economic response to river floods. *Nature Climate Change*, *8*(7), 594-598. https://doi.org/10.1038/s41558-018-0173-2

Winsemius, H. C., Aerts, J. C. J. H., van Beek, L. P. H., Bierkens, M. F. P., Bouwman, A., Jongman, B., . . . Ward, P. J. (2016). Global drivers of future river flood risk. *Nature Climate Change*, *6*(4), 381-385. https://doi.org/10.1038/nclimate2893

Winsemius, H. C., van Beek, L. P. H., Jongman, B., Ward, P. J., and Bouwman, A. (2013). A framework for global river flood risk assessments. *Hydrology and Earth System Sciences*, *17*(5), 1871-1892. https://doi.org/10.5194/hess-17-1871-2013

Wirtz, A., Kron, W., Löw, P., and Steuer, M. (2014). The need for data: natural disasters and the challenges of database management. *Natural Hazards*, *70*(1), 135-157. https://doi.org/10.1007/s11069-012-0312-4

Witte, J. C., Douglass, A. R., Da Silva, A., Torres, O., Levy, R., and Duncan, B. N. (2011). NASA A-Train and Terra observations of the 2010 Russian wildfires. *Atmospheric Chemistry and Physics*, *11*(17), 9287-9301. https://doi.org/10.5194/acp-11-9287-2011

World Bank. (2019). *World Development Report 2020: Trading for Development in the Age of Global Value Chains*. The World Bank. https://doi.org/10.1596/978-1-4648-1457-0

World Bank. (2021). *World Development Indicators* [DataBank]. WDI. https://data.worldbank.org

World Trade Organization. (2020). *Export prohibitions and restrictions*. https://www.wto.org/english/tratop_e/covid19_e/export_prohibitions_report_e.pdf

Wright, L. A., Kemp, S., and Williams, I. (2011). 'Carbon footprinting': towards a universally accepted definition. *Carbon Management*, *2*(1), 61-72. https://doi.org/10.4155/cmt.10.39

Wu, J., Li, N., Hallegatte, S., Shi, P., Hu, A., and Liu, X. (2012). Regional indirect economic impact evaluation of the 2008 Wenchuan Earthquake. *Environmental Earth Sciences*, *65*(1), 161-172. https://doi.org/10.1007/s12665-011-1078-9

Wyper, G. M. A., Assunção, R. M. A., Colzani, E., Grant, I., Haagsma, J. A., Lagerweij, G., . . . Devleesschauwer, B. (2021). Burden of disease methods: a guide to calculate COVID-19 disability-adjusted life years. *International Journal of Public Health*, *66*, 619011-619011. https://doi.org/10.3389/ijph.2021.619011

Xia, Y., Guan, D., Jiang, X., Peng, L., Schroeder, H., and Zhang, Q. (2016). Assessment of socioeconomic costs to China's air pollution. *Atmospheric*

Environment, *139*, 147-156. https://doi.org/10.1016/j.atmosenv.2016.05.036

Xia, Y., Guan, D., Meng, J., Li, Y., and Shan, Y. (2018). Assessment of the pollution-health-economics nexus in China. *Atmospheric Chemistry and Physics*, *18*(19), 14433-14443. https://doi.org/10.5194/acp-18-14433-2018

Xia, Y., Li, Y., Guan, D., Tinoco, D. M., Xia, J., Yan, Z., . . . Huo, H. (2018). Assessment of the economic impacts of heat waves: a case study of Nanjing, China. *Journal of Cleaner Production*, *171*, 811-819. https://doi.org/10.1016/j.jclepro.2017.10.069

Xie, R., Sabel, C. E., Lu, X., Zhu, W., Kan, H., Nielsen, C. P., and Wang, H. (2016). Long-term trend and spatial pattern of PM2.5 induced premature mortality in China. *Environment International*, *97*, 180-186. https://doi.org/10.1016/j.envint.2016.09.003

Xu, X., Li, B., and Huang, H. (1995). Air pollution and unscheduled hospital outpatient and emergency room visits. *Environmental Health Perspectives*, *103*(3), 286-289. https://doi.org/10.1289/ehp.95103286

Xu, Z., FitzGerald, G., Guo, Y., Jalaludin, B., and Tong, S. (2016). Impact of heatwave on mortality under different heatwave definitions: a systematic review and meta-analysis. *Environment International*, *89-90*, 193-203. https://doi.org/10.1016/j.envint.2016.02.007

Yamazaki, D., Kanae, S., Kim, H., and Oki, T. (2011). A physically based description of floodplain inundation dynamics in a global river routing model. *Water Resources Research*, *47*(4). https://doi.org/10.1029/2010WR009726

Yang, J., Xie, H., Yu, G., and Liu, M. (2021). Achieving a just-in-time supply chain: the role of supply chain intelligence. *International Journal of Production Economics*, *231*, 107878. https://doi.org/10.1016/j.ijpe.2020.107878

Yang, J., Yin, P., Sun, J., Wang, B., Zhou, M., Li, M., . . . Liu, Q. (2019). Heatwave and mortality in 31 major Chinese cities: definition, vulnerability and implications. *Science of the Total Environment*, *649*, 695-702. https://doi.org/10.1016/j.scitotenv.2018.08.332

Yin, Z., Hu, Y., Jenkins, K., He, Y., Forstenhäusler, N., Warren, R., . . . Guan, D. (2021). Assessing the economic impacts of future fluvial flooding in six countries under climate change and socio-economic development. *Climatic Change*, *166*(3), 38. https://doi.org/10.1007/s10584-021-03059-3

Zeng, Z. (2018). *Methodology and Applications of Flood Footprint Accounting For Determining Flood Induced Economic Costs Cascading throughout Production Supply Chains* [Doctoral Thesis, University of East Anglia]. Norwich, UK. https://ueaeprints.uea.ac.uk/id/eprint/69050/

Zeng, Z., and Guan, D. (2020). Methodology and application of flood footprint accounting in a hypothetical multiple two-flood event. *Philosophical Transactions of the Royal Society A: Mathematical, Physical and Engineering Sciences*, *378*(2168), 20190209. https://doi.org/10.1098/rsta.2019.0209

Zeng, Z., Guan, D., Steenge, A. E., Xia, Y., and Mendoza-Tinoco, D. (2019). Flood

footprint assessment: a new approach for flood-induced indirect economic impact measurement and post-flood recovery. *Journal of Hydrology*, *579*, 124204. https://doi.org/10.1016/j.jhydrol.2019.124204

Zhai, G., Fukuzono, T., and Ikeda, S. (2005). Modeling flood damage: case of Tokai Flood 2000. *Journal of the American Water Resources Association*, *41*(1), 77-92. https://doi.org/10.1111/j.1752-1688.2005.tb03719.x

Zhang, D., Lei, L., Ji, Q., and Kutan, A. M. (2019). Economic policy uncertainty in the US and China and their impact on the global markets. *Economic Modelling*, *79*, 47-56. https://doi.org/10.1016/j.econmod.2018.09.028

Zhang, P., Deschenes, O., Meng, K., and Zhang, J. (2018). Temperature effects on productivity and factor reallocation: evidence from a half million Chinese manufacturing plants. *Journal of Environmental Economics and Management*, *88*, 1-17. https://doi.org/10.1016/j.jeem.2017.11.001

Zhang, W., and Villarini, G. (2020). Deadly compound heat stress-flooding hazard across the central United States. *Geophysical Research Letters*, *47*(15), e2020GL089185. https://doi.org/10.1029/2020GL089185

Zhang, Y., Zhao, B., Jiang, Y., Xing, J., Sahu, S. K., Zheng, H., . . . Hao, J. (2022). Non-negligible contributions to human health from increased household air pollution exposure during the COVID-19 lockdown in China. *Environment International*, *158*, 106918. https://doi.org/10.1016/j.envint.2021.106918

Zhang, Z., Li, N., Cui, P., Xu, H., Liu, Y., Chen, X., and Feng, J. (2019). How to integrate labor disruption into an economic impact evaluation model for postdisaster recovery periods. *Risk Analysis*, *39*(11), 2443-2456. https://doi.org/10.1111/risa.13365

Zhang, Z., Li, N., Feng, J., Chen, X., Liu, L., and Bai, K. (2018). Quantitative assessment of changes in post-disaster resilience from the perspective of rescue funds and rescue efficiency: a case study of a flood disaster in Wuhan City on July 6, 2016 (in Chinese). *Journal of Catastrophology*, *33*(4), 211-216.

Zhang, Z., Li, N., Xu, H., and Chen, X. (2018). Analysis of the economic ripple effect of the United States on the world due to future climate change. *Earth's Future*, *6*(6), 828-840. https://doi.org/10.1029/2018EF000839

Zhao, J., Hu, J., and Chen, Q. (2021). Extreme weathers test the city's "extreme" management capabilities (in Chinese). *Business Management Review*, *8*, 98-100.

Zhao, M., Lee, J. K. W., Kjellstrom, T., and Cai, W. (2021). Assessment of the economic impact of heat-related labor productivity loss: a systematic review. *Climatic Change*, *167*, 22. https://doi.org/10.1007/s10584-021-03160-7

Zheng, H., Többen, J., Dietzenbacher, E., Moran, D., Meng, J., Wang, D., and Guan, D. (2021). Entropy-based Chinese city-level MRIO table framework. *Economic Systems Research*, 1-26. https://doi.org/10.1080/09535314.2021.1932764

Zheng, H., Zhang, Z., Wei, W., Song, M., Dietzenbacher, E., Wang, X., . . . Guan, D.

(2020). Regional determinants of China's consumption-based emissions in the economic transition. *Environmental Research Letters*, *15*(7), 074001. https://doi.org/10.1088/1748-9326/ab794f

Zhengzhou Municipal Bureau of Statistics. (2021). *Zhengzhou city's seventh national census bulletin (No. 1): the city's permanent population (in Chinese)*. Retrieved October 24, 2021 from http://tjj.zhengzhou.gov.cn/tjgb/5012681.jhtml

Zhou, M., Wang, H., Zhu, J., Chen, W., Wang, L., Liu, S., . . . Liang, X. (2016). Cause-specific mortality for 240 causes in China during 1990-2013: a systematic subnational analysis for the Global Burden of Disease Study 2013. *The Lancet*, *387*(10015), 251-272. https://doi.org/10.1016/S0140-6736(15)00551-6

Zscheischler, J., Martius, O., Westra, S., Bevacqua, E., Raymond, C., Horton, R. M., . . . Vignotto, E. (2020). A typology of compound weather and climate events. *Nature Reviews Earth & Environment*, *1*(7), 333-347. https://doi.org/10.1038/s43017-020-0060-z

Zscheischler, J., and Seneviratne, S. I. (2017). Dependence of drivers affects risks associated with compound events. *Science Advances*, *3*(6), e1700263. https://doi.org/10.1126/sciadv.1700263

Zscheischler, J., Westra, S., van den Hurk, B. J. J. M., Seneviratne, S. I., Ward, P. J., Pitman, A., . . . Zhang, X. (2018). Future climate risk from compound events. *Nature Climate Change*, *8*(6), 469-477. https://doi.org/10.1038/s41558-018-0156-3